Hepatitis C:
Host-virus interactions and their impact on treatment response

Inauguraldissertation

zur
Erlangung der Würde eines Doktors der Philosophie
vorgelegt der
Philosophisch-Naturwissenschaftlichen Fakultät
der Universität Basel

von

Michael Thomas Dill
aus Pratteln, Basel-Landschaft

Basel, 2012

Genehmigt von der Philosophisch-Naturwissenschaftlichen Fakultät
auf Antrag von

Fakultätsverantwortlicher: Prof. Dr. med. M. H. Heim

Korreferent: Prof. Dr. phil. D. Bumann

Basel, den 27.03.12

Prof. Dr. phil. M. Spiess
Dekan der Philosophisch-Naturwissenschaftlichen Fakultät

Dedicated to Anja

Acknowledgments

I would like to thank Markus Heim for taking me into his lab early on and giving me the opportunity to do my own research during my whole studies and as a PhD student. His leadership, the intensity he puts into scientific projects and his genuine interest into science are inspiring and motivating.

I am very grateful for the camaraderie of François Duong, who introduced me to almost every aspect of daily scientific research. I very much appreciate his abiding enthusiasm to help and assist with every imaginable problem.

I also want to especially thank Zuza Makowska for inspiring discussions and the outstanding collaborations we had on the acute HCV and the Interferon in vivo projects.

I would like to address my thanks to current and former members of the laboratory: Christine Bernsmeier, Tujana Boldanova, Sylvia Ketterer, Ilona Krol, Vijay Shanker, and Gaia Trincucci; Sonja Rothweiler and David Semela; Alex Blindenbacher, Verena Christen, Magdalena Filipowicz, Elke Moradpour, and Xueya Wang.

I always appreciated the excellent collaboration with Luigi Terracciano and Luigi Tornillo from the Institute of Pathology and our very informative discussions.

We had exceptional collaborations with Julia Vogt and Volker Roth from the Computer Science Department on the IL28B and the Intereron in vivo project. I'm also very grateful that they let me catch a glimpse of non-linear computational analyses and the random forest classifier.

I would like to thank Phil Demougin from the Life Sciences Training Facility to introduce me to all technical aspects of microarray processing.

Finally, I want to thank Thomas Baumert, Sarah Durand and Cathy Royer from the University of Strasbourg for the isolation and provision of primary human hepatocytes for my experiments.

Table of contents

Summary

Hepatitis C is a major cause of chronic liver disease with over 120 million infected people worldwide. Untreated chronic hepatitis C (CHC) infection leads in 20-50% to liver cirrhosis culminating in cirrhosis-related complications and hepatocellular carcinoma eventually leading to death. For the last decade a combination therapy of pegylated Interferon-alpha (pegIFN-α) and Ribavirin was the standard of care resulting in sustained virologic response (SVR) rates of approximately 50%. The antiviral effect of this naturally occurring cytokine is not achieved through a direct targeting of the virus but instead by creation of an antiviral state in infected host-cells and triggering of the host's immune system through induction of hundreds of interferon stimulated genes (ISGs). Interestingly, some patients with CHC who show a strong induction of ISGs in the liver even before treatment do not respond to administered pegIFN-α and do not clear the virus. The lack of response is most likely due to refractoriness of the IFN signaling. The reason for this preactivation of the IFN system in the liver in a subset of patients and the following non-response remains unclear.
It is the aim of this thesis to improve the understanding of host-virus interactions in hepatitis C infection with regard to the preactivation of the IFN system and its consequential failure to IFN-α based treatment regimens. The thesis consists of three different parts:

First, the host-response in the liver of patients in the acute phase of hepatitis C (AHC) infection, i.e. the first six months after transmission, was investigated. To elucidate molecular mechanisms involved in non-response, we wanted to exploit the fact that in AHC SVR rates to therapy with pegIFN-α are substantially better than in CHC (>90% versus 50%). Six liver biopsies of AHC patients were analyzed for ISG expression and IFN signaling by transcriptome, protein and immunohistochemical analyses and compared to a set of patients with CHC as well as control liver samples. Additionally, IFN-α and -γ specific gene sets were defined in primary human hepatocytes. While both AHC and CHC non-responders (CHC-NR) showed a strong induction of ISGs, enrichment analysis revealed that in CHC-NR mainly IFN-α stimulated genes were induced, in contrast to IFN-γ stimulated gene expression in AHC. IFN-γ was increased in AHC and correlated with the amount of infiltrating CD8+ T cells that by immunostaining were found to be co-localized with activated hepatocytes. Analysis of negative regulators of IFN signaling in the IFN-α stimulated gene set revealed exclusively in CHC-NR an upregulation of USP18, a key molecule in establishing refractoriness to IFN-α signaling. These results provide an explanation for the preserved

response to pegIFN-α in AHC and highlight USP18 as a potential therapeutical target to improve treatment in CHC patients with a pre-activated IFN system.

Second, a possible connection between genetic variants near the IL28B gene and ISG induction in livers of CHC patients was assessed. Four independent genome-wide association studies have revealed a highly significant association of single nucleotide polymorphisms (SNPs) near the IL28B gene with the outcome of therapy with pegIFN-α and ribavirin in CHC. We hypothesized that these genetic variants near the IL28B gene, which encodes for IFN-λ3, might be responsible for the preactivation of the IFN system in certain patients. 109 patients with CHC were genotyped for IL28B SNPs and the hepatic ISG expression was quantified. Interestingly, despite an association of the IL28B genotype with the expression of ISGs, stratification revealed that ISG expression is associated with response independent of its IL28B genotype making a direct link rather unlikely. A multivariate analysis using a random forest classifier analysis defined ISG expression, by the means of a 4-gene-classifier, as the strongest treatment predictor.

Third, the pharmacodynamics of pegIFN-α in the livers of patients with CHC was explored. Due to higher efficacy, pegIFN-α has replaced conventional IFN-α as standard of care. It is generally assumed that the improved pharmacokinetic properties of the former with a longer half-life leads to better effectiveness through a continuous induction of ISGs. However, basic studies *in vitro* and in mouse models suggest a long-lasting refractoriness of the IFN-α signaling that is not responsive to further stimulation. We therefore addressed this issue directly in CHC patients receiving treatment. To avoid non-response only patients with a non-preactivated IFN system were included. Each patient received a paired biopsy before and at a certain time point after the first injection with pegIFN-α. After transcriptome analyses, clusters of genes with distinctive temporal patterns were generated. The upregulation in the early ISG clusters was only transient and no prolonged upregulation or a second wave of induction could be noticed. Additionally, a direct comparison of the two commercially available pegIFNα, pegIFNα-2a versus -2b at 144h showed no significant difference in the amount or extension of upregulated ISGs, despite the longer serum half-life of pegIFNα-2a. This study indicates that the superior efficacy of pegIFN-α compared to conventional IFN-α cannot be explained by persistent signaling and ISG induction.

Abbreviations

AHC	acute hepatitis C
ALT	alanine-aminotransferase
AUC	area under the curve
cEVR	complete early virologic response
CHC	chronic hepatitis C
DAA	direct-acting antivirals
DNA	deoxyribonucleic acid
EGFR	epidermal growth factor receptor
ELISA	enzyme-linked immunosorbent assay
EoTR	end of treatment response
ERR	error rate
ES	enrichment score
EVR	early virologic response
GAS	gamma-activation sequence
GSEA	gene set enrichment analysis
GWAS	genome-wide association study
h	hour
HBV	hepatitis B virus
HCC	hepatocellular carcinoma
HCV	hepatitis C virus
HCVcc	cell-culture-derived hepatitis C virus
HIV	human immunodeficiency virus
IFNAR	Interferon alpha receptor
IFN-α	Interferon alpha
IFN-γ	Interferon gamma
IFN-λ	Interferon lambda
IL28B	Interleukin 28B
IP-10	Interferon-γ inducible protein 10
IRF	Interferon regulatory factor
IRES	internal ribosome entry site
ISG	Interferon stimulated gene
ISGF3	IFN-stimulated gene factor 3
ISRE	IFN-stimulated response element
Jak	Janus kinase
kb	kilobases
LDL	low density lipoprotein
MAVS	mitochondrial antiviral signaling protein
Mio	million
mRNA	messenger RNA
miRNA	microRNA
NCR	non-coding region
NLR	NOD-like receptor
NR	non-responder
NS	non-structural
ORF	open reading frame
PAMP	pathogen-associated molecular pattern
PBMC	peripheral blood mononuclear cell
PCR	polymerase chain reaction
pDC	plasmacytoid dendritic cell
PEG	polyethylene glycol
pegIFN-α	pegylated Interferon alpha
PKR	protein kinase R
PNR	primary non-response
PP2A	protein phosphatase 2A
PRMT1	protein arginine methyltransferase 1
PRR	pattern recognition receptor
pSTAT1	phosphorylated STAT1
R	responder
RdRp	RNA-dependent RNA polymerase
REL	relapse
RFFS	random forest feature score
RNA	ribonucleic acid
ROC	receiver operating characteristic
RVR	rapid virologic response
SNP	single nucleotide polymorphism
SOC	standard of care
SOCS	suppressor of cytokine signaling
STAT	signal transducer and activator of transcription
SVR	sustained virologic response
TLR	toll-like receptor
TRIF	TIR-domain-containing adapter-inducing interferon-β
USP18	Ubiquitin-specific peptidase 18
VL	viral load
VLDL	very low density lipoprotein

1. Introduction

1.1 Hepatitis C virus

Hepatitis C virus (HCV) infection is a major cause of chronic liver disease with development of liver cirrhosis and hepatocellular carcinoma (HCC). It is estimated that worldwide more than 120 million are infected with HCV with approximately 3-4 million new cases every year[1].

HCV was first isolated in 1989 by screening an expression library with serum from a patient with non-A, non-B hepatitis[2]. However, the low viral abundance in serum and liver tissue of patients, the lack of successful culture of HCV *in vitro*, and the limitation of infections occurring in humans and chimpanzees only made it very difficult to study its lifecycle, to identify and characterize viral products, and moreover to develop specific antiviral agents. Continuous efforts over the last 23 years led to great progress in the study of structure and replication of HCV by establishing *in vitro* models such as cellular expression systems[3], a subgenomic replicon system[4,5], and in 2005, 16 years after its discovery, for the first time a complete infectious cell-culture system (HCVcc)[6,7], producing HCV that was again infectious in chimpanzees, thus finally fulfilling Koch's postulates[8]. Additionally, a main objective has been to generate a mouse model fully supporting HCV infection for many years. First, different models with immunodeficient mice carrying chimeric livers with human hepatocytes were created[9,10], and recently a model with adenovirus-mediated delivery of essential receptors for HCV allowed to study HCV entry in further detail[11]. However, efforts to create a transgenic mouse model in immunocompetent mice that fully supports HCV entry as well as replication are still ongoing.

Nevertheless, all these models have been leading to big advances in the understanding of the viral structure and its lifecycle.

1.1.1 Genome and classification

HCV is a positive-strand RNA virus and is classified as *Hepacivirus* within the *Flaviviridae* family. The HCV genome has a size of 9.6 kilobases and is very heterogenous and prone to mutations due to a high replicative activity and the lack of proof-reading ability of the viral RNA-dependent RNA polymerase (RdRp).

HCV is classified into 7 major genotpyes (1-7) that differ up to 35% in their nucleotide sequence, and within subtypes that differ by 25%[12]. These genotypes have important implications for therapy, since treatment response to Interferon-based treatment regimens differs significantly according to HCV genotype, and new direct-acting antivirals (DAA) do not efficiently target viral proteins from every genotype.

HCV has a positive-strand RNA genome composed of a 5'-non-coding region (NCR) containing an internal ribosome entry site (IRES), an open reading frame (ORF) with 3 structural and 6 non-structural proteins, and a 3'-NCR. In the 5'-NCR binding sites for a liver specific microRNA (miRNA) miR-122 have been discovered[13]. Binding of miR-122 to the HCV 5'-NCR enhanced viral replication - a finding that provided a first example of a virus exploiting cellular miRNA[13]. The single ORF encodes a polyprotein precursor with a size of approximately 3300 amino acids that is posttranslationally processed by cellular and viral proteases into 3 structural proteins (core, envelope proteins E1 and E2), the p7 polypeptide and 6 non-structural proteins (NS2, NS3, NS4A, NS4B, NS5A and NS5B) (reviewed in [14] and [15]) (Figure 1.1).

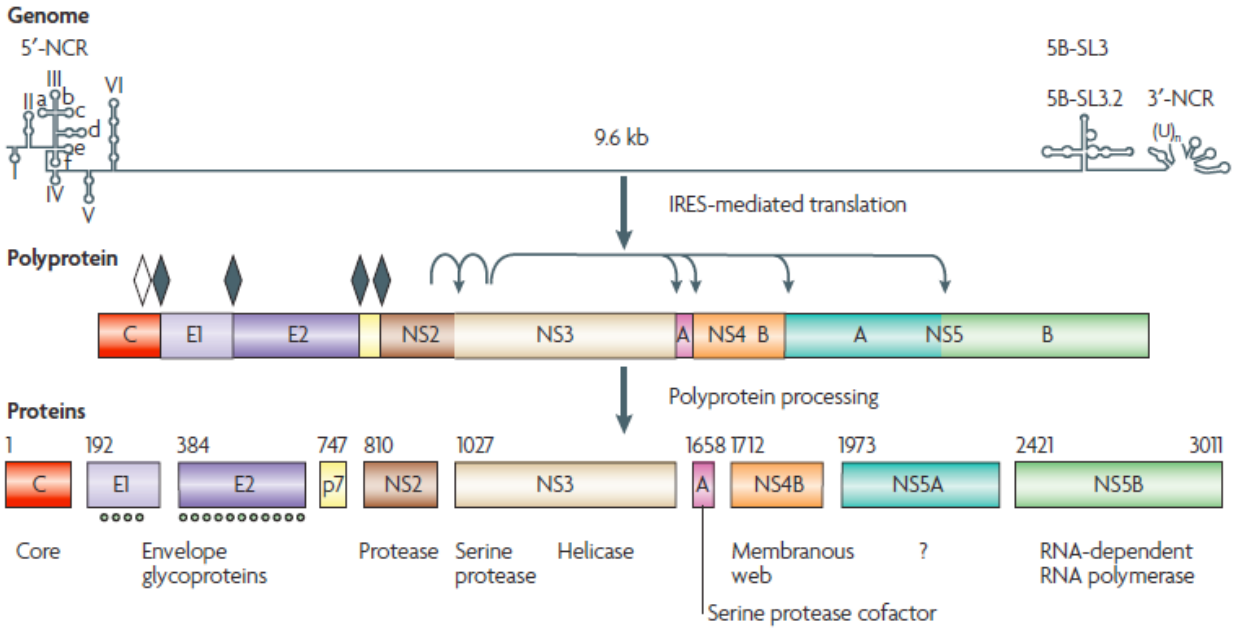

Figure 1.1. *Genetic organization and polyprotein processing of HCV* [14].

1.1.2 Structure and lifecycle

So far the HCV virions have not been definitely visualized, but based on filtration and electron microscopy studies the virions have a size of about 40-70 nm in diameter[7], and have been shown to be tightly associated with lipoproteins[16]. It is believed that multiple copies of core form a nucleocapsid containing the genomic RNA, and that the envelope glycoproteins E1 and E2 are anchored to a surrounding cell-derived double-layer lipid membrane[14].

Entry. Viral entry is the best studied phase of the lifecycle so far. HCV has a narrow host range, infecting humans and chimpanzees only. Hepatocytes are the main cells targeted by HCV but it has been reported that B lymphocytes, dendritic cells and also endothelial cells can be infected[17]. The first membrane-receptor described to bind HCV was CD81[18], followed by the LDL receptor[19], scavenger receptor class B type I (SR-BI)[20], Claudin-1[21] and Occludin[22]. More recently, epidermal growth factor receptor (EGFR)[23] and Niemann-Pick C1–like 1 cholesterol absorption receptor (NPC1L1)[24] have been identified as entry receptors, for both of which already pharmacological inhibitors exist. In an orchestrated process HCV virions sequentially bind to these receptors and then get internalized most likely by clathrin-mediated endocytosis[25].

Translation, Replication. The exact mechanisms regulating translation, replication and packaging of the viral genome remain to be elucidated. The 5'-NCR of the viral genome contains a highly conserved IRES that is essential for translation of the RNA. The polyprotein is posttranslationally cleaved by cellular enzymes and the viral protease NS3 with NS4A as a cofactor. NS3 has a range of catalytic sites containing a serine-type protease, RNA helicase and NTPase activity that are indispensable for polyprotein processing, RNA replication and possibly virion assembly (reviewed in [26]). The NS3-4A protease has therefore emerged as a main target of DAAs with newly approved drugs, Telaprevir and Boceprevir, now in clinical practice, and another wide range of protease inhibitors in clinical development[27].

NS4B, a highly hydrophobic protein, is then involved in creating an assembly of lipid vesicles in a membraneous matrix, designated as membraneous web which most likely functions as a scaffold for the assembly of the replication machinery[28].

The positive-strand RNA is copied by the NS5B RdRp into a negative-strand intermediate forming a double-strand replicative form, which serves as template for the production of new positive-strand genomes. The structure of NS5B has been comprehensively characterized[29,30] and NS5B inhibitors are currently tested in advanced phases of clinical development[31].

Assembly. Both, NS2 and the polypeptide p7 have been shown to be necessary for virion morphogenesis and release[32]. p7 forms oligomer complexes and has been shown to have a cation channel activity[33]. The full-length protein of NS2 including its protease domain but not its enzymatic activity is required for the production of infectious virus[34]. Several reports state that the formation of infectious particles and their release depends on members of the LDL and VLDL pathway, and that they require apolipoprotein E and other proteins[35,36,37] (Figure 1.2).

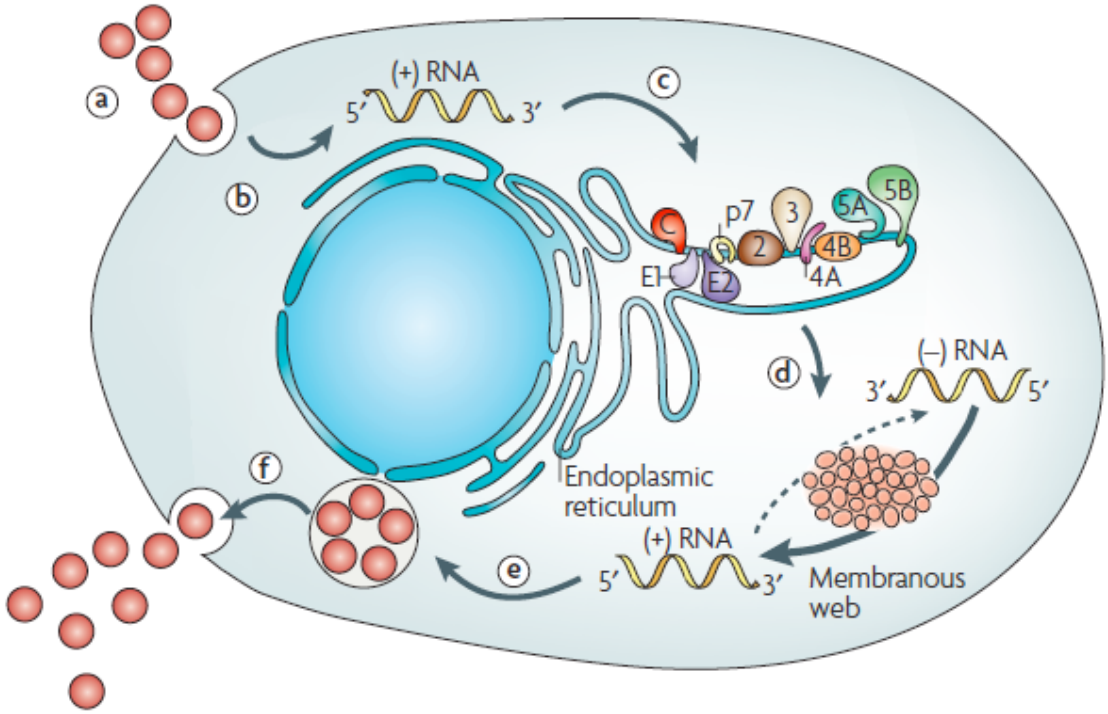

Figure 1.2. *Lifecycle of HCV. (a) Viral entry; (b) cytoplasmic release and uncoating; (c) IRES-mediated translation and polyprotein processing; (d) RNA replication; (e) packaging and assembly; (f) virion maturation and release*[14].

1.1.3 Natural history of hepatitis C virus infection

The discovery of HCV and the consequential emergence of serological and virological assays made it possible to understand the evolution of hepatitis C infection.

Transmission. Before HCV was detectable in human blood, transmission in blood-transfusion settings was the most common cause of infection (called initially non-A, non-B hepatitis) in industrialized countries[38]. Currently, intravenous drug use, unprotected sex with multiple

partners and viral exposure during medical procedures or in piercing and tattoo studios are the most common risk factors for infection[39].

Spontaneous clearance. Acute hepatitis C is defined as the period of the first 6 months after transmission with HCV. Unlike with other viral hepatitis infections, clinical symptoms at the acute onset of disease are usually mild and unspecific, such as fatigue, abdominal pain, or dyspepsia, while jaundice is reported in only 30%[39]. Thus, acutely infected patients rarely go to see a doctor and are therefore under-reported. This impedes of course the proper analysis of spontaneous clearance or progression of HCV infection. However, epidemiologic studies in well-defined patient cohorts that got infected by blood transfusion before the onset of HCV testing revealed that in about 75-85% of the cases the virus persisted and progressed to chronic infection[38,40]. Similar results were obtained in other settings of infection[41]. Interestingly, the rate of viral persistence seems to be significantly lower in children and young women (55-60%)[42,43].

Spontaneous clearance in the chronic phase of infection, i.e. later than 6 months after transmission, is extremely rare and negligible.

Fibrosis progression. Once a chronic infection is established in the liver, continuous inflammation generally leads to hepatic fibrogenesis and ultimately cirrhosis and HCC. With the prospect of lacking effective treatment options, many clinical studies had been performed to assess natural fibrosis progression. However, the risk to progress to cirrhosis varied considerably between different studies from 7% - 55%[41,44]. This variability most probably derives from biases obtained by different methodological approaches (prospective vs. retrospective), different patient collectives (liver clinic patients vs. community-based cohorts) and the difficulty to exactly assess the time point of infection due to the often clinically silent onset of disease. A recent meta-analysis including data from 111 clinical studies computed a mean prevalence of cirrhosis after 20 years of infection in 16% of patients[45]. Three main conclusions can be drawn from all these reports: first, there are huge inter-individual differences regarding the rate of progression depending on both host and viral factors[44]; second, the progression rate seems to remain linear over time[45]; and third, environmental factors like alcohol intake or HBV/HIV co-infection etc. can dramatically increase progression rate[46,44].

Importantly, once the causal agent of the liver disease, in this case HCV, is removed before cirrhosis has developed, liver fibrosis regresses almost completely again[47].

End-stage liver disease. Once cirrhosis is established the risk of impaired liver function as well as the development of HCC increases tremendously. In patients with HCV-induced

cirrhosis the 5-year cumulative incidence of HCC is very high with 17-31%[48] and HCV-related cirrhosis with its associated complications like variceal bleeding, spontaneous bacterial peritonitis, hepatic encephalopathy etc. increases overall mortality with a factor of three[49]. While in industrialized countries the incidence of newly acquired HCV infections is declining, the disease burden due to the slow fibrosis progression is still ascending, highlighting the urgent need for effective antiviral treatment regimens.

1.1.4 Interferon-based therapy of hepatitis C virus

Even before HCV was successfully isolated, first clinical trials with recombinant human IFN-α have been conducted[50] and for over 25 years IFN-α has remained the backbone of anti-HCV therapies. IFN-α has no direct interaction with HCV but rather indirect antiviral and immunomodulatory effects. Through the Jak-STAT pathway IFN-α induces interferon stimulated genes (ISGs) that lead to a non-virus-specific cellular antiviral state[51]. This rather special mode of action clearly distinguishes IFN-α from other conventional antiviral drugs.

Evolution of Interferon-therapy. In the late eighties, three times weekly subcutaneous injections of recombinant IFN-α (3 Mio units) for 48 weeks established itself as initial standard of care (SOC) therapy achieving overall a sustained virologic response (SVR, i.e. undetectable viral load 6 months after end of treatment) in 15-20%[52]. In 1998, a first randomized clinical trial testing a dual therapy with IFN-α2b and oral administration of the broad-spectrum antiviral ribavirin increased SVR rates considerably to 35-43% and replaced monotherapy[53]. 3 years later, pegylated IFN-α (pegIFN-α, IFN-α tethered with a polyethylene glycol (PEG)) with a much longer serum half-life was introduced. Injections could be reduced to once weekly and combination therapy with ribavirin led to higher overall SVR rates of approximately 55%[54].

PegIFN-α-2a vs. pegIFN-α-2b. Two different pegIFN-α are available which vary considerably in their pharmacologic properties. IFN-α-2b is covalently linked to a linear 12kDa PEG, while pegIFN-α-2a has a 40kDa PEG moiety, comprising two 20kDa chains linked to form a branched chain[55]. These molecular differences have a considerable effect on the pharmacokinetics and –dynamics of these drugs. The PEG bond with IFN-α-2b is unstable and undergoes hydrolysis, which leads to a quick release of IFN-α-2b that then circulates the body. Basically, pegIFN-α-2b is a pro-drug, and only IFN-α-2b interacts with the IFN

receptor. In contrast, pegIFN-α-2a is not subject to hydrolysis and therefore the entire pegylated molecule circulates the body and interacts with the receptor[55]. It has been shown that the attachment of the large PEG reduces the affinity of pegIFN-α-2a to the IFN receptor leading to an antiviral activity *in vitro* of only 7% compared to conventional IFN-α[55]. However, the advantage of pegIFN-α-2a is its greater stability and reduced clearance leading to a much longer serum half-life. Unlike with pegIFN-α-2a, more than half of the patients receiving pegIFN-α-2b have low serum levels at day 5 after injection, and over 90% at day 7[56].

Nevertheless, in the majority of the 18 trials where in direct comparison the antiviral efficacy by SVR was measured, no significant differences in SVR rates were obtained (reviewed in [55]). Thus, no recommendations exist to favor one drug over the other.

Side effects. Almost all patients are subject to adverse events during treatment, which is a main reason of discontinuation. In general, 10% to 14% of patients have to stop therapy due to an adverse event[57]. Most common are influenza-like symptoms, such as fatigue, headache, fever and rigors in more than half of the patients. Psychiatric effects like depression, insomnia, irratibility are also very common (20% to 30%). IFN has a bone marrow-suppressive effect that may lead to neutropenia, anemia and thrombocytopenia. Ribavirin additionally can lead to hemolytic anemia. Peg-IFN-α may lead to autoimmune disorders, such as autoimmune thyroiditis. Ribavirin has caused fetal death and abnormalities in toxicological animal studies and is therefore only allowed under strict contraception.

Treatment indication. The fact that only about half of the patients profit permanently from treatment and that these considerable side effects together with substantial costs arise from this therapy, led to recommendations for rational treatment decision making, balancing benefits and costs. Guidelines have been developed and the recommended minimal requirements to consider treatment are positive serum HCV RNA and significant fibrosis in the liver as assessed by liver biopsy[57]. Evidently, each individual patient's general and liver health, as well as social aspects have additionally to be taken into consideration.

1.1.5 Treatment predictors

Pre-treatment predictors. Considering the limited chance of SVR and the serious side effects accompanying IFN-α treatment, there has ever been the incentive to predict before treatment, which individual patient will profit from therapy. The most important predictor so far is the

viral genotype. SVR rates are much higher in patients infected with HCV genotype 2 or 3 (about 80%), while in genotype 1 rates are at 45%[57]. An additional viral factor is the viral load in the serum; less than 800,000 IU/mL seems to give higher likelihood for SVR[58]. Host characteristics that are generally less strongly associated with a positive response include female gender, age younger than 40 years, nonblack race, lower body weight (<75 kg), the absence of insulin resistance, and the absence of bridging fibrosis or cirrhosis on liver biopsy[58]. Additionally, there has been growing evidence that activation of the endogenous IFN system in the liver and genetic variants near the IL28B gene are highly associated with treatment response, which will be discussed in more detail in chapter 1.3.3 and 1.3.4.

On-treatment predictors. The most powerful predictors are the viral kinetics on treatment. A negative viral load at week 4 of treatment, so called rapid virological response (RVR, see table 1.1 for further definitions), is the strongest predictor of treatment outcome[58]. Achieving RVR is associated with 86-100% SVR rates regardless of the viral genotype[58]. However, only a minority of patients reach an RVR, and the negative predictive value is not very good, since many patients without RVR still achieve SVR. The best reason to stop therapy due to limited chance of SVR is the viral kinetics at week 12 of therapy. Not achieving an early virologic response (EVR, more than 2log^{10} drop of viral load compared to baseline) is associated with 0-3% of SVR[58], and therefore was implied as a stopping rule[57]. Figure 1.3 depicts the different types of virological responses in pegIFN- α/ribavirin regimens.

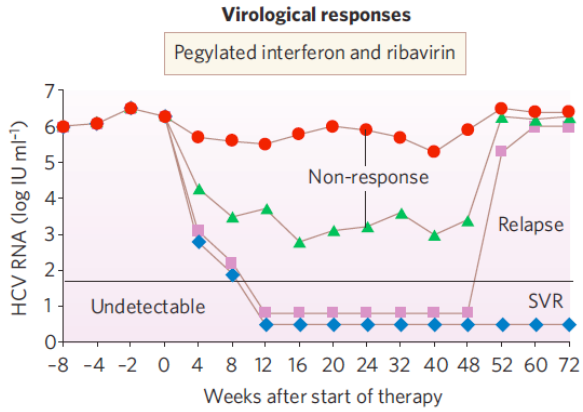

Figure 1.3. *Virological responses to HCV therapy. (red) primary non-response (PNR); (green) partial non-response with no end of treatment response (no EoTR); (lilac) relapse (REL); (blue) sustained virologic response (SVR)* [59].

Table 1.1. *Definitions of viral responses during treatment with pegIFN-α/ribavirin.*

Rapid virological response (RVR)	=	undetect. VL at 4 weeks
Complete early virologic response (cEVR)	=	undetect. VL at 12 weeks
Early virologic response (EVR)	=	> 2 log10 decline in VL at 12 weeks
End of treatment response (EoTR)	=	undetect. VL at end of treatment
Sustained virologic response (SVR)	=	undetect. VL 24 weeks after end of treatment
Primary non-response (PNR)	=	< 2 log10 decline in VL at 12 weeks
Partial non-response	=	> 2 log10 decline in VL at 12 weeks but still detectable at 24 weeks
Viral breakthrough	=	undetect. VL at any time and still on treatment re-detection of VL
Relapse (REL)	=	re-detection of VL after end of treatment response

Abbreviations: undetect., undetectable; VL, viral load

1.1.6 Direct-acting antivirals

In 2011, Boceprevir and Telaprevir, two NS3-4A protease inhibitors, were approved as therapeutics for patients infected with genotype 1. Monotherapy with these drugs has been shown to be very effective but quickly inducing viral resistance and leading to viral breakthrough[60]. Thus, so far IFN-α is still needed as the backbone of HCV therapy. Phase 3 randomized controlled trials of triple combination therapy showed improved SVR rates in treatment naïve genotype 1 patients compared to dual therapy from 40% to 68% for Boceprevir, and from 44% to 75% for Telaprevir, respectively[61,62] (Figure 1.4). Therefore, triple therapy in combination with pegIFN-α and ribavirin is now regarded as SOC for this group of patients[63]. Despite the big improvement of SVR rates in this difficult-to-treat patient group, the success comes at the cost of additional side effects, like severe anemia, rash or dysgeusia and pruritus[61,62], and strongly increased expenses. These two protease inhibitors though reflect a first promising tip of the iceberg of DAAs that are in development and let us look optimistically into the future of HCV treatment.

Nevertheless, promising DAAs for patients with genotype 2, 3 or 4 that did not respond to the combination therapy of pegIFN-α and ribavirin will not be available in the near future. Additionally, pegIFN-α is still essential in combination therapy. Therefore it is clinically absolutely relevant to identify patients that will respond to IFN-α, and on the other side to understand why certain patients show no response to IFN-α.

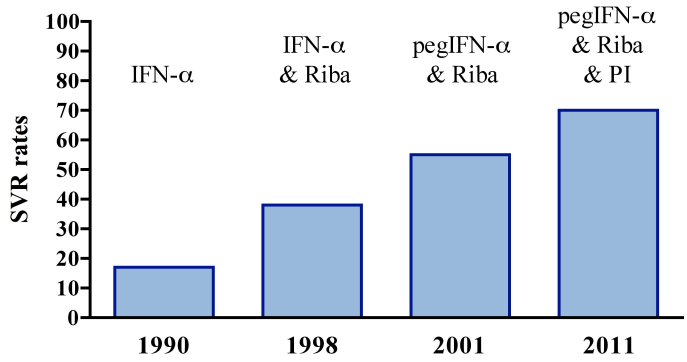

Figure 1.4. *Evolution of treatment responses. Triple combination therapy with proteinase inhibitors is only available for patients infected with Genotype 1. PI, proteinase inhibitor.*

1.2 Interferon signaling

In HCV infection the endogenous IFN system is not only activated during acute infection, but in some patients also during the chronic phase, which hasn't been described for any other chronic viral infection. Considering that exogenous IFN is also used as a therapeutic agent in this disease and many patients just do not respond to it, further underlines the need for better comprehension of these mechanisms. The basis for a thorough understanding of the host-virus interactions in HCV infection and its implications on treatment response is a detailed knowledge of Interferon signaling on the molecular level. In this chapter the different members of the IFN family, the pathways important for the sensing of HCV, the signal transduction through the Jak-STAT pathway and induction of ISGs, and last the negative regulation of IFN signaling will be outlined.

1.2.1 The Interferon family and its receptors

IFNs, first discovered by Isaacs and Lindenmann in 1957[64], belong to the class II cytokines and have important antiviral properties, are potent cell growth regulators, but also have immunomodulatory effects[65]. The IFNs have been grouped into three different classes: type I IFNs comprise of 13 IFN-α subtypes, IFN-β, IFN-ε, IFN-κ and IFN-ω; type II consists only of IFN-γ; and the most recent discovered type III IFNs include 3 IFN-λ (-1, -2 and -3) (Figure 1.5)[66].

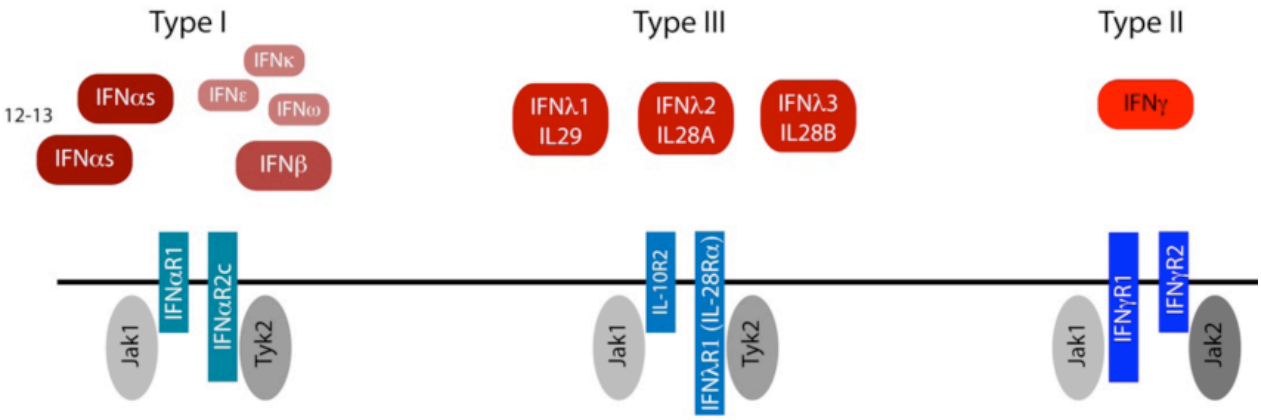

Figure 1.5. *Different types of IFN and their receptors. (from Heim MH, IFN Signaling in the Liver, EASL monothematic conference, 2010).*

Type I IFN. Type I IFNs bind to the IFN-α receptor (IFNAR), which consists of two chains (IFNAR1 and IFNAR2). It is assumed that type I IFN upon viral exposure are ubiquitously induced in basically any cell type, and these IFN are absolutely essential to fight viruses. IFNAR knockout mice are highly susceptible to viral infections and the outcome is fatal even at exposure of very low viral titers[67].

Type II IFN. IFN-γ engages the IFN-γR1 (IFNGR1) and IFN-γR2 (IFNGR2) chains to assemble its functional receptor complex[66]. It behaves quite different compared to type I IFN. IFN-γ is only produced by certain immune cells, including natural killer (NK) cells, CD4+ T helper cells and CD8+ cytotoxic T cells[65]. Accordingly, its function is more immunomodulatory by stimulating cell-mediated immune responses in an adaptive immunity setting[68]. Consequently, IFN-γ has complementary tasks compared to type I IFNs, and they work synergistically to fight viral infections[67].

Type III IFN. The IFN-λ family has only recently been discovered[69,70]. The IFN-λ1, -2 and -3 (also named IL29, IL28A, IL28B) bind to the IFN-λ receptor chain (IL28RA) that leads to the recruitment of the IL-10 receptor 2 chain (IL10RB). IFN-λ induces a similar set of ISGs like IFN-α, though with slower kinetics and a weaker induction[71]. While type III IFNs, similar to type I IFNs, seem to be inducible in any cell type, the expression of the IL28RA is mostly limited to epithelial cells, especially from the lung and gastrointestinal tract[72]. Consequently, thorough viral infection studies in mice lacking IFNAR and/or IL28RA revealed that IFN-λ plays an important role in fighting pneumotropic and gut-infecting viruses[72,73]. However, in the liver there is an apparent discrepancy between mice and human in regard to IL28RA expression. Human hepatocytes express IL28RA and are responsible to IFN-λ, which mouse hepatocytes clearly lack[72,74].

Function-wise type I and III IFN are more closely related than type II IFN, and the current knowledge suggests that type III IFN have evolutionarily evolved as an additional - and in some cases essential - support to type I IFN in fighting viral infections especially in locations frequently exposed to viruses, like the lung and gastrointestinal tract.

1.2.2 Viral sensory pathways in the context of HCV infection

The prerequisite for an effective IFN signaling is the proper sensing of viral pathogens. Pattern recognition receptors (PRRs) recognize pathogen-associated molecular patterns (PAMPs) in the extracellular environment as well as intracellularly. Four different classes of PRR families have been identified: the transmembrane toll-like receptors (TLR) and C-type lectin receptors, as well as the cytoplasmic retinoic acid-inducible gene (RIG)-I-like receptors and NOD-like receptors (NLRs)[75].

RIG-I. In the context of HCV evidence has been collected that sensing of intracellular HCV RNA occurs by RIG-I, a cytoplasmic RNA helicase, which recognizes a polyuridine motif in the 3'NCR of the virus, but also viral 5' triphosphate motifs[76,77]. Ubiquitination of RIG-I by TRIM25 is then needed to interact with mitochondrial antiviral signaling protein (MAVS, also known as CARDIF, VISA, IPS-1) to activate the signaling cascade[78]. RIG-I then interacts with MAVS, an adaptor protein connected to the mitochondrial membrane, by its CARD domain[75]. MAVS is able through binding to TRAF3 and TRAF6 to induce the IFN regulatory factor 3 (IRF3) and the NF-κB transcription activators that localize to the nucleus, bind to the IFN-β promoter, recruit co-factors and the RNA polymerase II to induce transcription.

TLR3. TL3, a membrane-bound receptor mainly located in the endosome, seems to sense HCV independent of RIG-I[79,80]. This receptor has first been described as a sensor of double stranded RNA and requires dimerization of TLR3 and phosporylation of a tyrosine residue to recruit the adaptor protein TIR-domain-containing adapter-inducing IFN-β (TRIF)[81]. The further downstream signaling pathway is common to the RIG-I signaling pathway downstream of MAVS (Figure 1.6)[75].

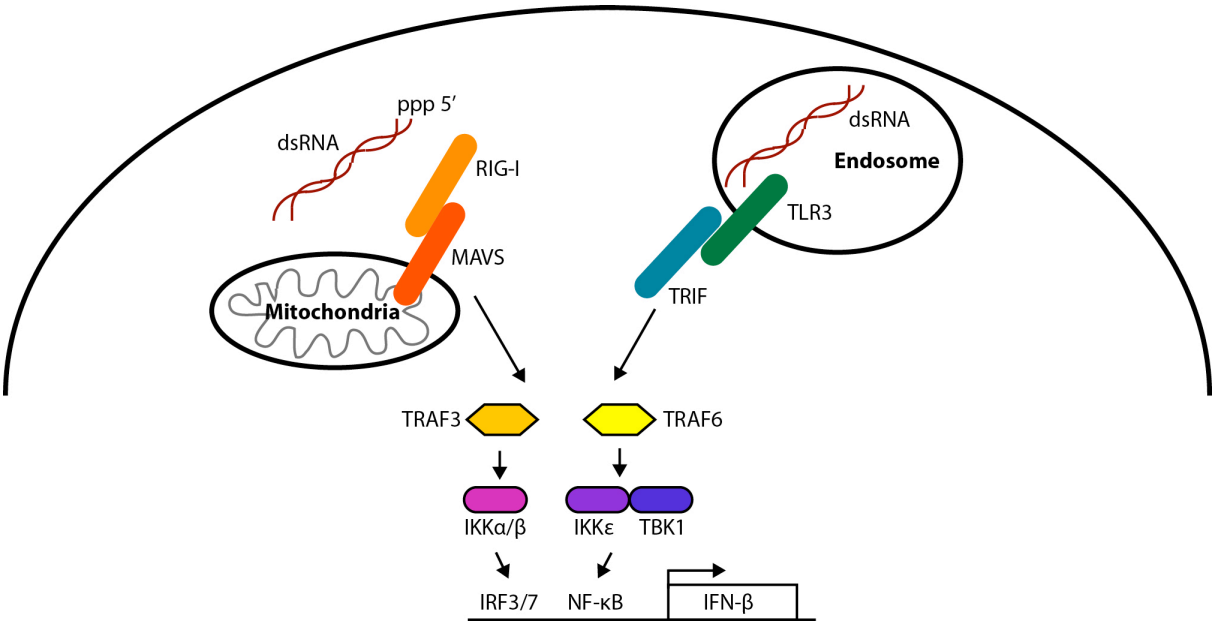

Figure 1.6. *Scheme of HCV sensing mechanisms. Depicted are simplifications of the RIG-I pathway, which senses cytoplasmic HCV RNA, and signals through MAVS, and the TLR3 pathway signaling through TRIF. Both transduce the signal through TRAFs and eventually induce NF-κB and IRF3/7 that enhance transcription of IFN-β.*

TLR7. One article focused on the role of TLR7 in plasmacytoid dendritic cells (pDCs) in HCV sensing[82]. pDCs are the most powerful type I IFN producing cells in the blood with the ability to release 200-1000 fold more cytokines than other cells[83]. TLR7 is only expressed in professional antigen expressing cells, localized in the endosome and recognizes single stranded RNA[84]. They show that cultured pDCs only upon direct contact with HCV-infected hepatocytes produce IFN through a TLR7-dependent pathway[82].

1.2.3 Jak-STAT pathway

As already mentioned, all IFN signal through the Jak-STAT pathway. This pathway consists, as its names reveals, of Janus kinases (Jaks) and signal transducers and activators of transcription (STATs). The canonical Jak-STAT pathway has been extensively studied and is well understood (reviewed in [85,86,87]). In mammals there are 4 Jak proteins (Jak1-3 and Tyk2) and 7 STAT genes (STAT1-4, STAT5A, STAT5B and STAT6) allowing for cell- and ligand-specificity, and to process diverse responses to extracellular signaling proteins. The signaling pathway is therefore not only used by IFN but by many other cytokines and growth

hormones. However, here it will be focused only on the signaling induced by the different IFN types, highlighting their similarities and their differences.

All IFNs have in common that binding to their receptors (e.g. IFNAR, IFNGR, IL28RA) induces an oligomerization of the two receptor chains, which leads to conformational changes of the associated Jak proteins, such that the Jaks can phosphorylate a tyrosine residue of each receptor chain. This phosphorylation creates a strong interaction site for the Src-homology 2 (SH2) domain of the STATs, that get recruited one to each receptor chain, then get phosphorylated on a tyrosine residue by the respective Jak protein, which allows the STATs to form stable dimers. They then translocate rapidly to the nucleus, where they bind to sequence motifs in the promoters of their respective target genes and enhance transcription of so called interferon stimulated genes (ISGs) (Figure 1.7).

Type I IFN bind to IFNAR1 and IFNAR2 that are associated with Tyk2 and Jak1, respectively. The receptor phosphorylation leads then to recruitment of each a STAT1 and a STAT2 molecule, the former getting phosphorylated on tyrosine 701 and the latter on tyrosine 689, leading to a strong heterodimer formation. After translocation to the nucleus the STAT1-STAT2 heterodimer interacts with IRF9 to build the IFN-stimulated gene factor 3 (ISGF3) that then binds to IFN-stimulated response elements (ISRE) in the promoters of classical ISGs. Again, signaling in response to type III IFN seems to follow a very similar pattern to that in response to type I IFN and also leads to ISGF3 formation that binds to ISRE[88]. On the other hand, type II IFN signaling is again different. IFNGR1 and IFNGR2 are associated with Jak1 and Jak2. Upon binding of the IFN-γ dimer to the receptor and the resulting receptor dimerization, Jak2 gets activated and first trans-phosphorylates Jak1, before both Jaks phosphorylate the receptor chains. Two STAT1 molecules get recruited that are phoshporylated at tyrosine 701 and form STAT1-STAT1 homodimers. They then translocate to the nucleus and bind to the gamma-activating sequence (GAS) elements that are distinct from ISRE.

It has to be noted, that these pathways are not exclusive and there is interplay between the canonical pathways. IFN-α is also able to partly induce STAT1 and STAT3 homo- and heterodimers, which then bind to GAS elements (Figure 1.7). What conditions apply to induce this cross-talk and to what extent this happens *in vivo* under physiological circumstances is not known.

Treatment of cells with IFN upregulates the expression of several hundred genes (ISGs), which specify the antiviral state. Transcriptome analysis of human peripheral blood

mononuclear cells (PBMCs) and human liver after treatment with pegIFN-α revealed that the ISG-sets induced is overlapping but also distinct, indicating a cell-type specific induction of ISGs[89]. Some of the ISGs, especially the ones encoding enzymes, have been studied thoroughly, e.g. protein kinase R (PKR), oligoadenylate synthetases (OAS), and Mx. In general different combinations of ISGs seem to be effective in different viruses, rather than one single ISG[84].

Recently, a very comprehensive overexpression screen has been performed to evaluate over 380 ISGs for their capability to inhibit the replication of several viruses, including HCV[90]. Among the strongest inhibitors of HCV replication were MDA5, RIG-I, IRF1 and IRF7[90]. Additionally, translational inhibition came out to be a general and potent mechanism to inhibit viral replication. Interestingly, several ISGs also enhanced the replication of some viruses, bringing forward another layer of complexity in virus-host interactions[90].

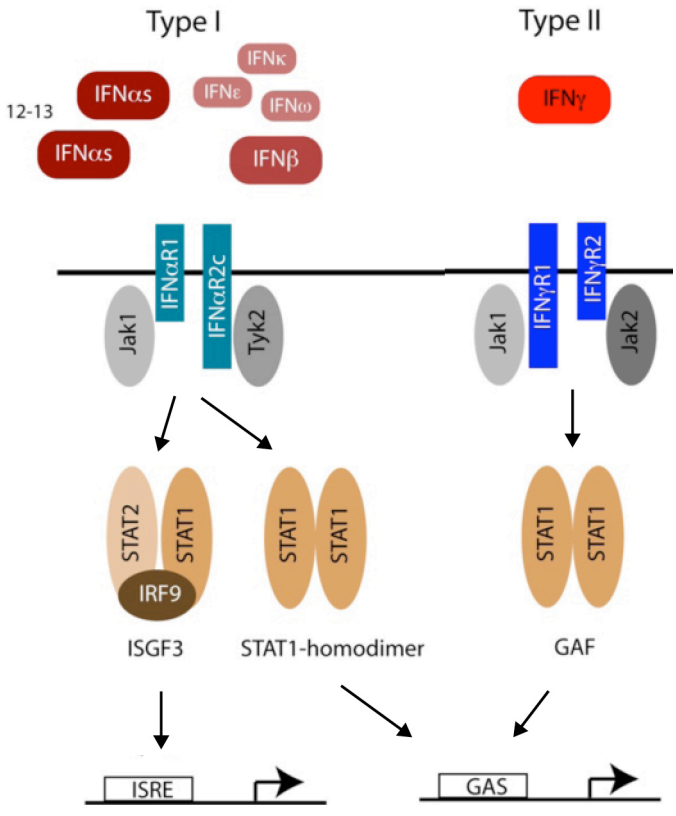

Figure 1.7. *Scheme of the proteins involved in the canonical Jak-STAT pathway of type I and II IFN (adapted from Heim MH, IFN Signaling in the Liver, EASL monothematic conference, 2010).*

1.2.4 Negative regulation of the Jak-STAT pathway

The activation of the Jak-STAT pathway is tightly controlled by several negative regulators that interfere at different steps of the pathway (Figure 1.8).

SOCS. A classical negative feedback loop in Jak-STAT signaling is the STAT-induced transcription of suppressor of cytokine signaling (SOCS) proteins. SOCS family members have a SH2 domain that can bind to phosphotyrosine residues of the cytokine receptor or the Jaks and the catalytic activity of the Jak proteins, or compete with STAT binding sites, or target bound signaling proteins for proteosomal degradation[91]. The exact mechanism remains to be elucidated.

PIAS. Another family of negative regulators that were discovered is called protein inhibitors of activated STATs (PIAS). PIAS acts in the nucleus by specifically binding to phosphorylated STATs and inhibiting their association with the DNA[92].

SHP. SH2 containing phosphatases (SHP) are ubiquitously expressed unspecific phosphatases that can attenuate cytokine signal transduction by dephosphorylating signaling intermediates such as JAK and its receptor[91].

USP18. More recently, ubiquitin-specific peptidase 18 (USP18), a classical ISG, has been identified as a novel negative regulator in Type I IFN signaling[93]. USP18 was first described to cleave ubiquitin-like modifier ISG15 from target proteins[94], but it has been demonstrated that it also blocks the Jak-STAT pathway, and this independently of its peptidase activity[93]. USP18 seems to bind specifically to the IFNAR2 receptor subunit and inhibits the activity of JAK1 by blocking the interaction between JAK1 and IFNAR2. Functionally, silencing of USP18 in cells infected with HCVcc potentiated the negative effect of IFN-α on the replication of HCVcc[95].

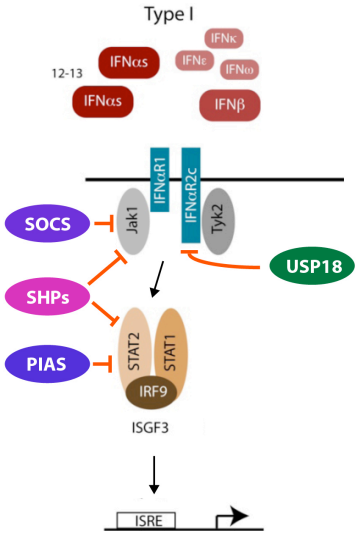

Figure 1.8. *Schematic overview of negative regulators at the different levels of the Jak-STAT pathway.*

1.2.5 Refractoriness to IFN signaling

It has been discovered many years ago that cultured cells treated with IFN-α become refractory within hours and remain unresponsive up to 3 days[96]. Refractoriness has also been demonstrated in livers of mice with continuous exposure to IFN-α[97]. A comprehensive study with different genetic mouse models revealed that while upregulation of SOCS proteins is responsible for an immediate negative regulation of the Jak-STAT pathway it cannot explain long-term refractoriness[97]. However, USP18 knockout mice remained responsive to further IFN-α stimulation suggesting a key function of USP18 in maintaining the cells refractory[97]. New evidence has been gathered *in vitro* and *in vivo* that this phenomenon of refractoriness is restricted to IFN-α signaling and does not affect IFN-β or IFN-λ signaling[98,74].

However, whether refractoriness to IFN-α signaling also occurs in the human liver has not been investigated so far, although this understanding would be important to improve IFN-α therapy regimens. pegIFN-α has replaced IFN-α because of its higher efficacy with more patients reaching SVR. It is commonly believed that the superior half-life of pegIFN-α with constant high serum levels is the reason for a better effectiveness by providing uninterrupted antiviral activity through continuous stimulation of the IFN signaling pathways[99]. Clearly, the evidence from cell culture and mouse models speaks against this hypothesis and pharmacodynamics studies in the human liver are needed if we want to understand the efficacy of pegIFN-α and its underlying molecular mechanisms.

1.3 Virus-host interactions

As indicated previously, proper small animal models to study HCV infection are still missing. So far the investigation of viral infection and the host's immune response has been limited to chimpanzees and human patients. Cell culture experiments in this context have clearly their limitations but have been helpful in discovering direct interactions of viral proteins with the host's intracellular defense mechanisms. This chapter will thus cover the gathered knowledge of the interference of HCV with the antiviral response, the dynamics of the host's immune response to HCV, the phenomenon of a pre-activated IFN system in CHC, and the relevance of IL28B genetic variations in HCV infection.

1.3.1 Molecular interactions of HCV with the host's immune response

It remains astounding, how HCV with its small genome, encoding for only 10 different proteins, is able to survive the immune response in most of the acutely infected persons and establish a lifelong persistent infection. One can only speculate which of the strategies discovered in different virus infections are predominantly useful for HCV to win the battle against the host's immune system, but one property that especially holds true for HCV with ever growing evidence is the ability to interfere directly with the molecular pathways involved in the IFN signaling pathways.

Viral sensing. As mentioned previously, the main sensing pathways responsible for HCV detection are the RIG-I pathway through adaptor protein MAVS and the TLR3 signaling via TRIF. Even before the discovery of the RIG-I pathway it has been shown that the NS3/4A protease is able to diminish the induction of IFN-β by an interaction upstream of IRF3[100]. It was only later revealed with the discovery of MAVS that this adaptor protein is the target cleaved by NS3/4A resulting in abrogated IFN-β induction *in vitro*[101,102,103]. Similarly, it has been shown that also TRIF gets cleaved *in vitro* by NS3/4A (Figure 1.9)[79,104].

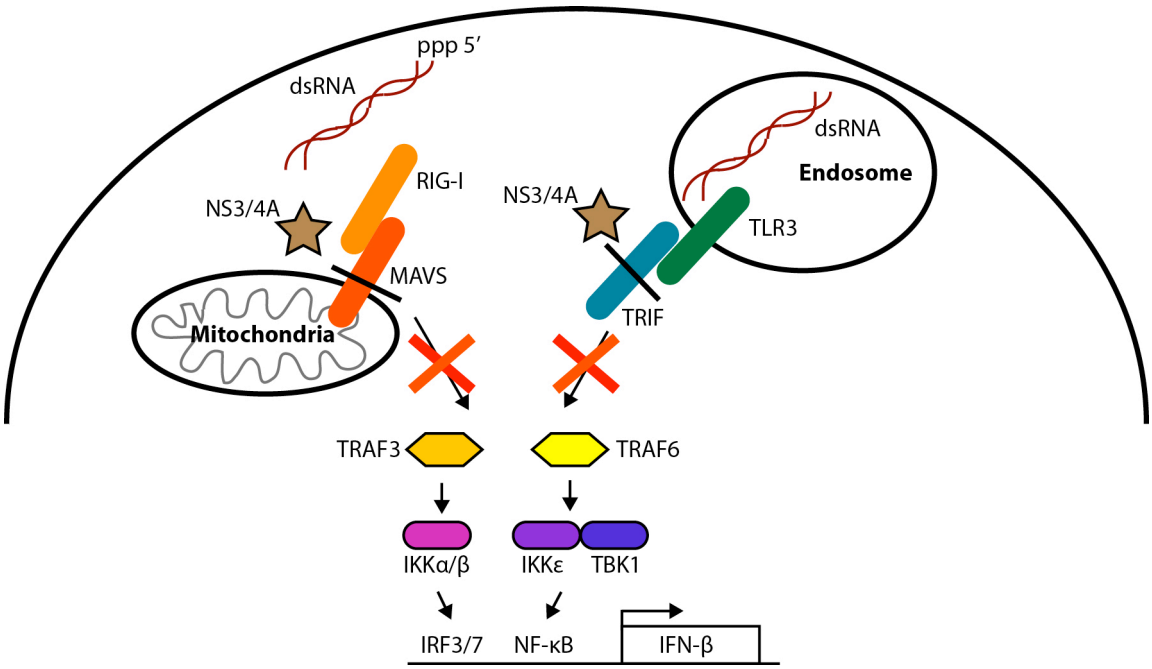

Figure 1.9. *NS3/4A of HCV cleaves MAVS and TRIF, and thus prevents the induction of IFN.*

Jak-STAT pathway. Overexpression of HCV core protein seems to interfere with IFN-signaling downstream of IFNAR, suggested by direct interaction with STAT1 leading to reduced STAT1 phosphorylation[105,106] (Figure 1.10). These findings are contrary to what has been shown when the whole HCV polyprotein is expressed in cells or in mouse liver, where STAT1 phosphorylation and nuclear translocation are not impaired but the binding of STATs to the DNA is abrogated[107,108]. This mechanism has been thoroughly investigated, introducing a model that the ubiquitously expressed protein phosphatase 2A (PP2A) is upregulated in infected hepatocytes probably due to an endoplasmatic reticulum stress response[109,110]. PP2A directly inhibitis the protein arginine methyltransferse 1 (PRMT1), which leads to a hypomethylation of STAT1, and promotes the association with the negative regulator PIAS1[111] (Figure 1.10) - a mechanism which has also been demonstrated in human liver biopsies[109,112].

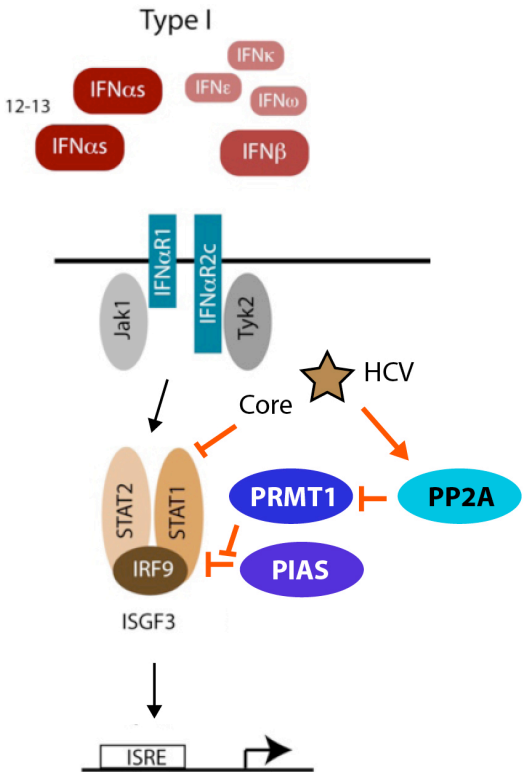

Figure 1.10. *Interference of HCV with the Jak-STAT pathway.*

IFN effector mechanisms. There has also been evidence that HCV proteins interact with IFN-induced effector proteins. Most prominent is dsRNA-activated protein kinase R (PKR), which seems to be bound and antagonized by NS5A[113,114]. PKR regulates cellular translation through dsRNA-stimulated autophosphorylation and subsequent phosphorylation of the translation initiation factor eIF2α, and it has been demonstrated that PKR inhibits the

replication of HCV *in vitro*[115]. Quite on the contrary is the following proposed model that HCV actually phosphorylates PKR which leads to an arrest of ISG translation, therefore favouring HCV replication[116]. However, all this data is derived from cell culture models and has not yet been confirmed in the liver of infected patients.

1.3.2 Host response to acute HCV infection

The study of the acute phase of HCV in human is hindered by rare clinical detection since most infections occur with unspecific symptoms or even asymptomatically. However, studies were conducted with subjects after needle stick injuries, which showed a very rapid increase of HCV viral load to maximal levels within the first 2 to 4 weeks[117]. Serial liver biopsies and blood sampling in artificially infected chimpanzees showed accordingly a very fast rise in viral load in the first 2 weeks followed by a slower rise for another couple of weeks and a concomitant induction of the innate immune system with upregulation of ISGs[118,119, 120]. HCV RNA levels only began to decrease with a significant rise of ALT (alanine-aminotransferase) – a marker of hepatocyte death - that coincided with infiltration of T cells in the liver, which happened approximately 8 to 12 weeks after infection[118,119]. The outcome then varied leading to either chronic infection with a lower steady level of viral load or to spontaneous clearance. Analyses of immunological determinants of spontaneous clearance in chimpanzees as well as humans revealed that only those subjects with a strong and multispecific T cell response were able to eradicate the virus[117,119]. It has to be noted, that all chimpanzees showed a strong hepatic ISG upregulation which however was not associated with any disease outcome[118]. The strong ISG upregulation would also argue against a very important role of MAVS cleavage by NS3/4A at the beginning of infection. However, MAVS cleavage in chimpanzees has not been studied (and neither in acutely infected humans) and it might be that NS3/4A is just not effective in cleaving chimpanzee MAVS. Interestingly, the only IFN that was measurable on the mRNA level during the whole phase of acute infection was IFN-γ which coincided with the T cell response and the rise in ALT[119,118,120]. The IFN responsible for the early induction of ISGs so far has not been identified.

1.3.3 Host response in chronic HCV infection

All studies performing transcriptome analyses from liver biopsy specimens obtained from patients with CHC uniformly observed an induction of the endogenous IFN system with a transcriptional upregulation of ISGs in a subpopulation of the patients[121,89,122]. More strikingly, this preactivation of the IFN system at baseline was very strongly associated with non-response to treatment with pegIFN-α and ribavirin, irrespective of the viral genotype the patient was infected with[89], while patients with a non-preactivated IFN system with ISG expression levels comparable to non-infected livers reached SVR. The phenomenon of an endogenously activated IFN system is restricted to the liver and does not occur for example in PBMCs[89]. While in humans only a part of the patients showed preactivation, all chimpanzees reaching CHC showed an induction of ISGs and consequently did not respond to therapy making the chimpanzee a suboptimal model to study this phenomenon[123,124]. An analysis of expression profiles in paired liver biopsies of 16 patients before and 4h after a single dose of pegIFN-α revealed that responder patients showed a strong induction of ISGs at 4h, while non-responder patients were not able to further increase transcription of ISGs[89]. Very interesting was the fact that the expression levels of >93% of the induced ISGs in the responder patients after 4h were not higher than the baseline expression levels in the non-responders, but obviously they were not able to clear the virus spontaneously. The reasons for non-response without a decrease in viral load in these patients also remain unclear, most likely this is due to a refractory state of the IFN system.

Explanations, why certain patients with CHC induce their IFN system and others do not, are also not truly found so far. A study with a comprehensive analysis of MAVS cleavage and ISG expression in liver biopsies showed a negative correlation between the amount of cleaved MAVS and ISG expression levels, meaning basically, the more successful HCV is in inhibiting antiviral defense the more susceptible it gets to treatment[125]. However, the correlation is not very strong and cannot wholly explain the activation of the endogeneous IFN system. Clearly, further factors that contribute to preactivation have to be identified.

1.3.4 Genetic variations near the IL28B gene

In 2009 four independent genome-wide association studies (GWAS) identified different single nucleotide polymorphisms (SNPs) near the IL28B gene to be highly associated with

treatment outcome to pegIFN-α and ribavirin[126,127,128,129]. These findings had a tremendous impact in the field. Not only was it the first genetic host marker to be linked to treatment response, but it also could explain to a big part the racial differences in response rates[126]. Due to different analysis platforms and different study populations different marker SNPs were identified to be most significant (Table 1.2). Homozygous carriers of the respective major (good-response) allele had a 2-fold higher chance to achieve SVR than carriers of the minor (bad-response) allele, and the effect of the minor allele seemed to be dominant, since heterozygous carriers had response rates similar to homozygous minor allele carriers. Interestingly, not only treatment response but also spontaneous clearance was associated with the IL28B genotype with an odds ratio between 2.3 and 3.1[129,130].

Table 1.2 *Strongest SNPs identified in 4 genome-wide association studies.*

GWAS	**Region**	**SNP (*P* value)**
Ge et al., [126]	North America	rs12979860 (1.21×10^{-28})
Tanaka et al., [127]	Japan	rs8099917 (3.11×10^{-15})
Suppiah et al., [128]	Australia, Northern Europe	rs8099917 (9.25×10^{-9})
Rauch et al., [129]	Switzerland	rs8099917 (5.47×10^{-8})

However, the causal variant has so far not been identified. GWAS merely narrow down an area where the functional variant may be localized. But neither direct sequencing of the region nor recombinant mapping were able to identify a causal variant due to the high linkage disequilibrium in the IL28B region[126,129]. The two strongest SNPs are localized 3 and 8 kilobases (kb) upstream of the IL28B gene, hinting at a possible influence in gene expression. First results of gene expression analyzed in PBMCs of these patients were contradictory. Two groups found lower IL28A/B gene expression, while the third group didn't find any differences[126,127,128]. These results were obtained in only a minor part of the study population though, and due to the high sequence similarity expression of IL28B and IL28A was not differentiated. Since the causal variant has not been identified, it is impossible to delineate how the polymorphisms influence treatment response and spontaneous clearance, whether it is through functional changes of the cytokine or differences in expression. However, since IL28B encodes for an IFN, IL28B polymorphisms would be a likely contributing factor to explain the preactivation of the IFN system in this subgroup of CHC patients, who through mechanisms that remain to be elucidated fail to therapy.

2. Aims of the PhD-thesis

The lack of proper *in vivo* models for HCV infection (besides chimpanzees) and the longstanding expertise of the Hepatology Laboratory to obtain valuable patient liver biopsy specimens for research purposes made it an obvious choice to study directly HCV-infected liver biopses for a better understanding of HCV-host interactions. Three main questions in the context of virus-host interactions and treatment response upon IFN-α in HCV infection were addressed:

1. In acute HCV infection more than 90% of the patients achieve an SVR with pegIFN-α monotherapy, while in CHC with a combination therapy of pegIFN-α/ribavirin SVR rates are in the range of only 50%. Reasons for this discrepancy are unknown. While the host reaction in the liver of CHC patients has been studied and an association of ISG induction and non-response to treatment has been established, none of this has so far been analyzed in the liver of patients with AHC. We therefore wanted to assess the host reaction upon AHC infection and to elucidate molecular mechanisms that might explain the discrepancies in response to IFN.

2. Genetic variants near the IL28B gene were the first genetic host factor discovered to be highly associated with treatment response. The fact that IL28B encodes for IFN-λ3, which is able to induce ISGs, which overexpressed has been shown to be strongly associated with non-response to treatment led us to the hypothesis that these genetic variants might be the driver of ISG induction in non-responder patients through upregulation of IFN- λ3. The aim was to address this hypothesis in a collection of CHC liver biopsies and also to assess all existing pre-treatment predictors to create a classifier that could be useful for prediction of treatment response in a clinical setting.

3. pegIFN-α is an essential therapeutic in HCV treatment regimens. It has replaced IFN-α due to higher efficacy, and it has been postulated that the reason is the superior half-life of pegIFN-α that leads to a strong and continuous induction of ISGs. However, *in vitro* and mouse studies suggest refractoriness to continuous IFN-α application. Thus, it was the aim to study for the first time the pharmacodynamics of pegIFN-α in the human liver.

3. Material and Methods

The materials and methods of the results of section 4.1 and 4.2 are described in the respective parts of the incorporated articles: Dill M.T. et al., Interferon gamma stimulated gene expression and lack of USP18 induction in the liver of patients with acute hepatitis C (submitted), and Dill M.T. et al., Interferon-Induced Gene Expression Is a Stronger Predictor of Treatment Response than IL28B Genotype in Patients with Hepatitis C, Gastroenterology. 2011 Mar;140(3):1021-1031.

The following material and methods refer to the results in section 4.3:

Patients. From November 2005 to April 2010, patients with CHC that were referred to the Hepatology Outpatient Clinic of the University Hospital Basel and gave written informed consent to use part of the diagnostic biopsy (B-1) for research purposes and were planned to receive treatment, were screened for hepatic ISG expression. Only patients with low ISG expression were asked to participate in the study which included a second paired biopsy (B-2) at a given time point in the first week after the first injection with pegIFN-α. 3 patients were included for the following time points: 16h, 48h, 96h, and 144h, and additionally data of 6 patients from a previous study biopsied at 4h (no. 1, 2, 6, 7, 8, 9) were included in the analysis[89]. The data reported in that previous paper have been deposited in the Gene Expression Omnibus (GEO) database, www.ncbi.nlm.nih.gov/geo (accession no. GSE11190). All patients received 1.5 μg/kg body weight pegIFN-α-2b (Essex Chemie, Switzerland). Weight-adjusted ribavirin treatment was initiated only after the second biopsy to avoid confounding effects. An additional 3 patients that were treated with pegIFN-α-2a (Roche, Switzerland) were included for the 144h time point. Blood for serum analysis was also taken. All patients gave written informed consent to the study, which was approved by the Ethics Committee of Basel. Serum HCV RNA was quantified using the COBAS AmpliPrep/COBAS Taqman HCV-Test and the Cobas Amplicor Monitor from Roche Molecular Systems.

Measurement of serum IFN-α.

Serum was collected before the first injection with pegIFN-α and at the time of the second biopsy. Serum levels of IFN-α-2b and peg-IFN-α-2a was measured with an enzyme-linked immunosorbent assay (ELISA) kit (Verikine #41100, PBL Interferonsource, Piscataway, NJ). Standard curves were prepared separately for peg-IFN-α-2a and -2b by a serial dilution

starting from 12.5 pg/ml in the sample diluent. The serum samples were diluted 10 times in sample diluent. Samples with concentration below 12.5 pg/ml were considered below the lower limit of detection.

RNA extraction and microarray hybridization. Total RNA was extracted from human liver tissue using Qiazol reagent and RNeasy Mini Kit (Qiagen) according to the manufacturer's instruction. Gene expression was assessed by microarray analysis using Affymetrix Human Genome U133 Plus 2.0 arrays (3' IVT array). 1 μg of total RNA from each sample was reverse transcribed using Genechip 3'IVT Express Kit (Affymetrix) according to the manufacturer's instructions. The Hybridization and Wash Kit (Affymetrix) was used to hybridize the samples.

Statistical analysis. Microarray analysis was performed with Bioconductor packages of R statistical environment[131]. Data were preprocessed using standard RMA algorithm. Batch effects observed between the human liver samples processed and hybridized at different times were corrected using the ComBat algorithm[132]. Probe sets with very low expression intensities (below 80 in the highest-expressing sample) as well as the control probe sets were excluded from the subsequent analyses. For the gene cluster analysis genes with fold change between B1 and B2 >2 up- or downregulated in 2/3 of the patients of the respective time point were included and normalized prior to the analysis. An infinite Gaussian mixture model with a Dirichlet process prior was used[133]. This non-parametric model suggests a growing number of Gaussians to describe the gene expressions. The model is fully probabilistic in nature, which means that on output samples from a distribution over partitions are given. By the special choice of a Dirichlet process prior, the number of clusters need not to be fixed in advance, but is inferred from the data. The results were tested for robustness by moderately changing the hyperparameters that control the Dirichlet process.
Additional statistical analyses were carried out using GraphPad Prism software version 4.0.

IL28B SNP genotyping. Genotyping for the rs12979860 SNP was performed with TaqMan SNP genotyping assays (Applied Biosystems Inc, Foster City, CA). TaqMan probes and primers were designed and synthesized by Applied Biosystems: forward 5'-TGTACT-GAACCAGGGAGCTC-3', reverse 5'-GCGCGGAGTGCAAT- TCAAC-3'; Vic probe 5'-TGGTTCGCGCCTTC-3', Fam probe 5'-CTGGTTCACGCCTTC-3'. Automated allele

calling was performed using SDS software from Applied Biosystems. Positive and negative controls were used in each genotyping assay.

Western blot. Whole cell extracts were obtained by homogenizing a 5mm cylinder of the liver biopsy lysis buffer (50mmol/L Tris pH8, 280mmol/L NaCl, 0.5% NP40, 0.2mmol/L EDTA, 2mmol/L EGTA, 10% glycerol, 100mol/L NaVO4, 1mmol/L PMSF, and protease inhibitors), incubating for 30 minutes on ice with regular vortexing, and centrifugation at 14,000g for 15 minutes. 10μg of total protein from human liver lysates was loaded for SDS/PAGE and transferred onto a nitrocellulose membrane (Schleicher & Schuell, Switzerland). The membranes were blocked in 3% BSA/milk (1:1) for 1h, washed with Tris-buffered saline Tween-20 (TBST), and then incubated with primary antibodies specific to tyrosine-phosphorylated STAT1 (PY701-STAT1; # 9171; Cell Signalling), STAT1 (C-terminus; 610186; BD Transduction Laboratories, BD Biosciences), USP18 (#4813; Cell Signalling) all 1:1000, and β -Actin (A5441; Sigma) 1:2000 in Tris-buffered saline Tween-20 (TBST) overnight at 4°C. After 3 washes with TBST, membranes were incubated with fluorescent secondary goat anti-mouse (IRDye 680) or anti-rabbit (IRDye 800) antibodies (both LI-COR Biosciences) for 1h at room temperature. Blots were scanned by Odyssey Infrared Imaging System (LI-COR). Quantification of the bands was done with ImageJ software.

4. Results

4.1 Interferon gamma stimulated gene expression and lack of USP18 induction in the liver of patients with acute hepatitis C

Dill M.T., Makowska Z., Duong F.H.T., Merkofer F., Filipowicz M., Baumert T.F., Tornillo L., Terracciano L., Heim M.H., Interferon gamma stimulated gene expression and lack of USP18 induction in the liver of patients with acute hepatitis C. (submitted manuscript)

Interferon gamma stimulated gene expression and lack of *USP18* induction in the liver of patients with acute hepatitis C

Michael T. Dill,[1,2] * Zuzanna Makowska,[1] * Francois H.T. Duong,[1] Franzisca Merkofer,[1] Magdalena Filipowicz,[1] Thomas F. Baumert,[4] Luigi Tornillo,[3] Luigi Terracciano,[3] and Markus H. Heim[1,2]

[1] Department of Biomedicine, Hepatology Laboratory, University of Basel, Basel, Switzerland

[2] Division of Gastroenterology and Hepatology, University Hospital Basel, Basel, Switzerland

[3] Institute of Pathology, University Hospital Basel, Basel, Switzerland

[4] Inserm, U748, University of Strasbourg, Strasbourg, France

* These authors contributed equally to this work.

Corresponding author:
Prof. Markus H. Heim
University of Basel
Department of Biomedicine, Zentrum für Lehre und Forschung
Hebelstrasse 20, 4031 Basel, Switzerland
tel. +41 61 265 33 62
fax. +41 61 265 38 47
email: markus.heim@unibas.ch

Short title: Hepatic gene expression in acute hepatitis C

Grant Support:

This work was supported by Swiss National Science Foundation (SNF) grant 320030_130243 to M.H.H. and SNF grant 323500-123714 to M.T.D.

Abbreviations:

AHC, acute hepatitis C; CHC, chronic hepatitis C; CHC-NR, CHC-non-responder; CHC-R, CHC-responder; GSEA, gene set enrichment analysis; HCV, hepatitis C virus; ISG, interferon stimulated gene; ES, enrichment score; PHH, primary human hepatocytes; pSTAT1, phosphorylated STAT1.

Disclosures:

The authors have no conflicting financial interests.

Acknowledgments:

We thank the patients who participated in this study. We are grateful to Tanja Uhle for excellent technical assistance with immunohistochemistry, Philippe Demougin (Life Sciences Training Facility, Pharmazentrum, Basel) for providing technical help with the processing of microarrays and Sarah Durand and Cathy Royer (Inserm U748) for isolation and culture of primary human hepatocytes.

Author contributions:

M.H.H. inititated and coordinated the study. M.T.D. and M.F. recruited patients and collected samples. M.T.D., Z.M. and F.H.T. performed the experiments. T.F.B. coordinated experiments performed in primary human hepatocytes. M.T.D., Z.M., F.M., L.T., L.T. and M.H.H analyzed the data. M.T.D., Z.M. and M.H.H. wrote the manuscript. All authors read and contributed to the manuscript.

Word count:

Title: 119 chars Abstract: 241 words Manuscript: 6153 words

Abstract

BACKGROUND & AIMS: Therapy of chronic hepatitis C (CHC) with pegylated interferon-α (pegIFN-α) and ribavirin achieves a sustained virological response (SVR) in approximately half of the patients. Non-response to treatment is associated with constitutively increased expression of IFN stimulated genes (ISGs) in the liver already before therapy. In acute hepatitis C (AHC), therapy is much more effective, with SVR rates > 90%. The aims of this study were to elucidate mechanisms responsible for the different treatment response rates between CHC and AHC.

METHODS: We analyzed IFN signaling and ISG expression in liver biopsies of patients with AHC, CHC and controls by microarray, immunohistochemical and protein analysis. By stimulating primary human hepatocytes with IFN-α or IFN-γ reference gene sets were created for gene set enrichment analysis.

RESULTS: Hundreds of genes, many of them IFN-γ stimulated genes, were differentially regulated in AHC compared to controls. There was only a limited overlap with the set of mostly IFN-α responsive genes dysregulated in patients with CHC. Expression analysis of negative regulators of IFN-α signaling showed no differences of SOCS1 or SOCS3 expression between AHC and CHC. However, USP18, another important negative regulator of IFN-α signaling, was strongly induced in CHC non-responders, but not in AHC.

CONCLUSIONS: The results provide an explanation for the preserved response to pegIFN-α in AHC despite strong ISG induction and identify USP18 as a therapeutic target for improving IFN-α responsiveness in CHC.

Key words: Hepatitis C virus; Jak-STAT signaling; host-virus interaction

Introduction

Chronic infection with hepatitis C virus (HCV) is a major cause of liver disease worldwide [1]. For the last decade, a combination of pegylated interferon α (pegIFN-α) with ribavirin was the standard therapy for chronic hepatitis C (CHC). This treatment achieves an overall sustained virological response (SVR) in ~55% of patients [2]. Recently, two HCV protease inhibitors used in conjunction with pegIFN-α and ribavirin have been approved for the treatment of CHC, and triple combination therapies will most likely be the standard of care for a majority of patients in developed countries [3]. However, non-response to pegIFN-α remains an important problem in the setting of triple therapy, because it significantly increases the rate of viral breakthrough during therapy caused by the emergence of HCV variants resistant to protease inhibitors [4, 5]. It has been well documented that non-response to pegIFN-α is associated with persistent induction of IFN stimulated genes (ISGs) in the liver [6-8]. The very same set of hundreds of ISGs is induced by therapeutically applied pegIFN-α in patients without pretreatment activation of ISGs who have a good response to treatment [7]. Paradoxically, activation of the endogenous IFN system not only is ineffective in clearing the infection, but also impedes response to pegIFN-α therapy, possibly because of refractoriness of the IFN-α signal transduction pathway. We have previously shown that IFN-α signaling in the mouse liver becomes unresponsive within hours after the injection of IFN-α and have identified USP18 as a key mediator of refractoriness [9].

Contrary to patients with CHC, most patients with acute hepatitis C (AHC) respond very well to monotherapy with (peg)IFN-α [10, 11]. The reasons for the discrepant response to pegIFN-α are unknown. Given the association of intrahepatic ISG expression and non-response to pegIFN-α in CHC, an obvious explanation for the good response to therapy in AHC could be a lack of ISG induction in AHC. The intrahepatic immune response has not been studied in patients with AHC, but serial liver biopsies in chimpanzees obtained during the first 6-8 months after infection with HCV have revealed a strong induction of ISGs [12-14]. In the present study, we analyzed inflammatory infiltrates, the activation of IFN signal transduction pathways and gene expression profiles in liver biopsies of 6 patients with AHC.

Materials and Methods

Patients.

All patients were recruited in the Hepatology Outpatient Clinic of the University Hospital Basel, Switzerland. From October 2007 to December 2010, 6 patients with AHC (between 0-6 months after the HCV transmission) gave written informed consent to participate in this study and donated a liver biopsy specimen for research purposes. The study was approved by the Ethics Committee of Basel.

Liver biopsies from 16 patients with CHC and 4 normal liver tissue samples were used for comparative analysis. These samples have been obtained during a previous study that has been published [7]. The data reported in that paper have been deposited in the Gene Expression Omnibus (GEO) database, www.ncbi.nlm.nih.gov/geo (accession no. GSE11190). Additional 16 liver biopsies of patients with CHC were used for immunohistochemical analyses. All patients with CHC were treated with pegIFN-α and ribavirin, the standard of care during the study period. Patients with a sustained virological response defined as undetectable HCV-RNA 6 months after the end of treatment were classified as responders (R), all others as non-responders (NR). Serum HCV RNA was quantified using the COBAS AmpliPrep/COBAS Taqman HCV-Test and the Cobas Amplicor Monitor from Roche Molecular Systems. AHC patients were closely monitored for transaminases and HCV-PCR and if there was no decline of the viral load below the limit of detection within a month after the first visit, they were treated with 1.5µg/kg body weight pegIFN-α-2b (PegIntron, Essex Chemie, Switzerland) monotherapy for 24 weeks, unless indicated otherwise (Table 4.1.1).

Isolation and treatment of primary human hepatocytes.

PHH were isolated from liver resections obtained from non-infected patients at described previously [15]. Freshly isolated PHH were seeded on 6-well-plates precoated with collagen (BD Biosciences) and maintained in culture in William's E medium (Sigma) supplemented with 1% Glutamax (Gibco), 1% insulin transferrin selenium (Gibco), 10-7 M dexamethasone (Sigma), 0.15% BSA (Sigma), and 10% FBS (PAN Biotec). PHH were treated with 1000U/mL of human IFN-α (Roferon, Roche) or human IFN-γ (BioLegend) for 6h and 24h.

RNA extraction and microarray hybridization.

Total RNA was extracted from human liver tissue and PHH using Qiazol reagent and RNeasy Mini Kit (Qiagen) according to the manufacturer's instruction. Gene expression was assessed by microarray analysis using Affymetrix Human Genome U133 Plus 2.0 arrays (3' IVT array) for human liver specimens and Affymetrix Human Gene 1.0 ST arrays (whole-transcript array) for PHH. For the 3' IVT arrays, 1 μg of total RNA from each sample was reverse transcribed using Genechip 3'IVT Express Kit (Affymetrix) according to the manufacturer's instructions. For the whole-transcript arrays, 500 ng of total RNA was reverse transcribed and biotinylated with the whole-transcript Expression Kit (Ambion) and whole-transcript Terminal Labeling Kit (Affymetrix) according to the manufacturer's instructions. The Hybridization and Wash Kit (Affymetrix) was used to hybridize all samples. All original array data are being deposited at the National Center for Biotechnology Information Gene Expression Omnibus database.

Statistical analysis.

Microarray analysis was performed with Bioconductor packages of R statistical environment [16]. Data were preprocessed using standard RMA algorithm. Batch effects observed between the human liver samples processed and hybridized at different times were corrected using the ComBat algorithm [17]. Probe sets with very low expression intensities (below 80 in the highest-expressing sample) as well as the control probe sets were excluded from the subsequent analyses. Genome-wide hierarchical clustering of the human liver samples was carried out using Ward's linkage method, with 1 – Pearson correlation as a distance metric. Differential gene expression for AHC, CHC-R and CHC-NR versus control samples was assessed using *limma* package [18], with fold change cutoff of 2 and false discovery rate (FDR) cutoff of 0.05. To calculate the FDR, moderated t-statistics were first generated using the empirical Bayes method, as implemented in the *limma* package, and the obtained p-values were corrected for multiple testing using Benjamini and Hochberg adjustment [19]. Enrichment of Gene Ontology Biological Process terms was performed using the list of genes significantly upregulated in AHC patients with respect to CTRL patients. Significance estimation of the enrichment analysis was carried out using a hypergeometric test as implemented in g:Profiler software. Terms with p-values below 10^{-6} were clustered into distinct groups based on the GO hierarchy. The enrichment scores were calculated for each cluster (–log10 of the geometric mean of the p-values for all categories in a cluster).

Area-proportional Venn diagrams were created with the help of BioVenn software [20].

Two gene sets for Gene Set Enrichment Analysis (GSEA) [21] were obtained as follows (Supplementary Figure 4.1.3A): (i) 2 initial probe set lists were derived from the PHH expression dataset based on upregulation in IFN-α or IFN-γ treated samples compared to untreated samples (fold change between the means of treated and untreated samples above 2 at least at one timepoint); (ii) within the 2 lists we selected probe sets for which at least at one time point there was more than a 2-fold difference between the means of α- and γ-IFN-treated samples, with the p-value from a Welch t-test between the corresponding samples below 0.05. These two lists were then annotated with gene symbols and their enrichment was assessed in AHC versus CHC-NR samples with javaGSEA software version 2.07 (Broad Institute), using signal-to-noise ratio as a ranking metric. On the GSEA plot, the *x* axis represents a list of all genes on the array rank-ordered according to their decreasing correlation with AHC phenotype (red: genes overexpressed in AHC, blue: genes overexpressed in CHC-NR). Black ticks along the *x* axis show positions of genes which are part of the tested gene set. The *y* axis unit is the enrichment score defined as a running-sum statistic calculated walking down the ranked gene list. The running-sum increases when a gene in the ordered list is present in the gene set in question and decreases when it is absent. The increment of the enrichment score depends on the value of the ranking metric.

Enrichment of KEGG pathways and Gene Ontology Biological Process terms in lists of genes significantly altered between AHC and CHC-NR was assessed using DAVID software version 6.7. To facilitate the interpretation, terms with p-values (modified Fisher exact test) below 0.05 were grouped based on the overlapping gene membership. The enrichment score is equal to –log10 of the geometric mean of the p-values for all categories in a cluster. Statistical analyses of real-time RT-PCR and immunohistochemical data were carried out using GraphPad Prism software version 4.0.

IL28B genotyping.

Extraction of DNA and genotyping for the single nucleotide polymporphism rs12979860 near the *IL28B* gene was performed as described previously [22].

Real-time RT-PCR.

RNA was reverse transcribed by Moloney murine leukemia virus reverse transcriptase (Promega Biosciences, Wallisellen, Switzerland) in the presence of random primers (Promega) and deoxynucleoside triphosphates. The reaction mixture was incubated for 5 min at 70°C and then for 1 h at 37°C. The reaction was stopped by heating at 95°C for 5 min. For

the measurement of IFNα and IFNβ genes containing only one exon, the same amount of RNA was also mock reverse transcribed to control for genomic DNA contamination. SYBR-realtime-PCR was performed using SYBR green (Applied Biosystems, Foster City, CA). The intron-spanning primers are listed in Supplementary Table VII. IFNα primers were designed to detect all 13 IFNα genes. All reactions were run in duplicate with an ABI 7500 Real-Time PCR System (Applied Biosystems). mRNA expression levels of the transcripts were normalized to *GAPDH* using the ΔCt method.

Western Blot.

Whole cell extracts and blotting of human liver samples were performed as described [7]. The membranes were incubated with primary antibodies (listed in Supplementary Table VIII) in Tris-buffered saline Tween-20 (TBST) overnight at 4°C. After 3 washes with TBST, membranes were incubated with fluorescent secondary goat anti-mouse (IRDye 680) or anti-rabbit (IRDye 800) antibodies (both LI-COR Biosciences) for 1h at room temperature. Blots were scanned by Odyssey Infrared Imaging System (LI-COR). For MAVS the membrane was incubated with HRP-conjugated goat anti-mouse antibody (Pierce) and developed on Biomax MR films (Kodak).

Immunohistochemistry.

4 µm-thick serial sections were cut from formalin-fixed, paraffin-embedded liver biopsy specimens, rehydrated, pretreated for 20 minutes in ER2 solution, incubated with the respective primary antibody and counterstained with haematoxilin. Standard indirect immunoperoxidase procedures were used for immunohistochemistry (ABC-Elite, Vectra Laboratories). The staining procedure was performed with an automated stainer (Bond, Vision BioSystems, UK). The primary antibodies are listed in Supplementary Table VIII.

For the co-localization analysis each section was photographed at 50x magnification with a 11.7 megapixel Axio Zeiss camera (picture size: 3900 x 3000 pixels) choosing the same area of the biopsy. 5 random high power fields (HPF, 279 x 252 pixels) were chosen within the parenchyma of the biopsy of the first section (Supplementary Figure 4.1.4). Then identical HPFs of the other sections were defined, all HPFs enlarged digitally and the amount of positive hepatocytes or immune cells were counted by two independent observers (MTD, FM) (Supplementary Table VI). To ensure the quality of the count on the digitally enlarged HPFs the corresponding HPFs were also counted by microscopic assessment. For the digital processing Adobe Photoshop and Illustrator version 5 were used.

Results

Host-virus interactions during acute hepatitis C induce a distinct pattern of gene expression in the liver.

Six patients with HCV monoinfection underwent a liver biopsy 2-5 months after HCV transmission, i.e. during the acute phase of HCV infection (Table 4.1.1). Gene expression in these liver biopsies was analyzed with Affymetrix U133 Plus 2.0 arrays and compared to 4 samples from patients without liver disease (controls) and 16 samples from patients with CHC recruited in a previous study [7]. We found between 203 and 492 genes (average 312) upregulated and 239 to 374 genes (average 294) downregulated more than 2-fold in the liver of patients with AHC compared to the healthy controls (Figure 4.1.1A). The extent of up- or downregulation was not associated with response to treatment, spontaneous clearance, estimated time from infection to biopsy, serum viral load or IL28B genotype (data not shown). Transcriptome profiles of AHC liver samples were highly homogenous: between 50 and 80% of genes altered in a particular patient were also changed in at least two other AHC patients (Figure 4.1.1A). Genes upregulated in AHC patients compared to healthy liver included chemokines and their receptors, ISGs, and genes involved in cellular immune responses (Figure 4.1.1B and Supplementary Table I). Many of the downregulated genes are involved in intermediate metabolism and lipid homeostasis (Supplementary Table II).

A comparable number of genes were dysregulated in the group of CHC patients who were non-responders to pegIFN-α (CHC-NR), but intersecting the sets of differentially regulated genes showed only a limited overlap between CHC and AHC patients, with 147 genes upregulated and 138 genes downregulated specifically in AHC (Figure 4.1.1B). Genome-wide unsupervised clustering of the healthy liver, CHC and AHC samples (Supplementary Figure 4.1.1) showed that AHC samples form a well-defined, separate cluster, further demonstrating the specific molecular signature of this group of patients.

Activation of Jak-STAT signaling and ISG induction in AHC.

As outlined above, functional annotation of the genes dysregulated in AHC identified several classical ISGs (Supplementary Table I). To investigate more rigorously to what extent ISGs were induced in AHC, we made use of a list of *bona fide* hepatic ISGs. This list was compiled

in a previous study where we obtained paired biopsies before and 4 hours after the first injection of pegIFN-α in 10 selected patients with CHC, who didn't show induction of ISGs before treatment and responded well to pegIFN-α [7]. It contains 167 genes (242 probe sets) significantly (paired t test, $P < 0.05$) changed >2-fold by pegIFN-α (157 upregulated, 10 downregulated). Of the 167, 125 were detected above the minimal expression cutoff in our dataset. Unexpectedly, only 30 of these 125 IFN-α-regulated genes were regulated > 2-fold in AHC. This low number of induced ISGs could be explained by a relatively weak activation of IFN signaling pathways in AHC. However, when we analyzed phoshorylation and nuclear translocation of STAT1 in the AHC samples, we found a strong activation of this central mediator of the IFN signaling pathway (Figure 4.1.2A-C). Alternatively, the absence of a broad induction of pegIFN-α induced genes in AHC could be explained by the activation of STAT1 by IFN-γ, another strong inducer of STAT1 phosphorylation [23] that has been implicated in the immune response during AHC in chimpanzees and human [24, 25]. We therefore measured the mRNA expression levels of IFN-γ, and found them indeed significantly upregulated in AHC biopsies compared to CHC (Figure 4.1.2D). IFN-γ induced signaling typically leads to pSTAT1 homodimers, while type I IFN signaling phosphorylates STAT1 and STAT2 that create heterodimers. We therefore hypothesized that in AHC we should observe exclusively STAT1 phosphorylation while CHC-NR should also show STAT2 phospohorylation signals. However, while AHC indeed only showed pSTAT1 we were not able to detect a pSTAT2 signal in the CHC-NR, which was only weakly detectable in liver biopsy samples from responder patients after 4h exposure to pegIFN-α (Figure 4.1.2E). But despite similar pSTAT1 levels in AHC and those liver samples under pegIFN-α treatment, pSTAT2 was limited to the latter. We therefore conclude that in AHC, STAT1 activation is caused by IFN-γ and not by IFN-α/β.

IFN-γ-specific gene signature is enriched in the AHC gene expression profiles, while IFN-α-induced transcription patterns characterize CHC-NR patients.

To further study the pattern of ISG induction in AHC and CHC-NR we generated IFN-α and IFN-γ-induced gene lists and compared them to the ISG expression in the biopsies. Because ISG expression differs considerably between different cells and tissues, we did not use published ISG lists obtained in non-hepatic cells, but stimulated primary human hepatocytes (PHH) from 2 donors with 1000 IU/ml of human α- and γ-IFN for 6 and 24 hours and performed microarray analysis (Figure 4.1.3A). There were 256 genes upregulated more than

2-fold in the PHH from both donors after IFN-α stimulation, with the majority of the genes induced already after 6 hours of treatment. IFN-γ induced a comparable number of genes (288), but with different kinetics. The majority of the IFN-γ induced genes were detected after 24 hours of treatment. Treatment of PHH with IFN-α led to a very broad gene downregulation: transcript levels of 850 genes were reduced more than 2-fold in PHH from both donors. Interestingly, the observed suppression was very transient and only 15 genes were found downregulated after 24 hours of IFN-α exposure. Gene downregulation after IFN-γ treatment involved 123 genes, with a slightly larger number of genes found suppressed after 24 hours of treatment (77) compared to 6 hours (60) and a limited overlap between the two time points (14).

Comparison of the gene sets induced by IFN-α or IFN-γ identified 149 common genes, but also similar number of genes specifically induced by either IFN-α or IFN-γ (Figure 4.1.3A and Supplementary Tables III and IV). This allowed us to generate two gene lists representative of IFN-α or IFN-γ stimulated genes (see Materials and Methods section and Supplementary Figure 4.1.2). These gene sets were then used to assess the enrichment of specific IFN-α and IFN-γ signatures in liver biopsies of AHC and CHC-NR patients using the gene set enrichment analysis (GSEA) algorithm [21] (Figure 4.1.3B and Supplementary Table V). We observed a significant enrichment of IFN-γ-regulated genes in AHC compared to CHC-NR (ES=0.52, p-value=0.04). On the other hand, the genes upregulated in PHH by IFN-α were enriched in CHC-NR samples (ES=-0.83, p-value<0.001). Selecting *IFI27* and *IFIT1* as IFN-α specific ISGs as well as *GBP5* and *HLA-DMB* for IFN-γ specificity we were able to confirm the data obtained from the microarrays in the PHH and the liver biopsies by quantitative RT-PCR (Supplementary Figure 4.1.4). These results disclose a predominant role of IFN-γ in driving the ISG transcription in the acute phase of HCV infection, whereas ISG expression in pre-activated patients in the chronic phase shows a type I IFN-specific pattern.

CD8+ T cells co-localize with pSTAT1 positive hepatocytes in AHC.

To investigate the source of IFN production in the infected liver, serial sections from AHC and CHC liver biopsy specimens were stained for phosphorylated STAT1 (pSTAT1) and markers for T cells (CD3, CD8), for B cells (CD20), for NK cells (CD56) and for plasmacytoid dendritic cells (CD123) (Supplementary Figure 3 and Supplementary Table VI). In general, the liver parenchyma of AHC showed more inflammatory infiltrates than CHC

and most of these cells were positive for CD3 (Figure 4.1.4B). Co-localization analysis revealed that in AHC areas with high amounts of pSTAT1 positive hepatic nuclei were associated with high numbers of CD3+ and CD8+ cells, but not with CD20+, CD56+ or CD123+ cells (Figure 4.1.4A). We did not observe a co-localization of any of these cell types with pSTAT1-positive hepatocytes in CHC-NR samples (Figure 4.1.4A). There was a statistically significant correlation of STAT1 phosphorylation with the amount of CD3+ cells (Spearman $r = 0.70$, $P < 0.0001$) and CD8+ cells in AHC (Spearman $r = 0.69$, $P < 0.0001$, Figure 4.1.4C). Additionally, we detected a positive correlation of CD8+ cells and IFN-γ mRNA levels in AHC that due to the low sample size slightly missed statistical significance (Figure 4.1.4D). Enrichment analysis of Gene Ontology terms and KEGG pathways revealed a significant overrepresentation of categories related to T-cell activation in the AHC compared to CHC-NR patients (Supplementary Figure 4.1.2B). Taken together, these data provide evidence that infiltrates of CD8+ T cells in the liver of patients with AHC are responsible for IFN-γ production and induction of the Jak-STAT signaling pathway.

***USP18* expression correlates with treatment response to pegIFN-α.**

Non-response to treatment with pegIFN-α and ribavirin in CHC is associated with a general upregulation of ISGs in the liver, but the molecular mechanism linking ISG induction to IFN non-response remains unknown [6-8]. In the present study, we found a similar extent of ISG upregulation in AHC samples, but most of the patients either cleared HCV spontaneously or responded to therapy (Figure 4.1.1 and Table 4.1.I). We therefore hypothesized that the IFN-α driven ISG set in CHC included specific genes that are not upregulated by IFN-γ in AHC. Because negative feed-back inhibition of Jak-STAT signaling pathways could underlie treatment non-response [9, 26], we analyzed the expression of pathway inhibitors in AHC and CHC liver biopsy samples. *SOCS1* and *SOCS3*, two IFN-induced negative regulators of IFN signaling, showed no difference between AHC and CHC (data not shown). However, *USP18*, a more recently discovered negative regulator that is instrumental for the refractory state of IFN signaling in the mouse liver [9, 27], was significantly upregulated in CHC-NR patients compared to CHC-R and AHC (Figure 4.1.5A). To investigate if the differential induction of *USP18* in CHC-NR versus AHC results from its preferential activation by IFN-α, we analyzed *USP18* induction in PHH stimulated by either IFN subtype. Indeed, *USP18* was almost exclusively induced by IFN-α (Figure 4.1.5B). This preferential induction of USP18 in CHC-NR was also apparent on the protein level (Figure 4.1.5C-D).

Discussion

The study of the acute phase of HCV in human is hampered by the fact that most infections are asymptomatic. Spontaneous clearance occurs in about 20-30% of patients [28]. Studies of subjects after needle stick injuries revealed a very rapid increase of HCV viral load to maximal levels within the first 2-4 weeks [25]. Viral replication is then slowed down, most likely by an innate immune response involving the induction of ISGs in the liver [14, 24]. HCV specific T cells are detectable 5-9 weeks after infection, accompanied by a rise in alanine aminotransferase (ALT) levels and a decline of the serum viral load [25]. Liver biopsy studies in chimpanzees documented the presence of HCV-specific CD8+ T cells and an increase in intrahepatic IFN-γ mRNA during this period of viral decline [14, 24]. In the present study, we analyzed human liver biopsies obtained 2-5 months after HCV infection, i.e. during the early phase of the adaptive immune response. In accordance with the chimpanzee studies, we found CD8+ T- cell infiltrates, increased intrahepatic IFN-γ mRNA expression, and ALT elevation. Importantly, T cell infiltrates were co-localized with hepatocytes positive for nuclear pSTAT1 immunostaining, providing evidence that the predominant mediator of STAT1 activation is IFN-γ that is secreted by infiltrating T cells which are in close contact to stimulated hepatocytes. The microarray analysis of ISG expression revealed a strong enrichment of IFN-γ specific ISGs in AHC liver biopsy samples, further confirming that the predominant IFN in this phase of HCV infection is IFN-γ and not IFN-α. These results do not support the hypothesis that liver infiltrating HCV-specific T cells are stunned, with impaired IFN-γ production, and are therefore not capable to clear the infection [25, 29, 30]. Our results are more consistent with a model where recruitment of T cells, IFN-γ secretion by T cells and IFN-signaling in hepatocytes is intact, but the induction of hundreds of ISGs is little effective, either because of a block of translation of ISG mRNAs [31] or because of interference of viral proteins with antiviral effector systems.

Upregulation of ISGs during the chronic phase of HCV infection is also ineffective in clearing the virus, and even strongly associated with non-response to therapy with pegIFN-α and ribavirin [6-8]. We have shown previously that in liver biopsies of CHC patients with persistently induced ISG expression, nuclear pSTAT1 staining is detectable in 40-80% of hepatocytes already in pre-treatment samples, and that this number does not increase in biopsies obtained 4 hours after the injection of pegIFN-α [7]. In such pre-activated livers, STAT1 phosphorylation seems to be refractory to further IFN-α stimulation. These findings

can explain why about half of the patients with CHC do not respond to treatment with pegIFN-α and ribavirin. On the other side, patients with AHC have an excellent, over 90% response rate to treatment with pegIFN-α, even when given as monotherapy. Before our present study, an attractive hypothesis to explain the efficacy of pegIFN-α in AHC postulated the lack of ISG induction in AHC. The seminal findings that the HCV protease NS3/4A can cleave an inactivate TRIF and MAVS, two important components of cellular pathways involved in viral sensing and IFN-β induction, provided a molecular mechanism to explain the lack of induction of the endogenous hepatic IFN system [32, 33]. However, we could not detect cleaved MAVS in any of the 6 AHC biopsy samples (Supplementary Figure 4.1.5). Furthermore, microarray analysis studies of liver biopsies from chimpanzees during the acute phase of HCV infection revealed a strong induction of ISGs [12, 13, 34]. These findings do not support the hypothesis that efficient MAVS cleavage is a central viral escape mechanism by preventing the induction of the IFN system. Our present study in human liver biopsies confirms these findings by showing a strong activation of STAT1 and ISG induction during AHC. However, whereas biopsies were obtained during the entire course of AHC in the chimpanzee studies, we obtained the biopsies in the "late" phase of AHC. Therefore, we cannot exclude that TRIF and/or MAVS cleavage are important viral escape mechanisms in the very first weeks after infection in humans.

In a previous study in mice we have identified USP18 as a key mediator of IFN-α refractoriness [9]. Here we show that USP18 is upregulated in CHC-NR but not in AHC patients. Comparison of responders versus non-responders to pegIFN-α in a combined analysis including AHC, CHC-R and CHC-NR showed that USP18 induction is associated with non-response to pegIFN-α. Its preferential induction by IFN-α can explain the low expression levels in patients with AHC, where ISG induction is predominantly IFN-γ driven. Because USP18 is an important mediator of refractoriness to IFN-α signaling, the apparent lack of its induction in AHC might explain the markedly improved response rate to pegIFN-α treatments in these patients compared to patients with CHC.

References

1. Lavanchy D. The global burden of hepatitis C. Liver Int 2009;29 Suppl 1:74-81.
2. Craxi A. EASL Clinical Practice Guidelines: Management of hepatitis C virus infection. Journal of Hepatology 2011.
3. Hofmann WP, Zeuzem S. A new standard of care for the treatment of chronic HCV infection. Nat Rev Gastroenterol Hepatol 2011;8:257-64.
4. Poordad F, McCone J, Jr., Bacon BR, et al. Boceprevir for untreated chronic HCV genotype 1 infection. New England Journal of Medicine 2011;364:1195-206.
5. Bacon BR, Gordon SC, Lawitz E, et al. Boceprevir for previously treated chronic HCV genotype 1 infection. New England Journal of Medicine 2011;364:1207-17.
6. Chen L, Borozan I, Feld J, et al. Hepatic gene expression discriminates responders and nonresponders in treatment of chronic hepatitis C viral infection. Gastroenterology 2005;128:1437-44.
7. Sarasin-Filipowicz M, Oakeley EJ, Duong FH, et al. Interferon signaling and treatment outcome in chronic hepatitis C. Proc Natl Acad Sci U S A 2008;105:7034-9.
8. Asselah T, Bieche I, Narguet S, et al. Liver gene expression signature to predict response to pegylated interferon plus ribavirin combination therapy in patients with chronic hepatitis C. Gut 2008;57:516-24.
9. Sarasin-Filipowicz M, Wang X, Yan M, et al. Alpha interferon induces long-lasting refractoriness of JAK-STAT signaling in the mouse liver through induction of USP18/UBP43. Mol Cell Biol 2009;29:4841-51.
10. Jaeckel E, Cornberg M, Wedemeyer H, et al. Treatment of acute hepatitis C with interferon alfa-2b. New England Journal of Medicine 2001;345:1452-7.
11. Wiegand J, Buggisch P, Boecher W, et al. Early monotherapy with pegylated interferon alpha-2b for acute hepatitis C infection: the HEP-NET acute-HCV-II study. Hepatology 2006;43:250-6.
12. Bigger CB, Brasky KM, Lanford RE. DNA microarray analysis of chimpanzee liver during acute resolving hepatitis C virus infection. J Virol 2001;75:7059-66.
13. Su AI, Pezacki JP, Wodicka L, et al. Genomic analysis of the host response to hepatitis C virus infection. Proc Natl Acad Sci U S A 2002;99:15669-74.
14. Major ME, Dahari H, Mihalik K, et al. Hepatitis C virus kinetics and host responses associated with disease and outcome of infection in chimpanzees. Hepatology 2004;39:1709-20.

15. Krieger SE, Zeisel MB, Davis C, et al. Inhibition of hepatitis C virus infection by anti-claudin-1 antibodies is mediated by neutralization of E2-CD81-claudin-1 associations. Hepatology 2010;51:1144-57.
16. RDevelopmentCoreTeam. R: A language and environment for statistical computing.: R Foundation for Statistical Computing, Vienna, Austria. ISBN 3-900051-07-0, URL http://www.R-project.org/, 2011.
17. Johnson WE, Li C, Rabinovic A. Adjusting batch effects in microarray expression data using empirical Bayes methods. Biostatistics 2007;8:118-27.
18. Smyth GK. Limma: linear models for microarray data. In: Gentleman R, Carey V, Dudoit S, Irizarry RA, Huber W, eds. Bioinformatics and Computational Biology Solutions using R and Bioconductor. New York: Springer, 2005:397-420.
19. Benjamini Y, Hochberg Y. Controlling the false discovery rate: A practical and powerful approach to multiple testing. J. Royal Stat. Soc. B 1995;57:289–300.
20. Hulsen T, de Vlieg J, Alkema W. BioVenn - a web application for the comparison and visualization of biological lists using area-proportional Venn diagrams. BMC Genomics 2008;9:488.
21. Subramanian A, Tamayo P, Mootha VK, et al. Gene set enrichment analysis: a knowledge-based approach for interpreting genome-wide expression profiles. Proc Natl Acad Sci U S A 2005;102:15545-50.
22. Dill MT, Duong FH, Vogt JE, et al. Interferon-Induced Gene Expression Is a Stronger Predictor of Treatment Response Than IL28B Genotype in Patients With Hepatitis C. Gastroenterology 2011;140:1021-1031 e10.
23. Shuai K, Stark GR, Kerr IM, et al. A single phosphotyrosine residue of Stat91 required for gene activation by interferon-gamma. Science 1993;261:1744-6.
24. Thimme R, Bukh J, Spangenberg HC, et al. Viral and immunological determinants of hepatitis C virus clearance, persistence, and disease. Proc Natl Acad Sci U S A 2002;99:15661-8.
25. Thimme R, Oldach D, Chang KM, et al. Determinants of viral clearance and persistence during acute hepatitis C virus infection. Journal of Experimental Medicine 2001;194:1395-406.
26. Makowska Z, Duong FH, Trincucci G, et al. Interferon-beta and interferon-lambda signaling is not affected by interferon-induced refractoriness to interferon-alpha in vivo. Hepatology 2011;53:1154-63.

27. Malakhova OA, Kim KI, Luo JK, et al. UBP43 is a novel regulator of interferon signaling independent of its ISG15 isopeptidase activity. Embo J 2006;25:2358-67.
28. Santantonio T, Wiegand J, Gerlach JT. Acute hepatitis C: current status and remaining challenges. Journal of Hepatology 2008;49:625-33.
29. Lechner F, Wong DK, Dunbar PR, et al. Analysis of successful immune responses in persons infected with hepatitis C virus. Journal of Experimental Medicine 2000;191:1499-512.
30. Urbani S, Boni C, Missale G, et al. Virus-specific CD8+ lymphocytes share the same effector-memory phenotype but exhibit functional differences in acute hepatitis B and C. Journal of Virology 2002;76:12423-34.
31. Garaigorta U, Chisari FV. Hepatitis C virus blocks interferon effector function by inducing protein kinase R phosphorylation. Cell Host Microbe 2009;6:513-22.
32. Meylan E, Curran J, Hofmann K, et al. Cardif is an adaptor protein in the RIG-I antiviral pathway and is targeted by hepatitis C virus. Nature 2005;437:1167-72.
33. Li K, Foy E, Ferreon JC, et al. Immune evasion by hepatitis C virus NS3/4A protease-mediated cleavage of the Toll-like receptor 3 adaptor protein TRIF. Proc Natl Acad Sci U S A 2005;102:2992-7.
34. Yu C, Boon D, McDonald SL, et al. Pathogenesis of hepatitis E virus and hepatitis C virus in chimpanzees: similarities and differences. Journal of Virology 2010;84:11264-78.

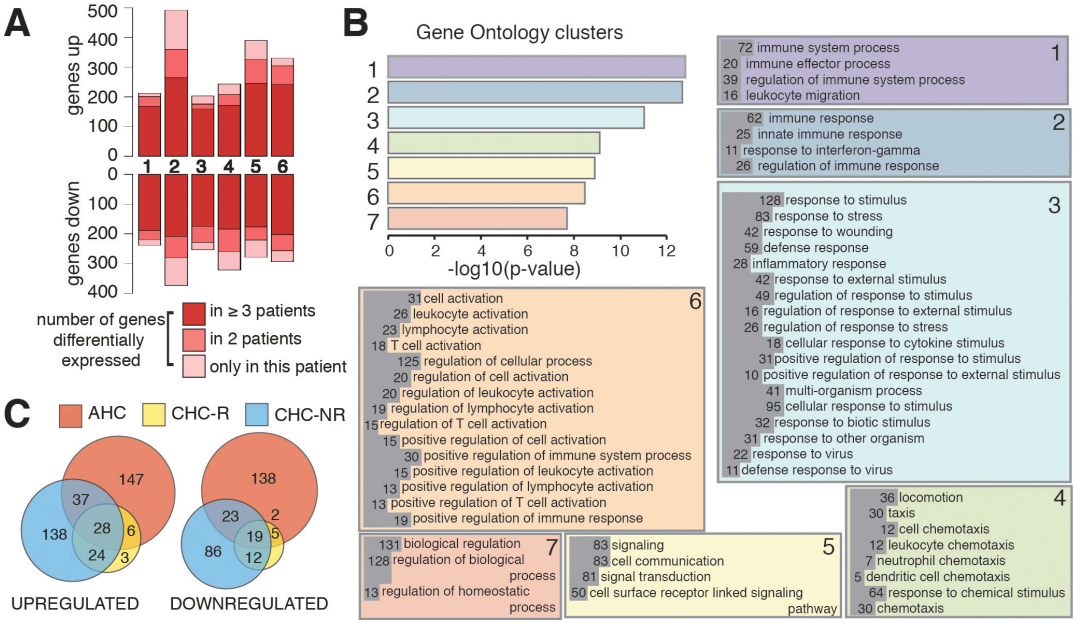

Figure 4.1.1.
Acute hepatitis C patients show a distinct pattern of gene expression in the liver.
(A) Number of genes 2-fold up- or downregulated in each AHC patient compared to the mean gene expression in healthy liver samples (n = 4). Different shades show the extent of overlap between patients as indicated.
(B) Enrichment of Gene Ontology Biological Process terms among genes upregulated in AHC patients with respect to CTRL patients. Terms with p-values below 10^{-6} were clustered based on the GO hierarchy. The barplot shows the enrichment score for each term. The numbers to the left from the term name show the number of genes which represent a given Gene Ontology term in AHC patients.
(C) Venn diagram of genes identified as up- or downregulated in AHC (n = 6), CHC-NR (n = 6) or CHC-R patients (n =10) compared to healthy liver. A gene was considered differentially regulated in a group if the fold change of expression values between the mean of the group and the mean of healthy liver samples was > 2 and the corresponding FDR < 0.05.

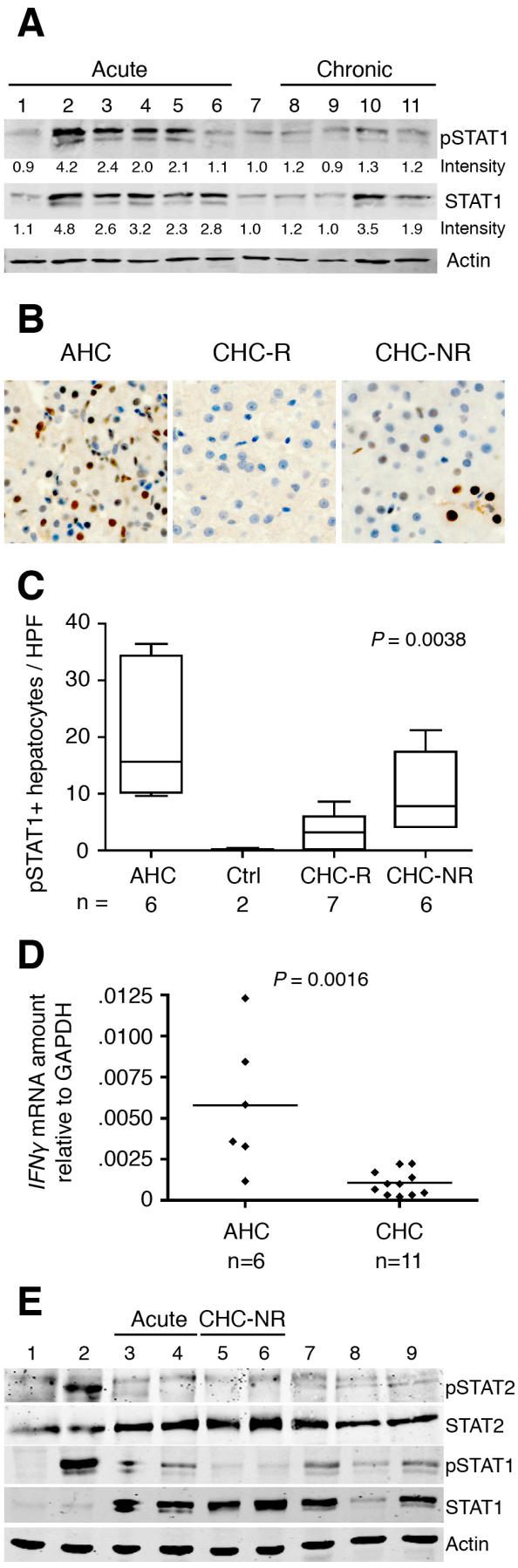
A
Acute
Chronic
1 2 3 4 5 6 7 8 9 10 11
pSTAT1
0.9 4.2 2.4 2.0 2.1 1.1 1.0 1.2 0.9 1.3 1.2
Intensity
STAT1
1.1 4.8 2.6 3.2 2.3 2.8 1.0 1.2 1.0 3.5 1.9
Intensity
Actin
B
AHC
CHC-R
CHC-NR
C
pSTAT1+ hepatocytes / HPF
40
30
20
10
0
P = 0.0038
AHC
Ctrl
CHC-R
CHC-NR
n =
6
2
7
6
D
IFNγ mRNA amount relative to GAPDH
.0125
.0100
.0075
.0050
.0025
0
P = 0.0016
AHC
n=6
CHC
n=11
E
Acute
CHC-NR
1 2 3 4 5 6 7 8 9
pSTAT2
STAT2
pSTAT1
STAT1
Actin

Figure 4.1.2.
Acute hepatitis C induces a distinct set of ISGs.
(A) STAT1 phosphorylation and STAT1 protein expression by Western Blot analysis using whole cell extracts of liver samples from AHC (lane 1-6, no. according to Table I), healthy liver (lane 7), CHC-R (lane 8-9) and CHC-NR (lane 10-11).
(B) Representative pictures of immunohistochemistry for pSTAT1 showing strong nuclear staining in AHC and moderate staining in CHC-NR, while CHC-R is not positively stained.
(C) Quantification of pSTAT1 nuclear staining in hepatocytes per high power field (HPF) in AHC, healthy liver (Ctrl) and CHC-R and -NR. There were significant differences of the mean amount of positive hepatocytes between the four groups (p-value obtained by one-way ANOVA).
(D) Measurement of hepatic expression of IFN-γ mRNA in AHC and CHC by quantitative PCR normalized to GAPDH. Each dot represesents one sample. P-value was obtained with Student's t-test.
(E) STAT1 and STAT2 phosphorylation and whole protein expression by Western Blot analysis using whole cell extracts of Huh7 cells untreated (lane 1) or treated for 30 min. with 1000 U/ml IFN-α (2); or of liver samples of AHC patients 2 and 3 (3-4), of 2 CHC-NR patients (5-6) and of 3 responder patients biopsied 4h after subcutaneous pegIFN-α injection (7-9) indicating a weak but distinguishable pSTAT2 band in the latter.

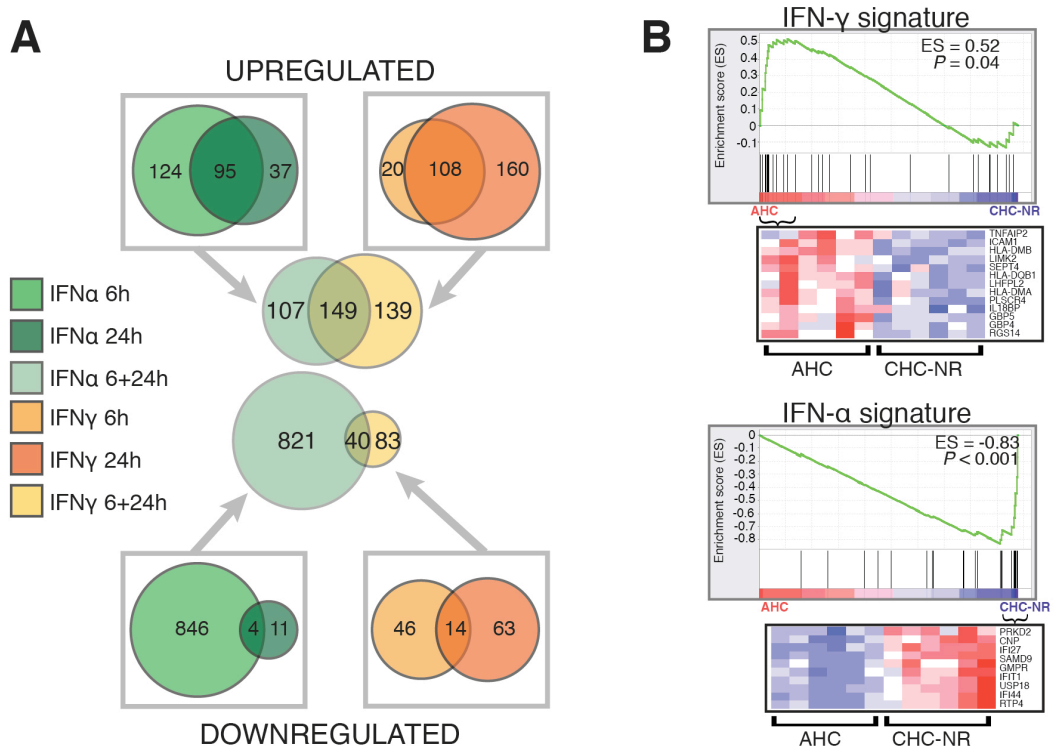

Figure 4.1.3.
IFN-γ-specific gene signature is enriched in the AHC gene expression profiles, while IFN-α-induced transcription patterns characterize CHC-NR patients.
(A) Venn diagrams of genes differentially expressed in primary human hepatocytes (PHH) upon IFN-α or IFN-γ treatment. A gene was considered differentially expressed if in PHH from both donors up- or downregulated more than 2-fold with respect to untreated samples. Diagrams in gray boxes show temporal patterns of IFN-induced gene expression in PHH, with genes differentially regulated at 6 and at 24 hours. In the middle the overlap between the sets of genes differentially regulated by IFN-α (green) and IFN-γ (orange) at any of the two time points is shown.
(B) Genes were rank-ordered based on differential expression between the AHC and CHC-NR patients and the overrepresentation of the experimentally defined IFN-α and IFN-γ-specific gene sets at the top and bottom of the list was assessed by GSEA algorithm. Below the GSEA plots are heatmaps of the genes which contribute to the enrichment score of the gene set tested.

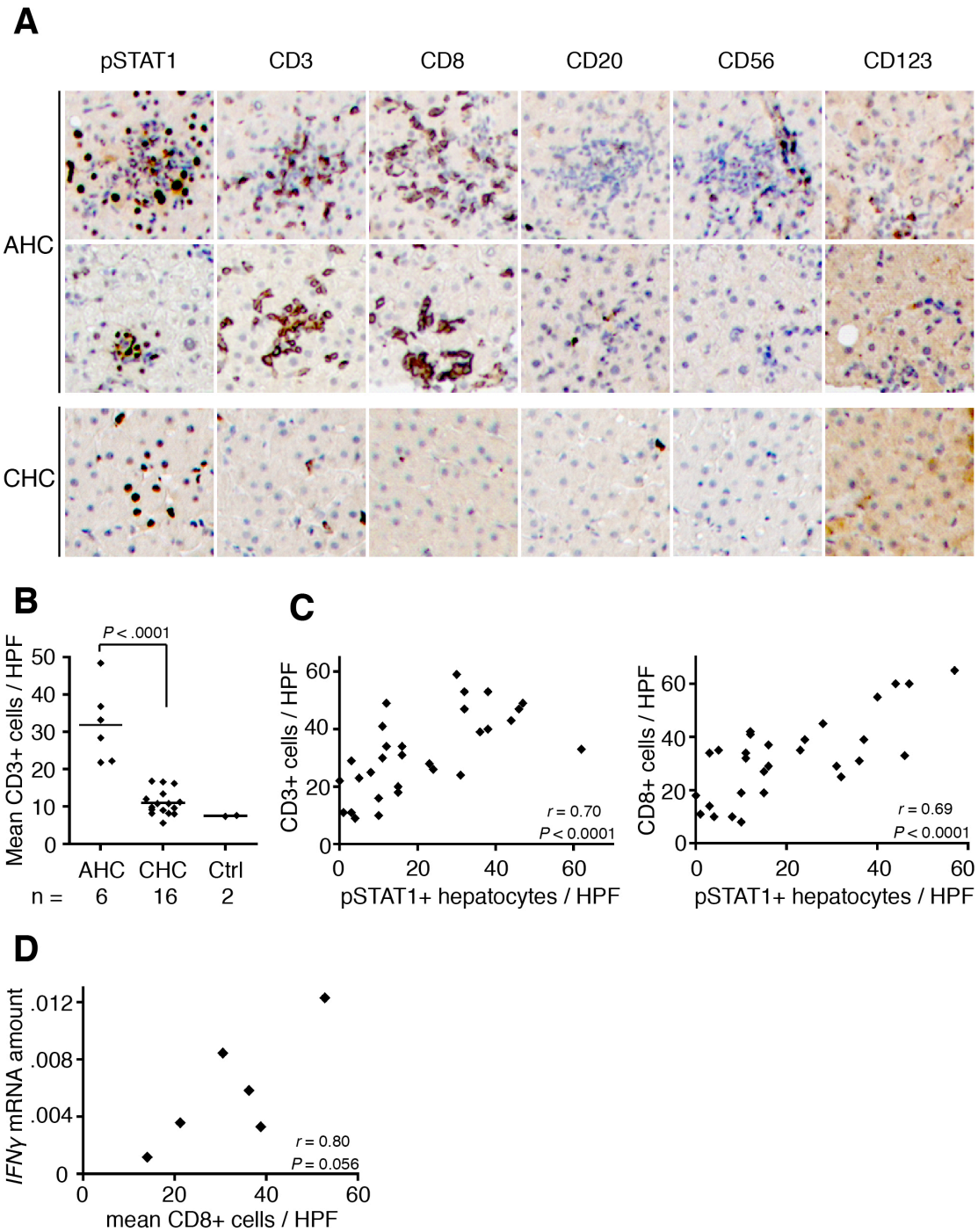
A
pSTAT1
CD3
CD8
CD20
CD56
CD123
AHC
CHC
B
P < .0001
Mean CD3+ cells / HPF
50
40
30
20
10
0
AHC
CHC
Ctrl
n =
6
16
2
C
CD3+ cells / HPF
60
40
20
0
r = 0.70
P < 0.0001
0
20
40
60
pSTAT1+ hepatocytes / HPF
CD8+ cells / HPF
60
40
20
0
r = 0.69
P < 0.0001
0
20
40
60
pSTAT1+ hepatocytes / HPF
D
IFNγ mRNA amount
.012
.008
.004
0
r = 0.80
P = 0.056
0
20
40
60
mean CD8+ cells / HPF

Figure 4.1.4.
In AHC pSTAT1 positive hepatocytes co-localize with CD8+ T cells.
(A) Number of mean CD3+ cells per high power field (HPF) of the liver parenchyma. Each dot represents the mean number per patient. P-value was obtained by Student's t-test.
(B)Representative pictures of serial sections from liver biopsies analyzed immunohistochemically for pSTAT1 and markers for T cells (CD3), cytotoxic T cells (CD8), B cells (CD20), NK cells (CD56) and plasmacytoid dendritic cells (CD123). For each section within the sample the same detail is shown. In AHC pSTAT1+ hepatocytes co-localized with immune cells positive for CD3 and CD8.
(C) Correlation analysis of the number of CD3+ cells and CD8+ cells / HPF with the number of nuclear pSTAT1 signals in hepatocytes / HPF (n=30). The values represent the number of positive cells counted in 5 random HPF in the parenchyma of each biopsy in AHC patients, which are shown in Supplementary Figure 3 and listed in Supplementary Table VI. Each dot represents one HPF. Association was assessed by Spearman correlation analysis.
(D) Correlation analysis of the mean number of CD8+ cells with the IFNγ mRNA amount in AHC (Pearson correlation).

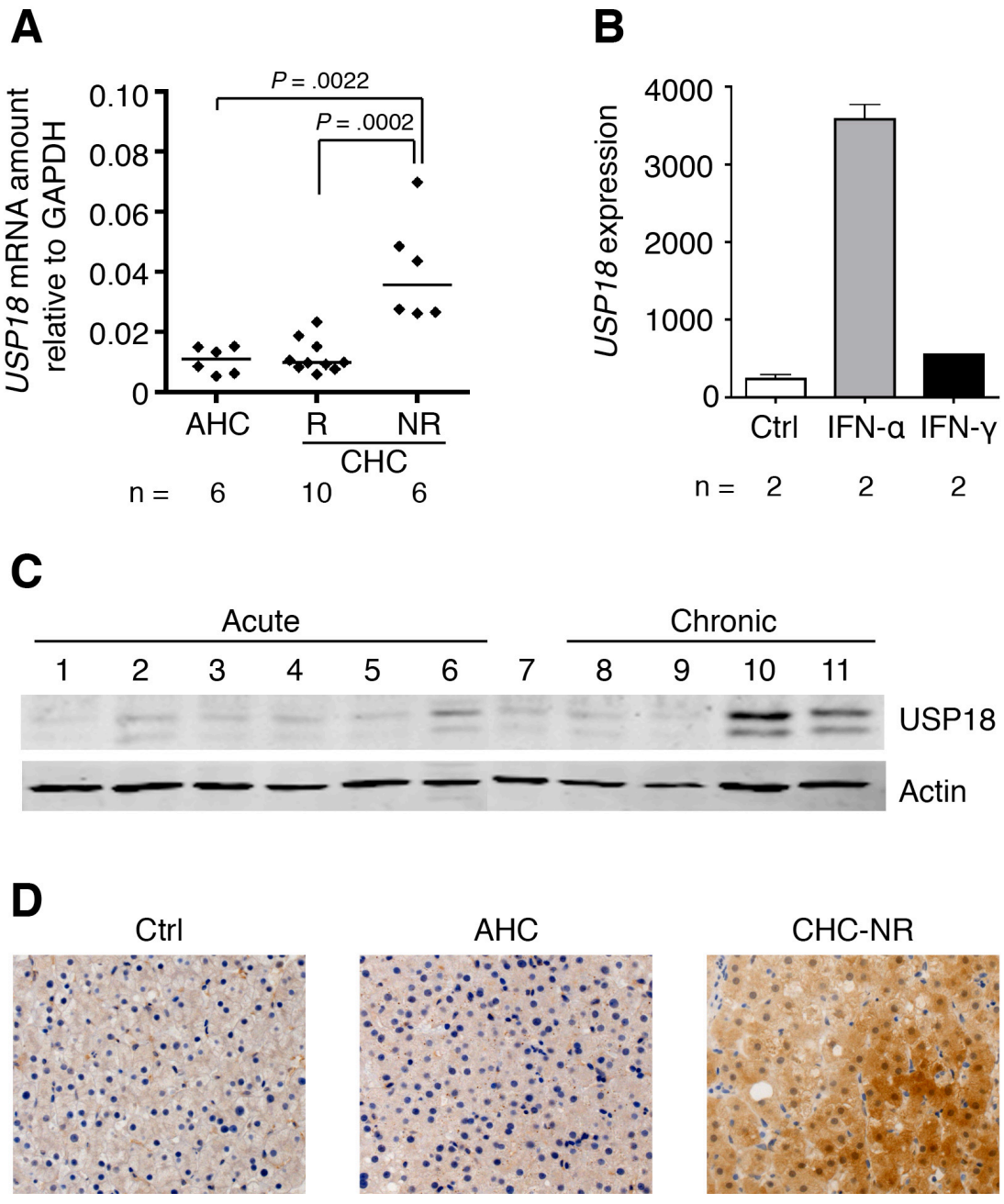
A
USP18 mRNA amount relative to GAPDH
0.10
0.08
0.06
0.04
0.02
0
P = .0022
P = .0002
AHC
R
NR
CHC
n = 6 10 6
B
USP18 expression
4000
3000
2000
1000
0
Ctrl
IFN-α
IFN-γ
n = 2 2 2
C
Acute
Chronic
1 2 3 4 5 6 7 8 9 10 11
USP18
Actin
D
Ctrl
AHC
CHC-NR

Figure 4.1.5.
USP18 expression in AHC and CHC liver biopsies.
(A) Hepatic expression of USP18 mRNA measured by quantitative PCR and normalized to GAPDH. Each dot represents one sample. The line indicates the median. P-values were obtained by Mann-Whitney tests.
(B) Expression of USP18 mRNA as measured by Human Gene 1.0 ST arrays in PHH treated with α- and γ-IFN for 6 hours, and untreated PHH (Ctrl). Mean+SD is shown.
(C) USP18 protein expression by Western Blot analysis using whole cell extracts of liver samples from AHC (lane 1-6, no. according to Table I), healthy liver (lane 7), CHC-R (lane 8-9) and CHC-NR (lane 10-11).
(D) Representative pictures of immunohistochemistry for USP18 in healthy liver (Ctrl), AHC and CHC-NR, showing a strong cytoplasmic and patchy staining in CHC-NR (magnification 400x).

Tables

Table 4.1.1: Patient characteristics

Patient no.	Age	Gender	HCV Genotype	Viral load at Bx, (log IU/mL)	ALT at Bx, (U/L)	IL28B rs12979860	Week 4 Response	Response	HIV	ΔT Inf-Bx
1	31	M	3	<12	60	CC	-	SC	-	3 months
2	17	F	1	<12	421	CT	-	SC	-	3 months
3	16	F	1	3.53	86	CT	RVR	SVR[a]	-	4 months
4	30	M	4	2.49	125	CT	RVR	SVR	-	2 months
5	44	M	3	5.98	571	CC	-	Interrupted	-	2-5 months
6	56	M	3	4.15	155	TT	RVR	EoTR[b]	-	3-4 months

Abbreviations: Bx, biopsy; EoTR, end of treatment response; Inf, infection;

RVR, rapid virological response (below limit of detection at week 4); SC, spontaneous clearance; SVR, sustained virologic response

[a] Treatment withPegIFN-α-2a for 12 weeks [b] Treatment with PegIFN-α-2b & Ribavirin

Supplementary Material

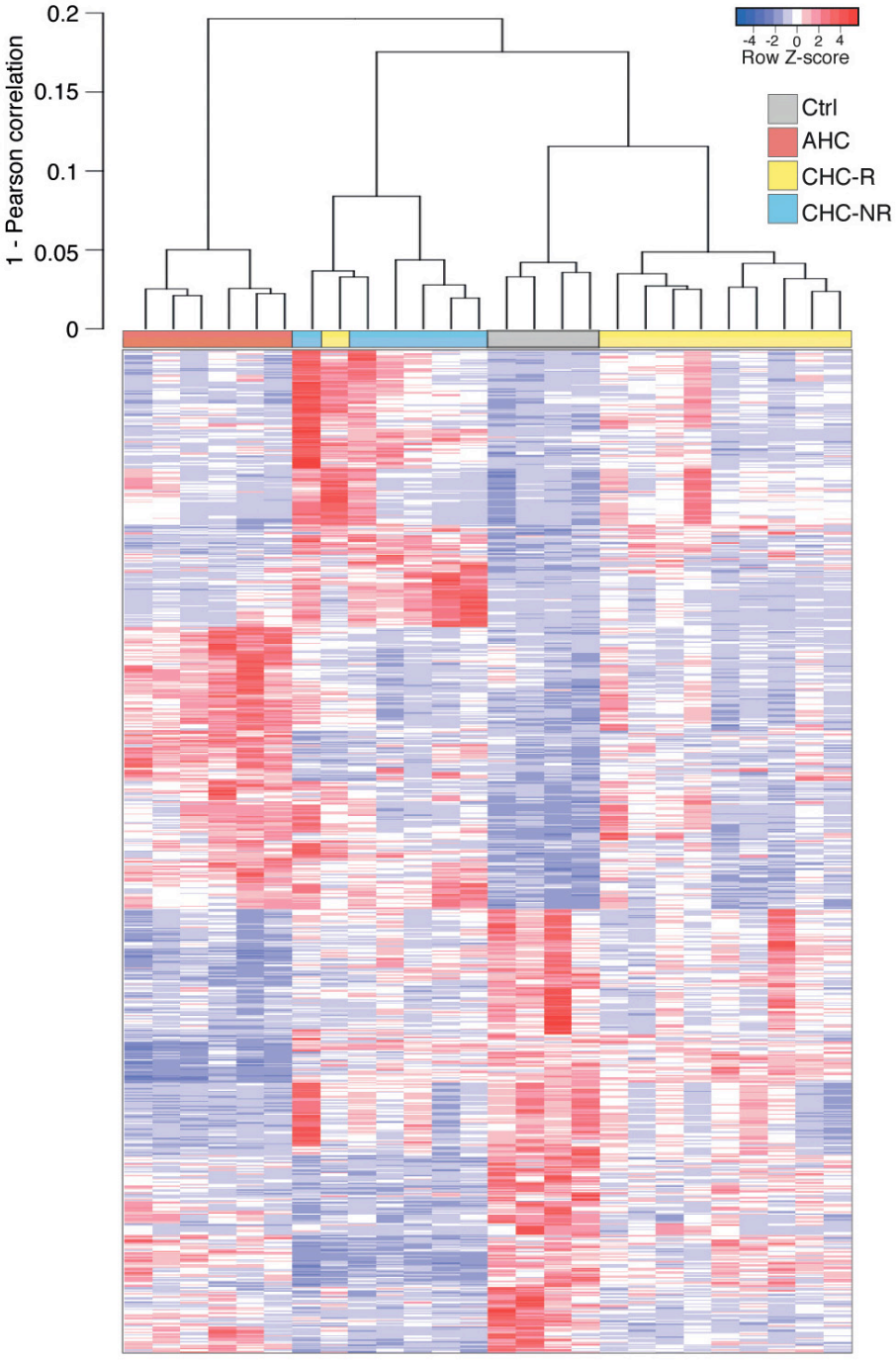

Supplementary Figure 4.1.1.
Genome-wide unsupervised hierarchical clustering groups all AHC patients in a distinct cluster, separate from the CHC or control samples. The heatmap shows the expression patterns of 1003 probe sets identified as up- or downregulated in at least one of AHC, CHC-NR or CHC-R compared to the healthy liver.

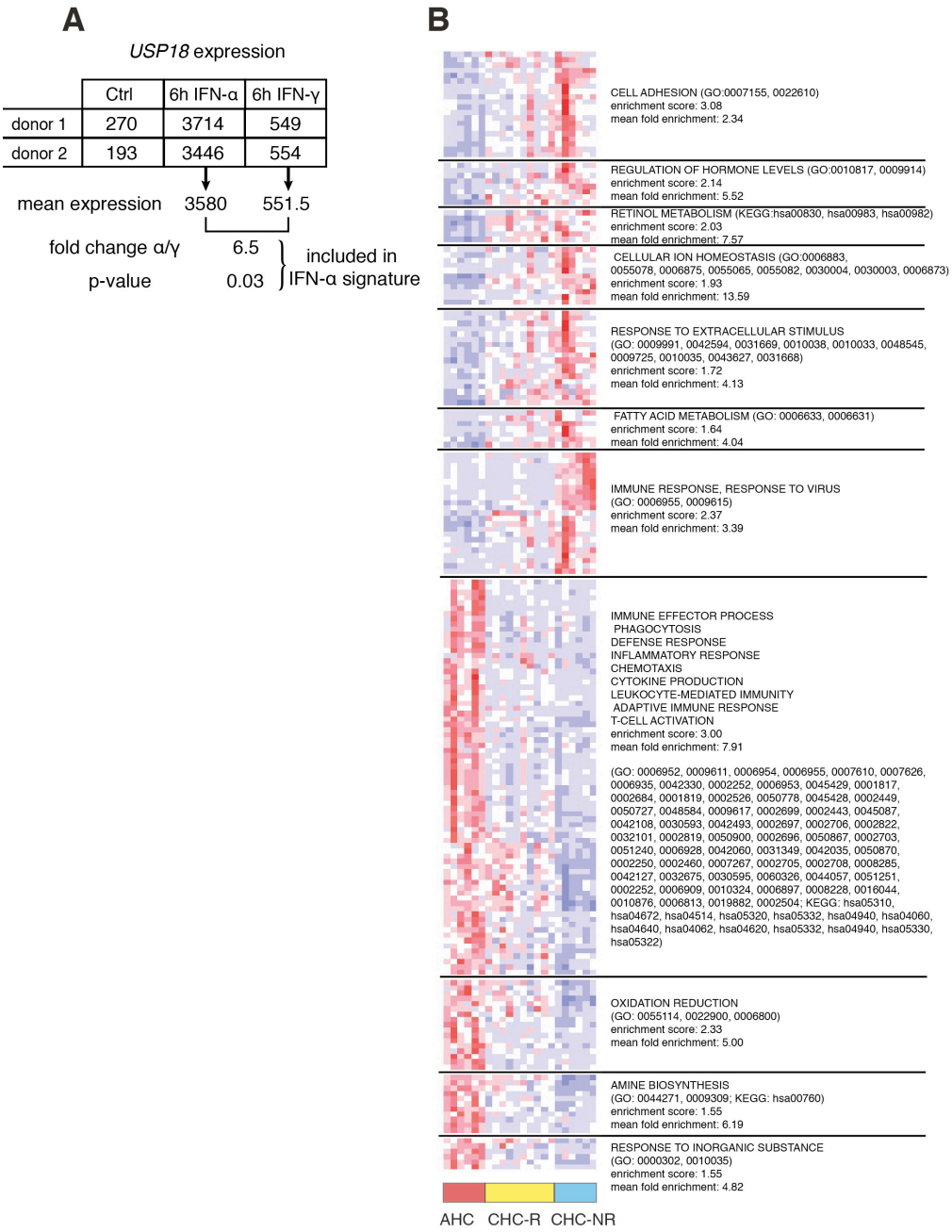

Supplementary Figure 4.1.2.

(A) Scheme representation of the generation of gene sets for GSEA.
A gene was included if the difference between the means of IFN-α and IFN-γ-treated PHH was larger than 2-fold and the p-value from a Welch t-test of the corresponding samples lower than 0.05. The example in the scheme shows expression values for USP18 after 6 hours of IFN-α or IFN-γ treatment.

(B) Gene Ontology Biological Process terms and KEGG collection pathways were tested for overrepresentation in lists of genes significantly altered between AHC and CHC-NR patients. Enriched categories were then clustered in order to bring together closely related terms. The heatmap shows expression patterns of all differentially expressed genes which belong to one of the enriched categories.

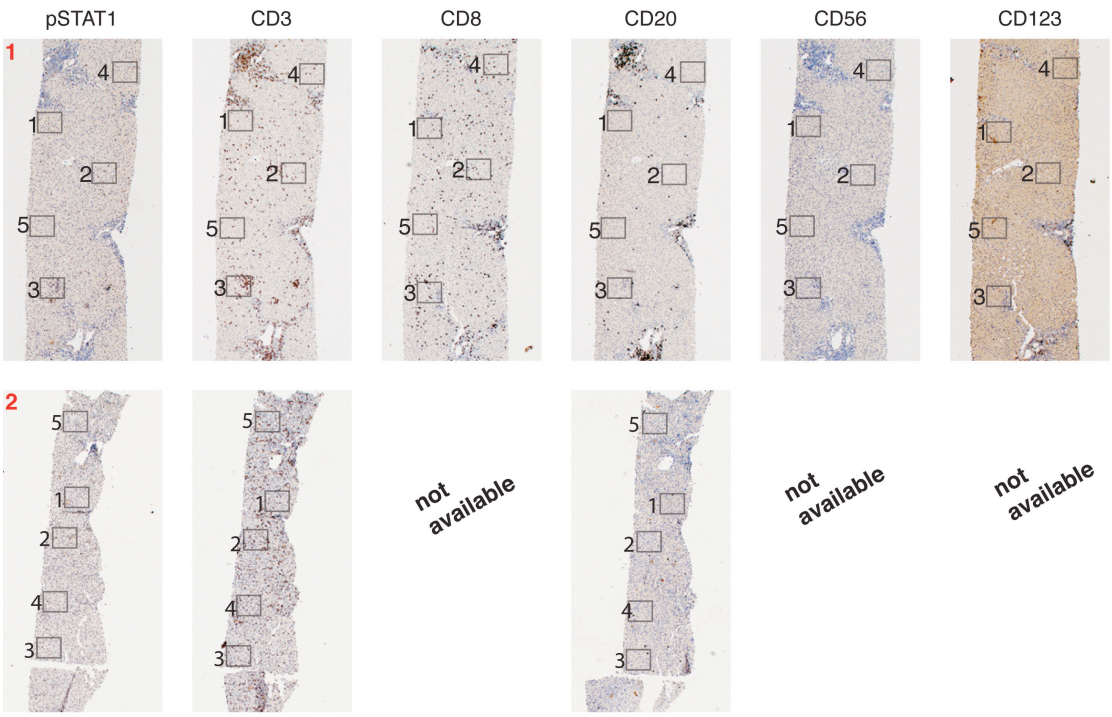
pSTAT1
CD3
CD8
CD20
CD56
CD123
1
2
not available
not available
not available

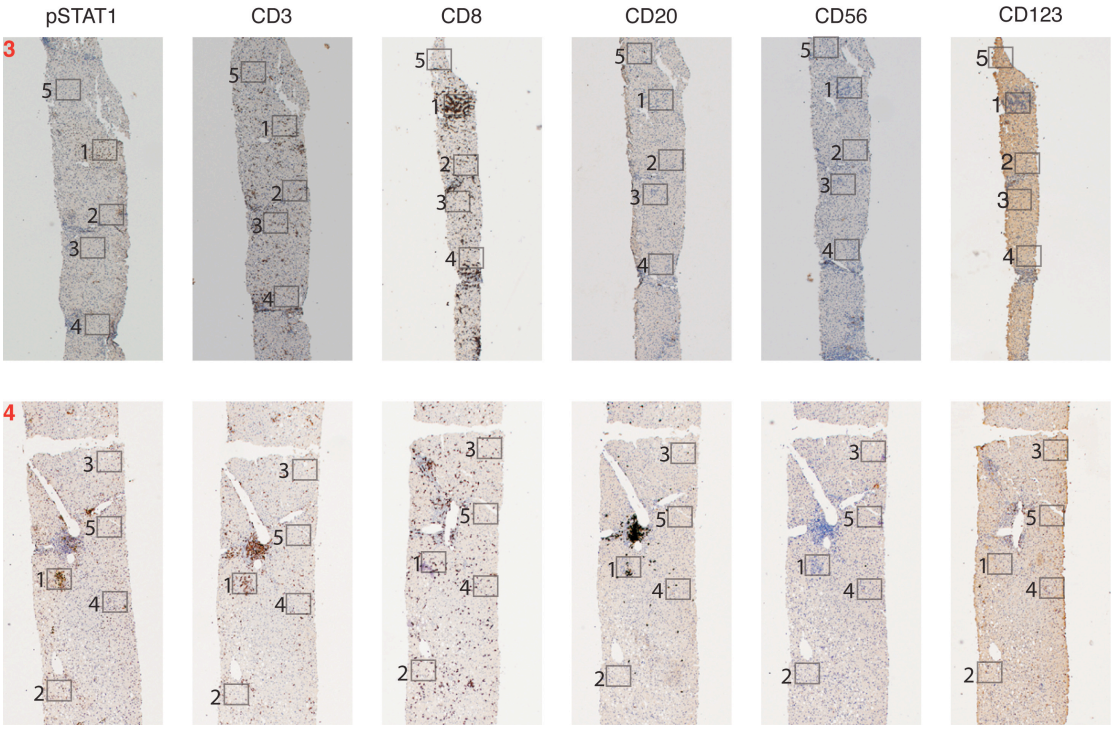
pSTAT1
CD3
CD8
CD20
CD56
CD123
3
4

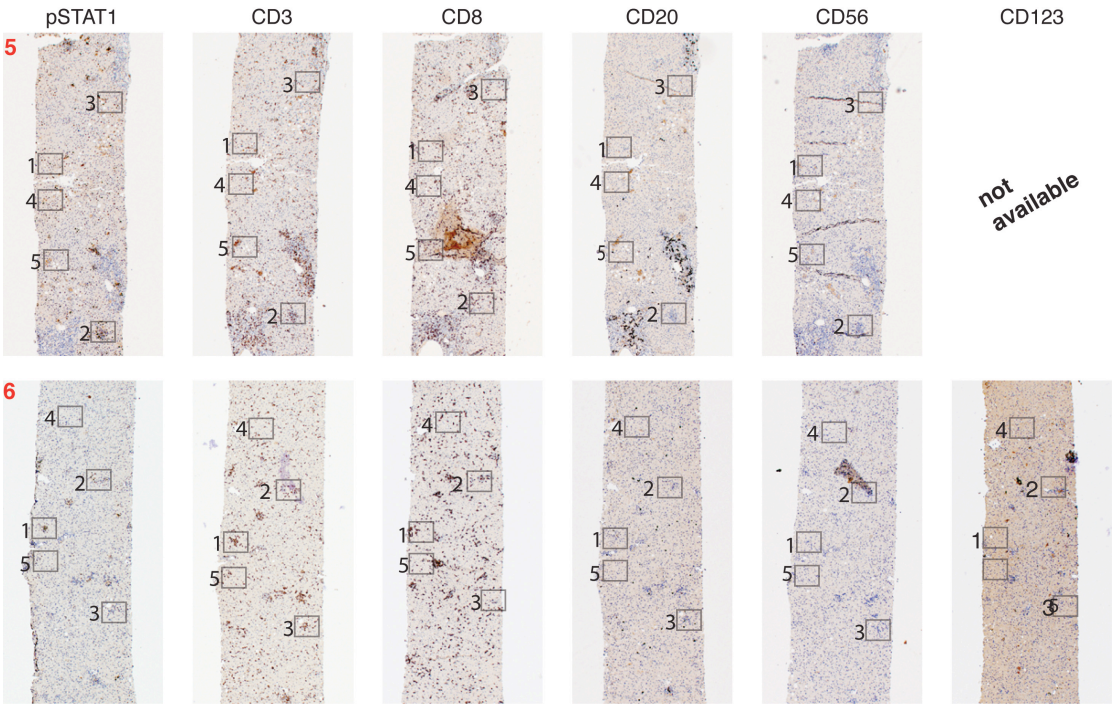

Supplementary Figure 4.1.3.
Collection of all liver biopsy serial sections from AHC patients no. 1-6 (red number), immunohistochemically stained for pSTAT1 and markers for T cells (CD3), cytotoxic T cells (CD8), B cells (CD20), NK cells (CD56) and plasmacytoid dendritic cells (CD123). The 5 boxes per slide indicate the high power fields in the liver parenchyma that were randomly chosen for the co-localization analysis.

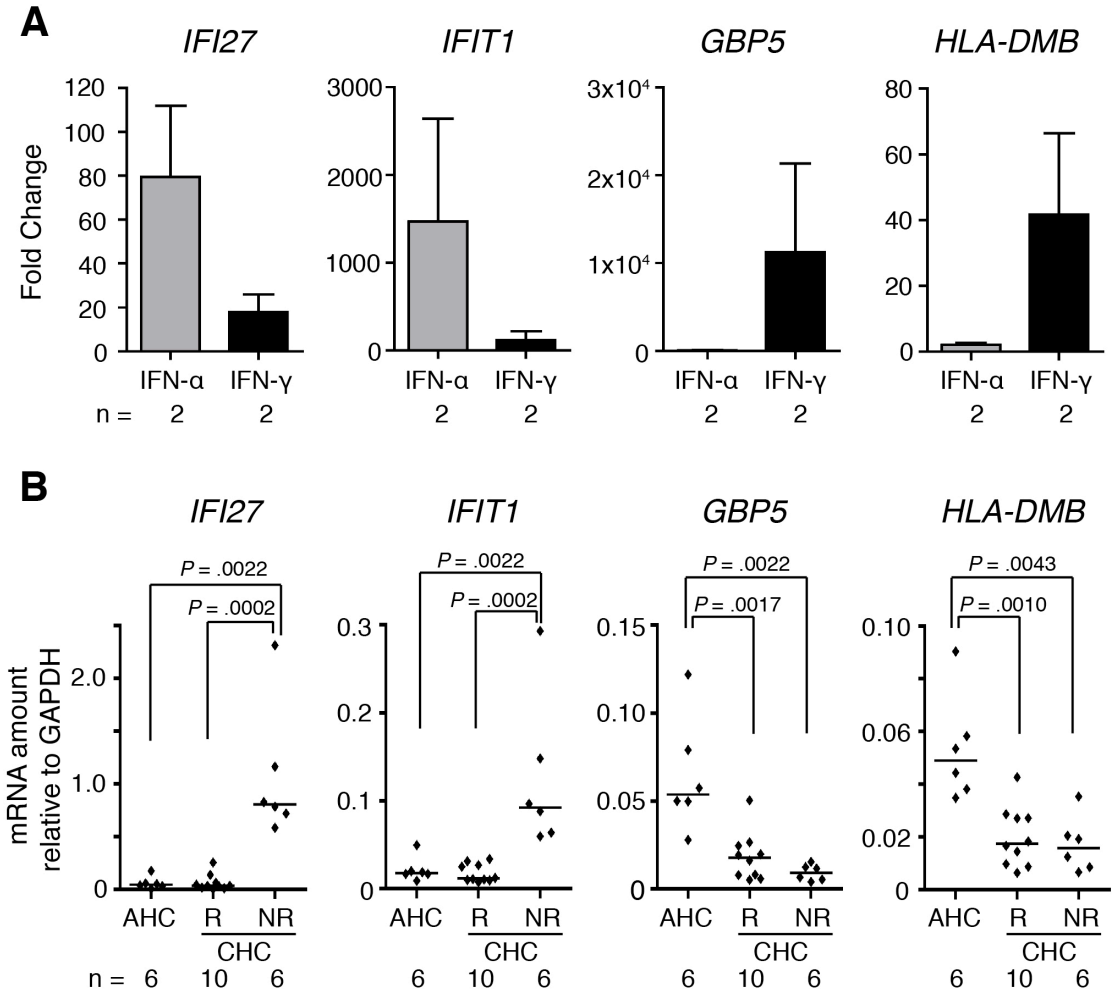

Supplementary Figure 4.1.4.
Confirmation of microarray data by quantitative RT-PCR.
(A) Quantification of IFN-α specific ISGs (IFI27 and IFIT1) and IFN-γ specific ISGs (GBP5 and HLA-DMB) by quantitative RT-PCR in IFN-α or IFN-γ treated PHH confirmed specific induction as previously assessed by the microarray analysis (time point 24h).
(B) Quantitative RT-PCR confirmed upregulation of IFN-α ISGs (IFI27 and IFIT1) in CHC-NR and upregulation of IFN-γ ISGs (GBP5 and HLA-DMB) in AHC. (p-values by Mann-Whitney test)

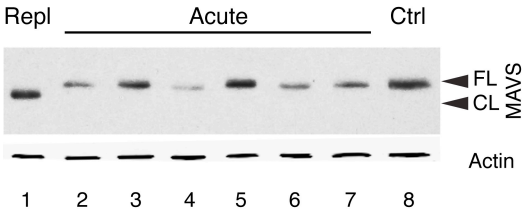

Supplementary Figure 4.1.5.
Analysis of MAVS cleavage by Western blot. Arrowheads indicate full-length (FL) and cleaved (CL) MAVS. Lysates from Huh-7.5 cells harboring a subgenomic HCV replicon (Repl, lane 1) and healthy liver (Ctrl, lane 8) served as controls for cleaved and full-length MAVS. Lysates from AHC patients 1-6 (according to Table I) are displayed on lanes 2-7.

For supplementary tables please refer to the appendix A of this thesis (p. 102).

Supplementary Table 1.
Fold changes of the upregulated genes in functional categories (fold change of at least 2 between the means of AHC and healthy liver samples with the corresponding FDR (Benjamini-Hochberg correction) below 0.05).
Supplementary Table 2.
Fold changes of the downregulated genes in functional categories (fold change of at least 2 between the means of AHC and healthy liver samples with the corresponding FDR (Benjamini-Hochberg correction) below 0.05).
Supplementary Table 3.
Fold changes of the upregulated genes in IFN-treated PHH. The table shows genes that in PHH from both donors were at least 2-fold upregulated between untreated and IFN-treated PHH samples.
Supplementary Table 4.
Fold changes of the downregulated genes in IFN-treated PHH. The table shows genes that in PHH from both donors were at least 2-fold downregulated between untreated and IFN-treated PHH samples.
Supplementary Table 5.
PHH-derived gene sets used for GSEA. The table shows genes that are preferentially induced by IFN-α or IFN-γ in PHH (at least at one time point the fold difference of expressions induced by the two cytokines is higher than 2, with the corresponding p-value below 0.05).
Supplementary Table 6.
Amount of cells positively stained for pSTAT1, CD3, CD8, CD20, CD56 and CD123 per high power field (HPF) in AHC. Shown are the numbers for each of the 5 HPF in each AHC patient. Below of each patient the mean is shown. Note that for patient no. 2 due to limitations of the biopsy section for CD8 not the same HPFs could be assessed (numbers in italics) and are therefore not directly comparable to the other HPFs.
Supplementary Table 7 and 8.
Primer sequences used for real-time RT-PCR analysis and primary antibodies used for immunohistochemistry.

4.2 The effect of genetic variations near the IL28B gene in the liver of patients with hepatitis C

4.2.1 Interferon-Induced Gene Expression Is a Stronger Predictor of Treatment Response than IL28B Genotype in Patients with Hepatitis C

Dill M.T., Duong F.H.T., Vogt J.E., Bibert S., Bochud P.Y., Terracciano L., Papassotiropoulos A., Roth V., Heim M.H., Interferon-Induced Gene Expression Is a Stronger Predictor of Treatment Response than IL28B Genotype in Patients with Hepatitis C, Gastroenterology. 2011 Mar;140(3):1021-1031.

For supplementary material please refer to the appendix B of this thesis.

Interferon-Induced Gene Expression Is a Stronger Predictor of Treatment Response Than *IL28B* Genotype in Patients With Hepatitis C

MICHAEL T. DILL,[*,‡] FRANCOIS H. T. DUONG,[*] JULIA E. VOGT,[§] STÉPHANIE BIBERT,[‖] PIERRE–YVES BOCHUD,[‖] LUIGI TERRACCIANO,[¶] ANDREAS PAPASSOTIROPOULOS,[#] VOLKER ROTH,[§] and MARKUS H. HEIM[*,‡]

[*]Department of Biomedicine, Hepatology Laboratory; [§]Computer Science Department; and [#]Division of Molecular Psychology, University of Basel, Basel; [‡]Division of Gastroenterology and Hepatology and [¶]Institute of Pathology, University Hospital Basel, Basel; and [‖]Infectious Diseases Service, Department of Medicine and Institute of Microbiology, University Hospital and University of Lausanne, Lausanne, Switzerland

BACKGROUND & AIMS: The host immune response during the chronic phase of hepatitis C virus infection varies among individuals; some patients have a no interferon (IFN) response in the liver, whereas others have full activation of IFN-stimulated genes (ISGs). Preactivation of this endogenous IFN system is associated with nonresponse to pegylated IFN-α (pegIFN-α) and ribavirin. Genome-wide association studies have associated allelic variants near the *IL28B* (*IFN*λ3) gene with treatment response. We investigated whether *IL28B* genotype determines the constitutive expression of ISGs in the liver and compared the abilities of ISG levels and *IL28B* genotype to predict treatment outcome. **METHODS:** We genotyped 109 patients with chronic hepatitis C for *IL28B* allelic variants and quantified the hepatic expression of ISGs and of *IL28B*. Decision tree ensembles, in the form of a random forest classifier, were used to calculate the relative predictive power of these different variables in a multivariate analysis. **RESULTS:** The minor *IL28B* allele was significantly associated with increased expression of ISG. However, stratification of the patients according to treatment response revealed increased ISG expression in nonresponders, irrespective of *IL28B* genotype. Multivariate analysis of ISG expression, *IL28B* genotype, and several other factors associated with response to therapy identified ISG expression as the best predictor of treatment response. **CONCLUSIONS: *IL28B* genotype and hepatic expression of ISGs are independent predictors of response to treatment with pegIFN-α and ribavirin in patients with chronic hepatitis C. The most accurate prediction of response was obtained with a 4-gene classifier comprising *IFI27*, *ISG15*, *RSAD2*, and *HTATIP2*.**

Keywords: Hepatitis C Virus; Jak-STAT Signaling; Host-Virus Interaction; Innate Immunity.

Chronic infection with hepatitis C virus (HCV) is a major cause of liver disease worldwide.[1] The current standard therapy of chronic hepatitis C (CHC) achieves an overall sustained virologic response (SVR) in ~55% of patients.[1] The treatment requires up to 72 weeks of weekly subcutaneous injection of pegylated interferon (pegIFN)-α combined with twice-daily intake of ribavirin tablets. Pretreatment predictors of response are useful for advising patients. SVR rates are higher in patients infected with HCV genotype non-1 (mostly genotypes 2 and 3) and in those with a viral load of less than 600,000 IU/mL.[1] Other less consistently reported baseline characteristics associated with a favorable response include female gender, age younger than 40 years, nonblack race, lower body weight (<75 kg), the absence of insulin resistance, and the absence of bridging fibrosis or cirrhosis on liver biopsy.[1] Infection with HCV can activate the endogenous IFN system in the liver. However, despite a strong induction of hundreds of IFN-stimulated genes (ISGs) in the liver, the activation of the endogenous IFN system in CHC is ineffective in clearing the infection and even impedes the response to therapy, most likely by inducing a refractory state of the IFN signaling pathway.[2–5] The causal factors and the mechanism underlying this preactivation of the IFN system in some patients with CHC are not well understood. We have shown that the cleavage of mitochondrial antiviral signaling protein by HCV NS3-4A protease correlates with a reduced activation of the endogenous IFN system.[6] Recently, several groups reported a strong association between allelic variants of the *IL28B* gene encoding *IFN*λ3 and response to treatment. Failure to respond to treatment was associated with the minor alleles of rs12979860 (T),[7] rs8099917 (G),[8–10] and rs12980275 (G).[10] The association was significant in HCV genotypes 1 and 4 but not in HCV genotypes 2 and 3.[8] Moreover, the *IL28B* genotype was also associated with the rate of spontaneous clearance of HCV infection.[8,11] The functional mechanism underlying the association of *IL28B* polymorphisms with response to

Abbreviations used in this paper: AUC, area under the curve; CHC, chronic hepatitis C; ERR, error rate; GAPDH, glyceraldehyde-3-phosphate dehydrogenase; ISG, interferon-stimulated gene; PBMC, peripheral blood mononuclear cell; pegIFN, pegylated interferon; RFFS, random forest feature score; ROC, receiver operating characteristic; RVR, rapid virologic response; SNP, single nucleotide polymorphism; SVR, sustained virologic response.

0016-5085/$36.00
doi:10.1053/j.gastro.2010.11.039

treatment is unknown, but 2 groups observed a lower expression of IFNλ3 in peripheral blood mononuclear cells (PBMCs) in individuals carrying the minor rs8099917 *IL28B* allele that is associated with nonresponse to treatment.[9,10] We hypothesized that allelic variants in *IL28B* might be responsible for the difference of endogenous IFN activation and studied the association between *IL28B* polymorphisms and hepatic ISG expression as well as the predictive power of the different factors. Here we show that *IL28B* genotype and hepatic ISG expression are independent predictors of treatment response in CHC. There is no direct link between altered IFNλ3 expression and preactivation of the endogenous IFN system in the liver. Importantly, hepatic ISG expression is by far the better predictor of treatment response than *IL28B* genotype.

Materials and Methods

Liver Biopsies and Patient Data

Liver biopsy specimens from white patients with CHC (n = 109) were obtained during routine diagnostic workup at the University Hospital Basel. Grading and staging of CHC was according to METAVIR classification. A specimen was frozen for research purposes if more than sufficient material was obtained for histopathologic examination and the patient gave his or her written informed consent in accordance with the Ethics Committee of Basel. Serum HCV RNA was quantified using the Cobas AmpliPrep/COBAS TaqMan HCV Test and the Cobas Amplicor Monitor from Roche Molecular Systems (Basel, Switzerland). Patients were treated with pegIFN-α 2a or 2b in combination with ribavirin according to current guidelines.[1] Definitions of response to treatment are as follows: SVR, HCV RNA level <12 IU/mL 6 months after end of treatment; relapse, HCV RNA level <12 IU/mL at the end of treatment but >12 IU/mL 6 months after the end of treatment; nonresponse, HCV RNA level >12 IU/mL at the end of treatment; rapid virologic response (RVR), HCV RNA level <12 IU/mL after 4 weeks of treatment. Patient characteristics are shown in Table 1 and Supplementary Table 1.

Measurement of Messenger RNA Levels in the Liver

Total RNA was extracted from human liver tissue using TRIzol reagent (Invitrogen, Basel, Switzerland) according to the manufacturer's instructions. RNA samples were then treated with deoxyribonuclease and purified on columns (Nucleospin kit; Machery-Nagel, Oensingen, Switzerland) according to the manufacturer's instructions. RNA was stored at −75°C. RNA was reverse transcribed by Moloney murine leukemia virus reverse transcriptase (Promega Biosciences, Wallisellen, Switzerland) in the presence of random primers (Promega) and deoxynucleoside triphosphate. The samples were incubated for 5 minutes at 70°C and then for 1 hour at 37°C. The reaction was stopped by heating at 95°C for 5 minutes. SYBR real-time polymerase chain reaction was performed using the SYBR Green PCR Master Mix (Applied Biosystems, Foster City, CA). Intron-spanning primers for *GAPDH*, *IFI44L*, *RSAD2*, *ISG15*, *IFI27*, *OAS3*, *LAMP3*, *LGALS3BP*, *HTATIP2*, *IL29*, *IL28RA*, and *IL10RB* were designed. To differentiate the very homologous *IL28A* and *IL28B* genes, primers were designed accordingly so that the last nucleotide of the 3′ end of each primer bound to a nucleotide differing in each gene. Primer sequences are displayed in Supplementary Table 2.

All reactions were performed in duplicate on an ABI 7500 Fast Real-Time PCR System (Applied Biosystems). For *IL28A* and *IL28B*, the polymerase chain reaction product was run on an agarose gel to exclude unspecific amplification from genomic DNA (data not shown). Messenger RNA (mRNA) expression levels of the transcripts were normalized to glyceraldehyde-3-phosphate dehydrogenase (GAPDH) using the ΔCt method. Supplementary Table 3 contains the complete result set.

Extraction of Genomic DNA

Genomic DNA was isolated from human liver tissue with TRIzol reagent (Invitrogen) and DNeasy Blood & Tissue Kit (Qiagen) according to the manufacturer's instructions.

Table 1. Patient Characteristics

	SVR	Relapse	Nonresponse	Total
Patients, n	33	9	31	109
Age (*y*), mean ± SD[a]	40.9 ± 10.2	45.9 ± 6.8	49.6 ± 8.6	45.9 ± 9.4
Sex, n				
Female	14	3	10	39
Male	19	6	21	70
HCV RNA (*IU/mL*), mean ± SE[b]	$3.1 \pm 0.9 \times 10^6$	$4.5 \pm 2.0 \times 10^6$	$3.9 \pm 1.2 \times 10^6$	$3.9 \pm 0.8 \times 10^6$
Genotypes 1/2/3/4, n	7/4/16/6	5/1/3/0	24/2/2/3	63/7/27/12
METAVIR stages F0–1/F2/F3/F4, n	5/13/7/8	0/3/2/4	1/11/7/12	16/41/21/31
METAVIR grades A1/A2/A3, n	6/19/8	3/5/1	5/14/12	30/49/30

[a]Range, 20–69 years.
[b]Range, 4.4×10^2 to 6.9×10^7.

Genotyping of IL28B *Single Nucleotide Polymorphisms*

Genotyping for rs8099917 and rs12979860 single nucleotide polymorphisms (SNPs) was with TaqMan SNP genotyping assays (Applied Biosystems Inc, Foster City, CA). TaqMan probes and primers were designed and synthesized by Applied Biosystems: rs12979860, forward 5′-TGTACTGAACCAGGGAGCTC-3′, reverse 5′-GCGCGGAGTGCAATTCAAC-3′; Vic probe 5′-TGGTTCGCGCCTTC-3′, Fam probe 5′-CTGGTTCACGCCTTC-3′; rs8099917, ABI reference C_11710096_10. Automated allele calling was performed using SDS software from Applied Biosystems. Positive and negative controls were used in each genotyping assay.

Statistical Analyses

All gene expression data were $\log_{10}$ transformed for analysis. After confirmation of normal distribution (Shapiro–Wilk), the data were analyzed with Student *t* test using GraphPad Prism V4 (GraphPad Software, San Diego, CA). The association of the SNPs with SVR was assessed with a logistic regression model, where the *IL28B* genotypes were encoded for an additive model based on the minor alleles. For building a suitable design matrix, these factors were represented internally by contrasting each level with the baseline level "0." Significance estimates for the remaining nonbaseline levels were computed in the standard way, that is, as 2-tailed *P* values corresponding to the z-ratio based on a normal reference distribution.

Decision Trees and Random Forest Classifier

A decision tree is a tree-structured classifier. The tree is iteratively built by selecting variables according to their relevance for discriminating between the classes, where relevance is measured in terms of information gain.[12]

The random forest classifier generalizes this concept by building an ensemble of decision trees. For each object to be classified (in our case each patient), a tree in the ensemble votes for membership in one of the classes, and finally a patient is assigned to the class with the most votes. During the training phase, the patients are randomly divided into a training set ("bag") and a test set ("out-of-bag") using resampling techniques. The average error on the "out-of-bag" sets serves as an estimate for the predictive error (ERR) on new patients. The random forest feature score (RFFS) is a measure of the predictive power of the variables for separating the classes. Because this measure is a "true" out-of-bag estimate, negative importance scores can occur, indicating overfitting phenomena, that is, weaker predictive performance despite an augmented set of variables used for learning the decision trees.

The large datasets from the previously reported genome-wide association studies were taken from Supplementary Table 2 in Suppiah et al[9] and extrapolated from Figure 1 (European-Americans) from Ge et al.[7] These data were run through the random forest classifier, and area under the curve (AUC), and ERR estimates were calculated as described previously.

Results

Minor Alleles of the IL28B *Gene Are Associated With Decreased Hepatic* IL28B *Expression*

We genotyped 109 patients with CHC who underwent a liver biopsy. The clinical characteristics of the patients are shown in Table 1, and the full dataset is available in Supplementary Table 1. Among 73 patients assessable for response to pegIFN-α and ribavirin treatment, 33 had an SVR, 9 had a relapse, and 31 were nonresponders. The allele frequencies in this group of 109 white patients and also in the subgroup of the 73 treated patients were comparable to the previously reported frequencies, and the association of the *IL28B* genotypes with SVR was statistically significant (Figure 1*A* and Supplementary Table 1).[7–10] We extracted RNA from all liver biopsy specimens and quantified the expression of *IL28A* (IFNλ2), *IL28B* (IFNλ3), *IL29* (IFNλ1), IL28 receptor α (IL28Rα, encoded by *IL28RA*), and IL-10 receptor β (*IL10Rβ*) (the 2 chains of the heterodimeric class II cytokine receptor that binds all IFNλs) by quantitative polymerase chain reaction. Homozygosity for the minor rs12979860 allele was significantly associated with decreased *IL28B* expression (Figure 1*B*). The minor rs8099917 allele was also associated with decreased *IL28B* expression, but the differences did not reach statistical significance (Figure 1*B*). There was no association of *IL28B* allele variants with the other members of the IFNλ family or with the IFNλ receptor chains (Supplementary Figure 1).

ISG Expression and Response to Treatment

We next quantified the expression of the classifier genes *IFI44L*, *RSAD2*, *ISG15*, *IFI27*, *LAMP3*, *OAS3*, *LGALS3BP*, and *HTATIP2* in the liver biopsy specimens of all 109 patients. These genes belong to the group of 29 genes previously identified as best predictors of response to treatment in a supervised classifier analysis of microarray data from liver biopsy specimens.[2] The first 6 genes of this subgroup are ISGs.[2] In accordance with previous reports,[2–5] ISG expression was significantly higher in nonresponders and patients who experienced a relapse compared with patients with an SVR (Figure 2*A*). The expression of *IL28A*, *IL28B*, *IL29*, *IL28RA*, and *IL10RB* did not differ between patients with and without SVR (Figure 2*B*).

IL28B *Polymorphisms and Activation of the Hepatic IFN System Are Independent Predictors of Response to Treatment*

The minor *IL28B* variants could be associated with poor treatment outcome because they induce the constitutive expression of ISGs in the liver during HCV infec-

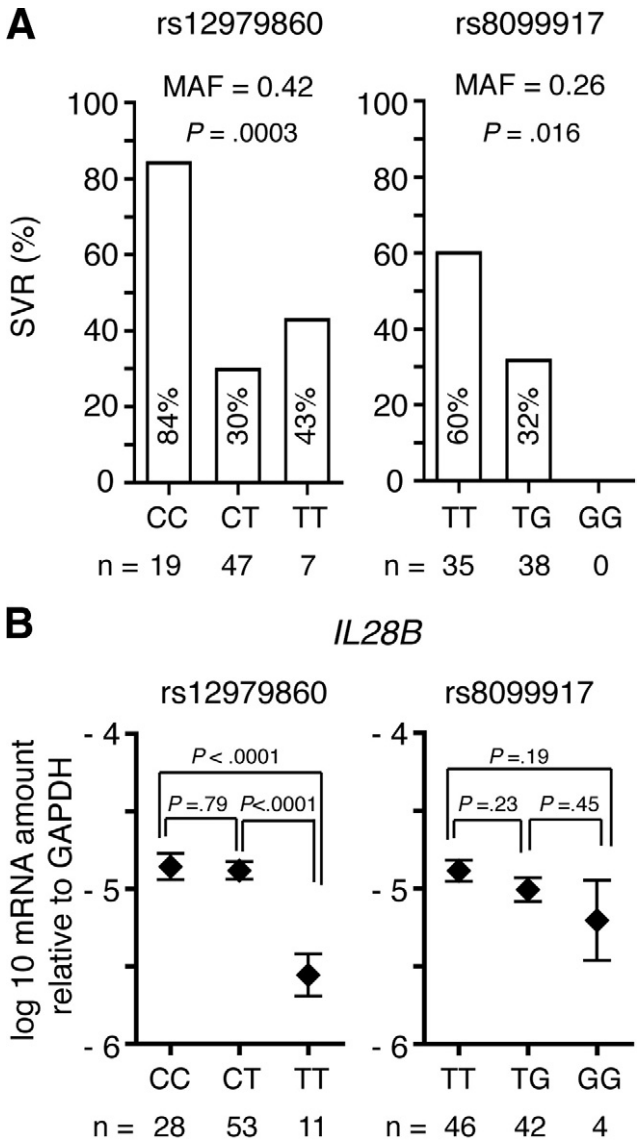

Figure 1. Association of *IL28B* SNPs with SVR and hepatic *IL28B* mRNA expression. (*A*) Percentage of SVR in different *IL28B* genotypes for the SNPs rs12979860 and rs8099917. The minor allele frequencies (MAF) for each SNP are indicated. Association of the major allele with SVR was assessed by a logistic regression model and is statistically significant for each SNP. (*B*) The minor *IL28B* allele correlates with lower expression of *IL28B* mRNA in the liver of patients with CHC. *IL28B* mRNA was determined by quantitative reverse-transcription polymerase chain reaction and normalized relative to GAPDH mRNA. Shown are the mean values (±SEM) after log transformation. The *P* values were obtained with Student *t* test. The *IL28B* genotypes for the rs12979860 and the rs8099917 SNPs and the number of patients in each group are shown below the plots.

tion. Compatibly with such a causal link, we found a statistically significant association between *IL28B* allele variants and the expression levels of the 6 ISGs (Figure 3*A* and Supplementary Figure 2*A*). As expected, the minor allele (poor response allele) was associated with an increased expression of ISGs.

To rigorously test the link between *IL28B* allelic variants and ISG expression, we compared ISG expression levels of SVR versus non-SVR patients within the different *IL28B* genotype groups. If the *IL28B* genotype would determine the expression level of ISGs in the liver, one would expect that both responders and nonresponders within the group of patients with the rs12979860 CC genotype have low ISG expression levels and that the patients with the rs12979860 CT or TT genotype have high expression levels irrespective of their treatment response. However, stratification of the samples according to treatment response revealed that ISG expression differed significantly between response groups within a given *IL28B* genotype group (Figure 3*B* and *C* and Supplementary Figures 2, 3, 4, 5*B* and *C*). In contrast, patients with an SVR had comparable ISG expression levels irrespective of their *IL28B* genotype. We conclude that the apparent correlation between *IL28B* genotype and ISG expression found in the nonstratified analysis (Figure 3*A*) is due to the unequal distribution of patients; there are few nonresponders in the rs12979860 CC group (3 of 19) but many in the rs12979860 CT group (33 of 47).

A significant correlation between *IL28B* genotypes and response to treatment has been reported for patients with HCV genotype 1 and 4 infections but not for HCV genotypes 2 and 3.[8] To exclude a potential confounding effect, we also analyzed our data after exclusion of HCV genotype 2 and 3 samples (Figure 4). Again, nonresponders had significantly higher ISG expression levels irrespective of the *IL28B* genotypes (Figure 4*B* and *C* and Supplementary Figures 3 and 5). We conclude that the *IL28B* genotype does not determine ISG expression. Rather, both ISG expression and *IL28B* genotype are associated with response to treatment but largely independent from each other.

Multivariate Analysis of Factors Associated With Final Treatment Response Identifies Hepatic Gene Expression of a Set of 4 Genes as Best Predictor

We used decision tree ensembles in the form of a random forest classifier[12] to quantify the relative predictive power of the *IL28B* allele variants; the hepatic expression of *IFI44L*, *RSAD2*, *ISG15*, *IFI27*, *LAMP3*, *OAS3*, *LGALS3BP*, and *HTATIP2*; the HCV genotype; viral load; sex; age; inflammatory grade; and fibrosis stage for prediction of response to treatment. As a result of this multivariate analysis, the predictive power of a variable for separating the 2 classes (eg, patients with an SVR vs patients without an SVR) is expressed as the RFFS. In the entire dataset including 73 patients, we identified the hepatic expression of *IFI27* (RFFS, 2.65), *ISG15* (RFFS, 2.01), and *RSAD2* (RFFS, 1.75) and the HCV genotype (RFFS, 1.77) as the strongest predictors (Figure 5*A*). The rs12979860 SNP followed at position 5. After exclusion of patients with HCV genotypes 2/3, the strongest predictors in this group of 45 patients with genotypes 1/4

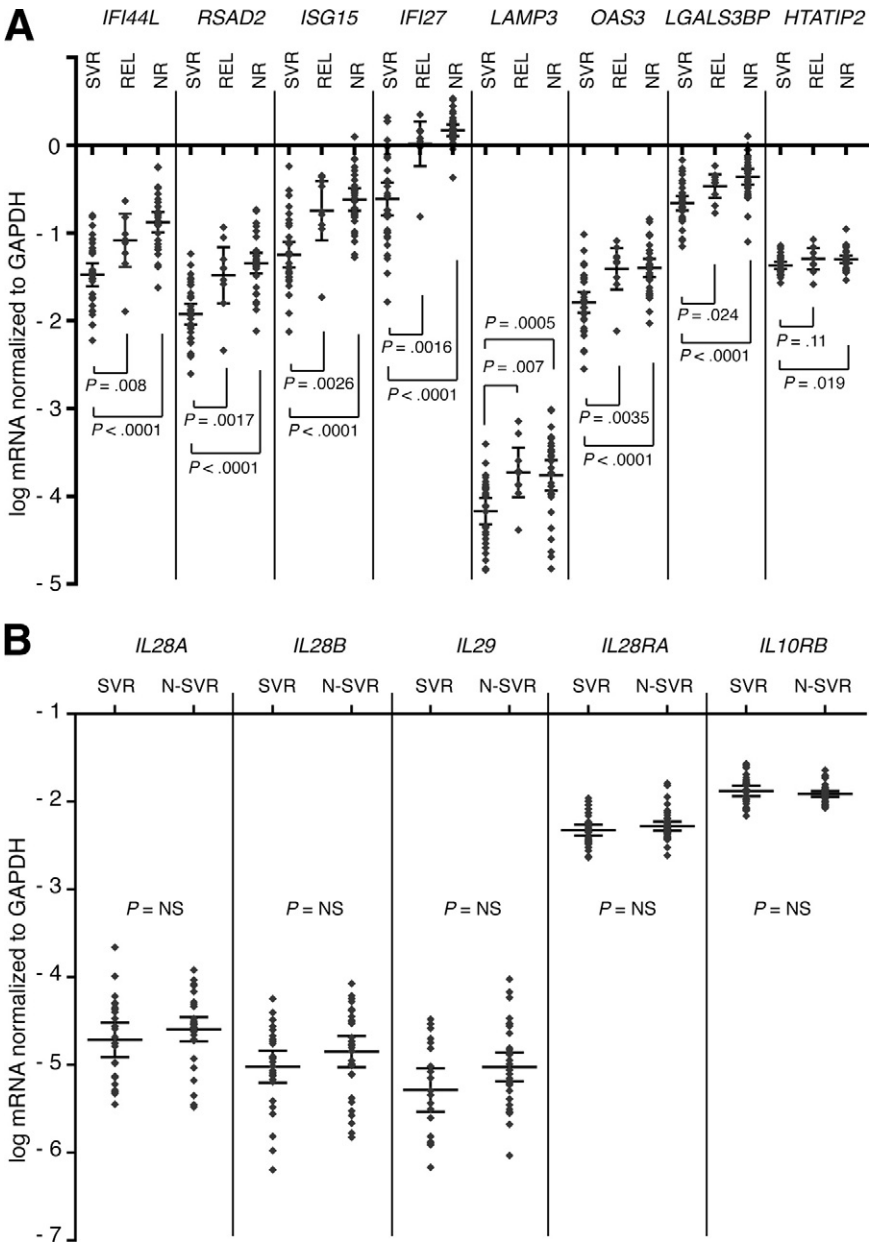

Figure 2. The expression of 8 classifier genes differs significantly between SVR, nonresponse, and relapse. *Aligned dot plot* of hepatic gene expression in patients with CHC stratified according to response to treatment (SVR, n = 33; relapse [REL], n = 9; nonresponse [NR], n = 31). Relative hepatic mRNA was assessed with quantitative polymerase chain reaction for (*A*) the 8 classifier genes (*IFI44L*, *RSAD2*, *ISG15*, *IFI27*, *LAMP3*, *OAS3*, *LGALS3BP*, and *HTATIP2*) and (*B*) genes from the IL28 cytokine family (*IL28A*, *IL28B*, *IL29*) and the IL28 receptor chains (*IL28RA*, *IL10RB*). Values are shown after log transformation and normalization to GAPDH. Each *dot* represents one sample. Mean ± SEM are shown. *P* values were obtained with Student *t* test.

infection were *IFI27* (RFFS, 2.87), *LGALS3BP* (RFFS, 2.53), *ISG15* (RFFS, 2.31), *RSAD2* (RFFS, 1.68), and *IFI44L* (RFFS, 1.49) (Figure 5*B*). The rs12979860 SNP followed at position 6.

We then calculated receiver operating characteristic (ROC) curves for the individual predictors. The HCV genotype had an AUC of 0.75 with an ERR of 0.27 (data not shown). In patients with HCV genotypes 1 and 4, the *IL28B* SNP variants rs12979860 and rs8099917 had AUCs/ERRs of 0.76/0.16 and 0.58/0.31, respectively (Figure 5*C*). These rather low values are not due to our small sample size, because we obtained similar values when using the published larger datasets for rs12979860 (0.69/0.32)[7] and rs8099917 (0.57/0.40).[9] When combining the 2 SNPs into one classifier, the AUC was 0.73 with an ERR of 0.16 (Figure 5*D*). By iteratively testing the predictive power of variable sets composed of the individual genes, we identified a set of 4 genes as having the best test performance: a random forest classifier using *IFI27*, *ISG15*, *RSAD2*, and *HTATIP2* had an AUC of 0.90 with an ERR of 0.12 (Figure 5*E*). The same 4 gene classifiers performed even slightly better in the HCV genotypes 1 and 4 subgroup (AUC, 0.92; ERR, 0.09) (Figure 5*E*). The performance was decreased by adding the information from the rs12979860 SNP (AUC, 0.90; ERR, 0.13) (Figure 5*F*). The weaker performance indicates that conditioned on the 4 genes *IFI27*, *ISG15*, *RSAD2*, and *HTATIP2*, the *IL28B* genotype carries no further discriminative information and only increases the model complexity, leading to overfitting phenomena.

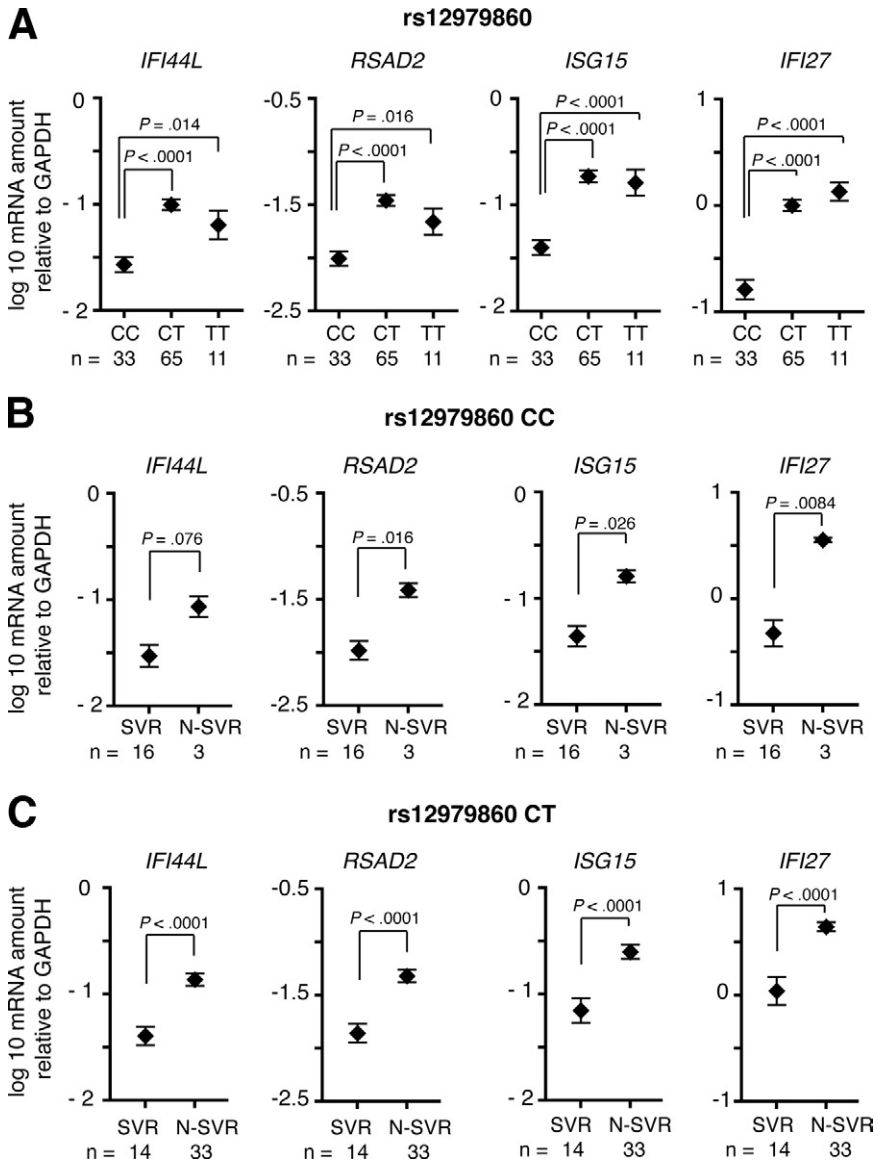

Figure 3. Hepatic ISG expression according to *IL28B* genotypes (SNP = rs12979860). (*A*) Expression of 4 ISGs (*IFI44L*, *RSAD2*, *ISG15*, *IFI27*) in the liver according to the *IL28B* genotype (rs12979860) in 109 patients with CHC. (*B*) Hepatic expression of 4 ISGs (*IFI44L*, *RSAD2*, *ISG15*, *IFI27*) in 19 patients with the rs12979860 CC genotype, stratified according to treatment response (SVR vs non-SVR). (*C*) Hepatic expression of 4 ISGs (*IFI44L*, *RSAD2*, *ISG15*, *IFI27*) in 47 patients with the rs12979860 CT genotype, stratified according to treatment response (SVR vs non-SVR). Shown are mean values (±SEM) after log transformation. *P* values were obtained with Student *t* test. The number of patients in each group is shown below the plots.

Multivariate Analysis of Factors Associated With Initial Treatment Response Identifies Hepatic Gene Expression of a Set of 5 Genes as Best Predictor

The prediction of the initial response to IFN-α could become important for future therapies with HCV protease or polymerase inhibitors, because patients with a preactivated endogenous IFN system would be exposed to direct antivirals without an effective protection against resistance development provided by coadministration of pegIFN-α/ribavirin. We therefore calculated a random forest classifier for predicting RVR, that is, a viral load <12 IU/mL after 4 weeks of treatment. In patients with HCV genotype 1 or 4, we identified the hepatic expression of *ISG15*, *RSAD2*, *IFI27*, *LAMP3*, and *IFI44L* as the strongest predictors (Figure 6*A*). ROC curves for the individual predictors showed an AUC of 0.6 with an ERR of 0.12 for the rs12979860 SNP (Figure 6*B*). The 5-gene classifier with *ISG15*, *RSAD2*, *IFI27*, *LAMP3*, and *HTATIP2* had an excellent performance with an AUC of 0.94 and an ERR of 0.04 (Figure 6*C*). The performance was not improved by adding the information from the rs12979860 SNP (AUC, 0.94; ERR, 0.06) (Figure 6*D*).

Discussion

The highly significant association of *IL28B* allelic variants with treatment outcome in CHC discovered recently by several research groups[7–10] opened up the perspective of developing *IL28B* genotyping as a pretreatment predictor of treatment response for individual patients. However, based on our ROC calculations with genotype data for *IL28B* SNPs rs12979860 and rs8099917, we conclude that the predictive power of such a test is insufficient for counseling individual patients with CHC. On the other hand, quantification of a set of

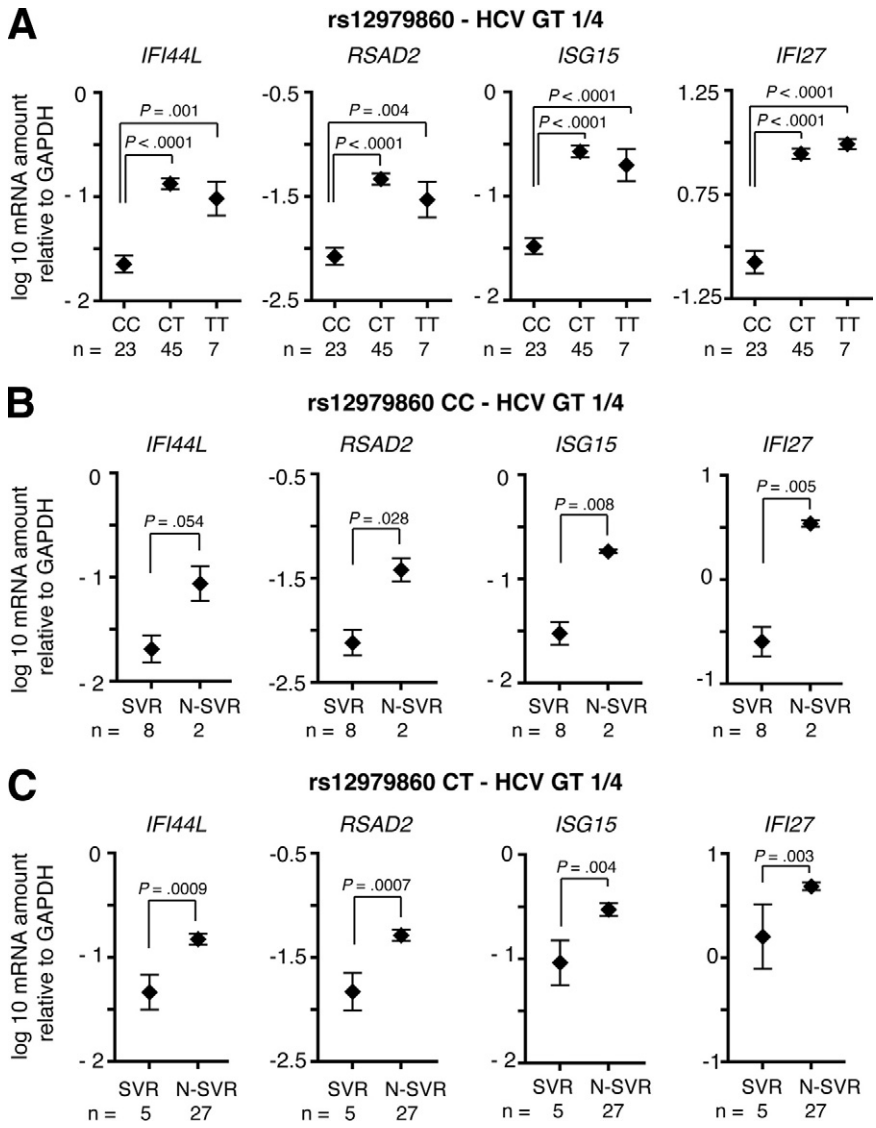

Figure 4. Hepatic ISG expression according to *IL28B* genotypes (SNP = rs12979860) in patients infected with HCV genotype 1 or 4. (*A*) Expression of 4 ISGs (*IFI44L*, *RSAD2*, *ISG15*, *IFI27*) in the liver according to the *IL28B* genotype (rs12979860) in 75 patients with CHC infected with HCV genotype 1 or 4. (*B*) Hepatic expression of 4 ISGs (*IFI44L*, *RSAD2*, *ISG15*, *IFI27*) in 10 patients with rs12979860 CC genotype, stratified according to treatment response (SVR vs non-SVR). (*C*) Hepatic expression of 4 ISGs (*IFI44L*, *RSAD2*, *ISG15*, *IFI27*) in 32 patients with rs12979860 CT genotype, stratified according to treatment response (SVR vs non-SVR). Shown are mean values (±SEM) after log transformation. *P* values were obtained with Student *t* test. The number of patients in each group is shown below the plots.

4 genes in pretreatment liver biopsy specimens allows prediction of treatment response to the current standard of care with pegIFN-α and ribavirin with an error rate of less than 15%. This classifier using *IFI27*, *ISG15*, *RSAD2*, and *HTATIP2* showed excellent test performance with an AUC of 0.90. Adding the *IL28B* genotype information to the 4-gene classifier did not improve the test performance.

For quantification of gene expression, a small piece of the liver biopsy specimen obtained during the workup of patients with CHC is stored at 4°C in buffer that stabilizes and protects cellular RNA. The samples can be shipped at ambient temperature to the laboratory. Extraction of RNA and quantification of classifier gene expression can be done within 1 day. Using standard expression values obtained from patients with known treatment response, the test allows us to predict the individual likelihood of a patient to have a response to therapy. In current clinical practice, liver biopsies are omitted in many patients, limiting the potential practicability of our test. PBMCs would be easier to obtain than liver biopsy material. Unfortunately, IFN-α induced quite distinct sets of genes in PBMCs versus liver,[2,13] and gene expression levels in PBMCs could not reliably classify patients into response groups in a supervised classifier analysis.[2] Quantitative serum protein analysis is also not a promising alternative to liver biopsy analysis, because none of the 4 classifier gene products identified in the present analysis and none of the 29 predictor genes identified in our previous analysis[2] is secreted from hepatocytes.

The causal factors and the mechanisms underlying the induction of ISGs in the liver of patients with CHC are not well understood. A genetic predisposition that regulates the host reaction to HCV infection could explain the observed interindividual differences in ISG induction. In this context, the *IL28B* genotype is a very attractive candidate for such a genetic factor, all the more because the

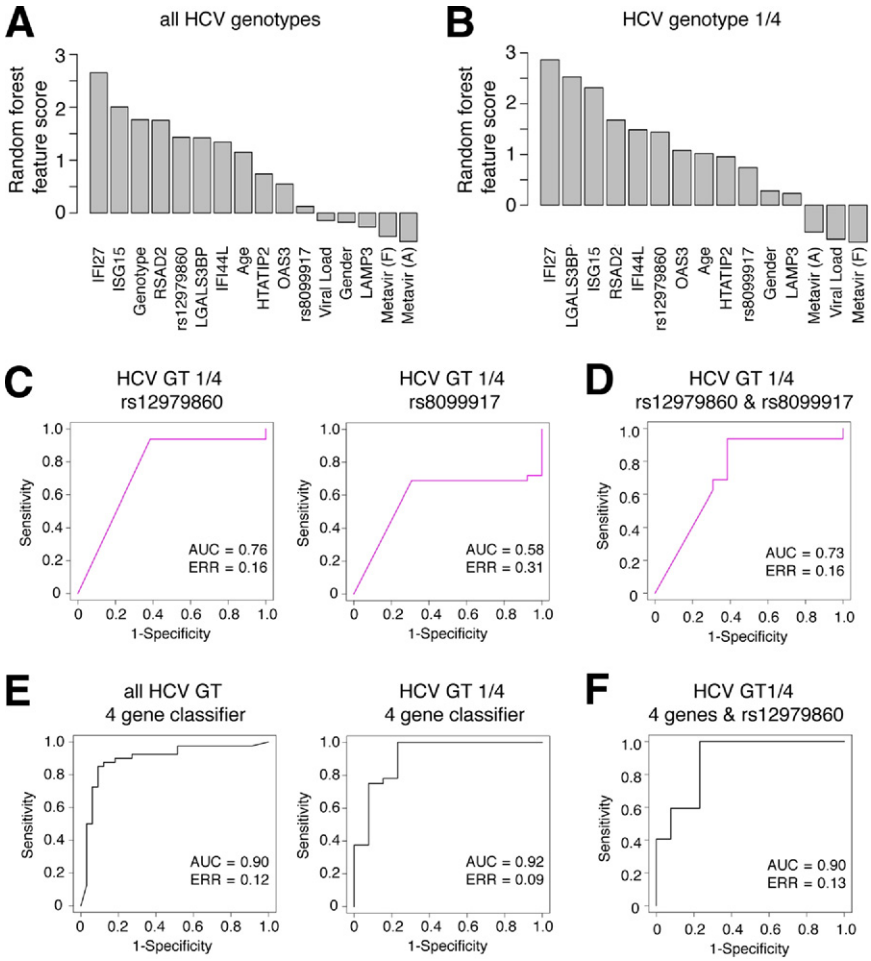

Figure 5. Hepatic expression of *IFI27*, *ISG15, RSAD2*, and *HTATIP2* is a better predictor of treatment response than *IL28B* allelic variants. (*A*) Importance plot of all variables in the entire 73 patient dataset (including all HCV genotypes). (*B*) Importance plot of all variables in the 45 treated patients with HCV genotypes 1 and 4. The RFFS is a measure of the predictive power of the variables for separating the classes. The importance of the variables is computed by permuting the values of a variable m in the out-of-bag case and putting these cases down the decision tree. The number of votes for the correct class in the permuted out-of-bag set is subtracted from the number of votes for the correct class in the untouched out-of-bag-set and averaged over all trees in the forest. This gives the importance score for variable m. Note that the importance score is computed on the out-of-bag set; hence, overfitting can occur. Negative importance scores imply that such overfitting phenomena indeed occur for some variables. (*C*) ROC curve for prediction of treatment response using the rs12979860 SNP (AUC, 0.76; ERR, 0.16) or the rs8099917 SNP (AUC, 0.58; ERR, 0.31) in patients with HCV genotype 1 or 4. (*D*) ROC curve with the combination of the rs12979860 and rs8099917 SNPs in patients with HCV genotypes 1 and 4 (AUC, 0.73; ERR, 0.16). (*E*) ROC curve for prediction of treatment response with a combination of *IFI27*, *ISG15*, *RSAD2*, and *HTATIP2* in the entire 73 patient dataset (AUC, 0.90; ERR, 0.12) or in the patients infected with HCV genotype 1 or 4 (AUC, 0.92; ERR, 0.09). (*F*) ROC curve using the combination of *IFI27*, *ISG15*, *RSAD2*, *HTATIP2*, and the rs12979860 SNP in patients with HCV genotypes 1 and 4 (AUC, 0.90; ERR, 0.13). Adding the *IL28B* genotype information to the 4-gene classifier impairs the performance of the classifier because of an increase in the complexity of the model without additional information gain (overfitting phenomenon).

IL28B gene product, IFNλ3, activates the same signal transduction pathways as type I IFNs and induces the same set of target genes.[14–18] Indeed, a recent study reported a strong association of hepatic ISG expression with *IL28B* genotype.[19] In this model, an increased expression of *IL28B/IFNλ3* in patients with the minor allele would result in higher ISG expression in the liver, which then would lead to nonresponse to pegIFN-α and ribavirin. However, our data do not support a direct link between *IL28B* genotype and hepatic ISG induction. First, the expression of *IL28B/IFNλ3* in the liver is decreased rather than increased in patients with the minor allele (Figure 1*B*). This finding is consistent with previous reports showing a lower expression of *IL28B/IFNλ3* in PBMCs from individuals with the minor allele.[9,10] Second, the strong association of higher ISG expression in the liver with the minor *IL28B* allele disappears after stratification for treatment response (Figures 3 and 4). If the *IL28B* genotype would determine ISG expression, we should have observed higher expression levels in responder patients with the minor allele compared with responders homozygous for the major allele, and the same genotype-dependent differences would also be present within the group of nonresponders. However, re-

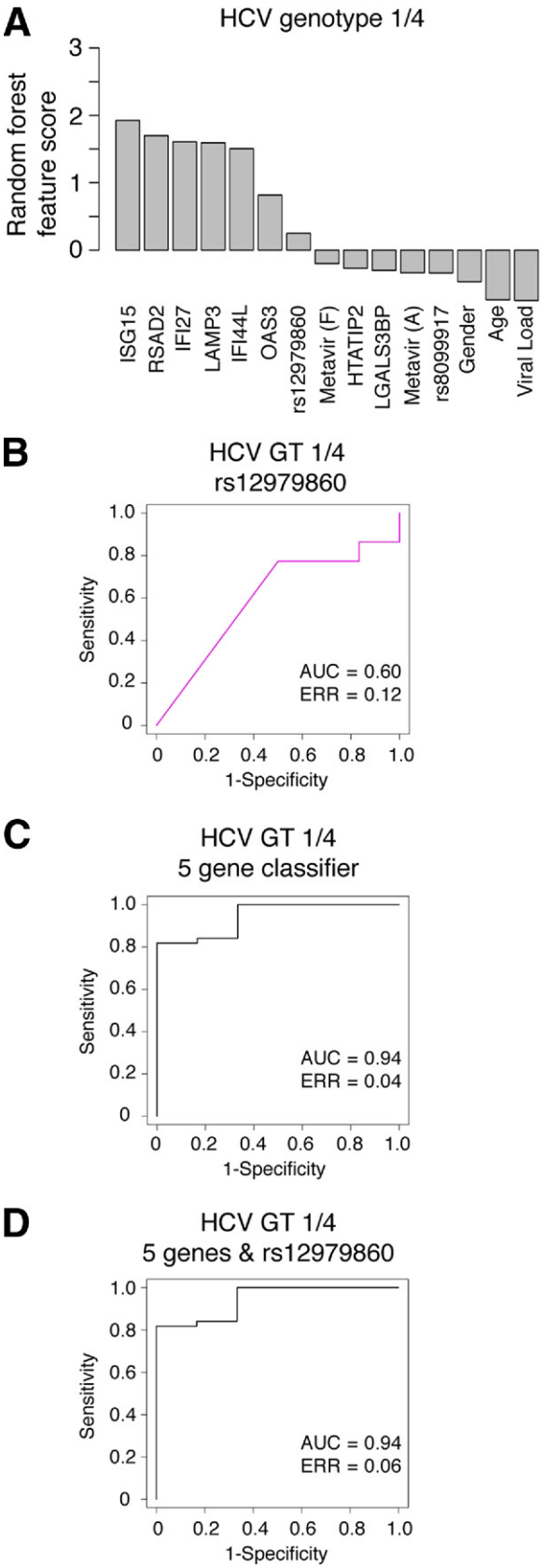

sponders had lower ISG expression levels than nonresponders irrespective of the genotype (Figures 3 and 4). We therefore conclude that IFN-induced gene expression in the liver and *IL28B* allelic variants are not causally linked but rather are independent predictors of response to therapy in CHC.

The association of *IL28B* allelic variants with response to pegIFN-α/ribavirin treatment has been discovered in large cohorts of HCV genotype 1–infected patients.[7–10] In patients with HCV genotype 2 or 3 infections, the response rates were also higher in rs8099917 TT patients compared to rs8099917 TG or GG (86% vs 80% SVR), but the difference did not reach statistical significance.[8] The same tendency without statistical significance was found in patients coinfected with HCV genotype 3 and human immunodeficiency virus (86% vs 81% SVR).[20] Genotype 4–infected patients behave more like genotype 1–infected patients and show large differences in SVR rates according to the *IL28B* genotype.[8,20] We believe that the absence of significant associations between SVR and *IL28B* genotype in genotype 2/3–infected patients is not caused by fundamental biological differences of the host-virus interactions. Rather, the published studies of patients with HCV genotype 2/3 were probably underpowered to detect associations between SVR rates and *IL28B* genotype because of the very high SVR rates found in HCV genotype 2/3–infected patients in general. We have included all HCV genotypes in our present analysis, because we have shown previously that pretreatment hepatic ISG expression levels and HCV genotype are independent predictors of response to treatment[2] and because we do not expect that the HCV genotype has an influence on the expression level of *IL28B* mRNA. Nevertheless, we have also analyzed the association between ISG expression and *IL28B* genotype separately for the patients infected with HCV genotype 1 and 4. As shown in Figure 4, ISG expression level analysis stratified according to treatment response showed significantly higher ISG expression in non-SVR patients independent of *IL28B* genotype even in this smaller group of patients infected with HCV genotype 1 and 4.

The discovery of the *IL28B* polymorphism has generated a strong interest in its potential usefulness for the pretreatment counseling of patients with CHC. Genotyping is a rather simple and straightforward procedure and does not require a liver biopsy, making it an attractive

Figure 6. Prediction of RVR in patients infected with HCV genotype 1 or 4. (*A*) Importance blot of all variables in the 50 patients infected with HCV genotype 1 or 4 and with RVR data available. (*B*) ROC curve with the rs12979860 SNP for prediction of RVR (AUC, 0.60; ERR, 0.12). (*C*) ROC curve using a combination of *IFI27*, *ISG15*, *RSAD2*, *HTATIP2*, and *LAMP3* as a 5-gene classifier to predict RVR (AUC, 0.94; ERR, 0.04). (*D*) ROC curve with the combination of *IFI27*, *ISG15*, *RSAD2*, *HTATIP2*, *LAMP3*, and the rs12979860 SNP to predict RVR (AUC, 0.94; ERR, 0.06).

alternative to hepatic ISG testing. However, there are some intrinsic limitations to genotyping. At present, *IL28B* genotyping is restricted to HCV genotype 1 infections. Also, genotyping has a high error rate in predicting SVR, because at least 1 in 5 patients with the favorable rs8099917 TT or rs12979860 CC genotype will not have an SVR. Likewise, genotyping has a high error rate in predicting nonresponse, because approximately 2 in 5 patients with rs8099917 TG/GG or rs12979860 CT/TT genotypes will still have an SVR. Genotyping can assign an individual patient to one of 2 (or maximal 3) groups with distinct mean SVR rates. On the other hand, hepatic ISG expression measurements can generate continuous probability values, allowing us to assign a distinct likelihood of SVR to an individual patient. Such classifiers using a limited number of ISGs seem to be more accurate for prediction of treatment response, independent from HCV genotypes. For patients with a liver biopsy specimen obtained during the routine diagnostic workup, tests that quantify the expression of a limited number of ISGs in the liver could become important for individualized patient counseling. Furthermore, pretreatment assessment of hepatic ISG induction could become an important tool for patient management in the upcoming era of directly acting antiviral therapy in CHC. Current experience with HCV protease and polymerase inhibitors has shown their strong antiviral activity but also the capacity of HCV to develop drug resistance within the first weeks of therapy. To some degree, the selection of drug-resistant strains can be prevented by the coadministration of pegIFN-α and ribavirin. However, combination therapy most likely will not effectively protect patients who do not respond to pegIFN-α at all (IFN-null responders) because of a highly preactivated endogenous IFN system in the liver.

In conclusion, *IL28B* genotype and hepatic ISG expression are both associated with response to treatment with pegIFN-α/ribavirin but not causally linked. The association of ISG expression with treatment outcome is dominant over the *IL28B* genotype, because patients with high pretreatment ISG expression do not respond to treatment despite a favorable *IL28B* genotype, whereas low ISG expression is strongly linked to SVR even in patients with an unfavorable *IL28B* genotype. In our analysis, the most accurate prediction of response was obtained with a 4-gene classifier comprising *IFI27*, *ISG15*, *RSAD2*, and *HTATIP2*.

Supplementary Material

Note: To access the supplementary material accompanying this article, visit the online version of *Gastroenterology* at www.gastrojournal.org, and at doi: 10.1053/j.gastro.2010.11.039.

References

1. Ghany MG, Strader DB, Thomas DL, et al. Diagnosis, management, and treatment of hepatitis C: an update. Hepatology 2009; 49:1335–1374.
2. Sarasin-Filipowicz M, Oakeley EJ, Duong FH, et al. Interferon signaling and treatment outcome in chronic hepatitis C. Proc Natl Acad Sci U S A 2008;105:7034–7039.
3. Chen L, Borozan I, Feld J, et al. Hepatic gene expression discriminates responders and nonresponders in treatment of chronic hepatitis C viral infection. Gastroenterology 2005;128:1437–1444.
4. Asselah T, Bieche I, Narguet S, et al. Liver gene expression signature to predict response to pegylated interferon plus ribavirin combination therapy in patients with chronic hepatitis C. Gut 2008;57:516–524.
5. Sarasin-Filipowicz M, Wang X, Yan M, et al. Alpha interferon induces long-lasting refractoriness of JAK-STAT signaling in the mouse liver through induction of USP18/UBP43. Mol Cell Biol 2009;29:4841–4851.
6. Bellecave P, Sarasin-Filipowicz M, Donze O, et al. Cleavage of mitochondrial antiviral signaling protein in the liver of patients with chronic hepatitis C correlates with a reduced activation of the endogenous interferon system. Hepatology 2010;51:1127–1136.
7. Ge D, Fellay J, Thompson AJ, et al. Genetic variation in IL28B predicts hepatitis C treatment-induced viral clearance. Nature 2009;461:399–401.
8. Rauch A, Kutalik Z, Descombes P, et al. Genetic variation in IL28B is associated with chronic hepatitis C and treatment failure: a genome-wide association study. Gastroenterology 2010; 138:1338–1345, 1345 e1–7.
9. Suppiah V, Moldovan M, Ahlenstiel G, et al. IL28B is associated with response to chronic hepatitis C interferon-alpha and ribavirin therapy. Nat Genet 2009;41:1100–1104.
10. Tanaka Y, Nishida N, Sugiyama M, et al. Genome-wide association of IL28B with response to pegylated interferon-alpha and ribavirin therapy for chronic hepatitis C. Nat Genet 2009;41:1105–1109.
11. Thomas DL, Thio CL, Martin MP, et al. Genetic variation in IL28B and spontaneous clearance of hepatitis C virus. Nature 2009; 461:798–801.
12. Breiman L. Random forests. Machine Learning 2001;45:5–32.
13. Lanford RE, Guerra B, Lee H, et al. Genomic response to interferon-alpha in chimpanzees: implications of rapid downregulation for hepatitis C kinetics. Hepatology 2006;43:961–972.
14. Kotenko SV, Gallagher G, Baurin VV, et al. IFN-lambdas mediate antiviral protection through a distinct class II cytokine receptor complex. Nat Immunol 2003;4:69–77.
15. Sheppard P, Kindsvogel W, Xu W, et al. IL-28, IL-29 and their class II cytokine receptor IL-28R. Nat Immunol 2003;4:63–68.
16. Doyle SE, Schreckhise H, Khuu-Duong K, et al. Interleukin-29 uses a type 1 interferon-like program to promote antiviral responses in human hepatocytes. Hepatology 2006;44:896–906.
17. Marcello T, Grakoui A, Barba-Spaeth G, et al. Interferons alpha and lambda inhibit hepatitis C virus replication with distinct signal transduction and gene regulation kinetics. Gastroenterology 2006;131:1887–1898.
18. Zhou Z, Hamming OJ, Ank N, et al. Type III interferon (IFN) induces a type I IFN-like response in a restricted subset of cells through signaling pathways involving both the Jak-STAT pathway and the mitogen-activated protein kinases. J Virol 2007;81:7749–7758.
19. Honda M, Sakai A, Yamashita T, et al. Hepatic ISG expression is associated with genetic variation in interleukin 28B and the outcome of IFN therapy for chronic hepatitis C. Gastroenterology 2010;139:499–509.
20. Rallon NI, Naggie S, Benito JM, et al. Association of a single nucleotide polymorphism near the interleukin-28B gene with response to hepatitis C therapy in HIV/hepatitis C virus-coinfected patients. AIDS 2010;24:F23–F29.

Received August 10, 2010. Accepted November 10, 2010.

Reprint requests

Address requests for reprints to: Prof. Markus H. Heim, MD, University Hospital Basel, Petersgraben 4, CH-4031 Basel, Switzerland. e-mail: markus.heim@unibas.ch; fax: (41) 61 265 53 52.

Acknowledgments

M.T.D. and F.H.T.D. contributed equally to this work.

Conflicts of interest

The authors disclose no conflicts.

Funding

Supported by Swiss National Science Foundation (SNF) grant 320030-116106 and Oncosuisse (OCS) grant 02192-02-2008 (to M.H.H.), SNF grant 323500-123714 (to M.T.D.), SNF grant 32003B-127613/1 and a Leenaards foundation grant (to P.-Y.B.), and the LiverX grant of the SNF (to V.R. and M.H.H.).

4.2.2 IL28B genotype affects the susceptibility to IFN-α in the liver of patients with hepatitis C but not in non-infected primary human hepatocytes

Stronger induction of a subset of ISGs in CC carriers upon pegIFN-α-2b injection *in vivo*.

So far the mechanism by which the effect of the IL28B polymporphisms on treatment response is achieved could not be identified by direct sequencing and association studies, and functional studies are direly needed. The lack of a defined functional mutation limits the use of possible genetic constructs and restricts the research so far to human samples. We had a look at the transcriptome data from a previous study where paired liver biopsies were obtained from patients with CHC before treatment and 4h after the first injection with pegIFN-α-2b[89]. 10 patients who had shown low pretreatment ISG transcript levels in the liver and had responded well with over 3 log10 drop of viral load within 4 weeks were selected for further analysis, and IL28B genotype (rs12979860) was determined. 7 patients carried the favorable CC genotype, and 3 were CT carriers. Of a total of 157 upregulated ISGs an amount of 26 genes, of which 3 representative genes are depicted in Figure 4.2.1, were significantly higher induced in CC than CT carriers at 4h after pegIFN-α-2b injection (t test, $P < 0.005$). We hypothesized that these 26 genes represents a subset of differently regulated ISGs which is affected by IL28B genetic variants rendering them more susceptible to IFN-α stimulation. However, we cannot exclude due to the relative small sample size that these 26 genes are false positives, despite the application of a stringent P value of < 0.005.

ISG induction after IFN-α or IFN-λ treatment in primary human hepatocytes is not affected by IL28B genotype.

Thus, we next wanted to explore, whether this effect was reproducible in a cell culture model of primary human hepatocytes (PHH), which would give us the means to properly study possible underlying mechanisms. PHH were genotyped for IL28B, and treated with IFN-α or IFN-λ for 4h. However, neither by IFN-α nor by IFN-λ any difference in fold induction between PHH with CC and CT alleles was observed looking at *BATF2*, *IFIT3* and *RSAD2* (Figure 4.2.2), rendering this an unsuitable model to study the effect we observed *in vivo*.

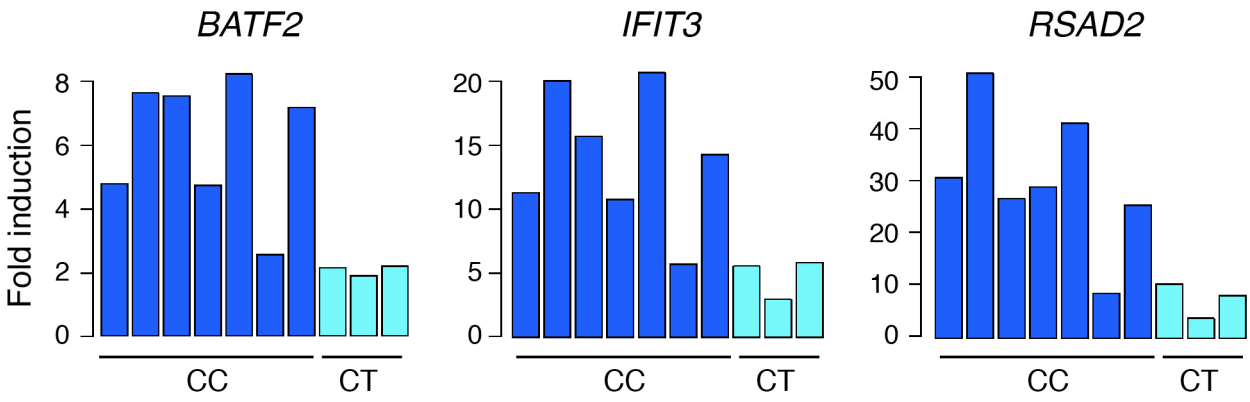

Figure 4.2.1. *Three exemplary genes differentially induced in IL28B CC and CT carriers. 10 rapid responder patients of Sarasin-Filipowicz et al.* [89]*, were genotyped for IL28B rs12979860 SNP. Stratification of paired transcriptome data according to IL28B genotype revealed a stronger induction of 26 ISGs in CC than CT carriers. Shown is fold induction between pre-treatment biopsy and the paired biopsy 4h after pegIFN-α-2b injection. Student's t test, P < 0.005.*

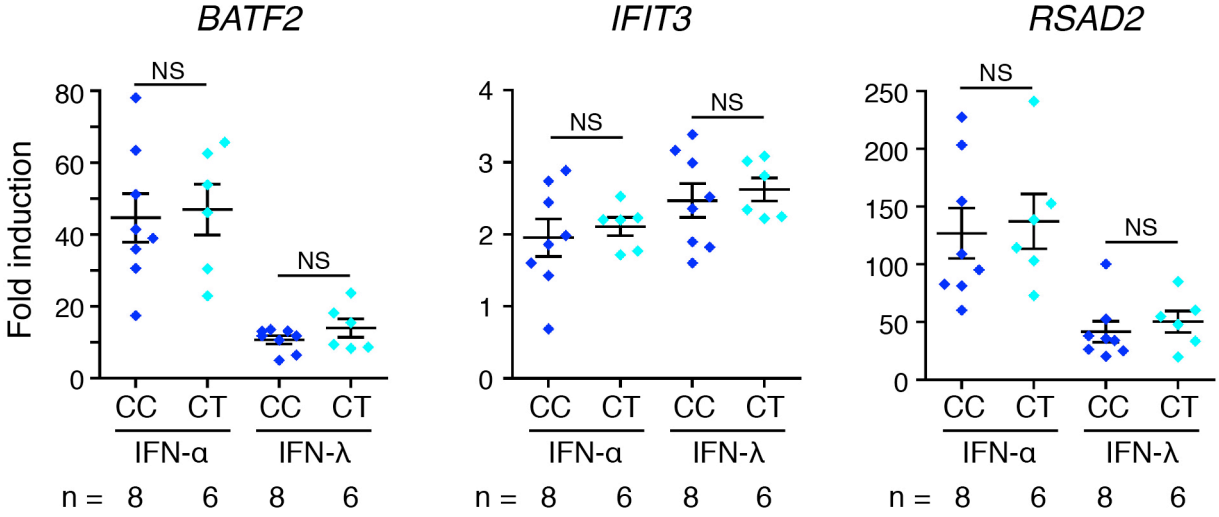

Figure 4.2.2. *Gene induction in PHH carrying different IL28B genotypes. PHH were genotyped for IL28B and treated with IFN-α (1000 U/ml) or IFN-λ (100ng/ml) for 4h. Shown is the fold induction compared to untreated PHH of the same donor. Student's t test. P value <0.05 was considered significant.*

4.3 Despite persistent high serum levels, peg-IFNα only transiently induces ISGs in the liver of patients with chronic hepatitis C

Transient induction of the Jak-STAT pathway in the liver upon administration of peg-IFN-α-2b.

To study the long-term pharmacodynamics of pegIFN-α-2b in the liver of patients with CHC 12 subjects were included to undergo a second paired biopsy (B2) at one of the following time points within a week after the first subcutaneous injection of pegIFN-α-2b: 16h, 48h, 96, or 144h (Figure 4.3.1A). Additional data from 6 responder patients derived from an earlier study in the Hepatology Laboratory were included for a 4h time point[89]. Patients were only asked to participate after decision for treatment has been already taken and gene expression analysis in the diagnostic liver biopsy (B1) by real-time RT-PCR revealed low ISG expression with a high chance to accomplish good response to pegIFN-α. Indeed, all included patients achieved cEVR and 94% SVR upon treatment with pegIFN-α-2b and ribavirin irrespective of viral or Il28B genotype, fibrosis stage or any other factor known to be associated with response (Table 4.3.1).

For most of the patients serum was available to test for IFN-α-2b levels at the time of the second biopsy. Serum levels measured by ELISA were very similar to those described in previous studies[56,134], with a peak at the 16h time point around 1000 pg/ml following a decline to 200 pg/ml, but without reaching pre-treatment levels even at 144h (Figure 4.3.1B). In contrast, despite continuous elevated serum IFN-α levels, phosphorylation of STAT1 (pSTAT1) reflecting induction of the Jak-STAT pathway in the liver was mainly induced in the first 16h and was not prolonged (Figure 4.3.1C-D).

Formation of temporally distinct clusters of interferon regulated genes.

We next analyzed gene expression in the B1 and B2 liver samples with Affymetrix U133 Plus 2.0 arrays. A considerable amount of genes were up- or downregulated with a fold change > 2.0 between B2 and B1 in 2/3 of the patients at each time point with a maximum at 16h (Figure 4.3.2A). Interestingly, these results differ from what has been observed in healthy chimpanzees, where maximum induction has been seen at 4h and most genes had again basal expression levels at 24h[135]. Since clearly not all genes were already upregulated immediately at 4h, we wanted to further dissect possible different transcriptional patterns. Rather than focusing on single genes

we chose a global clustering approach. The data was normalized in order to avoid that the difference in fold induction amplitude of the genes affects the clustering which was merely focused on temporal distribution. Using a Dirichlet process we were able to let the clustering algorithm define the amount of clusters from the data itself in an unbiased way. The algorithm produced four robust clusters of upregulated genes, which we termed early (number of genes: 144), intermediate (31), late (299), and very late ISG cluster (20); and two downregulated gene clusters with 143 and 98 genes, respectively (Figure 4.3.2B-C). We observed that the majority of genes were maximally upregulated at 4h and 16h and didn't show prolonged nor any second wave of induction. It has been shown that the IFN signaling cascade gets refractory to continuous IFNα exposure *in vitro* and *in vivo*[96,97], and that the main negative regulator responsible for this refractoriness in the mouse liver has been identified to not be SOCS1 or SOCS3, two important negative regulators, but USP18[97]. Consistently, mRNA levels of SOCS1 and SOCS3 were only upregulated initially or weakly induced, while USP18 showed elevated mRNA levels throughout the observation period, and also continuous higher protein expression than at baseline (Figure 4.3.2D-E).

PegIFN-α-2a does not induce the IFN signaling differently than PegIFN-α-2b at 144h, despite continuous high serum levels.

The different design of pegIFN-α-2b and pegIFN-α-2a leads to very distinct pharmacokinetic properties. While the single chain PEG moiety of pegIFN-α-2b is subject to hydrolysis, which leads to a release of IFN-α-2b into the human body and faster elimination of the drug, pegIFN-α-2a is not hydrolyzed, has a lower absorption rate and is much slower eliminated. Pharmacokinetic studies have shown that unlike pegIFN-α-2b with a serum level peak around 24h and subsequent gradual decline, pegIFN-α-2a achieves maximum serum levels around 80h which sustain up to 168h[56,134]. Accordingly, in our three study patients treated with pegIFN-α-2a serum levels of 6800, 7200, and 20'000 pg/ml at 144h were comparable to those assessed in previous studies. We wanted to exploit this difference in pharmacokinetic behavior to gain more evidence that IFN signaling is indeed refractory regardless of the amount of pegIFN-α circulating the body. Indeed, even with high level of pegIFN-α-2a in the serum STAT1 phosphorylation in the liver was not markedly increased at 144h (Figure 4.3.3A).

We next tried to assess with several approaches whether pegIFN-α-2a leads to a different and stronger induction of ISGs at 144h than pegIFN-α-2b. The amount of genes expressed over 2 fold in 2/3 of the patients in each group was similar (49 vs. 59), and genes with the highest absolute expression levels from each group or the biggest fold change compared to B1 didn't

show significant differences than the usual inter-individual variabilities. We also assessed different genes from each representing cluster, to see whether some clusters might be specifically affected by continuous high exposure to pegIFN-α. However, again genes of all clusters behaved identically between the two groups. Taken together, this evidence suggests that in the human liver the gene induction is refractory to continuous IFN-α exposure and thus does not support the hypothesis that the superiority of pegIFN-α in antiviral therapy is due to longer serum half-life.

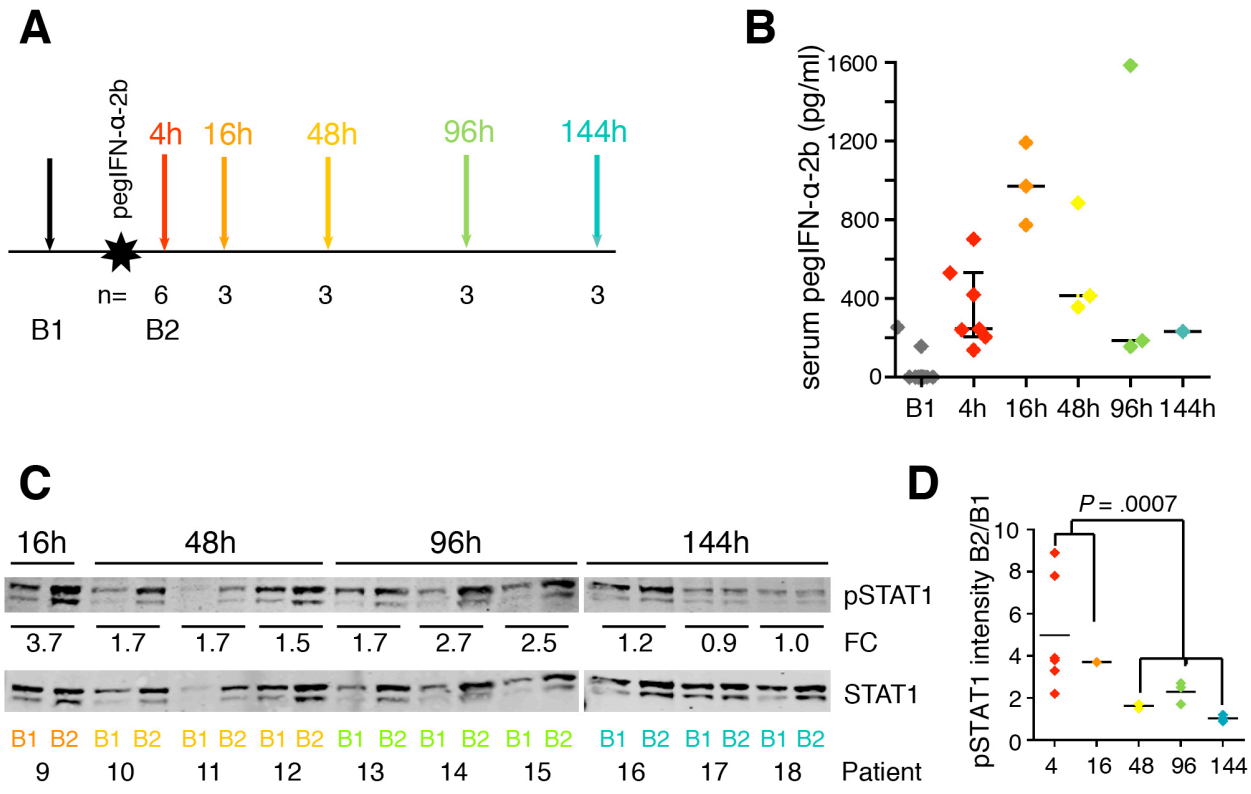

Figure 4.3.1. *Transient induction of the Jak-STAT pathway in the liver upon administration of peg-IFN-α-2b. (A) Study design. All patients had a diagnostic biopsy before therapy (B1). Paired second biopsies (B2) were taken at the indicated time points. Numbers of patients are indicated below the plot. (B) Serum concentration of pegIFN-α-2b measured by ELISA. Median is indicated. (C) Phosphorylated STAT1 (pSTAT1) and STAT1 protein expression by Western Blot analysis using whole cell extracts of liver samples from B1 and B2 of each patient. At TP 16h only liver material from patient 9 was left for protein analysis. (D) Graphical representation of the induction of pSTAT1 between B2 and B1. The intensity of the pSTAT1 bands on the Western blots has been assessed by ImageJ. The values of time point 4h have been taken from Sarasin-Filipowicz et al.[89]. P-value obtained by Mann-Whitney test. Patient numbers as indicated in Table 1.*

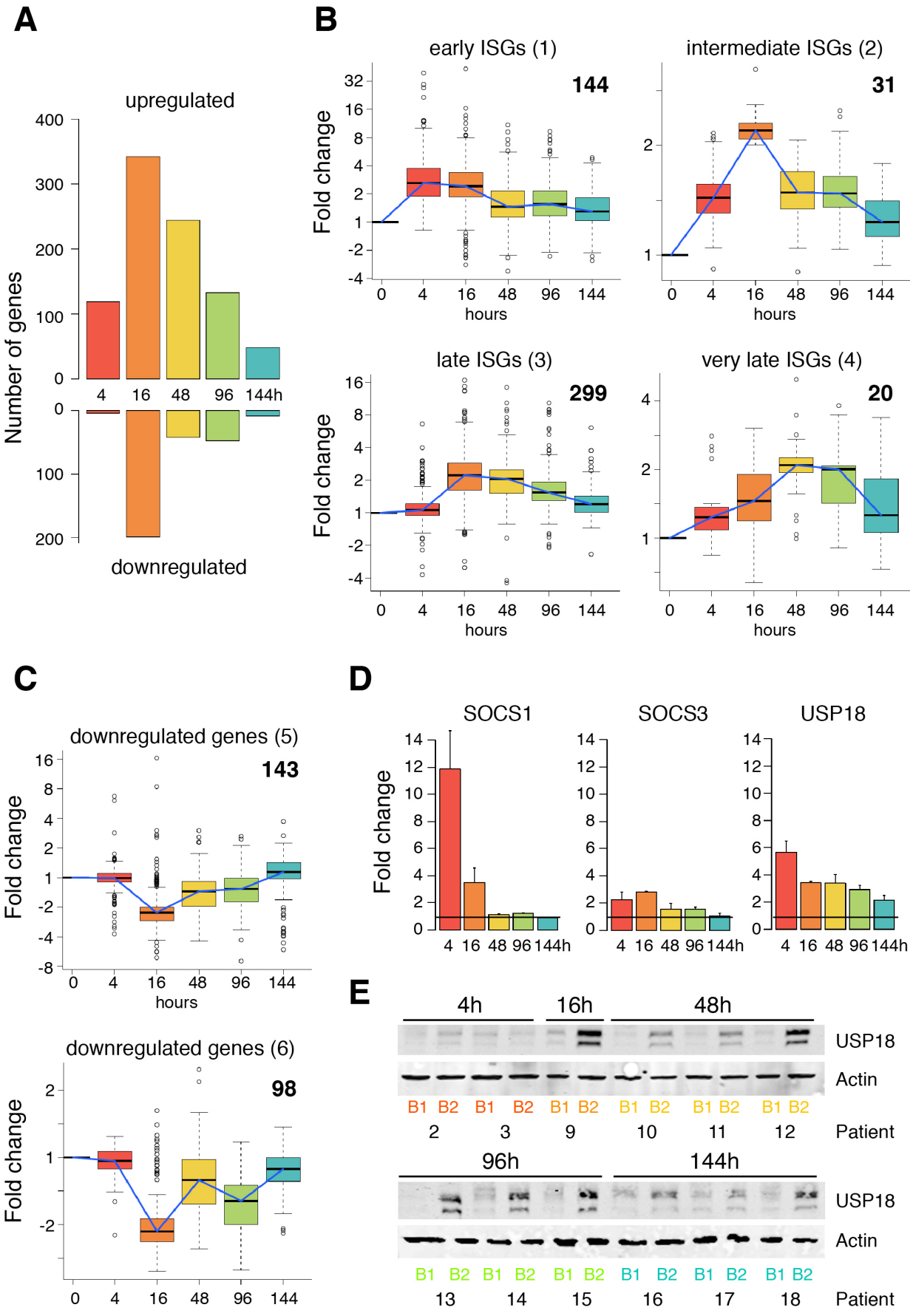
A
upregulated
Number of genes
400
300
200
100
0
4
16
48
96
144h
0
100
200
downregulated
B
early ISGs (1)
144
Fold change
hours
intermediate ISGs (2)
31
late ISGs (3)
299
very late ISGs (4)
20
C
downregulated genes (5)
143
downregulated genes (6)
98
D
SOCS1
SOCS3
USP18
E
4h
16h
48h
96h
144h
USP18
Actin
B1 B2
2 3 9 10 11 12
13 14 15 16 17 18
Patient

Figure 4.3.2. *ISGs are induced in temporally distinct clusters. (A) Number of genes > 2-fold up- or downregulated at each time point in 2/3 of the patients. (B) Clustering analysis of the upregulated genes produced four robust clusters (1-4) that comprised of early, intermediate, late, and very late ISGs. Blue line indicates the median expression. The number of genes in each cluster is provided in the plot. (C) Two clusters of downregulated genes (5-6). (D) Bar plot of the fold change of mRNA expression between B1 and B2 of SOCS1, SOCS3 and USP18. Shown are mean with SEM. Black line indicates baseline. (E) USP18 protein expression by Western blot analysis using whole cell extracts of liver samples from B1 and B2. Patient numbers as indicated in Table 1.*

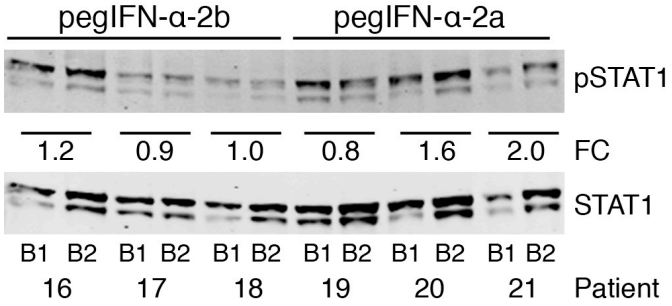

Figure 4.3.3. *PegIFN-α-2a does not induce the IFN signaling differently than pegIFN-α-2b at 144h, despite continuous high serum levels. Phosphorylated STAT1 (pSTAT1) and STAT1 protein expression by Western Blot analysis using whole cell extracts of liver samples from B1 and B2 of each patient. Fold induction of the pSTAT1 bands is indicated.*

Table 1: Patient characteristics

				Viral load, log IU/mL			Response						
Patient no.	Age	Sex	HCV GT	Baseline	4-week	12-week	4-week	12-week	Follow-up	METAVIR	IL28B GT	Time point	Medication
1	52	m	3	7.14	neg	neg	RVR	cEVR	SVR	A2/F2	CC	4h	
2	37	m	3	4.9	neg	neg	RVR	cEVR	SVR	A1/F2	CT	4h	
3	54	f	2	4.95	neg	neg	RVR	cEVR	SVR	A3/F3	CT	4h	
4	57	m	3	5.25	2.15	neg	RR	cEVR	Relapse	A3/F4	CC	4h	
5	38	m	4	4.08	1.66	neg	RR	cEVR	SVR	A2/F2	CT	4h	
6	51	f	1	6.82	3.52	neg	RR	cEVR	SVR	A1/F2	CT	4h	
7	26	m	3	4.58	neg	neg	RVR	cEVR	SVR	A1/F1	TT	16h	
8	42	f	3	5.49	neg	neg	RVR	cEVR	SVR	A1/F2	CT	16h	
9	41	m	3	5.66	neg	neg	RVR	cEVR	SVR	A1/F2	CT	16h	PegIFNα-2b
10	30	m	3	7.07	neg	neg	RVR	cEVR	SVR	A2/F2	CT	48h	
11	57	f	1	5.95	neg	neg	RVR	cEVR	SVR	A2/F2	CC	48h	
12	37	m	3	6.72	1.28	neg	RR	cEVR	SVR	A3/F2	CT	48h	
13	62	m	4	7.16	neg	neg	RVR	cEVR	SVR	A3/F4	CT	96h	
14	43	m	1	5.6	1.63	neg	RR	cEVR	SVR	A3/F2	CC	96h	
15	40	m	1	5.16	1.41	neg	RR	cEVR	SVR	A3/F4	CT	96h	
16	25	f	1	2.64	neg	neg	RVR	cEVR	SVR	A2/F2	CC	144h	
17	70	m	2	6.86	1.84	neg	RR	cEVR	SVR	A2/F3	CT	144h	
18	34	m	3	5.56	neg	neg	RVR	cEVR	SVR	A2/F2	CT	144h	
19	57	f	2	5.18	neg	neg	RVR	cEVR	SVR	A2/F2	CC	144h	PegIFNα-2a
20	57	m	1	6.54	4.59	3.33	Non-RR	EVR	interrupted	A3/F4	CT	144h	
21	38	f	4	6.32	5.07	neg	Non-RR	cEVR	SVR	A3/F4	CC	144h	

5. Discussion

5.1 The host response in acute hepatitis C infection

In this first study, human liver biopsies obtained 2-5 months after HCV infection, i.e. during the early phase of the adaptive immune response, were analyzed. In accordance with data obtained from experimentally infected chimpanzees that were then biopsied during acute infection[118,119,120], we found CD8+ T- cell infiltrates, increased intrahepatic IFN-γ mRNA expression, and ALT elevation. Importantly, T cell infiltrates were co-localized with hepatocytes positive for nuclear pSTAT1 immunostaining, providing evidence that the predominant mediator of STAT1 activation in that phase of infection is IFN-γ that is secreted by infiltrating T cells which are in close contact to stimulated hepatocytes. The microarray analysis of ISG expression revealed a strong enrichment of IFN-γ specific ISGs in AHC liver biopsy samples, further confirming that the predominant IFN in this phase of HCV infection is IFN-γ and not IFN-α. These results do not support the hypothesis that liver infiltrating HCV-specific T cells are stunned, with impaired IFN-γ production, and are therefore not capable to clear the infection[117,136]. We were however not able to draw any conclusions on possible molecular factors that favour viral persistence or spontaneous clearance due to the small sample size and the ethical necessity to treat those patients while they were still in the acute phase of infection with greater chances of achieving SVR.

It is puzzling that in this phase of infection the vast majority of typical IFN-α stimulated genes are not induced. Interference of HCV with the innate immune system could explain these findings. However, the Jak-STAT pathway doesn't seem to be impaired as IFN-γ signaling is very effective with strong pSTAT1 signals and IFN-γ stimulated gene induction. We weren't able to detect MAVS cleavage and thus impairment of the viral sensing mechanism in any of the AHC patients either. This is clearly in contrast to CHC, where MAVS cleavage has been identified in about half of the patients[125]. The lack of detection of cleaved MAVS in our AHC patients might be due the low viral load in these patients rendering MAVS cleavage below detection levels, or that MAVS cleavage is an important viral escape mechanism in the very first weeks after infection in humans which we fail to detect at our observation period.

It would also be very interesting to find the time range after unsuccessful spontaneous clearance when preactivation of the IFN system is induced. So far we do not know whether

this actually happens early after persistence to chronic infection and or whether it occurs only later. This would allow us to better understand the mechanisms that are involved in the establishment of preactivation. This assessement is however limited by the fact that it is rather impossible to extrapolate the exact time of infection in most of the patients, as long as they were not diagnosed during acute infection.

One aim of this study was to find possible molecular explanations for the difference in response rates to pegIFN-α in AHC (SVR >90%) and CHC (SVR 50%). The idea that AHC patients did not induce hepatic ISGs clearly proved to be wrong. However, since we were able to dissect these ISG expression profiles into IFN-γ driven in AHC or IFN-α driven in CHC-NR, we could thoroughly examine possible differences. A candidate molecule that immediately attracted attention was USP18. In a previous study in mice USP18 has been identified as a key mediator of IFN-α refractoriness[97]. Similarly, an association between induction of USP18 and impaired IFN signaling has been seen in the livers of responder patients upon injection with pegIFN-α (Figure 4.3.2). Comparison of responders versus non-responders to pegIFN-α in a combined analysis including AHC, CHC-R and CHC-NR showed that USP18 induction is associated with non-response to pegIFN-α (Figure 4.1.5). Therefore the apparent lack of USP18 induction in AHC might explain the improved response rate to pegIFN-α treatments in these patients compared to patients with CHC, and it could be worthwile to investigate USP18 as a potential therapeutical target to improve response to IFN-α.

5.2 IL28B genetic variations and the host response in chronic hepatitis C infection

The discovery of polymorphisms around the IL28B gene and its association with treatment response had a tremendous impact on hepatitis C research. For one the possibility to predict treatment response in the clinical setting was considered, and on the other hand the first genetic factor was uncovered that would allow new means to explore and better understand the interplay between the immune system and HCV infection. However, IL28B genotype has so far not been compared with other predictive factors, especially hepatic ISG induction. We therefore wanted to assess the power of different treatment predictors, and explore if IL28B genetic variants could explain the preactivation of the IFN system in some CHC patients.

First, by analyzing a large cohort of CHC patients we have shown that a 4-gene classifier measuring hepatic mRNA expression levels had much better predictive power than IL28B genotyping. IL28B genotyping is just one variable that gives only three distinct outputs while measurement of ISG expression levels allows for continuous variable measurements. A combination of ISGs thus creates continuous probability values that can much better define the likelihood for treatment response in an individual patient than IL28B genotyping. It can also be speculated, that hepatic ISG expression is a more immediate phenotype more accurately representing the actual situation in the liver before treatment that dictates response to pegIFN-α.

The arrival of two protease inhibitors Boceprevir and Telaprevir to the therapy of CHC patients infected with genotype 1 HCV infection adds further complexity. Phase 1 studies have clearly shown that monotherapy is not applicable and only leads to selection of resistant virus strains[97]. Therefore triple combination with pegIFN-α and ribavirin is the treatment of choice. However, about 30% of the patients still do not respond to this treatment and from our current knowledge it has to be hypothesized that the majority of these non-responders would be probably preactivated with high ISG levels and thus do not respond to pegIFN-α, rendering the addition of a protease inhibitor useless. Prediction of non-response in the era of triple therapy could therefore be very useful to avoid the rising of resistant strains, and it should be tested if high expression of hepatic ISGs indeed predicts non-response in this setting.

The drawback of hepatic ISG expression measurement is the requirement of a liver biopsy, which is invasive and has a small risk of complications. While a diagnostic liver biopsy is still included in the American Association of the Study of Liver Diseases (AASLD) guidelines[57], biopsies are often omitted in current clinical practice. An appropriate alternative with more easy to obtain material would be very promising. I just discussed that IL28B genotyping to our opinion is not suitable, and analysis of ISG expression in PBMCs revealed that it does not represent the situation of IFN activation in the liver[89,135]. Recently, measurement of IFN-γ inducible protein 10 (IP-10), a chemokine secreted to the blood, came forward as a potential predictor of non-response that was able to improve the predictive power of IL28B genotyping[137–139]. However, whether this is superior or at least equal to our four gene classifier or hepatic ISG levels in general has not been investigated. In our study a combination of IL28B genotype with ISG expression did not improve our classifier, and we didn't have blood samples to test for IP-10 levels, and thus compare its predictive power.

In our study we have seen that hepatic ISG induction representing the activation of the endogenous IFN system is associated with genetic polymorphisms near the IL28B gene. However, this association is lost when the patients are stratified to treatment response, which led us to the conclusion that it is very unlikely that IL28B genetic variants are the only and direct cause of preactivation of the endogenous hepatic IFN system. Whether this is really the cause is still under debate since our conclusions diverge from two other studies[140,141]. However, three more recently published articles again drew similar conclusions that IL28B genotype and ISG expression are rather independent factors associated with treatment response[142,143,144]. To clearly settle this matter, a thorough understanding of the effect of the IL28B genotype would be necessary.

One hypothesis is that the genetic variations lead to difference in expression, since no obvious variation in the coding sequence could be discovered. But analyses of IL28B mRNA levels led to very contradictory results in the field. The expression seems to be very low and the high sequence similarity between IL28A and IL28B makes it difficult to properly design assays to distinguish them. In two GWAS publications IL28 mRNA expression was measured in PBMCs indicating paradoxically lower expression in minor allele carriers, which are the ones showing higher hepatic ISG expression. We observed a similar trend in the liver (Section 4.2.1, Figure 1), while others could not detect a significant difference[141]. Despite discrepant data none has so far described higher IL28B levels in minor allele carriers and this hypothesis thus can probably be abolished. How lower levels of IL28B might explain higher ISG induction remains a mystery.

By looking at our data from 10 responder patients with paired liver biopsies, one before and one after 4h of pegIFN-α injection, we hoped to gain some insight of the effect of IL28B genetic variants on the response to pegIFN-α. Although the sample size was relatively low, there was a consistent and significant difference in induction of a subset of ISGs according to the IL28B genotype. It has to be stated that all these patients had low pretreatment ISG levels and virologically responded well to therapy, limiting the risk of any bias interfering with response to IFN. However, we were however not able to reproduce these findings in an *in vitro* model using PHH. It might very well be that HCV infection is necessary, or that a complex interaction of different cell types as in an infected liver is required to see that effect. PHH are not very easily infected with HCVcc and the replication rate is usually very low. Marukian et al. infected fetal liver cells with different IL28B genotypes with HCVcc and looked at HCV-induced ISG induction[145]. Similarly, they were not able to see an IL28B genotype driven difference in ISG expression. Another group has investigated the effect of

IL28 polymorphisms on the induction of ISGs in PBMCs upon treatment in CHC patients[143]. They saw a stronger induction of ISGs in patients with the favorable CC genotype, and thus concluded that the non-response associated T allele carriers had an aberrant baseline induction of the innate immune system. These interpretations should be considered with some caution since they did not control for hepatic ISG induction in these patients and it has been shown that PBMCs do not reflect the hepatic immune response in the case of HCV infection[89,135]. Thus, the effect of IL28B polymorphisms in HCV infection remains unclear, and more research is needed to uncover the underlying mechanisms.

5.3 Refractoriness to pegIFN-α therapy

In our study of the pharmacodynamics of pegIFN-α in the liver we were able to show that the IFN signaling is transient with peak pSTAT1 levels in the first 16 hours and also a peak induction of ISGs at 16h. The majority of genes thereafter decrease steadily back to baseline and do not show prolonged or a second wave of induction. This refractoriness was associated with a permanent increase in USP18 mRNA and protein levels, which has been shown to be a key mediator of refractoriness to IFN-α in the mouse liver[97].

A first analysis of uninfected chimpanzees which were treated with either human or chimpanzee IFN-α or human pegIFN-α and then serially liver biopsied at 4h, 8h and 24h revealed with all three treatments a rapid induction with a maximal response for most ISGs at 4h, a decline at 8h and baseline levels at 24h[135]. Those data are surprisingly different from our observations in humans where we clearly see a majority of ISGs maximally increased at 16h (Section 4.3, figure 2). In this chimpanzee study the rapid downregulation has been interpreted with the IFNAR receptor and the Jak-STAT pathway getting desensitized. A more rapid induction of USP18 in the chimpanzees could be a possible explanation for this phenomenon. However, USP18 as a key negative regulator has not yet been discovered at that time, and thus has not been looked at.

We describe here for the first time different clusters of interferon regulated genes in the liver that differ in their temporal transcription pattern upon pegIFN-α treatment. We have identified 4 clusters of upregulated genes (early, intermediate, late, and very late), as well as two downregulated gene clusters. It would be interesting to learn how these different transcription patterns arise. One obvious explanation would be a first induction of additional transcription

activators that in a second wave induce further ISGs. A biocomputional approach looking at main transcription factor binding sites in the promoter of the genes in the different clusters revealed however, that in each cluster, be it early or late ISGs, ISRE binding sites that are bound by the phosphorylated STATs were the absolutely dominant motifs (data not shown) rendering this possibility unlikely. Clearly further research has to be done to understand the orchestrated process of ISG induction over time.

The canonical Jak-STAT pathway and the regulation of transcription upon IFN stimulation is very well understood on the molecular level. In our analysis we did also see over 200 genes transcriptionally downregulated more than 2-fold upon IFN-α stimulation. While repression of genes upon IFN-α treatment has already been described earlier[135], it is not clear how this is actually achieved. One could think of induction of transcriptional repressors or epigenetic changes, and it would be worthwile to further elucidate these mechanisms for a more thorough understanding of IFN signaling.

We could definitely observe that at late time points the liver is refractory to circulating IFN-α. Even constant high serum levels of pegIFN-α did not lead to a continuous upregulation of ISGs to remain a constant antiviral state. Therefore we still have no proof that the superiority of pegIFN-α is explained by permanent ISG induction until the next injection is received, but rather evidence for the opposite. We are aware that we do not have a treatment arm that received IFN-α injections instead of pegIFN-α to directly compare possible differences in pharmacodynamics, since it would be ethically not correct to provide a sub-standard of care treatment to those patients. Nevertheless, no differences in ISG induction between IFN-α and pegIFN-α application have been found in chimpanzees and our data clearly also indicate a transient induction albeit with slower kinetics than in the chimpanzees. It would be very interesting to investigate if the patients are again as responsive to a second injection of pegIFN-α after 7 days as they were to the first injection, but this would require 3 biopsies per patient and is thus not really realizable.

Taken together, we provide first evidence for refractoriness to IFN-α in the human liver and our data might be a helpful resource for further research of IFN-signaling in the liver.

5.4 Outlook: Visualization of HCV

One completely unresolved question remains why patients with a preactivated IFN system who show similar induction of ISGs like responder patients upon pegIFN-α treatment are not able to spontaneously clear the virus.
One could imagine that the infected cells are repressed to induce ISGs by the means which HCV has to inhibit the Jak-STAT pathway, and therefore ISGs are expressed only in non-infected hepatocytes, where they are ineffective. A model derived from *in vitro* data also postulates that HCV is effectively blocking translation by phosphorylating PKR, and thus also inhibits the translation of ISG mRNA[116].
The limitation that so far hampered the investigation and proof of these important concepts *in vivo* was the inability to reliably visualize HCV in liver biopsies. Several immunohistochemical protocols with different antibodies have not been reproducible. Another approach combining 2-photon microscopy with virus-specific, fluorescent, semiconductor probes has also not been reproduced so far[146].

Additionally, the source that is responsible for this ISG induction has also not been identified. We failed to measure hepatic IFN-α or IFN-β mRNA levels in CHC patients, as did earlier studies in chimpanzees[123,147] and more recently also in humans[148]. IFN-λ levels again are also very low expressed and not different between responders and non-responders, and IFN-γ is induced in the late acute phase, but not in CHC. It remains puzzling that despite strong induction of ISGs the respective source is not measurable in liver biopsies, and it leads to the question, whether a so far unidentified IFN or cytokine might be responsible. An IFN that has slightly different properties compared to IFN-α making it unsuccessful to clear the virus effectively.

New visualization techniques and more sensitive measuring techniques are therefore one of the most direly needed advances that would help to unravel the unresolved questions in the field of virus-host interactions in HCV infection.

5.5 Concluding remarks

With the experimental approaches outlined in this thesis we were able to contribute to the understanding of host-virus interactions in acute and chronic hepatitis C. Analyzing liver biopsy samples, we were able to dissect the molecular differences between the host response in acute and chronic hepatitis C together with a possible explanation to the difference in treatment susceptibility, and we have shed some light on the connection of IL28B genetic variants and preactivation of the IFN system, additionally providing a test to predict treatment response that could be readily used in the clinical setting. Last, we describe for the first time the pharmacodynamics of pegIFN-α in the human liver gathering evidence that IFN-α signaling gets refractory, questioning a ten-year-old theory that the superior pharmacokinetics of pegIFN-α are responsible for the better efficacy in the treatment of CHC.

Altogether these findings provide insights that help to better understand hepatitis C infection and IFN-signaling in the human liver, knowledge that should be eventually helpful to improve the care of patients suffering from this important liver disease.

References

1. Shepard CW, Finelli L, Alter MJ. Global epidemiology of hepatitis C virus infection. The Lancet Infectious Diseases 2005;5:558–567.

2. Choo QL, Kuo G, Weiner AJ, et al. Isolation of a cDNA clone derived from a blood-borne non-A, non-B viral hepatitis genome. Science 1989;244:359–362.

3. Grakoui A, McCourt DW, Wychowski C, et al. Characterization of the hepatitis C virus-encoded serine proteinase: determination of proteinase-dependent polyprotein cleavage sites. Journal of Virology 1993;67:2832 –2843.

4. Lohmann V, Körner F, Koch J-O, et al. Replication of Subgenomic Hepatitis C Virus RNAs in a Hepatoma Cell Line. Science 1999;285:110 –113.

5. Blight KJ, Kolykhalov AA, Rice CM. Efficient Initiation of HCV RNA Replication in Cell Culture. Science 2000;290:1972 –1974.

6. Lindenbach BD, Evans MJ, Syder AJ, et al. Complete replication of hepatitis C virus in cell culture. Science 2005;309:623–626.

7. Wakita T, Pietschmann T, Kato T, et al. Production of infectious hepatitis C virus in tissue culture from a cloned viral genome. Nat Med 2005;11:791–796.

8. Lindenbach BD, Meuleman P, Ploss A, et al. Cell culture-grown hepatitis C virus is infectious in vivo and can be recultured in vitro. Proceedings of the National Academy of Sciences of the United States of America 2006;103:3805 –3809.

9. Mercer DF, Schiller DE, Elliott JF, et al. Hepatitis C virus replication in mice with chimeric human livers. Nat Med 2001;7:927–933.

10. Bissig K-D, Wieland SF, Tran P, et al. Human liver chimeric mice provide a model for hepatitis B and C virus infection and treatment. Journal of Clinical Investigation 2010;120:924–930.

11. Dorner M, Horwitz JA, Robbins JB, et al. A genetically humanized mouse model for hepatitis C virus infection. Nature 2011;474:208–211.

12. Kuiken C, Simmonds P. Nomenclature and Numbering of the Hepatitis C Virus. In: Tang H, ed. *Hepatitis C: Methods and Protocols*.Vol 510. Totowa, NJ: Humana Press; :33–53.

13. Jopling CL, Yi M, Lancaster AM, et al. Modulation of Hepatitis C Virus RNA Abundance by a Liver-Specific MicroRNA. Science 2005;309:1577 –1581.

14. Moradpour D, Penin F, Rice CM. Replication of hepatitis C virus. Nat Rev Micro 2007;5:453–463.

15. Poenisch M, Bartenschlager R. New Insights into Structure and Replication of the Hepatitis C Virus and Clinical Implications. Semin Liver Dis 2010;30:333–347.

16. André P, Perlemuter G, Budkowska A, et al. Hepatitis C Virus Particles and Lipoprotein Metabolism. Seminars in Liver Disease 2005;25:93–104.

17. Fletcher NF, Wilson GK, Murray J, et al. Hepatitis C Virus Infects the Endothelial Cells of the Blood-Brain Barrier. Gastroenterology.

18. Pileri P, Uematsu Y, Campagnoli S, et al. Binding of Hepatitis C Virus to CD81. Science 1998;282:938 –941.

19. Agnello V, Ábel G, Elfahal M, et al. Hepatitis C virus and other Flaviviridae viruses enter cells via low density lipoprotein receptor. Proceedings of the National Academy of Sciences 1999;96:12766 –12771.

20. Scarselli E, Ansuini H, Cerino R, et al. The human scavenger receptor class B type I is a novel candidate receptor for the hepatitis C virus. EMBO J 2002;21:5017–5025.

21. Evans MJ, Hahn T von, Tscherne DM, et al. Claudin-1 is a hepatitis C virus co-receptor required for a late step in entry. Nature 2007;446:801–805.

22. Ploss A, Evans MJ, Gaysinskaya VA, et al. Human occludin is a hepatitis C virus entry factor required for infection of mouse cells. Nature 2009;457:882–886.

23. Lupberger J, Zeisel MB, Xiao F, et al. EGFR and EphA2 are host factors for hepatitis C virus entry and possible targets for antiviral therapy. Nat. Med. 2011;17:589–595.

24. Sainz B, Barretto N, Martin DN, et al. Identification of the Niemann-Pick C1-like 1 cholesterol absorption receptor as a new hepatitis C virus entry factor. Nat Med 2012;advance online publication.

25. Blanchard E, Belouzard S, Goueslain L, et al. Hepatitis C Virus Entry Depends on Clathrin-Mediated Endocytosis. Journal of Virology 2006;80:6964 –6972.

26. Morikawa K, Lange CM, Gouttenoire J, et al. Nonstructural protein 3–4A: the Swiss army knife of hepatitis C virus. Journal of Viral Hepatitis 2011;18:305–315.

27. Ciesek S, Hahn T von, Manns MP. Second-wave Protease Inhibitors: Choosing an Heir. Clinics in Liver Disease 2011;15:597–609.

28. Egger D, Wölk B, Gosert R, et al. Expression of Hepatitis C Virus Proteins Induces Distinct Membrane Alterations Including a Candidate Viral Replication Complex. Journal of Virology 2002;76:5974 –5984.

29. Ago H, Adachi T, Yoshida A, et al. Crystal structure of the RNA-dependent RNA polymerase of hepatitis C virus. Structure 1999;7:1417–1426.

30. Lesburg CA, Cable MB, Ferrari E, et al. Crystal structure of the RNA-dependent RNA polymerase from hepatitis C virus reveals a fully encircled active site. Nat. Struct. Biol. 1999;6:937–943.

31. Legrand-Abravanel F, Nicot F, Izopet J. New NS5B polymerase inhibitors for hepatitis C. Expert Opinion on Investigational Drugs 2010;19:963–975.

32. Jones CT, Murray CL, Eastman DK, et al. Hepatitis C Virus p7 and NS2 Proteins Are Essential for Production of Infectious Virus. Journal of Virology 2007;81:8374 –8383.

33. Luik P, Chew C, Aittoniemi J, et al. The 3-dimensional structure of a hepatitis C virus p7 ion channel by electron microscopy. Proceedings of the National Academy of Sciences 2009;106:12712 –12716.

34. Jirasko V, Montserret R, Appel N, et al. Structural and Functional Characterization of Nonstructural Protein 2 for Its Role in Hepatitis C Virus Assembly. Journal of Biological Chemistry 2008;283:28546 –28562.

35. Chang K-S, Jiang J, Cai Z, et al. Human apolipoprotein e is required for infectivity and production of hepatitis C virus in cell culture. J. Virol. 2007;81:13783–13793.

36. Gastaminza P, Cheng G, Wieland S, et al. Cellular determinants of hepatitis C virus assembly, maturation, degradation, and secretion. J. Virol. 2008;82:2120–2129.

37. Huang H, Sun F, Owen DM, et al. Hepatitis C virus production by human hepatocytes dependent on assembly and secretion of very low-density lipoproteins. Proc. Natl. Acad. Sci. U.S.A. 2007;104:5848–5853.

38. Aach RD, Stevens CE, Hollinger FB, et al. Hepatitis C virus infection in post-transfusion hepatitis. An analysis with first- and second-generation assays. N. Engl. J. Med. 1991;325:1325–1329.

39. Santantonio T, Wiegand J, Tilman Gerlach J. Acute hepatitis C: Current status and remaining challenges. Journal of Hepatology 2008;49:625–633.

40. Alter HJ, Purcell RH, Shih JW, et al. Detection of antibody to hepatitis C virus in prospectively followed transfusion recipients with acute and chronic non-A, non-B hepatitis. N. Engl. J. Med. 1989;321:1494–1500.

41. Seeff LB. The history of the "natural history" of hepatitis C (1968–2009). Liver International 2009;29:89–99.

42. Locasciulli A, Testa M, Pontisso P, et al. Prevalence and natural history of hepatitis C infection in patients cured of childhood leukemia. Blood 1997;90:4628–4633.

43. Kenny-Walsh E. Clinical outcomes after hepatitis C infection from contaminated anti-D immune globulin. Irish Hepatology Research Group. N. Engl. J. Med. 1999;340:1228–1233.

44. Missiha SB, Ostrowski M, Heathcote EJ. Disease Progression in Chronic Hepatitis C: Modifiable and Nonmodifiable Factors. Gastroenterology 2008;134:1699–1714.

45. Thein H, Yi Q, Dore GJ, et al. Estimation of stage‐specific fibrosis progression rates in chronic hepatitis C virus infection: A meta‐analysis and meta‐regression. Hepatology 2008;48:418–431.

46. Hutchinson SJ, Bird SM, Goldberg DJ. Influence of alcohol on the progression of hepatitis C virus infection: a meta-analysis. Clin. Gastroenterol. Hepatol. 2005;3:1150–1159.

47. Poynard T, McHutchison J, Davis GL, et al. Impact of interferon alfa‐2b and ribavirin on progression of liver fibrosis in patients with chronic hepatitis C. Hepatology 2000;32:1131–1137.

48. Fattovich G, Stroffolini T, Zagni I, et al. Hepatocellular carcinoma in cirrhosis: Incidence and risk factors. Gastroenterology 2004;127:S35–S50.

49. Degos F, Christidis C, Ganne-Carrie N, et al. Hepatitis C virus related cirrhosis: time to occurrence of hepatocellular carcinoma and death. Gut 2000;47:131 –136.

50. Hoofnagle JH, Mullen KD, Jones DB, et al. Treatment of chronic non-A,non-B hepatitis with recombinant human alpha interferon. A preliminary report. N. Engl. J. Med. 1986;315:1575–1578.

51. Sen GC. Viruses and interferons. Annu. Rev. Microbiol. 2001;55:255–281.

52. Poynard T, Leroy V, Cohard M, et al. Meta-analysis of interferon randomized trials in the treatment of viral hepatitis C: effects of dose and duration. Hepatology 1996;24:778–789.

53. Poynard T, Marcellin P, Lee SS, et al. Randomised trial of interferon α2b plus ribavirin for 48 weeks or for 24 weeks versus interferon α2b plus placebo for 48 weeks for treatment of chronic infection with hepatitis C virus. The Lancet 1998;352:1426–1432.

54. Manns MP, McHutchison JG, Gordon SC, et al. Peginterferon alfa-2b plus ribavirin compared with interferon alfa-2b plus ribavirin for initial treatment of chronic hepatitis C: a randomised trial. The Lancet 2001;358:958–965.

55. Foster GR. Pegylated Interferons for the Treatment of Chronic Hepatitis C. Drugs 2010;70:147–165.

56. Bruno R, Sacchi P, Ciappina V, et al. Viral dynamics and pharmacokinetics of peginterferon alpha-2a and peginterferon alpha-2b in naive patients with chronic hepatitis c: a randomized, controlled study. Antivir. Ther. (Lond.) 2004;9:491–497.

57. Ghany MG, Strader DB, Thomas DL, et al. Diagnosis, management, and treatment of hepatitis C: An update. Hepatology 2009;49:1335–1374.

58. Kau A, Vermehren J, Sarrazin C. Treatment predictors of a sustained virologic response in hepatitis B and C. Journal of Hepatology 2008;49:634–651.

59. Feld JJ, Hoofnagle JH. Mechanism of action of interferon and ribavirin in treatment of hepatitis C. Nature 2005;436:967–972.

60. Liu-Young G, Kozal MJ. Review: Hepatitis C Protease and Polymerase Inhibitors in Development. AIDS Patient Care STDS 2008;22:449–457.

61. Poordad F, McCone J Jr, Bacon BR, et al. Boceprevir for untreated chronic HCV genotype 1 infection. N. Engl. J. Med. 2011;364:1195–1206.

62. Jacobson IM, McHutchison JG, Dusheiko G, et al. Telaprevir for previously untreated chronic hepatitis C virus infection. N. Engl. J. Med. 2011;364:2405–2416.

63. Ghany MG, Nelson DR, Strader DB, et al. An update on treatment of genotype 1 chronic hepatitis C virus infection: 2011 practice guideline by the American Association for the Study of Liver Diseases. Hepatology 2011;54:1433–1444.

64. ISAACS A, LINDENMANN J. Virus interference. I. The interferon. Proc. R. Soc. Lond., B, Biol. Sci. 1957;147:258–267.

65. Katze MG, He Y, Gale M. Viruses and interferon: A fight for supremacy. Nature Reviews Immunology 2002;2:675–687.

66. Donnelly RP, Kotenko SV. Interferon-Lambda: A New Addition to an Old Family. Journal of Interferon & Cytokine Research 2010;30:555–564.

67. Müller U, Steinhoff U, Reis LF, et al. Functional role of type I and type II interferons in antiviral defense. Science 1994;264:1918–1921.

68. Lu B, Ebensperger C, Dembic Z, et al. Targeted disruption of the interferon-γ receptor 2 gene results in severe immune defects in mice. Proceedings of the National Academy of Sciences 1998;95:8233 –8238.

69. Kotenko SV, Gallagher G, Baurin VV, et al. IFN-[lambda]s mediate antiviral protection through a distinct class II cytokine receptor complex. Nat Immunol 2003;4:69–77.

70. Sheppard P, Kindsvogel W, Xu W, et al. IL-28, IL-29 and their class II cytokine receptor IL-28R. Nat Immunol 2003;4:63–68.

71. Marcello T, Grakoui A, Barba-Spaeth G, et al. Interferons [alpha] and [lambda] Inhibit Hepatitis C Virus Replication With Distinct Signal Transduction and Gene Regulation Kinetics. Gastroenterology 2006;131:1887–1898.

72. Mordstein M, Michiels T, Staeheli P. What Have We Learned from the IL28 Receptor Knockout Mouse? Journal of Interferon & Cytokine Research 2010;30:579–584.

73. Pott J, Mahlakõiv T, Mordstein M, et al. IFN-λ determines the intestinal epithelial antiviral host defense. Proceedings of the National Academy of Sciences 2011;108:7944 –7949.

74. Makowska Z, Duong FHT, Trincucci G, et al. Interferon-β and interferon-λ signaling is not affected by interferon-induced refractoriness to interferon-α in vivo. Hepatology 2011;53:1171–1180.

75. Takeuchi O, Akira S. Pattern Recognition Receptors and Inflammation. Cell 2010;140:805–820.

76. Sumpter R, Loo Y-M, Foy E, et al. Regulating Intracellular Antiviral Defense and Permissiveness to Hepatitis C Virus RNA Replication through a Cellular RNA Helicase, RIG-I. Journal of Virology 2005;79:2689 –2699.

77. Saito T, Owen DM, Jiang F, et al. Innate immunity induced by composition-dependent RIG-I recognition of hepatitis C virus RNA. Nature 2008;454:523–527.

78. Gack MU, Shin YC, Joo C-H, et al. TRIM25 RING-finger E3 ubiquitin ligase is essential for RIG-I-mediated antiviral activity. Nature 2007;446:916–920.

79. Wang N, Liang Y, Devaraj S, et al. Toll-Like Receptor 3 Mediates Establishment of an Antiviral State against Hepatitis C Virus in Hepatoma Cells. Journal of Virology 2009;83:9824 –9834.

80. Li K, Li NL, Wei D, et al. Activation of chemokine and inflammatory cytokine response in HCV-infected hepatocytes depends on TLR3 sensing of HCV dsRNA intermediates. Hepatology.

81. Kumar H, Kawai T, Akira S. Toll-like receptors and innate immunity. Biochemical and Biophysical Research Communications 2009;388:621–625.

82. Takahashi K, Asabe S, Wieland S, et al. Plasmacytoid dendritic cells sense hepatitis C virus–infected cells, produce interferon, and inhibit infection. Proceedings of the National Academy of Sciences 2010;107:7431 –7436.

83. Gilliet M, Cao W, Liu Y-J. Plasmacytoid dendritic cells: sensing nucleic acids in viral infection and autoimmune diseases. Nat Rev Immunol 2008;8:594–606.

84. Randall RE, Goodbourn S. Interferons and viruses: an interplay between induction, signalling, antiviral responses and virus countermeasures. Journal of General Virology 2008;89:1 –47.

85. Darnell JE Jr, Kerr IM, Stark GR. Jak-STAT pathways and transcriptional activation in response to IFNs and other extracellular signaling proteins. Science 1994;264:1415–1421.

86. Heim MH. The Jak-Stat Pathway: Cytokine Signalling from the Receptor to the Nucleus. Journal of Receptors and Signal Transduction 1999;19:75–120.

87. Aaronson DS, Horvath CM. A Road Map for Those Who Don't Know JAK-STAT. Science 2002;296:1653 –1655.

88. Zhou Z, Hamming OJ, Ank N, et al. Type III Interferon (IFN) Induces a Type I IFN-Like Response in a Restricted Subset of Cells through Signaling Pathways Involving both the Jak-STAT Pathway and the Mitogen-Activated Protein Kinases. J. Virol. 2007;81:7749–7758.

89. Sarasin-Filipowicz M, Oakeley EJ, Duong FHT, et al. Interferon signaling and treatment outcome in chronic hepatitis C. Proc Natl Acad Sci U S A 2008;105:7034–7039.

90. Schoggins JW, Wilson SJ, Panis M, et al. A diverse range of gene products are effectors of the type I interferon antiviral response. Nature 2011;472:481–485.

91. Wormald S, Hilton DJ. Inhibitors of Cytokine Signal Transduction. Journal of Biological Chemistry 2004;279:821 –824.

92. Liu B, Liao J, Rao X, et al. Inhibition of Stat1-mediated gene activation by PIAS1. Proceedings of the National Academy of Sciences 1998;95:10626 –10631.

93. Malakhova OA, Kim KI, Luo J-K, et al. UBP43 is a novel regulator of interferon signaling independent of its ISG15 isopeptidase activity. EMBO J 2006;25:2358–2367.

94. Liu LQ, Ilaria R Jr, Kingsley PD, et al. A novel ubiquitin-specific protease, UBP43, cloned from leukemia fusion protein AML1-ETO-expressing mice, functions in hematopoietic cell differentiation. Mol. Cell. Biol. 1999;19:3029–3038.

95. Randall G, Chen L, Panis M, et al. Silencing of USP18 Potentiates the Antiviral Activity of Interferon Against Hepatitis C Virus Infection. Gastroenterology 2006;131:1584–1591.

96. Larner AC, Chaudhuri A, Darnell JE. Transcriptional induction by interferon. New protein(s) determine the extent and length of the induction. Journal of Biological Chemistry 1986;261:453 – 459.

97. Sarasin-Filipowicz M, Wang X, Yan M, et al. Alpha Interferon Induces Long-Lasting Refractoriness of JAK-STAT Signaling in the Mouse Liver through Induction of USP18/UBP43. Mol. Cell. Biol. 2009;29:4841–4851.

98. François-Newton V, Magno de Freitas Almeida G, Payelle-Brogard B, et al. USP18-Based Negative Feedback Control Is Induced by Type I and Type III Interferons and Specifically Inactivates Interferon α Response. PLoS ONE 2011;6:e22200.

99. Zeuzem S, Feinman SV, Rasenack J, et al. Peginterferon alfa-2a in patients with chronic hepatitis C. N. Engl. J. Med. 2000;343:1666–1672.

100. Foy E, Li K, Wang C, et al. Regulation of interferon regulatory factor-3 by the hepatitis C virus serine protease. Science 2003;300:1145–1148.

101. Meylan E, Curran J, Hofmann K, et al. Cardif is an adaptor protein in the RIG-I antiviral pathway and is targeted by hepatitis C virus. Nature 2005;437:1167–1172.

102. Li X-D, Sun L, Seth RB, et al. Hepatitis C virus protease NS3/4A cleaves mitochondrial antiviral signaling protein off the mitochondria to evade innate immunity. Proceedings of the National Academy of Sciences of the United States of America 2005;102:17717–17722.

103. Loo Y-M, Owen DM, Li K, et al. Viral and therapeutic control of IFN-β promoter stimulator 1 during hepatitis C virus infection. Proceedings of the National Academy of Sciences 2006;103:6001 –6006.

104. Li K, Foy E, Ferreon JC, et al. Immune evasion by hepatitis C virus NS3/4A protease-mediated cleavage of the Toll-like receptor 3 adaptor protein TRIF. Proceedings of the National Academy of Sciences of the United States of America 2005;102:2992 –2997.

105. Lin W, Kim SS, Yeung E, et al. Hepatitis C Virus Core Protein Blocks Interferon Signaling by Interaction with the STAT1 SH2 Domain. Journal of Virology 2006;80:9226 –9235.

106. Bode JG, Ludwig S, Ehrhardt C, et al. IFN-α antagonistic activity of HCV core protein involves induction of suppressor of cytokine signaling-3. The FASEB Journal 2003.

107. Heim MH, Moradpour D, Blum HE. Expression of Hepatitis C Virus Proteins Inhibits Signal Transduction through the Jak-STAT Pathway. J. Virol. 1999;73:8469–8475.

108. Blindenbacher A, Duong FHT, Hunziker L, et al. Expression of hepatitis c virus proteins inhibits interferon [alpha] signaling in the liver of transgenic mice. Gastroenterology 2003;124:1465–1475.

109. Duong FHT, Filipowicz M, Tripodi M, et al. Hepatitis C virus inhibits interferon signaling through up-regulation of protein phosphatase 2A. Gastroenterology 2004;126:263–277.

110. Christen V, Treves S, Duong FHT, et al. Activation of endoplasmic reticulum stress response by hepatitis viruses up-regulates protein phosphatase 2A. Hepatology 2007;46:558–565.

111. Duong FHT, Christen V, Berke JM, et al. Upregulation of Protein Phosphatase 2Ac by Hepatitis C Virus Modulates NS3 Helicase Activity through Inhibition of Protein Arginine Methyltransferase 1. J. Virol. 2005;79:15342–15350.

112. Duong FHT, Christen V, Filipowicz M, et al. S-adenosylmethionine and betaine correct hepatitis C virus induced inhibition of interferon signaling <I>in vitro</I>. Hepatology 2006;43:796–806.

113. Gale MJ Jr, Korth MJ, Tang NM, et al. Evidence that hepatitis C virus resistance to interferon is mediated through repression of the PKR protein kinase by the nonstructural 5A protein. Virology 1997;230:217–227.

114. Pflugheber J, Fredericksen B, Sumpter R Jr, et al. Regulation of PKR and IRF-1 during hepatitis C virus RNA replication. Proc. Natl. Acad. Sci. U.S.A. 2002;99:4650–4655.

115. Jiang D, Guo H, Xu C, et al. Identification of three interferon-inducible cellular enzymes that inhibit the replication of hepatitis C virus. J. Virol. 2008;82:1665–1678.

116. Garaigorta U, Chisari FV. Hepatitis C Virus Blocks Interferon Effector Function by Inducing PKR Phosphorylation. Cell Host Microbe 2009;6:513–522.

117. Thimme R, Oldach D, Chang K-M, et al. Determinants of Viral Clearance and Persistence during Acute Hepatitis C Virus Infection. The Journal of Experimental Medicine 2001;194:1395 – 1406.

118. Major ME, Dahari H, Mihalik K, et al. Hepatitis C virus kinetics and host responses associated with disease and outcome of infection in chimpanzees. Hepatology 2004;39:1709–1720.

119. Thimme R, Bukh J, Spangenberg HC, et al. Viral and immunological determinants of hepatitis C virus clearance, persistence, and disease. Proc. Natl. Acad. Sci. U.S.A 2002;99:15661–15668.

120. Su AI, Pezacki JP, Wodicka L, et al. Genomic analysis of the host response to hepatitis C virus infection. Proceedings of the National Academy of Sciences of the United States of America 2002;99:15669 –15674.

121. Chen L, Borozan I, Feld J, et al. Hepatic Gene Expression Discriminates Responders and Nonresponders in Treatment of Chronic Hepatitis C Viral Infection. Gastroenterology 2005;128:1437–1444.

122. Asselah T, Bieche I, Narguet S, et al. Liver gene expression signature to predict response to pegylated interferon plus ribavirin combination therapy in patients with chronic hepatitis C. Gut 2008;57:516–524.

123. Bigger CB, Guerra B, Brasky KM, et al. Intrahepatic Gene Expression during Chronic Hepatitis C Virus Infection in Chimpanzees. J. Virol. 2004;78:13779–13792.

124. Lanford RE, Guerra B, Bigger CB, et al. Lack of Response to Exogenous Interferon-α in the Liver of HCV Chronically Infected Chimpanzees. Hepatology 2007;46:999–1008.

125. Bellecave P, Sarasin-Filipowicz M, Donzé O, et al. Cleavage of mitochondrial antiviral signaling protein in the liver of patients with chronic hepatitis C correlates with a reduced activation of the endogenous interferon system. Hepatology 2010;51:1127–1136.

126. Ge D, Fellay J, Thompson AJ, et al. Genetic variation in IL28B predicts hepatitis C treatment-induced viral clearance. Nature 2009;461:399–401.

127. Tanaka Y, Nishida N, Sugiyama M, et al. Genome-wide association of IL28B with response to pegylated interferon-[alpha] and ribavirin therapy for chronic hepatitis C. Nat Genet 2009;41:1105–1109.

128. Suppiah V, Moldovan M, Ahlenstiel G, et al. IL28B is associated with response to chronic hepatitis C interferon-alpha and ribavirin therapy. Nat. Genet. 2009;41:1100–1104.

129. Rauch A, Kutalik Z, Descombes P, et al. Genetic Variation in IL28B Is Associated With Chronic Hepatitis C and Treatment Failure: A Genome-Wide Association Study. Gastroenterology 2010;138:1338–1345.e7.

130. Thomas DL, Thio CL, Martin MP, et al. Genetic variation in IL28B and spontaneous clearance of hepatitis C virus. Nature 2009;461:798–801.

131. R Development Core Team (2008). R: A language and environment for statistical computing. R Foundation for Statistical Computing, Vienna, Austria. ISBN 3-900051-07-0, URL http://www.R-project.org.

132. Johnson WE, Li C, Rabinovic A. Adjusting batch effects in microarray expression data using empirical Bayes methods. Biostatistics 2007;8:118–127.

133. Ferguson TS. A Bayesian Analysis of Some Nonparametric Problems. The Annals of Statistics 1973;1:209–230.

134. Silva M, Poo J, Wagner F, et al. A randomised trial to compare the pharmacokinetic, pharmacodynamic, and antiviral effects of peginterferon alfa-2b and peginterferon alfa-2a in patients with chronic hepatitis C (COMPARE). Journal of Hepatology 2006;45:204–213.

135. Lanford RE, Guerra B, Lee H, et al. Genomic response to interferon-alpha in chimpanzees: Implications of rapid downregulation for hepatitis C kinetics. Hepatology 2006;43:961–972.

136. Lechner F, Wong DKH, Dunbar PR, et al. Analysis of Successful Immune Responses in Persons Infected with Hepatitis C Virus. The Journal of Experimental Medicine 2000;191:1499–1512.

137. Darling JM, Aerssens J, Fanning G, et al. Quantitation of pretreatment serum interferon-γ-inducible protein-10 improves the predictive value of an IL28B gene polymorphism for hepatitis C treatment response. Hepatology 2011;53:14–22.

138. Lagging M, Askarieh G, Negro F, et al. Response prediction in chronic hepatitis C by assessment of IP-10 and IL28B-related single nucleotide polymorphisms. PLoS ONE 2011;6:e17232.

139. Fattovich G, Covolo L, Bibert S, et al. IL28B polymorphisms, IP-10 and viral load predict virological response to therapy in chronic hepatitis C. Aliment. Pharmacol. Ther. 2011;33:1162–1172.

140. Honda M, Sakai A, Yamashita T, et al. Hepatic ISG Expression Is Associated With Genetic Variation in Interleukin 28B and the Outcome of IFN Therapy for Chronic Hepatitis C. Gastroenterology 2010;139:499–509.

141. Urban TJ, Thompson AJ, Bradrick SS, et al. IL28B genotype is associated with differential expression of intrahepatic interferon-stimulated genes in patients with chronic hepatitis C. Hepatology 2010;52:1888–1896.

142. Asahina Y, Tsuchiya K, Muraoka M, et al. Association of gene expression involving innate immunity and genetic variation in interleukin 28B with antiviral response. Hepatology 2012;55:20–29.

143. Naggie S, Osinusi A, Katsounas A, et al. Dysregulation of innate immunity in HCV genotype 1 IL28B unfavorable genotype patients: Impaired viral kinetics and therapeutic response. Hepatology.

144. McGilvray I, Feld JJ, Chen L, et al. Hepatic Cell–Specific Gene Expression Better Predicts HCV Treatment Outcome Than IL28B Genotype. Gastroenterology.

145. Marukian S, Andrus L, Sheahan TP, et al. Hepatitis C virus induces interferon-λ and interferon-stimulated genes in primary liver cultures. Hepatology 2011;54:1913–1923.

146. Liang Y, Shilagard T, Xiao S-Y, et al. Visualizing Hepatitis C Virus Infections in Human Liver by Two-Photon Microscopy. Gastroenterology 2009;137:1448–1458.

147. Bigger CB, Brasky KM, Lanford RE. DNA Microarray Analysis of Chimpanzee Liver during Acute Resolving Hepatitis C Virus Infection. J. Virol. 2001;75:7059–7066.

148. Jouan L, Chatel-Chaix L, Melançon P, et al. Targeted impairment of innate antiviral responses in the liver of chronic hepatitis C patients. Journal of Hepatology 2012;56:70–77.

Appendix

Appendix A: Supplementary Tables of Section 4.1

Appendix B: Supplementary Material of Section 4.2

Appendix C: Curriculum Vitae

Supplementary Table I.

Fold changes of the upregulated genes in functional categories (fold change of at least 2 between the means of AHC and healthy liver samples with the corresponding FDR (Benjamini-Hochberg correction) below 0.05).

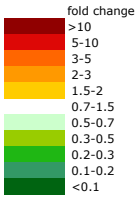

Chemokines, receptors and related

probe set ID	Symbol	pat1	pat2	pat3	pat4	pat5	pat6	CHC-R	CH-NR	Gene Name
32128_at	CCL18	3.5	8.1	3.9	5.7	9.0	11.0	2.0	1.8	chemokine (C-C motif) ligand 18 (pulmonary and activation-regulated)
210072_at	CCL19	5.5	2.0	9.5	4.5	2.4	3.1	8.1	7.4	chemokine (C-C motif) ligand 19
216598_s_at	CCL2	3.3	2.9	4.4	2.9	5.6	2.7	2.0	1.8	chemokine (C-C motif) ligand 2
205476_at	CCL20	8.4	7.1	5.7	2.8	42.6	5.1	3.4	6.7	chemokine (C-C motif) ligand 20
204606_at	CCL21	3.0	2.6	2.6	3.1	1.4	1.8	3.1	4.6	chemokine (C-C motif) ligand 21
204103_at	CCL4	1.8	3.2	2.4	1.9	5.1	3.7	1.4	1.2	chemokine (C-C motif) ligand 4
1405_i_at	CCL5	2.2	5.5	3.6	2.7	5.7	5.4	2.2	2.3	chemokine (C-C motif) ligand 5
214038_at	CCL8	2.1	8.5	2.0	2.6	7.2	6.6	1.8	2.3	chemokine (C-C motif) ligand 8
206991_s_at	CCR5	1.5	2.3	2.4	2.1	2.0	2.4	1.5	1.6	chemokine (C-C motif) receptor 5
204533_at	CXCL10	9.7	13.1	20.4	11.3	23.3	31.3	11.5	19.8	chemokine (C-X-C motif) ligand 10
211122_s_at	CXCL11	6.6	10.9	13.8	11.0	13.4	17.0	5.8	10.1	chemokine (C-X-C motif) ligand 11
203915_at	CXCL9	3.6	7.2	18.3	10.8	21.4	19.8	8.6	4.0	chemokine (C-X-C motif) ligand 9
217028_at	CXCR4	1.6	2.0	3.1	1.7	2.5	3.6	2.3	2.8	chemokine (C-X-C motif) receptor 4
206974_at	CXCR6	1.4	3.2	2.6	2.7	2.6	3.0	1.3	1.3	chemokine (C-X-C motif) receptor 6
210354_at	IFNG	1.7	4.7	3.5	3.2	4.2	3.8	1.2	0.9	interferon, gamma
222868_s_at	IL18BP	2.4	3.3	2.1	2.1	2.9	2.4	1.3	1.3	interleukin 18 binding protein
205067_at	IL1B	2.1	2.7	1.9	1.7	3.9	2.3	1.2	1.1	interleukin 1, beta
204116_at	IL2RG	1.8	3.2	2.5	1.9	2.7	2.4	1.7	1.6	interleukin 2 receptor, gamma (severe combined immunodeficiency)
203828_s_at	IL32	1.7	2.5	2.0	1.6	4.1	2.0	1.6	2.2	interleukin 32
202859_x_at	IL8	3.4	3.1	3.9	1.5	15.7	4.0	2.2	2.2	interleukin 8
209035_at	MDK	2.9	4.1	1.9	1.5	2.8	3.0	1.3	3.5	midkine (neurite growth-promoting factor 2)
206366_x_at	XCL1	2.1	1.8	2.4	1.4	3.2	1.7	1.3	1.2	chemokine (C motif) ligand 1

ISGs

probe set ID	Symbol	pat1	pat2	pat3	pat4	pat5	pat6	CHC-R	CH-NR	Gene Name
202269_x_at	GBP1	4.1	5.9	4.2	4.9	4.5	4.6	1.9	2.0	guanylate binding protein 1, interferon-inducible, 67kDa
202748_at	GBP2	2.3	3.0	2.3	2.3	2.3	1.7	1.3	1.3	guanylate binding protein 2, interferon-inducible
235574_at	GBP4	2.1	3.5	2.7	2.6	2.2	2.8	1.3	1.5	guanylate binding protein 4
229625_at	GBP5	1.9	3.3	2.1	3.2	2.2	2.0	1.2	1.0	guanylate binding protein 5
205483_s_at	ISG15	2.2	3.3	1.5	1.5	2.0	4.5	2.1	15.4	ISG15 ubiquitin-like modifier
204698_at	ISG20	4.0	5.6	2.7	2.4	3.3	4.5	2.2	5.7	interferon stimulated exonuclease gene 20kDa
205569_at	LAMP3	6.1	5.0	11.3	6.4	4.7	15.7	4.8	29.2	lysosomal-associated membrane protein 3
204972_at	OAS2	1.8	3.6	1.7	1.4	1.7	3.9	1.4	6.5	2'-5'-oligoadenylate synthetase 2, 69/71kDa
205660_at	OASL	3.8	5.2	3.2	2.4	5.6	9.0	7.5	21.7	2'-5'-oligoadenylate synthetase-like

Cellular immune response

probe set ID	Symbol	pat1	pat2	pat3	pat4	pat5	pat6	CHC-R	CH-NR	Gene Name
205831_at	CD2	2.0	3.9	3.6	2.6	3.7	3.7	2.3	2.3	CD2 molecule
213539_at	CD3D	1.8	3.4	3.1	2.6	3.1	3.3	2.1	2.1	CD3d molecule, delta (CD3-TCR complex)
34210_at	CD52	1.6	3.3	2.2	1.6	3.3	2.7	2.0	1.9	CD52 molecule
205758_at	CD8A	2.1	5.0	4.1	2.8	5.4	4.9	2.0	1.7	CD8a molecule
204440_at	CD83	2.0	2.2	2.5	2.0	3.0	2.5	1.6	1.7	CD83 molecule
204118_at	CD48	1.6	3.0	2.0	1.7	2.3	2.1	1.5	1.5	CD48 molecule
203416_at	CD53	1.8	2.7	2.1	1.7	2.4	2.3	1.3	1.3	CD53 molecule
210895_s_at	CD86	1.7	3.5	1.9	1.8	2.6	2.6	1.3	1.1	CD86 molecule
209835_x_at	CD44	2.2	3.0	1.7	1.7	2.5	1.6	1.2	1.0	CD44 molecule (Indian blood group)
215925_s_at	CD72	1.6	3.1	1.6	2.0	2.7	2.6	1.3	0.9	CD72 molecule
205159_at	CSF2RB	2.1	3.4	1.7	2.0	2.5	2.2	1.5	1.4	colony stimulating factor 2 receptor, beta, low-affinity (granulocyte-macrophage)
231496_at	FCAMR	7.3	5.4	4.0	3.4	10.6	4.7	4.5	3.4	Fc receptor, IgA, IgM, high affinity
1554899_s_at	FCER1G	2.0	3.1	1.7	1.9	2.0	1.8	1.0	0.9	Fc fragment of IgE, high affinity I, receptor for; gamma polypeptide
214511_x_at	FCGR1B	3.0	5.3	2.3	3.1	3.1	2.3	0.9	0.9	Fc fragment of IgG, high affinity Ib, receptor (CD64)
203561_at	FCGR2A	1.7	2.8	1.9	1.5	2.6	2.4	1.1	1.1	Fc fragment of IgG, low affinity IIa, receptor (CD32)
205488_at	GZMA	1.4	3.4	2.4	2.2	2.7	2.7	1.3	1.2	granzyme A (granzyme 1, cytotoxic T-lymphocyte-associated serine esterase 3)
206082_at	HCP5	3.6	4.8	3.1	5.2	3.1	5.2	2.2	4.1	HLA complex P5
203932_at	HLA-DMB	1.9	3.3	2.3	2.1	2.6	2.9	1.4	1.3	major histocompatibility complex, class II, DM beta
213537_at	HLA-DPA1	3.8	7.5	1.8	4.8	4.6	5.5	1.8	1.6	major histocompatibility complex, class II, DP alpha 1
212998_x_at	HLA-DQB1	1.5	4.3	3.0	1.8	2.2	4.0	1.4	1.1	major histocompatibility complex, class II, DQ beta 1
210982_s_at	HLA-DRA	1.7	2.5	2.1	1.8	2.5	2.5	1.4	1.4	major histocompatibility complex, class II, DR alpha
204806_x_at	HLA-F	1.8	2.4	2.0	2.6	1.6	2.9	1.5	2.7	major histocompatibility complex, class I, F
216491_x_at	IGHM	7.1	3.0	3.2	11.1	4.8	2.6	5.2	4.7	immunoglobulin heavy constant mu
234884_x_at	IGL@	2.8	1.2	2.1	2.7	2.3	1.8	2.5	2.5	Immunoglobulin lambda locus
234764_x_at	IGLV1-44	5.7	2.1	3.3	5.8	4.0	2.4	5.2	3.1	Immunoglobulin lambda variable 1-44
206420_at	IGSF6	1.7	2.6	2.1	1.5	3.0	3.0	1.1	0.8	immunoglobulin superfamily, member 6
211339_s_at	ITK	1.6	3.1	3.6	2.6	3.7	3.9	2.1	2.3	IL2-inducible T-cell kinase
214470_at	KLRB1	1.3	3.6	1.8	2.6	2.2	2.2	1.1	1.0	killer cell lectin-like receptor subfamily B, member 1
1555691_a_at	KLRK1	1.3	3.1	2.5	1.7	2.5	2.6	1.2	1.1	killer cell lectin-like receptor subfamily K, member 1
204890_s_at	LCK	2.1	3.7	2.8	2.1	3.0	2.7	1.8	1.7	lymphocyte-specific protein tyrosine kinase
205269_at	LCP2	1.7	2.9	1.8	1.8	2.3	2.2	1.4	1.4	lymphocyte cytosolic protein 2 (SH2 domain containing leukocyte protein of 76kDa)
208949_s_at	LGALS3	2.7	3.7	2.3	1.7	3.3	2.8	1.7	2.2	lectin, galactoside-binding, soluble, 3
210732_s_at	LGALS8	2.8	3.5	2.2	2.1	2.2	1.9	1.3	1.0	lectin, galactoside-binding, soluble, 8
206881_s_at	LILRA3	2.0	2.6	1.6	1.8	2.5	1.7	1.0	1.0	leukocyte immunoglobulin-like receptor, subfamily A (without TM domain), member 3
203523_at	LSP1	2.1	2.8	2.4	2.2	2.3	2.5	1.7	1.7	lymphocyte-specific protein 1
1555745_a_at	LYZ	5.4	4.2	1.9	3.4	12.1	7.4	5.3	3.9	lysozyme (renal amyloidosis)
206247_at	MICB	2.2	3.6	2.1	2.0	3.0	2.4	1.8	2.1	MHC class I polypeptide-related sequence B
214770_at	MSR1	1.3	2.6	1.6	1.7	2.6	3.2	0.9	1.0	macrophage scavenger receptor 1
219788_at	PILRA	1.6	3.0	1.8	1.5	3.0	2.7	1.1	1.1	paired immunoglobin-like type 2 receptor alpha
202963_at	RFX5	1.7	2.5	1.7	1.9	2.1	2.4	1.6	2.0	regulatory factor X, 5 (influences HLA class II expression)
229723_at	TAGAP	1.7	3.4	2.6	2.1	2.9	2.9	2.0	2.4	T-cell activation RhoGTPase activating protein
202307_s_at	TAP1	2.3	3.1	1.9	2.5	2.3	2.4	1.4	1.9	transporter 1, ATP-binding cassette, sub-family B (MDR/TAP)
225973_at	TAP2	1.9	3.0	2.2	3.3	1.6	2.9	1.8	2.9	transporter 2, ATP-binding cassette, sub-family B (MDR/TAP)
1555565_s_at	TAPBP	1.9	2.7	1.7	2.9	1.3	2.0	1.2	1.1	TAP binding protein (tapasin)
218746_at	TAPBPL	2.6	2.4	1.7	2.8	2.2	1.9	1.3	1.5	TAP binding protein-like
209670_at	TRAC	1.5	2.9	3.2	2.1	2.7	2.8	1.9	1.7	T cell receptor alpha constant
213193_x_at	TRBC1	2.1	4.7	4.1	2.9	4.3	4.0	2.4	2.4	T cell receptor beta constant 1

Transcription factors

probe set ID	Symbol	pat1	pat2	pat3	pat4	pat5	pat6	CHC-R	CH-NR	Gene Name
212420_at	ELF1	2.3	3.3	2.2	2.6	1.9	2.5	1.5	1.6	E74-like factor 1 (ets domain transcription factor)
223287_s_at	FOXP1	2.3	2.1	2.3	2.4	1.9	2.2	1.9	1.9	forkhead box P1
202431_s_at	MYC	1.9	3.1	1.6	1.3	4.3	2.5	1.2	1.3	v-myc myelocytomatosis viral oncogene homolog (avian)
233446_at	ONECUT2	2.9	1.7	3.0	2.9	2.5	1.9	1.4	1.5	one cut homeobox 2
209969_s_at	STAT1	3.6	5.5	3.6	4.9	3.0	6.4	2.6	5.8	signal transducer and activator of transcription 1, 91kDa

Signal transduction

probe set ID	Symbol	pat1	pat2	pat3	pat4	pat5	pat6	CHC-R	CH-NR	Gene Name
242961_x_at	DDX58	2.0	3.4	1.7	1.7	1.5	2.4	1.2	2.1	DEAD (Asp-Glu-Ala-Asp) box polypeptide 58
207651_at	GPR171	1.6	3.3	3.5	2.0	4.5	3.2	1.7	1.5	G protein-coupled receptor 171
210279_at	GPR18	1.5	3.5	2.4	2.1	3.0	2.4	1.7	1.6	G protein-coupled receptor 18
209631_s_at	GPR37	1.9	2.4	2.8	1.2	2.5	2.1	1.1	1.9	G protein-coupled receptor 37 (endothelin receptor type B-like)
1552611_a_at	JAK1	2.1	2.2	2.4	3.3	1.7	2.3	1.5	1.3	Janus kinase 1
229560_at	TLR8	2.2	3.2	2.4	2.0	3.2	2.5	1.3	1.2	toll-like receptor 8

Lipid homeostasis-related

probe set ID	Symbol	pat1	pat2	pat3	pat4	pat5	pat6	CHC-R	CH-NR	Gene Name
221087_s_at	APOL3	2.2	2.9	2.3	2.9	2.7	3.5	1.8	3.1	apolipoprotein L, 3
38241_at	BTN3A3	1.7	2.3	2.4	2.8	1.6	2.7	1.4	1.9	butyrophilin, subfamily 3, member A3
220029_at	ELOVL2	2.0	2.1	3.6	1.4	1.6	2.4	2.2	2.5	elongation of very long chain fatty acids (FEN1/Elo2, SUR4/Elo3, yeast)-like 2
202345_s_at	FABP5	3.2	4.8	3.1	2.1	5.5	4.2	1.5	1.7	fatty acid binding protein 5 (psoriasis-associated)
209785_s_at	PLA2G4C	1.8	2.4	2.4	2.4	2.0	2.9	1.5	1.8	phospholipase A2, group IVC (cytosolic, calcium-independent)
206214_at	PLA2G7	2.4	5.5	3.1	1.8	6.5	5.2	1.1	1.2	phospholipase A2, group VII (platelet-activating factor acetylhydrolase, plasma)
211708_s_at	SCD	1.5	2.6	2.4	3.8	1.1	3.3	1.6	1.6	stearoyl-CoA desaturase (delta-9-desaturase)
220232_at	SCD5	1.9	3.3	1.8	2.9	1.3	2.3	1.0	0.8	stearoyl-CoA desaturase 5
204881_s_at	UGCG	3.0	2.5	2.2	1.3	3.0	1.6	1.5	1.7	UDP-glucose ceramide glucosyltransferase

Apoptosis-related

probe set ID	Symbol	pat1	pat2	pat3	pat4	pat5	pat6	CHC-R	CH-NR	Gene Name
224461_s_at	AIFM2	1.9	2.4	1.6	1.6	2.9	2.7	1.3	1.7	apoptosis-inducing factor, mitochondrion-associated, 2
211367_s_at	CASP1	2.2	3.5	1.8	2.0	2.0	2.1	1.3	1.6	caspase 1, apoptosis-related cysteine peptidase (interleukin 1, beta, convertase)

Ubiquitination, proteasome

probe set ID	Symbol	pat1	pat2	pat3	pat4	pat5	pat6	CHC-R	CH-NR	Gene Name
204279_at	PSMB9	2.8	3.5	2.8	3.5	2.7	3.2	1.6	2.4	proteasome (prosome, macropain) subunit, beta type, 9 (large multifunctional peptidase 2)
222600_s_at	UBA6	2.2	3.1	2.0	2.9	1.7	2.1	1.2	1.7	ubiquitin-like modifier activating enzyme 6
226035_at	USP31	2.7	2.0	3.3	2.6	2.1	2.5	1.7	1.4	ubiquitin specific peptidase 31

Antiviral

probe set ID	Symbol	pat1	pat2	pat3	pat4	pat5	pat6	CHC-R	CH-NR	Gene Name
204205_at	APOBEC3G	1.8	3.6	2.2	1.8	2.7	3.1	1.9	2.3	apolipoprotein B mRNA editing enzyme, catalytic polypeptide-like 3G
204502_at	SAMHD1	1.7	3.3	1.7	1.6	2.0	2.3	1.2	1.3	SAM domain and HD domain 1

Metabolism

probe set ID	Symbol	pat1	pat2	pat3	pat4	pat5	pat6	CHC-R	CH-NR	Gene Name
206561_s_at	AKR1B10	8.4	25.4	2.0	5.8	23.7	6.9	2.2	4.8	aldo-keto reductase family 1, member B10 (aldose reductase)
209646_x_at	ALDH1B1	2.0	2.3	2.3	2.7	1.9	2.7	1.4	1.7	aldehyde dehydrogenase 1 family, member B1
203922_s_at	CYBB	2.1	3.7	1.8	1.6	2.7	1.9	1.1	0.9	cytochrome b-245, beta polypeptide
210272_at	CYP2B7P1	3.3	2.0	5.2	4.4	2.9	4.3	2.4	3.5	cytochrome P450, family 2, subfamily B, polypeptide 7 pseudogene 1
224009_x_at	DHRS9	2.2	3.6	3.6	2.9	4.4	5.2	1.3	1.4	dehydrogenase/reductase (SDR family) member 9
210029_at	IDO1	2.0	3.5	3.1	3.8	2.9	2.9	2.0	1.7	indoleamine 2,3-dioxygenase 1
204059_s_at	ME1	1.7	3.1	1.9	1.8	2.5	3.3	1.6	1.5	malic enzyme 1, NADP(+)-dependent, cytosolic
210154_at	ME2	1.8	2.6	2.0	1.9	1.9	2.1	1.0	1.1	malic enzyme 2, NAD(+)-dependent, mitochondrial
201761_at	MTHFD2	2.5	3.2	1.9	1.6	2.6	1.8	1.3	1.5	methylenetetrahydrofolate dehydrogenase (NADP+ dependent) 2, methenyltetrahydrofolate cyclohydrolase
223298_s_at	NT5C3	2.0	2.9	1.5	1.6	2.0	2.7	1.2	2.5	5'-nucleotidase, cytosolic III
200628_s_at	WARS	2.2	3.1	2.0	2.8	1.8	1.6	1.1	0.9	tryptophanyl-tRNA synthetase

Cell membrane, adhesion, extracellular matrix

probe set ID	Symbol	pat1	pat2	pat3	pat4	pat5	pat6	CHC-R	CH-NR	Gene Name
214701_s_at	FN1	2.0	1.8	4.4	2.7	2.0	2.0	1.4	1.0	fibronectin 1
207165_at	HMMR	1.8	3.5	1.2	1.6	2.6	2.9	1.5	1.5	hyaluronan-mediated motility receptor (RHAMM)
219403_s_at	HPSE	1.7	3.3	2.1	1.5	2.9	3.3	1.1	1.3	heparanase
219697_at	HS3ST2	3.2	5.4	3.8	2.9	8.9	6.9	1.2	1.3	heparan sulfate (glucosamine) 3-O-sulfotransferase 2
202746_at	ITM2A	2.4	3.8	2.1	1.8	5.7	3.2	2.1	2.5	integral membrane protein 2A
219574_at	MARCH1	2.7	4.9	1.8	2.3	2.5	2.5	1.3	1.7	membrane-associated ring finger (C3HC4) 1

Cell cycle

probe set ID	Symbol	pat1	pat2	pat3	pat4	pat5	pat6	CHC-R	CH-NR	Gene Name
210559_s_at	CDC2	1.8	3.2	1.6	1.2	2.7	2.8	1.4	1.5	cell division cycle 2, G1 to S and G2 to M
208727_s_at	CDC42	1.5	5.9	1.4	1.7	2.9	4.6	1.5	1.2	cell division cycle 42 (GTP binding protein, 25kDa)
224851_at	CDK6	1.9	2.5	2.5	4.0	1.6	3.1	1.4	1.3	cyclin-dependent kinase 6
210416_s_at	CHEK2	1.8	2.8	1.7	2.6	2.4	4.8	1.6	2.2	CHK2 checkpoint homolog (S. pombe)

Kinases/phosphatases and related

probe set ID	Symbol	pat1	pat2	pat3	pat4	pat5	pat6	CHC-R	CH-NR	Gene Name
226702_at	CMPK2	1.9	4.0	1.3	1.7	1.4	3.2	1.5	6.7	cytidine monophosphate (UMP-CMP) kinase 2, mitochondrial
203302_at	DCK	1.9	2.8	2.1	1.8	2.0	2.1	1.5	1.4	deoxycytidine kinase
201251_at	PKM2	2.2	3.3	2.3	1.9	2.9	1.9	1.5	1.4	pyruvate kinase, muscle
212588_at	PTPRC	1.7	2.9	2.7	1.8	2.5	2.6	1.5	1.5	protein tyrosine phosphatase, receptor type, C
204960_at	PTPRCAP	1.4	2.6	1.9	1.8	2.7	2.4	1.4	1.6	protein tyrosine phosphatase, receptor type, C-associated protein
202693_s_at	STK17A	1.5	3.1	2.0	1.4	2.8	2.2	1.5	1.7	serine/threonine kinase 17a

DNA damage-related

probe set ID	Symbol	pat1	pat2	pat3	pat4	pat5	pat6	CHC-R	CH-NR	Gene Name
222850_s_at	DNAJB14	2.6	2.8	2.3	2.7	2.9	2.8	1.4	1.4	DnaJ (Hsp40) homolog, subfamily B, member 14
1558080_s_at	DNAJC3	2.6	4.5	1.6	4.0	2.4	2.3	1.4	1.5	DnaJ (Hsp40) homolog, subfamily C, member 3
218627_at	DRAM1	1.7	2.4	1.6	1.9	2.4	2.2	1.3	1.2	DNA-damage regulated autophagy modulator 1

Other

probe set ID	Symbol	pat1	pat2	pat3	pat4	pat5	pat6	CHC-R	CH-NR	Gene Name
221008_s_at	AGXT2L1	1.5	1.8	1.8	3.0	2.0	3.3	1.9	3.0	alanine-glyoxylate aminotransferase 2-like 1
238439_at	ANKRD22	4.3	6.5	2.3	5.7	3.2	1.8	1.0	0.6	ankyrin repeat domain 22
238332_at	ANKRD29	1.6	1.8	2.4	2.1	1.7	2.7	1.8	2.9	ankyrin repeat domain 29
213503_x_at	ANXA2	1.8	2.7	1.9	1.3	2.3	2.4	2.0	2.3	annexin A2
225285_at	BCAT1	2.2	2.9	1.9	1.7	2.5	3.3	1.4	2.3	branched chain aminotransferase 1, cytosolic
205681_at	BCL2A1	2.3	3.5	2.8	2.2	4.1	2.4	1.3	1.1	BCL2-related protein A1
210538_s_at	BIRC3	3.0	2.9	3.6	2.5	6.8	2.9	1.8	1.9	baculoviral IAP repeat-containing 3
226054_at	BRD4	2.3	1.8	2.1	3.0	1.9	2.5	1.8	1.8	bromodomain containing 4
205548_s_at	BTG3	2.1	2.3	2.0	1.6	2.7	1.6	1.3	1.3	BTG family, member 3
201850_at	CAPG	2.6	3.6	3.6	2.1	3.3	3.5	1.6	1.7	capping protein (actin filament), gelsolin-like
1552701_a_at	CARD16	2.3	3.2	1.8	1.7	2.3	1.6	1.7	2.4	caspase recruitment domain family, member 16
228323_at	CASC5	2.1	1.8	2.5	2.4	1.8	2.7	1.9	2.9	cancer susceptibility candidate 5
226425_at	CLIP4	1.9	3.0	2.2	1.7	2.7	2.5	2.2	2.8	CAP-GLY domain containing linker protein family, member 4
209536_s_at	EHD4	2.1	2.4	1.6	1.8	2.0	2.3	1.4	1.8	EH-domain containing 4
227609_at	EPSTI1	2.4	4.7	1.9	2.0	2.0	3.6	1.4	5.7	epithelial stromal interaction 1 (breast)
217234_s_at	EZR	2.4	2.8	2.0	2.7	2.0	1.8	1.3	1.3	ezrin
203305_at	F13A1	3.7	3.1	1.9	2.1	2.2	1.2	2.3	2.2	coagulation factor XIII, A1 polypeptide
231769_at	FBXO6	1.7	2.6	1.7	1.9	1.9	2.6	1.5	2.0	F-box protein 6
230422_at	FPR3	1.7	3.4	2.5	1.7	3.0	3.2	1.3	1.5	formyl peptide receptor 3
205285_s_at	FYB	1.3	3.2	1.4	2.0	2.4	2.5	1.2	1.1	FYN binding protein (FYB-120/130)
221521_s_at	GINS2	2.1	2.3	1.6	2.1	2.5	3.1	2.0	1.9	GINS complex subunit 2 (Psf2 homolog)
35820_at	GM2A	1.7	2.7	1.6	1.9	2.2	2.5	1.3	1.3	GM2 ganglioside activator
224863_at	GNAQ	1.9	1.7	2.3	2.5	1.6	2.1	1.4	1.7	Guanine nucleotide binding protein (G protein), q polypeptide
201141_at	GPNMB	2.3	4.0	4.6	2.1	5.2	5.5	1.3	1.2	glycoprotein (transmembrane) nmb
227614_at	HKDC1	4.9	18.3	2.4	1.5	17.1	6.3	2.6	10.5	hexokinase domain containing 1
211597_s_at	HOPX	2.3	3.4	2.1	1.3	3.9	2.1	1.6	1.7	HOP homeobox
200598_s_at	HSP90B1	1.9	2.8	1.9	2.0	2.6	2.1	1.3	1.2	heat shock protein 90kDa beta (Grp94), member 1
211006_s_at	KCNB1	1.4	2.0	2.0	4.8	4.1	3.7	1.1	0.9	potassium voltage-gated channel, Shab-related subfamily, member 1
244111_at	KRT222	1.8	1.9	1.7	2.9	1.8	3.8	1.8	4.2	keratin 222
201151_s_at	MBNL1	2.0	2.6	3.1	2.8	1.8	2.1	1.4	1.2	muscleblind-like (Drosophila)
202107_s_at	MCM2	1.8	2.1	1.6	1.8	2.2	3.0	2.0	1.5	minichromosome maintenance complex component 2
216237_s_at	MCM5	2.2	2.5	1.4	2.0	2.2	2.6	2.0	1.7	minichromosome maintenance complex component 5
201930_at	MCM6	2.2	3.4	1.8	2.1	3.3	3.5	2.1	1.9	minichromosome maintenance complex component 6
225325_at	MFSD6	2.2	3.1	1.7	1.8	2.2	1.9	1.5	1.8	major facilitator superfamily domain containing 6
224726_at	MIB1	2.4	1.7	2.1	3.0	1.9	2.3	1.5	1.7	mindbomb homolog 1 (Drosophila)
218883_s_at	MLF1IP	2.4	2.9	1.6	2.6	3.2	4.8	2.1	2.4	MLF1 interacting protein
204959_at	MNDA	2.2	3.3	1.8	2.0	2.2	1.7	1.3	1.2	myeloid cell nuclear differentiation antigen
202149_at	NEDD9	2.0	2.5	2.1	1.7	1.7	2.5	1.8	1.9	neural precursor cell expressed, developmentally down-regulated 9
218039_at	NUSAP1	1.8	2.6	1.6	1.6	2.3	2.5	1.4	1.3	nucleolar and spindle associated protein 1
200906_s_at	PALLD	3.1	2.6	1.3	1.8	3.0	1.2	1.3	1.5	palladin, cytoskeletal associated protein
207469_s_at	PIR	2.5	2.8	1.7	1.8	2.9	2.1	1.3	1.3	pirin (iron-binding nuclear protein)
201927_s_at	PKP4	2.5	2.1	2.0	2.9	2.0	1.8	1.6	1.8	plakophilin 4
221538_s_at	PLXNA1	2.4	2.0	2.4	2.1	2.7	2.8	1.6	1.8	plexin A1
213241_at	PLXNC1	1.7	2.6	2.4	1.6	2.7	2.4	1.6	1.8	plexin C1
208879_x_at	PRPF6	3.3	3.0	2.3	3.3	1.9	2.0	1.6	1.5	PRP6 pre-mRNA processing factor 6 homolog (S. cerevisiae)
204897_at	PTGER4	1.6	2.9	1.8	1.6	2.7	2.3	1.3	1.2	prostaglandin E receptor 4 (subtype EP4)
203554_x_at	PTTG1	2.0	3.3	1.6	2.0	2.5	2.5	1.5	1.3	pituitary tumor-transforming 1

207419_s_at	RAC2	1.8	3.0	2.0	2.6	1.7	2.2	1.4	1.4	ras-related C3 botulinum toxin substrate 2 (rho family, small GTP binding protein Rac2)
200607_s_at	RAD21	2.8	3.1	2.6	3.2	2.5	2.6	1.7	1.5	RAD21 homolog (S. pombe)
221872_at	RARRES1	1.9	3.4	2.1	2.1	5.3	4.3	1.7	1.5	retinoic acid receptor responder (tazarotene induced) 1
205590_at	RASGRP1	1.6	2.6	2.8	2.2	2.8	2.3	1.9	2.1	RAS guanyl releasing protein 1 (calcium and DAG-regulated)
201890_at	RRM2	3.6	4.4	1.6	2.7	4.0	3.7	1.6	2.3	ribonucleotide reductase M2
220330_s_at	SAMSN1	1.7	3.6	1.8	2.0	3.0	2.8	1.2	1.1	SAM domain, SH3 domain and nuclear localization signals 1
202062_s_at	SEL1L	1.9	2.4	2.1	2.6	2.6	2.8	1.3	1.0	sel-1 suppressor of lin-12-like (C. elegans)
209723_at	SERPINB9	1.8	2.8	1.4	1.6	3.0	2.3	1.8	2.5	serpin peptidase inhibitor, clade B (ovalbumin), member 9
219159_s_at	SLAMF7	3.5	6.5	3.6	3.8	5.0	3.4	2.2	1.3	SLAM family member 7
219386_s_at	SLAMF8	3.1	5.1	5.6	3.7	5.7	6.2	2.0	2.2	SLAM family member 8
202800_at	SLC1A3	1.6	2.4	2.0	1.5	2.7	2.6	0.9	1.0	solute carrier family 1 (glial high affinity glutamate transporter), member 3
212295_s_at	SLC7A1	2.5	3.2	2.0	1.6	2.4	2.0	1.8	1.9	solute carrier family 7 (cationic amino acid transporter, y+ system), member 1
201996_s_at	SPEN	2.9	2.5	2.0	4.4	1.6	2.4	1.4	1.7	spen homolog, transcriptional regulator (Drosophila)
209875_s_at	SPP1	6.0	8.6	1.7	1.4	6.8	1.2	2.5	3.4	secreted phosphoprotein 1
1554690_a_at	TACC1	2.2	2.4	1.7	2.7	1.6	2.1	1.3	1.3	transforming, acidic coiled-coil containing protein 1
201813_s_at	TBC1D5	2.6	2.9	2.5	2.5	2.7	2.6	1.7	1.5	TBC1 domain family, member 5
208691_at	TFRC	4.0	1.8	3.1	1.7	4.3	1.5	1.7	1.6	transferrin receptor (p90, CD71)
202643_s_at	TNFAIP3	2.0	1.7	2.4	2.1	2.9	2.3	1.6	1.7	tumor necrosis factor, alpha-induced protein 3
219725_at	TREM2	2.1	3.0	1.7	1.5	3.3	2.7	1.3	1.5	triggering receptor expressed on myeloid cells 2
1568592_at	TRIM69	2.0	3.3	1.9	2.7	1.9	2.9	1.2	2.1	tripartite motif-containing 69
218245_at	TSKU	2.2	1.8	2.8	2.0	2.6	2.8	1.3	1.4	tsukushin
202589_at	TYMS	1.7	2.1	1.3	1.4	3.4	3.1	1.9	2.1	thymidylate synthetase
238657_at	UBXN10	1.6	3.4	1.4	1.9	3.9	5.6	2.2	2.2	UBX domain protein 10
208998_at	UCP2	2.2	2.9	1.7	2.1	2.5	2.6	1.3	1.1	uncoupling protein 2 (mitochondrial, proton carrier)
214382_at	UNC93A	2.2	2.4	2.9	7.0	3.0	6.2	7.6	7.0	unc-93 homolog A (C. elegans)
222387_s_at	VPS35	2.1	2.7	2.7	2.7	1.5	1.6	1.5	1.3	vacuolar protein sorting 35 homolog (S. cerevisiae)
204026_s_at	ZWINT	1.8	3.0	1.3	1.9	3.2	3.7	1.7	1.8	ZW10 interactor
227918_s_at	ZYG11B	2.7	2.6	2.1	5.1	1.5	3.0	1.3	1.1	zyg-11 homolog B (C. elegans)

_Unannotated

probe set ID	Symbol	pat1	pat2	pat3	pat4	pat5	pat6	CHC-R	CH-NR	Gene Name
219099_at	C12orf5	1.5	3.1	1.6	1.5	3.2	3.0	1.3	2.0	chromosome 12 open reading frame 5
225105_at	C12orf75	2.4	3.0	1.8	1.6	3.0	1.2	1.6	2.2	chromosome 12 open reading frame 75
219757_s_at	C14orf101	1.9	1.9	2.5	2.6	1.8	2.0	1.0	1.1	chromosome 14 open reading frame 101
223484_at	C15orf48	3.2	6.9	3.5	2.6	5.1	4.7	2.3	2.2	chromosome 15 open reading frame 48
226456_at	C16orf75	2.2	3.3	1.7	2.1	3.0	3.9	2.0	2.3	chromosome 16 open reading frame 75
235377_at	C6orf142	3.1	5.3	3.0	3.8	3.5	3.4	0.7	0.8	chromosome 6 open reading frame 142
217967_s_at	FAM129A	2.9	2.8	2.5	2.0	2.4	1.8	1.7	1.9	family with sequence similarity 129, member A
229391_s_at	FAM26F	1.6	3.6	1.9	2.6	2.3	2.4	0.9	0.7	family with sequence similarity 26, member F

Supplementary Table II.

Fold changes of the downregulated genes in functional categories (fold change below 0.5 between the means of AHC and healthy liver samples with the corresponding FDR (Benjamini-Hochberg correction) below 0.05).

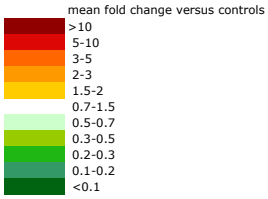

Metabolism

probe set ID	Symbol	pat1	pat2	pat3	pat4	pat5	pat6	CHC-R	CH-NR	Gene Name
214829_at	AASS	0.40	0.35	0.69	0.64	0.38	0.55	0.64	0.50	aminoadipate-semialdehyde synthase
203559_s_at	ABP1	0.18	0.34	0.53	0.87	0.15	0.42	0.23	0.09	amiloride binding protein 1 (amine oxidase (copper-containing))
227962_at	ACOX1	0.44	0.35	0.62	0.47	0.64	0.52	0.88	0.74	acyl-Coenzyme A oxidase 1, palmitoyl
231675_s_at	ADH4	0.28	0.30	0.37	0.30	0.36	0.29	0.47	0.49	alcohol dehydrogenase 4 (class II), pi polypeptide
214423_x_at	ALDOB	0.22	0.26	0.30	0.32	0.25	0.28	0.44	0.57	Aldolase B, fructose-bisphosphate
231662_at	ARG1	0.17	0.30	0.30	0.23	0.29	0.38	0.49	0.53	Arginase, liver
201171_at	ATP6V0E1	0.36	0.64	0.36	0.43	0.48	0.53	0.55	0.65	ATPase, H+ transporting, lysosomal 9kDa, V0 subunit e1
232449_at	BCO2	0.26	0.16	0.62	0.22	0.46	0.39	0.41	0.43	beta-carotene oxygenase 2
231591_at	BHMT	0.26	0.37	0.67	0.41	0.35	0.60	0.62	0.68	Betaine-homocysteine methyltransferase
231672_at	CES4	0.27	0.34	0.30	0.24	0.37	0.33	0.54	0.67	Carboxylesterase 4-like
206424_at	CYP26A1	0.06	0.22	0.22	0.23	0.14	0.28	0.27	0.27	cytochrome P450, family 26, subfamily A, polypeptide 1
219903_s_at	CYP2C8	0.29	0.34	0.50	0.33	0.35	0.45	0.59	0.66	cytochrome P450, family 2, subfamily C, polypeptide 8
214420_s_at	CYP2C9	0.22	0.25	0.36	0.20	0.36	0.27	0.56	0.58	Cytochrome P450, family 2, subfamily C, polypeptide 9
222100_at	CYP2E1	0.36	0.46	0.47	0.53	0.35	0.51	0.62	0.52	Cytochrome P450, family 2, subfamily E, polypeptide 1
1554931_at	CYP4A11	0.52	0.22	0.70	0.62	0.19	0.30	0.59	0.56	cytochrome P450, family 4, subfamily A, polypeptide 11
213868_s_at	DHRS7	0.34	0.36	0.38	0.44	0.30	0.40	0.56	0.81	Dehydrogenase/reductase (SDR family) member 7
235305_s_at	ECHDC2	0.55	0.22	0.57	0.76	0.41	0.49	0.49	0.38	enoyl Coenzyme A hydratase domain containing 2
211934_x_at	GANAB	0.30	0.37	0.33	0.18	0.75	0.36	0.99	0.93	glucosidase, alpha; neutral AB
231686_at	GATM	0.28	0.29	0.23	0.21	0.21	0.17	0.46	0.54	Glycine amidinotransferase (L-arginine:glycine amidinotransferase)
210328_at	GNMT	0.18	0.19	0.16	0.32	0.13	0.14	0.49	0.29	glycine N-methyltransferase
220801_s_at	HAO2	0.57	0.34	0.69	0.86	0.27	0.36	0.70	0.73	hydroxyacid oxidase 2 (long chain)
204110_at	HNMT	0.26	0.30	0.29	0.34	0.51	0.36	0.61	0.64	histamine N-methyltransferase
209703_x_at	METTL7A	0.37	0.41	0.43	0.37	0.33	0.40	0.76	0.58	methyltransferase like 7A
219959_at	MOCOS	0.46	0.35	0.57	0.76	0.16	0.62	0.79	0.99	molybdenum cofactor sulfurase
231559_at	NNMT	0.25	0.39	0.17	0.23	0.21	0.17	0.30	0.26	Nicotinamide N-methyltransferase
203515_s_at	PMVK	0.43	0.53	0.38	0.36	0.73	0.47	0.99	0.84	phosphomevalonate kinase
204476_s_at	PC	0.38	0.45	0.26	0.18	0.73	0.26	0.69	0.56	pyruvate carboxylase
242662_at	PCSK6	0.42	0.27	0.72	0.68	0.37	0.63	0.71	0.54	Proprotein convertase subtilisin/kexin type 6
237248_at	PDE11A	0.35	0.28	0.82	0.49	0.54	0.51	0.61	0.80	phosphodiesterase 11A
1562321_at	PDK4	0.16	0.15	0.46	0.36	0.15	0.39	0.45	0.35	pyruvate dehydrogenase kinase, isozyme 4
217383_at	PGK1	0.42	0.41	0.27	0.36	0.42	0.24	0.46	0.61	Phosphoglycerate kinase 1
222049_s_at	RBP4	0.31	0.38	0.40	0.29	0.35	0.38	0.53	0.59	Retinol binding protein 4, plasma
1566472_s_at	RETSAT	0.41	0.60	0.40	0.31	0.74	0.56	0.82	0.79	retinol saturase (all-trans-retinol 13,14-reductase)
219934_s_at	SULT1E1	0.42	0.25	0.74	0.76	0.19	0.35	0.74	0.42	sulfotransferase family 1E, estrogen-preferring, member 1
1555189_a_at	TAT	0.19	0.34	0.27	0.35	0.25	0.71	0.40	0.35	tyrosine aminotransferase
231702_at	TDO2	0.29	0.46	0.35	0.48	0.25	0.52	0.44	0.59	Tryptophan 2,3-dioxygenase
224043_s_at	UPB1	0.28	0.26	0.36	0.22	0.41	0.30	1.01	0.77	ureidopropionase, beta

Immune response

probe set ID	Symbol	pat1	pat2	pat3	pat4	pat5	pat6	CHC-R	CH-NR	Gene Name
201641_at	BST2	0.31	0.45	0.29	0.18	0.99	0.51	0.79	2.04	bone marrow stromal cell antigen 2
1554459_s_at	CFHR3	0.51	0.26	0.69	0.70	0.32	0.22	0.40	0.12	complement factor H-related 3
207874_s_at	CFHR4	0.56	0.37	0.70	0.63	0.36	0.26	0.47	0.20	complement factor H-related 4
208088_s_at	CFHR5	0.55	0.64	0.39	0.45	0.61	0.30	0.51	0.23	complement factor H-related 5
220305_at	MAVS	0.50	0.53	0.50	0.35	0.77	0.42	0.78	0.64	mitochondrial antiviral signaling protein

Lipid-related genes

probe set ID	Symbol	pat1	pat2	pat3	pat4	pat5	pat6	CHC-R	CH-NR	Gene Name
231359_at	APOH	0.33	0.36	0.33	0.26	0.31	0.30	0.47	0.64	Apolipoprotein H (beta-2-glycoprotein I)
231693_at	FABP1	0.33	0.52	0.27	0.24	0.45	0.40	0.58	0.67	Fatty acid binding protein 1, liver
207584_at	LPA	0.54	0.33	0.59	0.57	0.32	0.35	0.42	0.15	lipoprotein, Lp(a)
220675_s_at	PNPLA3	0.37	0.41	0.23	0.30	0.57	0.44	0.91	1.01	patatin-like phospholipase domain containing 3

Apoptosis

probe set ID	Symbol	pat1	pat2	pat3	pat4	pat5	pat6	CHC-R	CH-NR	Gene Name
208478_s_at	BAX	0.42	0.57	0.28	0.23	1.20	0.52	1.14	1.63	BCL2-associated X protein

Translation and ribosomes

probe set ID	Symbol	pat1	pat2	pat3	pat4	pat5	pat6	CHC-R	CH-NR	Gene Name
213087_s_at	EEF1D	0.23	0.34	0.20	0.25	0.25	0.25	0.46	0.44	eukaryotic translation elongation factor 1 delta (guanine nucleotide exchange protein)
219138_at	RPL14	0.36	0.42	0.39	0.39	0.55	0.44	0.58	0.58	ribosomal protein L14
212044_s_at	RPL27A	0.47	0.44	0.46	0.56	0.31	0.38	0.66	0.76	Ribosomal protein L27a
213350_at	RPS11	0.41	0.47	0.39	0.57	0.35	0.48	0.70	0.75	Ribosomal protein S11
230034_x_at	MRPL41	0.46	0.51	0.42	0.59	0.42	0.42	0.69	0.81	mitochondrial ribosomal protein L41
223292_s_at	MRPS15	0.29	0.42	0.25	0.21	0.37	0.26	0.49	0.52	mitochondrial ribosomal protein S15

Blood-related genes

probe set ID	Symbol	pat1	pat2	pat3	pat4	pat5	pat6	CHC-R	CH-NR	Gene Name
231684_at	ANGPTL3	0.22	0.35	0.47	0.35	0.47	0.49	0.52	0.56	Angiopoietin-like 3
209116_x_at	HBB	0.32	0.52	0.36	0.40	0.27	0.22	0.36	0.27	hemoglobin, beta
240033_at	PLG	0.60	0.32	0.84	0.56	0.43	0.40	0.54	0.44	plasminogen
1558603_at	PLGLB2	0.32	0.39	0.42	0.37	0.29	0.34	0.40	0.34	plasminogen-like B2

RNA binding or processing

probe set ID	Symbol	pat1	pat2	pat3	pat4	pat5	pat6	CHC-R	CH-NR	Gene Name
225191_at	CIRBP	0.52	0.35	0.47	0.38	0.50	0.40	0.65	0.65	cold inducible RNA binding protein
231011_at	LARP2	0.24	0.27	0.18	0.17	0.22	0.17	0.37	0.35	La ribonucleoprotein domain family, member 2
242837_at	SFRS4	0.43	0.21	0.64	0.31	0.70	0.42	0.64	0.65	Splicing factor, arginine/serine-rich 4
212266_s_at	SFRS5	0.45	0.45	0.52	0.32	0.64	0.40	0.84	0.85	splicing factor, arginine/serine-rich 5
226670_s_at	PABPC1L	0.54	0.30	0.51	0.42	0.45	0.48	0.63	0.67	poly(A) binding protein, cytoplasmic 1-like
227244_s_at	SSU72	0.26	0.34	0.22	0.31	0.22	0.23	0.46	0.78	SSU72 RNA polymerase II CTD phosphatase homolog (S. cerevisiae)

DNA binding

probe set ID	Symbol	pat1	pat2	pat3	pat4	pat5	pat6	CHC-R	CH-NR	Gene Name
221646_s_at	ZDHHC11	0.61	0.42	0.65	0.40	0.44	0.36	0.87	1.07	zinc finger, DHHC-type containing 11
224445_s_at	ZFYVE21	0.49	0.60	0.45	0.31	0.73	0.48	0.90	0.84	zinc finger, FYVE domain containing 21
206373_at	ZIC1	0.18	0.40	0.28	0.29	0.51	0.66	0.30	0.15	Zic family member 1 (odd-paired homolog, Drosophila)
1557953_at	ZKSCAN1	0.58	0.39	0.56	0.51	0.53	0.43	0.78	0.90	zinc finger with KRAB and SCAN domains 1
239937_at	ZNF207	0.29	0.16	0.36	0.15	0.47	0.25	0.64	0.61	Zinc finger protein 207
215012_at	ZNF451	0.47	0.34	0.64	0.33	0.71	0.49	0.71	0.71	zinc finger protein 451
205594_at	ZNF652	0.51	0.50	0.37	0.48	0.61	0.54	1.01	0.91	zinc finger protein 652

Protein phosphatases/kinases and related

probe set ID	Symbol	pat1	pat2	pat3	pat4	pat5	pat6	CHC-R	CH-NR	Gene Name
218744_s_at	PACSIN3	0.55	0.49	0.34	0.35	0.52	0.36	0.92	0.61	protein kinase C and casein kinase substrate in neurons 3
240187_at	PPP1R3C	0.26	0.11	0.39	0.41	0.13	0.18	0.32	0.37	protein phosphatase 1, regulatory (inhibitor) subunit 3C
222351_at	PPP2R1B	0.24	0.26	0.33	0.22	0.54	0.45	0.42	0.55	protein phosphatase 2 (formerly 2A), regulatory subunit A, beta isoform
200637_s_at	PTPRF	0.44	0.48	0.34	0.29	0.75	0.34	0.84	0.61	protein tyrosine phosphatase, receptor type, F
209622_at	STK16	0.35	0.44	0.38	0.21	0.67	0.40	0.76	0.71	serine/threonine kinase 16

Ubiquitination

probe set ID	Symbol	pat1	pat2	pat3	pat4	pat5	pat6	CHC-R	CH-NR	Gene Name
236235_at	ITCH	0.34	0.29	0.58	0.40	0.39	0.31	0.75	0.53	Itchy E3 ubiquitin protein ligase homolog (mouse)
225179_at	UBE2K	0.41	0.44	0.38	0.32	0.53	0.36	0.85	0.83	ubiquitin-conjugating enzyme E2K (UBC1 homolog, yeast)

Ras oncogene-related

probe set ID	Symbol	pat1	pat2	pat3	pat4	pat5	pat6	CHC-R	CH-NR	Gene Name
215506_s_at	DIRAS3	0.45	0.28	0.49	0.71	0.23	0.24	0.57	0.52	DIRAS family, GTP-binding RAS-like 3
228161_at	RAB32	0.38	0.59	0.45	0.36	0.65	0.67	0.61	0.69	RAB32, member RAS oncogene family
231075_x_at	RAPH1	0.48	0.42	0.33	0.64	0.39	0.52	0.87	0.94	Ras association (RalGDS/AF-6) and pleckstrin homology domains 1
213409_s_at	RHEB	0.35	0.29	0.64	0.64	0.23	0.33	0.56	0.46	Ras homolog enriched in brain

SLC family

probe set ID	Symbol	pat1	pat2	pat3	pat4	pat5	pat6	CHC-R	CH-NR	Gene Name
219915_s_at	SLC16A10	0.52	0.26	0.47	0.78	0.24	0.28	0.67	0.39	solute carrier family 16, member 10 (aromatic amino acid transporter)
221661_at	SLC22A7	0.45	0.32	0.35	0.40	0.42	0.30	0.51	0.57	solute carrier family 22 (organic anion transporter), member 7
209236_at	SLC23A2	0.26	0.25	0.41	0.25	0.56	0.36	0.67	0.42	solute carrier family 23 (nucleobase transporters), member 2
218136_s_at	SLC25A37	0.44	0.48	0.47	0.52	0.44	0.41	0.52	0.39	solute carrier family 25, member 37
205799_s_at	SLC3A1	0.49	0.56	0.35	0.32	0.30	0.18	0.44	0.28	solute carrier family 3 (cystine, dibasic and neutral amino acid transporters, activator of cystine, dibasic and n
233123_at	SLC40A1	0.49	0.36	0.76	0.33	0.61	0.44	0.63	0.66	Solute carrier family 40 (iron-regulated transporter), member 1
219820_at	SLC6A16	0.44	0.29	0.44	0.37	0.28	0.24	0.67	0.58	solute carrier family 6, member 16

Other

probe set ID	Symbol	pat1	pat2	pat3	pat4	pat5	pat6	CHC-R	CH-NR	Gene Name
205730_s_at	ABLIM3	0.51	0.54	0.46	0.28	0.81	0.37	0.56	0.58	actin binding LIM protein family, member 3
211489_at	ADRA1A	0.53	0.36	0.71	0.32	0.58	0.36	0.49	0.49	adrenergic, alpha-1A-, receptor
232810_at	AIG1	0.30	0.20	0.47	0.32	0.35	0.32	0.57	0.48	androgen-induced 1
214425_at	AMBP	0.37	0.45	0.36	0.42	0.29	0.35	0.53	0.64	Alpha-1-microglobulin/bikunin precursor
226663_at	ANKRD10	0.29	0.14	0.44	0.18	0.46	0.23	0.60	0.59	ankyrin repeat domain 10
216563_at	ANKRD12	0.50	0.32	0.32	0.59	0.55	0.57	0.66	0.76	Ankyrin repeat domain 12
203747_at	AQP3	0.51	0.51	0.38	0.38	0.74	0.44	0.79	0.61	aquaporin 3 (Gill blood group)
209824_s_at	ARNTL	0.33	0.38	0.77	0.28	0.61	0.42	0.48	0.57	aryl hydrocarbon receptor nuclear translocator-like
211852_s_at	ATRN	0.44	0.38	0.55	0.27	0.88	0.49	0.96	0.80	attractin
215460_x_at	BRD1	0.52	0.47	0.49	0.42	0.63	0.47	0.89	1.07	bromodomain containing 1
229163_at	CAMK2N1	0.34	0.35	0.28	0.44	0.32	0.32	0.54	0.64	calcium/calmodulin-dependent protein kinase II inhibitor 1
214475_x_at	CAPN3	0.45	0.31	0.56	0.60	0.39	0.52	0.45	0.36	calpain 3, (p94)
226736_at	CHURC1	0.75	0.38	0.37	0.28	0.38	0.39	0.74	0.72	churchill domain containing 1
227953_at	CMTM6	0.32	0.61	0.27	0.32	0.51	0.37	0.63	0.69	CKLF-like MARVEL transmembrane domain containing 6
206417_at	CNGA1	0.65	0.34	0.63	0.35	0.61	0.38	0.68	0.63	cyclic nucleotide gated channel alpha 1
216389_s_at	DCAF11	0.45	0.50	0.50	0.40	0.57	0.45	0.88	0.75	DDB1 and CUL4 associated factor 11
225549_at	DDX6	0.39	0.29	0.51	0.27	0.76	0.45	0.94	1.03	DEAD (Asp-Glu-Ala-Asp) box polypeptide 6
213645_at	ENOSF1	0.57	0.38	0.46	0.64	0.38	0.42	0.78	0.71	enolase superfamily member 1
201216_at	ERP29	0.38	0.46	0.38	0.25	0.68	0.42	0.91	0.91	endoplasmic reticulum protein 29
212697_at	FAM134C	0.31	0.34	0.35	0.18	0.72	0.41	1.03	1.22	family with sequence similarity 134, member C
215600_x_at	FBXW12	0.55	0.39	0.56	0.44	0.60	0.47	0.83	0.81	F-box and WD repeat domain containing 12
214417_s_at	FETUB	0.28	0.35	0.49	0.28	0.44	0.48	0.63	0.80	Fetuin B
203391_at	FKBP2	0.38	0.57	0.38	0.33	0.71	0.49	0.95	0.88	FK506 binding protein 2, 13kDa
200959_at	FUS	0.38	0.40	0.30	0.17	0.71	0.33	1.13	1.18	fusion (involved in t(12;16) in malignant liposarcoma)
236548_at	GIPC2	0.42	0.38	0.50	0.73	0.36	0.53	0.86	0.82	GIPC PDZ domain containing family, member 2
224997_x_at	H19	0.71	0.43	0.71	0.40	0.30	0.25	0.71	1.05	H19, imprinted maternally expressed transcript (non-protein coding)
1557100_s_at	HECTD1	0.33	0.29	0.47	0.26	0.51	0.33	0.59	0.50	HECT domain containing 1
219976_at	HOOK1	0.58	0.53	0.41	0.48	0.60	0.41	0.67	0.78	hook homolog 1 (Drosophila)
227139_s_at	HPS3	0.51	0.54	0.48	0.41	0.52	0.43	0.77	0.87	Hermansky-Pudlak syndrome 3
202718_at	IGFBP2	0.25	0.16	0.22	0.03	0.51	0.13	1.12	1.28	insulin-like growth factor binding protein 2, 36kDa
203424_s_at	IGFBP5	0.48	0.28	0.33	0.35	0.24	0.25	0.63	0.58	insulin-like growth factor binding protein 5
229125_at	KANK4	0.55	0.48	0.48	0.72	0.38	0.28	0.64	0.43	KN motif and ankyrin repeat domains 4
210078_s_at	KCNAB1	0.31	0.29	0.32	0.62	0.26	0.31	0.52	0.42	potassium voltage-gated channel, shaker-related subfamily, beta member 1
242931_at	LONRF3	0.52	0.41	0.70	0.51	0.46	0.38	0.60	0.71	LON peptidase N-terminal domain and ring finger 3
231640_at	LYRM5	0.35	0.38	0.31	0.42	0.32	0.30	0.57	0.64	LYR motif containing 5
232168_x_at	MACF1	0.54	0.40	0.55	0.39	0.66	0.48	0.75	0.66	microtubule-actin crosslinking factor 1
212708_at	MSL1	0.46	0.54	0.36	0.31	0.82	0.52	0.89	0.99	male-specific lethal 1 homolog (Drosophila)
217546_at	MT1M	0.65	0.40	0.10	0.61	0.38	0.16	0.17	0.13	metallothionein 1M
214753_at	N4BP2L2	0.38	0.24	0.66	0.26	0.45	0.34	0.57	0.70	NEDD4 binding protein 2-like 2
1558515_at	NCRNA00182	0.28	0.19	0.47	0.18	0.54	0.37	0.61	0.63	non-protein coding RNA 182
206453_s_at	NDRG2	0.26	0.26	0.26	0.11	0.46	0.22	1.17	1.10	NDRG family member 2
224566_at	NEAT1	0.40	0.31	0.50	0.33	0.50	0.44	0.53	0.52	nuclear paraspeckle assembly transcript 1 (non-protein coding)
225355_at	NEURL1B	0.48	0.54	0.39	0.37	0.69	0.43	1.18	1.44	neuralized homolog 1B (Drosophila)
232158_x_at	NIPAL1	0.43	0.36	0.49	0.36	0.31	0.36	0.89	0.95	NIPA-like domain containing 1
207202_s_at	NR1I2	0.46	0.47	0.58	0.54	0.38	0.61	0.67	0.80	nuclear receptor subfamily 1, group I, member 2
1570188_at	NR1I3	0.30	0.16	0.39	0.39	0.27	0.33	0.49	0.40	nuclear receptor subfamily 1, group I, member 3
224582_s_at	NUCKS1	0.38	0.32	0.41	0.24	0.41	0.23	1.07	0.88	nuclear casein kinase and cyclin-dependent kinase substrate 1
226643_s_at	NUDCD2	0.28	0.30	0.39	0.38	0.25	0.43	0.58	0.65	NudC domain containing 2
205728_at	ODZ1	0.54	0.25	0.79	0.64	0.41	0.50	0.65	0.52	odz, odd Oz/ten-m homolog 1(Drosophila)
228881_at	PARL	0.24	0.36	0.33	0.30	0.38	0.39	0.58	0.65	presenilin associated, rhomboid-like
1567213_at	PNN	0.43	0.38	0.56	0.33	0.42	0.39	0.54	0.66	pinin, desmosome associated protein
219392_x_at	PRR11	0.46	0.42	0.56	0.38	0.56	0.51	0.81	0.78	proline rich 11
203354_s_at	PSD3	0.28	0.38	0.41	0.31	0.52	0.75	1.03	1.05	pleckstrin and Sec7 domain containing 3
207330_at	PZP	0.38	0.34	0.34	0.23	0.35	0.11	0.09	0.04	pregnancy-zone protein
210751_s_at	RGN	0.52	0.52	0.50	0.47	0.46	0.46	1.05	1.32	regucalcin (senescence marker protein-30)
212482_at	RMND5A	0.40	0.38	0.52	0.34	0.50	0.38	0.88	0.85	required for meiotic nuclear division 5 homolog A (S. cerevisiae)
228806_at	RORC	0.60	0.43	0.52	0.59	0.33	0.35	0.73	0.77	RAR-related orphan receptor C
216962_at	RPAIN	0.32	0.42	0.34	0.33	0.35	0.46	0.55	0.70	RPA interacting protein
206211_at	SELE	0.47	0.43	0.13	0.19	0.55	0.08	0.14	0.05	selectin E
230707_at	SORL1	0.49	0.21	0.58	0.67	0.29	0.36	0.57	0.43	sortilin-related receptor, L(DLR class) A repeats-containing
212468_at	SPAG9	0.44	0.38	0.30	0.43	0.45	0.41	0.76	0.67	sperm associated antigen 9
208610_s_at	SRRM2	0.62	0.40	0.28	0.77	0.40	0.47	0.53	0.52	serine/arginine repetitive matrix 2
214064_at	TF	0.48	0.29	0.77	0.52	0.26	0.44	0.58	0.58	transferrin
221871_s_at	TFG	0.39	0.42	0.56	0.49	0.43	0.51	0.70	0.70	TRK-fused gene
229302_at	TMEM178	0.55	0.41	0.59	0.32	0.60	0.50	0.72	0.86	transmembrane protein 178
226083_at	TMEM70	0.49	0.46	0.44	0.50	0.60	0.52	0.55	0.72	transmembrane protein 70
229574_at	TRA2A	0.39	0.24	0.69	0.35	0.49	0.40	0.62	0.71	transformer 2 alpha homolog (Drosophila)
237350_at	TTC36	0.59	0.39	0.60	0.60	0.43	0.41	0.73	0.47	tetratricopeptide repeat domain 36
208844_at	VDAC3	0.38	0.41	0.39	0.28	0.42	0.34	0.54	0.73	voltage-dependent anion channel 3
205506_at	VIL1	0.38	0.41	0.37	0.28	0.30	0.20	0.44	0.34	villin 1
242234_at	XAF1	0.41	0.31	0.35	0.27	0.50	0.60	0.53	0.90	XIAP associated factor 1
213999_at	YIPF4	0.46	0.52	0.38	0.60	0.36	0.46	0.67	0.76	Yip1 domain family, member 4

Unannotated

probe set ID	Symbol	pat1	pat2	pat3	pat4	pat5	pat6	CHC-R	CH-NR	Gene Name
231538_at	C11orf1	0.40	0.60	0.36	0.75	0.37	0.53	0.71	0.82	Chromosome 11 open reading frame 1
227535_at	C15orf24	0.31	0.48	0.24	0.25	0.35	0.35	0.61	0.96	Chromosome 15 open reading frame 24
216483_s_at	C19orf10	0.43	0.62	0.35	0.25	1.07	0.46	1.21	1.14	chromosome 19 open reading frame 10
230213_at	C19orf43	0.42	0.35	0.41	0.36	0.56	0.37	0.61	0.67	chromosome 19 open reading frame 43
230256_at	C1orf104	0.26	0.20	0.16	0.17	0.31	0.24	0.44	0.39	Chromosome 1 open reading frame 104
223126_s_at	C1orf21	0.41	0.39	0.48	0.60	0.35	0.49	0.87	0.80	chromosome 1 open reading frame 21
230424_at	C5orf13	0.56	0.43	0.38	0.47	0.25	0.27	0.52	0.44	chromosome 5 open reading frame 13
213089_at	LOC100272216	0.65	0.35	0.63	0.35	0.72	0.40	0.75	0.79	hypothetical LOC100272216
213810_s_at	LOC100292682	0.41	0.37	0.37	0.32	0.44	0.32	0.58	0.83	hypothetical protein LOC100292682
231258_at	LOC100293390	0.45	0.59	0.42	0.41	0.33	0.36	0.60	0.64	hypothetical protein LOC100293390
1560679_at	LOC151438	0.49	0.28	0.65	0.81	0.28	0.53	0.82	0.83	hypothetical protein LOC151438
225762_x_at	LOC284801	0.42	0.62	0.37	0.38	0.73	0.57	0.72	0.88	hypothetical protein LOC284801
237889_s_at	LOC553137	0.14	0.10	0.23	0.10	0.23	0.14	0.30	0.23	Hypothetical LOC553137
239432_at	FLJ31306	0.44	0.28	0.75	0.41	0.58	0.40	0.61	0.62	hypothetical LOC379025
238127_at	FLJ41484	0.30	0.42	0.43	0.39	0.39	0.56	0.76	0.71	hypothetical LOC650669

Supplementary Table III.

Fold changes of the upregulated genes in IFN-treated PHH. The table shows genes that in PHH from both donors were at least 2-fold upregulated between untreated and IFN-treated PHH samples.

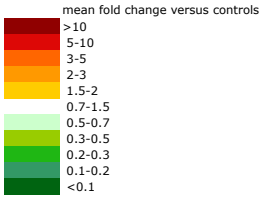

> 2-fold induced in both donors IFN-alpha, but not in IFN-gamma

		IFN-alpha				IFN-gamma				
		6h		24h		6h		24h		
probeSetID	Symbol	D1	D2	D1	D2	D1	D2	D1	D2	GeneName
8170704	ABCD1	2.5	2.5	1.7	2.4	1.1	1.3	1.4	1.3	ATP-binding cassette, sub-family D (ALD), member 1 (ABCD1), mRNA.
7947462	ABTB2	2.2	2.1	1.5	1.5	1.3	1.1	1.2	1.2	ankyrin repeat and BTB (POZ) domain containing 2 (ABTB2), mRNA.
8141648	ACHE	1.9	4.5	2.1	6.5	1.1	3.3	1.5	6.6	acetylcholinesterase (Yt blood group) (ACHE), transcript variant E4-E5, mRNA.
7905233	ADAMTSL4	2.1	2.3	1.3	2.2	1.4	2.4	1.7	3.0	ADAMTS-like 4 (ADAMTSL4), transcript variant 1, mRNA.
7900087	ADPRHL2	2.7	2.4	1.4	1.7	1.7	1.6	1.3	1.6	ADP-ribosylhydrolase like 2 (ADPRHL2), nuclear gene encoding mitochondrial protein, mRNA.
8011599	ANKFY1	2.1	2.3	1.7	1.9	1.5	1.4	1.7	1.9	ankyrin repeat and FYVE domain containing 1 (ANKFY1), transcript variant 1, mRNA.
8073062	APOBEC3B	5.5	4.3	1.8	2.0	1.5	1.3	1.2	1.1	apolipoprotein B mRNA editing enzyme, catalytic polypeptide-like 3B (APOBEC3B), mRNA.
8180374	APOBEC3F	4.9	3.1	2.2	2.3	1.5	1.0	2.0	1.6	apolipoprotein B mRNA editing enzyme, catalytic polypeptide-like 3F (APOBEC3F), transcript varia
8016215	ARHGAP27	2.3	2.8	1.3	2.2	0.9	1.4	1.1	1.8	Rho GTPase activating protein 27 (ARHGAP27), transcript variant 1, mRNA.
8142098	ATXN7L1	2.1	1.4	2.2	2.3	0.9	0.8	1.4	1.5	ataxin 7-like 1 (ATXN7L1), transcript variant 1, mRNA.
8035304	BST2	2.3	2.1	3.2	3.8	1.1	1.1	1.8	2.7	bone marrow stromal cell antigen 2 (BST2), mRNA.
7996403	C16orf70	2.2	2.2	1.3	1.7	0.9	1.1	1.4	1.5	chromosome 16 open reading frame 70 (C16orf70), mRNA.
7899394	C1orf38	3.1	2.2	1.4	1.1	0.8	0.5	1.6	1.0	chromosome 1 open reading frame 38 (C1orf38), transcript variant 3, mRNA.
7930577	CASP7	2.2	2.3	1.7	1.6	2.5	1.9	1.9	1.7	caspase 7, apoptosis-related cysteine peptidase (CASP7), transcript variant delta, mRNA.
8126371	CCND3	2.3	2.6	1.6	2.3	1.2	1.2	1.6	2.0	cyclin D3 (CCND3), transcript variant 2, mRNA.
8007188	CNP	3.4	3.6	2.0	2.3	1.3	1.1	1.8	2.1	2',3'-cyclic nucleotide 3' phosphodiesterase (CNP), mRNA.
8086330	CSRNP1	2.9	2.3	1.7	1.9	1.7	1.9	1.1	1.9	cysteine-serine-rich nuclear protein 1 (CSRNP1), mRNA.
7916616	CYP2J2	2.3	1.7	2.1	2.4	1.1	1.0	1.5	1.5	cytochrome P450, family 2, subfamily J, polypeptide 2 (CYP2J2), mRNA.
8018922	CYTH1	2.1	2.3	1.7	1.9	1.1	1.3	1.3	1.4	cytohesin 1 (CYTH1), transcript variant 1, mRNA.
8128843	DDO	3.2	2.6	3.1	2.9	1.2	1.1	1.8	1.7	D-aspartate oxidase (DDO), transcript variant 1, mRNA.
7987772	EHD4	3.4	2.8	1.5	1.7	1.3	1.3	1.0	1.5	EH-domain containing 4 (EHD4), mRNA.
8098439	EPCAM	2.0	30.9	1.0	24.8	1.8	28.9	0.5	17.5	epithelial cell adhesion molecule (EPCAM), mRNA.
8127778	FAM46A	1.3	1.8	2.1	2.4	1.4	1.2	1.5	2.0	family with sequence similarity 46, member A (FAM46A), mRNA.
7904361	FAM46C	3.8	2.6	1.1	1.2	1.6	1.7	1.7	1.9	family with sequence similarity 46, member C (FAM46C), mRNA.
8152812	FAM84B	2.3	2.5	1.2	1.5	1.0	1.1	1.0	0.9	family with sequence similarity 84, member B (FAM84B), mRNA.
8119198	FTSJD2	2.8	1.9	2.1	2.3	1.2	1.3	1.5	2.0	FtsJ methyltransferase domain containing 2 (FTSJD2), mRNA.
8142687	GPR37	2.7	3.0	1.3	1.9	1.3	1.5	1.1	1.4	G protein-coupled receptor 37 (endothelin receptor type B-like) (GPR37), mRNA.
7917472	GTF2B	2.5	2.5	1.3	1.4	1.8	1.8	1.4	1.9	general transcription factor IIB (GTF2B), mRNA.
8072926	H1F0	1.2	1.0	2.2	2.5	1.0	1.2	1.8	1.9	H1 histone family, member 0 (H1F0), mRNA.
8096361	HERC5	8.2	8.0	13.1	9.3	1.1	0.6	2.1	1.9	hect domain and RLD 5 (HERC5), mRNA.
7919619	HIST2H2AA3	1.7	2.3	2.4	3.2	0.9	1.6	1.3	2.2	histone cluster 2, H2aa3 (HIST2H2AA3), mRNA.
8026533	HSH2D	3.8	5.7	3.0	6.4	1.2	1.8	1.7	3.4	hematopoietic SH2 domain containing (HSH2D), mRNA.
7914127	IFI6	2.2	1.8	3.0	3.0	1.5	0.5	1.9	2.0	interferon, alpha-inducible protein 6 (IFI6), transcript variant 1, mRNA.
8132694	IGFBP1	2.4	2.5	0.9	1.5	1.8	1.8	1.1	1.3	insulin-like growth factor binding protein 1 (IGFBP1), mRNA.
7913768	IL22RA1	3.5	3.9	1.8	5.0	0.7	1.8	1.5	2.2	interleukin 22 receptor, alpha 1 (IL22RA1), mRNA.
7924058	IRF6	2.9	4.7	1.2	3.1	0.9	2.8	0.4	2.4	interferon regulatory factor 6 (IRF6), mRNA.
7945462	IRF7	4.0	2.6	2.7	2.5	1.3	1.0	1.4	1.5	interferon regulatory factor 7 (IRF7), transcript variant d, mRNA.
7936242	ITPRIP	2.9	3.3	1.6	2.0	1.8	1.7	1.7	1.6	inositol 1,4,5-triphosphate receptor interacting protein (ITPRIP), mRNA.
7992685	KCTD5	2.2	2.4	1.2	1.7	1.5	2.1	0.9	1.6	potassium channel tetramerisation domain containing 5 (KCTD5), mRNA.
8093230	KIAA0226	2.3	3.6	1.2	2.1	1.5	2.1	1.5	2.1	KIAA0226 (KIAA0226), transcript variant 1, mRNA.
7926679	KIAA1217	2.8	3.0	1.3	1.7	1.9	2.0	1.7	1.8	KIAA1217 (KIAA1217), transcript variant 1, mRNA.
8015133	KRT23	1.8	22.7	2.2	30.2	0.6	13.6	1.1	10.2	keratin 23 (histone deacetylase inducible) (KRT23), mRNA.
7994237	LCMT1	2.3	2.9	1.1	1.5	1.2	1.5	1.2	2.2	leucine carboxyl methyltransferase 1 (LCMT1), transcript variant 1, mRNA.
8018975	LGALS3BP	1.8	1.2	2.2	2.3	1.4	0.8	1.9	1.9	lectin, galactoside-binding, soluble, 3 binding protein (LGALS3BP), mRNA.
8097773	MAB21L2	9.4	2.1	2.4	1.2	1.5	1.2	1.7	1.3	mab-21-like 2 (C. elegans) (MAB21L2), mRNA.
8131091	MAFK	2.1	2.5	1.2	2.0	1.5	1.9	0.7	1.4	v-maf musculoaponeurotic fibrosarcoma oncogene homolog K (avian) (MAFK), mRNA.
7926821	MASTL	2.3	3.1	2.4	3.1	1.1	1.1	1.4	1.5	microtubule associated serine/threonine kinase-like (MASTL), transcript variant 1, mRNA.
8118116	MICB	2.2	3.3	1.3	2.0	1.4	2.3	1.8	2.7	MHC class I polypeptide-related sequence B (MICB), mRNA.
7915861	MOBKL2C	3.3	2.8	1.6	1.6	2.0	1.8	2.0	1.8	MOB1, Mps One Binder kinase activator-like 2C (yeast) (MOBKL2C), transcript variant 1, mRNA.
8151334	MSC	2.0	4.2	1.4	5.0	1.5	2.7	1.1	4.0	musculin (MSC), mRNA.
8042503	MXD1	2.2	2.9	1.3	1.7	1.5	1.6	1.8	2.8	MAX dimerization protein 1 (MXD1), mRNA.
8078729	MYD88	3.1	3.4	1.9	2.5	1.4	1.7	1.7	2.0	myeloid differentiation primary response gene (88) (MYD88), transcript variant 1, mRNA.
8001317	N4BP1	2.1	2.2	2.2	2.3	1.4	1.7	1.7	2.1	NEDD4 binding protein 1 (N4BP1), mRNA.
8031899	NA	2.4	2.5	1.5	2.1	1.3	1.5	1.4	1.6	similar to envelope protein, mRNA (cDNA clone MGC:16737 IMAGE:4129886), complete cds.
8037913	NAPA	2.1	2.3	1.8	2.4	1.4	1.5	1.5	1.9	N-ethylmaleimide-sensitive factor attachment protein, alpha (NAPA), mRNA.
8063955	OGFR	3.5	3.7	1.7	2.2	1.7	2.0	1.7	2.3	opioid growth factor receptor (OGFR), mRNA.
8090018	PARP9	1.5	1.5	2.4	2.2	1.6	1.2	1.6	1.7	poly (ADP-ribose) polymerase family, member 9 (PARP9), transcript variant 1, mRNA.
7899455	PHACTR4	2.4	2.8	1.7	2.1	1.4	1.7	1.5	1.9	phosphatase and actin regulator 4 (PHACTR4), transcript variant 1, mRNA.
8038225	PLEKHA4	5.3	4.4	2.3	2.3	1.7	1.2	1.5	1.9	pleckstrin homology domain containing, family A (phosphoinositide binding specific) member 4 (P
8052331	PNPT1	1.7	2.8	3.8	4.6	1.1	1.3	0.9	1.6	polyribonucleotide nucleotidyltransferase 1 (PNPT1), mRNA.
7941214	POLA2	2.8	2.0	1.3	1.4	1.0	1.0	1.1	0.9	polymerase (DNA directed), alpha 2 (70kD subunit) (POLA2), mRNA.
8037794	PRKD2	5.0	4.8	2.2	2.8	1.4	1.4	1.2	1.5	protein kinase D2 (PRKD2), transcript variant 1, mRNA.
8132031	PRR15	2.7	3.6	1.0	1.2	1.1	1.2	1.6	1.7	proline rich 15 (PRR15), mRNA.
8090529	RAB43	2.4	2.0	1.0	1.2	1.3	1.2	1.6	1.7	RAB43, member RAS oncogene family (RAB43), mRNA.
7941865	RAD9A	2.7	2.6	1.2	1.4	1.1	1.0	1.2	1.7	RAD9 homolog A (S. pombe) (RAD9A), mRNA.
7927120	RET	6.8	3.9	3.4	3.9	1.5	1.0	1.7	1.6	ret proto-oncogene (RET), transcript variant 2, mRNA.
8116622	RIPK1	2.7	2.2	1.6	1.7	1.7	2.0	1.9	2.7	receptor (TNFRSF)-interacting serine-threonine kinase 1 (RIPK1), mRNA.
7920297	S100A14	2.6	3.7	1.1	1.8	1.5	3.2	1.2	2.1	S100 calcium binding protein A14 (S100A14), mRNA.
8064418	SDCBP2	2.1	3.4	1.1	2.4	1.3	2.9	0.9	1.9	syndecan binding protein (syntenin) 2 (SDCBP2), transcript variant 1, mRNA.
8123598	SERPINB1	2.1	2.1	1.0	1.3	1.3	1.5	1.2	1.9	serpin peptidase inhibitor, clade B (ovalbumin), member 1 (SERPINB1), mRNA.
8021635	SERPINB2	1.1	41.3	2.2	51.3	0.7	41.2	0.7	25.2	serpin peptidase inhibitor, clade B (ovalbumin), member 2 (SERPINB2), transcript variant 1, mRN
8081710	SIDT1	6.0	5.1	2.1	2.7	1.1	0.9	1.7	1.6	SID1 transmembrane family, member 1 (SIDT1), mRNA.
8068810	SLC37A1	2.3	2.4	1.5	1.7	1.6	2.5	1.6	2.9	solute carrier family 37 (glycerol-3-phosphate transporter), member 1 (SLC37A1), mRNA.
7984364	SMAD3	2.2	2.2	1.5	2.0	1.2	1.5	1.1	1.6	SMAD family member 3 (SMAD3), transcript variant 1, mRNA.
8048926	SP140L	2.8	2.3	1.7	1.5	1.9	1.6	1.6	2.0	SP140 nuclear body protein-like (SP140L), mRNA.
7914904	STK40	2.1	2.2	0.9	1.4	1.2	1.7	0.9	1.5	serine/threonine kinase 40 (STK40), mRNA.
7916584	TACSTD2	2.0	11.1	1.8	7.7	0.8	6.3	0.8	6.1	tumor-associated calcium signal transducer 2 (TACSTD2), mRNA.
7971813	THSD1	2.4	2.7	1.3	1.5	1.4	1.6	1.4	1.8	thrombospondin, type I, domain containing 1 (THSD1), transcript variant 1, mRNA.
8032899	TICAM1	2.1	3.0	1.3	2.5	1.3	1.9	1.5	2.0	toll-like receptor adaptor molecule 1 (TICAM1), mRNA.
7978208	TINF2	2.7	2.7	1.3	1.5	1.1	1.3	1.3	1.4	TERF1 (TRF1)-interacting nuclear factor 2 (TINF2), transcript variant 2, mRNA.
8098611	TLR3	0.9	0.7	2.4	2.5	1.0	0.6	1.6	1.3	toll-like receptor 3 (TLR3), mRNA.
7966448	TMEM116	2.6	2.1	1.7	2.0	0.9	0.9	1.0	1.1	transmembrane protein 116 (TMEM116), mRNA.
8106170	TMEM171	3.5	2.3	1.3	1.2	0.9	0.9	1.8	2.3	transmembrane protein 171 (TMEM171), transcript variant 1, mRNA.
7983157	TMEM62	2.2	2.1	1.9	2.1	1.1	1.0	1.5	1.6	transmembrane protein 62 (TMEM62), mRNA.
8008289	TMEM92	2.6	3.9	1.3	3.6	1.1	2.1	1.0	1.9	transmembrane protein 92 (TMEM92), transcript variant 1, mRNA.
8149762	TNFRSF10A	2.3	3.2	1.4	2.6	1.3	2.2	0.9	1.5	tumor necrosis factor receptor superfamily, member 10a (TNFRSF10A), mRNA.
8163825	TRAF1	3.1	3.3	2.0	3.3	2.1	1.7	1.3	1.7	TNF receptor-associated factor 1 (TRAF1), mRNA.
8086125	TRANK1	3.7	3.4	2.0	1.9	1.4	0.9	1.3	1.3	tetratricopeptide repeat and ankyrin repeat containing 1 (TRANK1), mRNA.
8016847	TRIM25	2.3	2.1	1.4	1.5	1.8	2.0	1.6	2.2	tripartite motif-containing 25 (TRIM25), mRNA.
8179638	TRIM26	2.9	2.8	1.5	1.6	1.4	1.6	1.8	2.0	tripartite motif-containing 26 (TRIM26), mRNA.
8117321	TRIM38	3.1	3.8	2.1	2.1	1.6	1.1	2.3	1.7	tripartite motif-containing 38 (TRIM38), mRNA.
8135064	TRIM56	3.0	2.8	1.5	1.5	2.1	1.7	1.4	1.5	tripartite motif-containing 56 (TRIM56), mRNA.
7905428	TUFT1	2.5	2.4	1.3	1.8	1.3	1.3	0.7	0.9	tuftelin 1 (TUFT1), transcript variant 1, mRNA.
8087485	UBA7	3.2	1.9	2.6	3.0	0.9	0.5	1.1	0.8	ubiquitin-like modifier activating enzyme 7 (UBA7), mRNA.
7949904	UNC93B1	2.9	2.8	2.5	3.0	1.1	0.8	1.8	1.9	unc-93 homolog B1 (C. elegans) (UNC93B1), mRNA.
7921738	USF1	2.9	3.2	1.4	1.8	1.6	1.5	1.8	2.0	upstream transcription factor 1 (USF1), transcript variant 1, mRNA.
8131387	USP42	2.2	2.6	1.6	1.8	1.8	2.5	1.8	2.1	ubiquitin specific peptidase 42 (USP42), mRNA.
8108631	VTRNA1-3	2.2	2.1	1.6	1.2	1.2	1.4	1.9	1.1	vault RNA 1-3 (VTRNA1-3), non-coding RNA.

8084232	YEATS2	2.1	2.0	1.5	1.5	1.4	1.2	1.4	1.6	YEATS domain containing 2 (YEATS2), mRNA.
8067221	ZBP1	7.0	4.8	3.5	5.3	1.3	1.4	1.2	2.7	Z-DNA binding protein 1 (ZBP1), transcript variant 1, mRNA.
7979757	ZFYVE26	2.5	2.3	1.3	1.3	1.2	1.0	1.5	1.2	zinc finger, FYVE domain containing 26 (ZFYVE26), mRNA.

> 2-fold induced in both donors IFN-alpha and in IFN-gamma

		IFN-alpha				IFN-gamma				
		6h		24h		6h		24h		
probeSetID	Symbol	D1	D2	D1	D2	D1	D2	D1	D2	GeneName
7922598	ANGPTL1	1.6	1.1	5.8	4.1	1.5	0.7	2.7	2.2	angiopoietin-like 1 (ANGPTL1), mRNA.
8073081	APOBEC3F	5.3	4.2	2.0	2.7	1.4	1.2	2.5	3.3	apolipoprotein B mRNA editing enzyme, catalytic polypeptide-like 3F (APOBEC3F), transcript varia
8073088	APOBEC3G	10.2	6.4	3.7	5.3	1.4	0.9	4.4	5.8	apolipoprotein B mRNA editing enzyme, catalytic polypeptide-like 3G (APOBEC3G), mRNA.
8072735	APOL1	2.7	2.1	1.9	1.9	2.5	1.7	3.3	4.1	apolipoprotein L, 1 (APOL1), transcript variant 2, mRNA.
8075720	APOL2	4.0	3.5	1.6	1.7	2.3	2.6	2.5	3.6	apolipoprotein L, 2 (APOL2), transcript variant alpha, mRNA.
8075695	APOL3	6.4	4.3	2.9	2.9	5.8	3.8	9.4	8.3	apolipoprotein L, 3 (APOL3), transcript variant alpha/a, non-coding RNA.
8075709	APOL4	2.6	4.9	1.2	2.1	6.2	3.2	20.9	22.5	apolipoprotein L, 4 (APOL4), transcript variant a, mRNA.
8072108	ASPHD2	2.2	2.5	0.9	1.1	1.4	1.6	2.2	3.4	aspartate beta-hydroxylase domain containing 2 (ASPHD2), mRNA.
7909610	ATF3	6.2	3.2	1.5	2.4	4.5	2.7	2.5	3.2	activating transcription factor 3 (ATF3), transcript variant 4, mRNA.
7949340	BATF2	14.2	21.6	6.0	9.2	10.7	13.3	14.6	19.9	basic leucine zipper transcription factor, ATF-like 2 (BATF2), mRNA.
7953993	BCL2L14	7.1	8.6	1.7	2.6	5.4	4.8	6.3	9.8	BCL2-like 14 (apoptosis facilitator) (BCL2L14), transcript variant 2, mRNA.
8117435	BTN3A2	2.0	0.9	2.5	2.3	1.1	0.7	3.1	2.7	butyrophilin, subfamily 3, member A2 (BTN3A2), mRNA.
8025551	C19orf66	3.5	2.7	2.5	3.1	1.2	1.3	2.2	2.3	chromosome 19 open reading frame 66 (C19orf66), mRNA.
8094550	C4orf19	2.1	2.5	1.0	2.1	2.2	3.3	2.0	3.6	chromosome 4 open reading frame 19 (C4orf19), transcript variant 1, mRNA.
8047403	CASP10	3.1	2.7	1.5	1.5	2.2	2.4	3.2	6.0	caspase 10, apoptosis-related cysteine peptidase (CASP10), transcript variant D, mRNA.
8096808	CCDC109B	2.3	2.2	1.6	1.6	2.3	2.5	4.6	6.8	coiled-coil domain containing 109B (CCDC109B), mRNA.
8006453	CCL8	33.6	1.9	18.4	1.0	20.1	3.9	34.0	42.4	chemokine (C-C motif) ligand 8 (CCL8), mRNA.
8122334	CCRL1	3.0	3.0	4.3	8.0	3.9	4.0	58.3	65.3	chemokine (C-C motif) receptor-like 1 (CCRL1), transcript variant 1, mRNA.
8154233	CD274	8.4	18.2	4.1	9.0	24.7	30.6	21.7	41.5	CD274 molecule (CD274), mRNA.
8063156	CD40	2.2	2.5	1.6	2.3	1.9	2.2	3.7	6.2	CD40 molecule, TNF receptor superfamily member 5 (CD40), transcript variant 1, mRNA.
8050102	CMPK2	14.7	12.5	10.3	11.1	7.4	5.0	9.4	10.2	cytidine monophosphate (UMP-CMP) kinase 2, mitochondrial (CMPK2), nuclear gene encoding mit
8062409	CTNNBL1	2.5	2.2	1.2	1.3	1.5	1.2	2.0	2.1	catenin, beta like 1 (CTNNBL1), mRNA.
7996027	CX3CL1	7.9	9.9	2.5	3.6	10.3	12.5	8.1	13.7	chemokine (C-X3-C motif) ligand 1 (CX3CL1), mRNA.
8101126	CXCL10	64.6	63.9	45.6	58.2	67.3	69.2	76.8	80.2	chemokine (C-X-C motif) ligand 10 (CXCL10), mRNA.
8101131	CXCL11	29.7	24.4	35.0	35.6	49.1	35.8	75.1	69.3	chemokine (C-X-C motif) ligand 11 (CXCL11), mRNA.
8101118	CXCL9	16.5	5.5	6.6	2.8	157.5	113.8	265.2	265.9	chemokine (C-X-C motif) ligand 9 (CXCL9), mRNA.
7990391	CYP1A1	2.5	4.2	0.9	0.7	5.1	4.3	0.4	0.4	cytochrome P450, family 1, subfamily A, polypeptide 1 (CYP1A1), mRNA.
8157610	DAB2IP	2.7	3.3	1.3	2.1	1.6	2.5	2.0	2.6	DAB2 interacting protein (DAB2IP), transcript variant 1, mRNA.
8160559	DDX58	3.8	4.1	6.6	6.4	5.1	3.0	3.3	5.1	DEAD (Asp-Glu-Ala-Asp) box polypeptide 58 (DDX58), mRNA.
8103563	DDX60	2.9	1.7	8.7	9.7	4.7	2.3	9.8	8.9	DEAD (Asp-Glu-Ala-Asp) box polypeptide 60 (DDX60), mRNA.
8103601	DDX60L	3.6	3.3	4.6	7.3	4.1	3.0	3.4	5.4	DEAD (Asp-Glu-Ala-Asp) box polypeptide 60-like (DDX60L), mRNA.
7946478	DENND5A	3.0	2.7	1.5	1.3	2.3	1.7	2.1	2.1	DENN/MADD domain containing 5A (DENND5A), mRNA.
8015511	DHX58	8.2	5.1	6.6	6.0	2.6	1.3	3.6	3.4	DEXH (Asp-Glu-X-His) box polypeptide 58 (DHX58), mRNA.
8051501	EIF2AK2	1.9	2.3	3.6	3.4	2.0	1.5	2.0	2.6	eukaryotic translation initiation factor 2-alpha kinase 2 (EIF2AK2), transcript variant 1, mRNA.
7943293	ENDOD1	2.4	3.2	1.3	1.7	2.6	5.4	2.4	5.5	endonuclease domain containing 1 (ENDOD1), mRNA.
7971296	EPSTI1	5.9	6.2	6.9	9.6	4.5	3.2	8.7	11.1	epithelial stromal interaction 1 (breast) (EPSTI1), transcript variant 1, mRNA.
8107044	ERAP2	1.2	4.7	2.5	11.2	2.7	9.0	2.9	11.1	endoplasmic reticulum aminopeptidase 2 (ERAP2), transcript variant 1, mRNA.
7953981	ETV6	2.8	3.0	1.3	1.0	2.1	2.0	2.3	2.0	ets variant 6 (ETV6), mRNA.
8125993	ETV7	4.5	3.8	2.3	2.4	3.4	3.0	6.5	6.1	ets variant 7 (ETV7), mRNA.
8169995	FAM122C	4.2	4.1	2.0	2.9	1.2	1.4	2.3	2.4	family with sequence similarity 122C (FAM122C), transcript variant 1, mRNA.
8030339	FLT3LG	2.2	2.1	1.6	1.8	1.5	1.5	2.1	2.0	fms-related tyrosine kinase 3 ligand (FLT3LG), mRNA.
8105302	FST	1.9	2.5	2.0	3.4	2.2	2.9	3.9	7.0	follistatin (FST), transcript variant FST317, mRNA.
8041542	GALM	3.5	2.2	1.3	1.3	1.0	0.6	2.1	2.2	galactose mutarotase (aldose 1-epimerase) (GALM), mRNA.
7917503	GBP3	1.1	1.1	2.7	3.1	2.1	2.0	3.4	4.4	guanylate binding protein 3 (GBP3), mRNA.
7917561	GBP4	20.3	18.4	6.6	6.7	29.6	27.3	38.7	51.0	guanylate binding protein 4 (GBP4), mRNA.
7917576	GBP5	12.7	4.0	4.3	1.9	50.6	9.8	225.5	153.9	guanylate binding protein 5 (GBP5), transcript variant 1, mRNA.
8117034	GMPR	6.1	4.5	3.1	3.6	1.2	1.0	2.2	2.9	guanosine monophosphate reductase (GMPR), mRNA.
8073039	GTPBP1	3.1	2.8	1.8	2.4	1.8	1.8	2.0	2.2	GTP binding protein 1 (GTPBP1), mRNA.
8118111	HCP5	1.0	0.6	2.6	2.9	0.8	0.6	2.6	2.6	HLA complex P5 (HCP5), mRNA.
8090193	HEG1	2.6	4.1	1.1	2.3	2.2	3.2	1.9	4.1	HEG homolog 1 (zebrafish) (HEG1), mRNA.
8096335	HERC6	4.9	4.2	7.9	7.3	2.6	1.5	4.7	6.2	hect domain and RLD 6 (HERC6), transcript variant 1, mRNA.
7948982	HRASLS2	11.5	5.4	14.2	14.4	1.4	1.0	5.8	4.5	HRAS-like suppressor 2 (HRASLS2), mRNA.
8146092	IDO1	54.8	4.7	6.4	1.5	122.2	21.8	522.6	447.3	indoleamine 2,3-dioxygenase 1 (IDO1), mRNA.
7906400	IFI16	1.6	1.0	3.6	2.4	3.2	1.8	3.5	3.1	interferon, gamma-inducible protein 16 (IFI16), mRNA.
7976443	IFI27	3.3	1.8	12.5	11.7	1.4	0.8	4.4	5.1	interferon, alpha-inducible protein 27 (IFI27), transcript variant 1, mRNA.
8007446	IFI35	6.1	4.4	7.7	9.4	3.1	3.3	6.7	10.4	interferon-induced protein 35 (IFI35), mRNA.
7902553	IFI44	7.1	6.1	16.8	14.4	5.0	1.0	6.8	5.7	interferon-induced protein 44 (IFI44), mRNA.
7902541	IFI44L	16.2	8.7	50.1	41.1	11.0	2.0	30.8	22.2	interferon-induced protein 44-like (IFI44L), mRNA.
8056285	IFIH1	4.1	4.2	8.6	7.0	4.1	2.0	5.6	6.1	interferon induced with helicase C domain 1 (IFIH1), mRNA.
7929065	IFIT1	40.6	40.0	42.7	36.0	3.9	0.6	7.2	9.4	interferon-induced protein with tetratricopeptide repeats 1 (IFIT1), transcript variant 2, mRNA.
7929047	IFIT2	17.9	21.4	20.7	21.2	18.9	11.8	21.7	23.5	interferon-induced protein with tetratricopeptide repeats 2 (IFIT2), mRNA.
7929052	IFIT3	7.8	9.2	9.2	9.1	9.6	7.5	9.4	9.9	interferon-induced protein with tetratricopeptide repeats 3 (IFIT3), transcript variant 2, mRNA.
7929072	IFIT5	1.2	1.6	3.2	3.1	2.7	2.8	2.5	3.4	interferon-induced protein with tetratricopeptide repeats 5 (IFIT5), mRNA.
7937335	IFITM1	10.0	5.5	17.5	13.6	3.5	1.7	14.2	10.7	interferon induced transmembrane protein 1 (9-27) (IFITM1), mRNA.
7931899	IL15RA	2.7	2.9	1.7	1.9	2.0	2.2	2.1	2.4	interleukin 15 receptor, alpha (IL15RA), transcript variant 1, mRNA.
8044574	IL1RN	11.7	4.9	2.9	3.6	2.3	2.0	3.4	5.0	interleukin 1 receptor antagonist (IL1RN), transcript variant 1, mRNA.
8114010	IRF1	6.4	5.7	2.3	2.1	11.3	12.3	11.7	12.5	interferon regulatory factor 1 (IRF1), mRNA.
8103911	IRF2	2.7	2.8	1.6	1.7	1.8	2.0	2.5	2.3	interferon regulatory factor 2 (IRF2), mRNA.
7896817	ISG15	7.2	4.0	7.5	7.9	2.2	1.1	2.4	3.4	ISG15 ubiquitin-like modifier (ISG15), mRNA.
7985777	ISG20	4.5	3.9	3.4	3.8	3.5	2.3	4.0	3.8	interferon stimulated exonuclease gene 20kDa (ISG20), mRNA.
8028908	ITPKC	2.2	2.5	1.2	1.7	4.5	6.5	2.2	5.1	inositol 1,4,5-trisphosphate 3-kinase C (ITPKC), mRNA.
7922474	KIAA0040	4.4	6.7	1.7	2.0	2.8	3.9	2.7	4.5	KIAA0040 (KIAA0040), transcript variant 2, mRNA.
8092348	LAMP3	19.7	19.5	23.1	29.1	7.0	3.2	15.7	19.4	lysosomal-associated membrane protein 3 (LAMP3), mRNA.
8094259	LAP3	2.9	2.7	3.2	3.1	2.6	2.0	4.5	4.7	leucine aminopeptidase 3 (LAP3), mRNA.
8028744	LGALS17A	4.4	2.3	1.3	1.5	10.5	4.4	53.8	57.8	lectin, galactoside-binding, soluble, 14-like (LOC400696), mRNA.
8005809	LGALS9	3.2	1.8	5.6	4.6	0.9	0.6	2.6	2.8	lectin, galactoside-binding, soluble, 9 (LGALS9), transcript variant 1, mRNA.
8013450	LGALS9B	3.5	2.1	5.4	5.3	1.1	0.8	3.0	3.2	lectin, galactoside-binding, soluble, 9B (LGALS9B), mRNA.
8005458	LGALS9C	3.5	2.2	5.2	4.8	1.1	0.8	2.9	3.0	lectin, galactoside-binding, soluble, 9C (LGALS9C), mRNA.
7975687	LIN52	3.9	3.1	1.7	1.8	2.2	2.3	3.4	4.7	lin-52 homolog (C. elegans) (LIN52), mRNA.
8148572	LY6E	2.1	1.6	3.1	3.8	1.2	1.1	2.1	2.8	lymphocyte antigen 6 complex, locus E (LY6E), transcript variant 1, mRNA.
8123606	MGC39372	2.8	2.0	1.3	1.8	1.0	1.1	2.5	2.8	hypothetical protein MGC39372, mRNA (cDNA clone IMAGE:5089466), complete cds.
8002778	MLKL	3.7	4.1	2.7	3.0	3.0	3.1	3.9	5.3	mixed lineage kinase domain-like (MLKL), transcript variant 1, mRNA.
8090180	MUC13	1.2	1.3	2.3	3.6	0.9	1.0	3.1	2.9	mucin 13, cell surface associated (MUC13), mRNA.
8068713	MX1	5.9	4.7	4.9	4.9	3.1	1.7	3.7	4.1	myxovirus (influenza virus) resistance 1, interferon-inducible protein p78 (mouse) (MX1), transcri
8068697	MX2	36.5	18.1	49.7	40.9	4.8	1.3	10.2	15.3	myxovirus (influenza virus) resistance 2 (mouse) (MX2), mRNA.
8027377	NA	8.8	2.0	3.3	1.8	2.8	0.9	6.3	3.0	cDNA FLJ16183 fis, clone BRTHA2002702.
8048976	NA	1.0	0.9	2.9	2.4	3.2	1.4	4.5	2.6	ncrna:misc_RNA chromosome:GRCh37:2:231371816:231372099:1 gene:ENSG00000222252
7995926	NLRC5	4.8	4.8	2.4	2.8	3.0	3.0	3.8	3.5	NLR family, CARD domain containing 5 (NLRC5), mRNA.
8055702	NMI	2.5	2.4	2.8	2.5	3.1	1.9	3.4	3.2	N-myc (and STAT) interactor (NMI), mRNA.
7995539	NOD2	2.7	2.1	1.4	1.7	2.3	1.7	2.0	3.1	nucleotide-binding oligomerization domain containing 2 (NOD2), mRNA.
7912520	NPPB	2.4	7.5	1.6	4.4	2.6	6.7	0.9	2.6	natriuretic peptide precursor B (NPPB), mRNA.
8180396	NT5C3	2.4	3.8	4.1	3.9	2.3	1.5	2.7	3.2	5'-nucleotidase, cytosolic III (NT5C3), transcript variant 1, mRNA
8180397	NT5C3	3.1	5.0	5.9	6.2	3.1	1.8	3.9	4.3	5'-nucleotidase, cytosolic III (NT5C3), transcript variant 3, mRNA
7923753	NUAK2	2.3	5.4	1.4	2.9	2.8	3.9	1.2	2.5	NUAK family, SNF1-like kinase, 2 (NUAK2), mRNA.
8137414	NUB1	2.7	2.6	2.2	1.9	1.9	2.0	2.4	2.8	negative regulator of ubiquitin-like proteins 1 (NUB1), mRNA.
7958884	OAS1	6.1	4.4	6.6	6.2	1.9	1.1	4.1	4.1	2',5'-oligoadenylate synthetase 1, 40/46kDa (OAS1), transcript variant 1, mRNA.
7958913	OAS2	6.1	4.9	7.0	7.5	2.9	1.7	5.0	6.0	2'-5'-oligoadenylate synthetase 2, 69/71kDa (OAS2), transcript variant 2, mRNA.
7958895	OAS3	5.8	4.0	7.3	6.7	3.0	1.6	5.4	5.8	2'-5'-oligoadenylate synthetase 3, 100kDa (OAS3), mRNA.
7967117	OASL	25.3	22.1	16.4	21.4	4.4	2.4	7.5	10.1	2'-5'-oligoadenylate synthetase-like (OASL), transcript variant 1, mRNA.
8082100	PARP14	1.1	1.1	2.9	2.9	3.5	2.6	3.8	4.2	poly (ADP-ribose) polymerase family, member 14 (PARP14), mRNA.
8154245	PDCD1LG2	2.3	2.6	3.7	4.3	4.0	3.8	12.3	9.2	programmed cell death 1 ligand 2 (PDCD1LG2), mRNA.
8108080	PHF15	3.5	2.8	2.3	2.2	1.2	1.0	2.3	2.2	PHD finger protein 15 (PHF15), mRNA.
8027398	PLEKHF1	2.2	2.5	1.1	1.6	2.3	2.2	2.0	2.1	pleckstrin homology domain containing, family F (with FYVE domain) member 1 (PLEKHF1), mRN
8091327	PLSCR1	1.8	2.0	3.4	3.1	2.5	2.1	3.0	3.3	phospholipid scramblase 1 (PLSCR1), mRNA.
7984779	PML	3.9	4.3	2.1	3.1	2.6	2.8	3.2	4.1	promyelocytic leukemia (PML), transcript variant 2, mRNA.
8067680	PRIC285	5.1	4.6	3.1	3.8	2.6	2.0	2.2	2.9	peroxisomal proliferator-activated receptor A interacting complex 285 (PRIC285), transcript variar
8062108	PROCR	2.0	3.9	2.0	4.9	1.7	2.5	3.8	6.1	protein C receptor, endothelial (EPCR) (PROCR), mRNA.
8178211	PSMB9	3.2	3.0	3.4	4.5	2.5	2.3	5.2	6.1	proteasome (prosome, macropain) subunit, beta type, 9 (large multifunctional peptidase 2) (PSM
7962884	RND1	6.2	2.5	1.1	2.1	2.6	2.4	1.3	2.1	Rho family GTPase 1 (RND1), mRNA.
8063369	RNF114	2.3	2.4	1.6	1.5	1.9	2.0	2.2	2.4	ring finger protein 114 (RNF114), mRNA.

8150186	RNF122	6.1	8.8	1.8	2.2	2.9	3.1	1.3	4.0	ring finger protein 122 (RNF122), mRNA.
7914603	RNF19B	4.2	4.8	1.7	2.2	4.3	4.9	4.0	5.7	ring finger protein 19B (RNF19B), transcript variant 1, mRNA.
8010426	RNF213	3.5	3.8	2.4	2.6	3.4	2.8	4.1	4.0	ring finger protein 213 (RNF213), transcript variant 1, mRNA.
8064766	RNF24	3.0	2.3	1.1	1.3	2.2	2.2	2.3	2.6	ring finger protein 24 (RNF24), transcript variant 3, mRNA.
8040080	RSAD2	104.5	119.5	68.3	114.3	30.4	13.8	29.7	57.6	radical S-adenosyl methionine domain containing 2 (RSAD2), mRNA.
8079415	RTP3	3.7	3.3	1.5	1.2	2.0	2.1	0.7	0.7	receptor (chemosensory) transporter protein 3 (RTP3), mRNA.
8084732	RTP4	12.8	11.9	10.6	9.8	5.8	4.8	6.6	6.8	receptor (chemosensory) transporter protein 4 (RTP4), mRNA.
8140967	SAMD9	1.4	0.8	9.1	9.7	2.3	0.5	3.3	3.8	sterile alpha motif domain containing 9 (SAMD9), mRNA.
8140971	SAMD9L	1.1	0.6	7.6	7.0	5.5	2.0	8.9	9.4	sterile alpha motif domain containing 9-like (SAMD9L), mRNA.
8066117	SAMHD1	2.7	2.6	4.3	3.8	2.4	1.8	5.2	5.2	SAM domain and HD domain 1 (SAMHD1), mRNA.
8019486	SECTM1	14.9	15.9	5.7	11.5	8.7	13.6	33.4	49.3	secreted and transmembrane 1 (SECTM1), mRNA.
8123609	SERPINB9	3.2	2.2	1.0	0.8	2.4	2.0	1.0	0.9	serpin peptidase inhibitor, clade B (ovalbumin), member 9 (SERPINB9), mRNA.
7948493	SLC15A3	4.3	2.7	5.6	6.0	2.3	1.1	4.1	3.7	solute carrier family 15, member 3 (SLC15A3), transcript variant 1, mRNA.
7935639	SLC25A28	5.4	5.1	2.9	2.7	3.5	2.8	3.7	4.4	solute carrier family 25, member 28 (SLC25A28), mRNA.
8006531	SLFN5	4.0	6.2	3.4	5.1	3.6	4.4	3.2	6.0	schlafen family member 5 (SLFN5), mRNA.
7999423	SOCS1	4.8	6.0	1.5	2.1	4.4	4.9	8.1	10.8	suppressor of cytokine signaling 1 (SOCS1), mRNA.
8059650	SP110	5.0	5.4	4.5	6.0	3.7	3.7	4.3	6.1	SP110 nuclear body protein (SP110), transcript variant c, mRNA.
7990839	STARD5	6.0	5.3	2.5	3.2	1.9	2.1	3.4	5.9	StAR-related lipid transfer (START) domain containing 5 (STARD5), mRNA.
8057744	STAT1	2.6	2.3	3.6	3.4	2.5	2.0	3.5	2.9	signal transducer and activator of transcription 1, 91kDa (STAT1), transcript variant alpha, mRNA.
7964119	STAT2	5.6	4.7	3.6	4.0	2.8	2.2	5.2	5.8	signal transducer and activator of transcription 2, 113kDa (STAT2), transcript variant 1, mRNA.
8140840	STEAP4	24.9	3.7	1.0	1.6	61.6	27.7	33.7	95.7	STEAP family member 4 (STEAP4), mRNA.
8125512	TAP1	3.8	4.1	2.5	3.6	4.0	3.9	4.9	5.5	transporter 1, ATP-binding cassette, sub-family B (MDR/TAP) (TAP1), mRNA.
8180034	TAP2	3.1	3.1	2.6	3.8	2.6	2.9	4.6	5.8	transporter 2, ATP-binding cassette, sub-family B (MDR/TAP) (TAP2), transcript variant 1, mRNA.
8178841	TAP2	3.0	3.1	2.6	3.7	2.6	2.9	4.5	5.7	transporter 2, ATP-binding cassette, sub-family B (MDR/TAP) (TAP2), transcript variant 2, mRNA.
8156688	TDRD7	3.2	3.5	2.7	3.1	2.0	1.6	2.2	2.6	tudor domain containing 7 (TDRD7), mRNA.
7915718	TESK2	4.1	3.5	1.3	1.6	5.8	4.0	4.5	6.7	testis-specific kinase 2 (TESK2), mRNA.
8156060	TLE4	6.7	6.7	2.3	2.8	1.3	1.3	2.2	2.8	transducin-like enhancer of split 4 (E(sp1) homolog, Drosophila) (TLE4), mRNA.
8019622	TMEM106A	4.0	10.6	1.4	6.1	1.3	5.1	2.2	6.6	transmembrane protein 106A (TMEM106A), mRNA.
8088054	TMEM110	3.3	3.9	1.7	2.5	1.2	1.4	2.0	2.5	transmembrane protein 110 (TMEM110), mRNA.
8136388	TMEM140	3.1	3.2	2.5	3.1	2.5	2.8	3.1	3.7	transmembrane protein 140 (TMEM140), mRNA.
8070584	TMPRSS3	2.2	2.5	1.6	2.5	2.1	4.3	5.0	8.3	transmembrane protease, serine 3 (TMPRSS3), transcript variant A, mRNA.
8122265	TNFAIP3	2.8	2.0	1.6	1.5	2.3	1.2	2.3	2.1	tumor necrosis factor, alpha-induced protein 3 (TNFAIP3), mRNA.
8092169	TNFSF10	8.5	8.7	5.9	4.9	4.9	3.0	9.7	9.2	tumor necrosis factor (ligand) superfamily, member 10 (TNFSF10), mRNA.
7969986	TNFSF13B	3.9	3.9	3.3	4.9	2.1	0.9	9.1	8.3	tumor necrosis factor (ligand) superfamily, member 13b (TNFSF13B), transcript variant 1, mRNA.
7958828	TRAFD1	5.3	5.1	2.0	1.9	4.4	5.0	5.1	6.6	TRAF-type zinc finger domain containing 1 (TRAFD1), transcript variant 1, mRNA.
8177760	TRIM15	2.2	3.1	1.1	1.4	5.6	7.3	3.9	6.2	tripartite motif-containing 15 (TRIM15), mRNA.
7945962	TRIM21	3.3	2.9	2.3	2.5	2.0	2.7	2.1	2.8	tripartite motif-containing 21 (TRIM21), mRNA.
7938035	TRIM22	1.9	1.7	2.8	2.7	2.1	1.2	3.2	3.1	tripartite motif-containing 22 (TRIM22), mRNA.
7904726	TXNIP	3.0	3.0	2.2	3.0	1.2	0.8	2.5	2.8	thioredoxin interacting protein (TXNIP), mRNA.
8178295	UBD	2.3	2.2	1.3	1.3	3.2	4.6	6.3	8.2	ubiquitin D (UBD), mRNA.
7948274	UBE2L6	2.4	2.1	2.3	2.6	1.8	1.2	3.2	2.9	ubiquitin-conjugating enzyme E2L 6 (UBE2L6), transcript variant 1, mRNA.
8071155	USP18	18.3	11.6	9.9	10.5	2.9	2.1	3.9	6.2	ubiquitin specific peptidase 18 (USP18), mRNA.
7981290	WARS	3.9	3.1	1.8	2.6	4.8	4.3	7.9	8.3	tryptophanyl-tRNA synthetase (WARS), transcript variant 1, mRNA.
7976766	WDR25	2.4	2.1	0.9	1.5	1.7	1.9	2.2	2.4	WD repeat domain 25 (WDR25), transcript variant 1, mRNA.
8004184	XAF1	0.8	0.5	4.1	3.4	2.5	1.4	3.7	3.7	XIAP associated factor 1 (XAF1), transcript variant 1, mRNA.
8051322	XDH	2.5	2.2	1.0	2.1	1.1	1.4	2.6	4.3	xanthine dehydrogenase (XDH), mRNA.
8143279	ZC3HAV1	2.2	2.7	1.8	1.8	2.2	2.3	1.7	1.9	zinc finger CCCH-type, antiviral 1 (ZC3HAV1), transcript variant 1, mRNA.
8057418	ZNF385B	2.6	2.0	1.4	1.6	1.7	1.3	3.6	2.2	zinc finger protein 385B (ZNF385B), transcript variant 1, mRNA.
8066905	ZNFX1	4.5	4.3	3.0	3.2	2.9	3.0	2.8	3.2	zinc finger, NFX1-type containing 1 (ZNFX1), mRNA.

> 2-fold induced in both donors IFN-gamma, but not in IFN-alpha

		IFN-alpha				IFN-gamma				
		6h		24h		6h		24h		
probeSetID	Symbol	D1	D2	D1	D2	D1	D2	D1	D2	GeneName
8017039	SEPT4	1.1	1.0	0.9	0.9	1.1	1.2	3.2	3.1	septin 4 (SEPT4), transcript variant 2, mRNA.
8122807	AKAP12	1.0	1.6	1.1	2.1	4.0	4.6	2.7	4.4	A kinase (PRKA) anchor protein 12 (AKAP12), transcript variant 1, mRNA.
8096919	ALPK1	2.6	1.7	1.6	0.9	3.3	1.5	5.2	4.1	alpha-kinase 1 (ALPK1), transcript variant 1, mRNA.
7957861	ANO4	1.1	1.0	0.9	1.1	1.1	1.0	2.8	9.6	anoctamin 4 (ANO4), mRNA.
8073072	APOBEC3D	3.5	1.8	1.9	1.9	1.2	1.4	3.1	2.6	apolipoprotein B mRNA editing enzyme, catalytic polypeptide-like 3D (APOBEC3D), mRNA.
8072710	APOL6	1.7	1.5	1.4	1.3	2.4	2.3	2.5	2.7	apolipoprotein L, 6 (APOL6), mRNA.
8099760	ARAP2	1.0	0.6	1.4	1.6	3.2	1.6	2.7	2.9	ArfGAP with RhoGAP domain, ankyrin repeat and PH domain 2 (ARAP2), mRNA.
7927732	ARID5B	0.7	0.7	1.3	2.0	2.2	2.4	1.6	1.9	AT rich interactive domain 5B (MRF1-like) (ARID5B), mRNA.
7954527	ARNTL2	0.9	1.1	0.9	0.9	2.4	1.6	2.1	2.1	aryl hydrocarbon receptor nuclear translocator-like 2 (ARNTL2), mRNA.
8125017	BAT5	1.6	1.6	1.3	1.8	1.3	1.4	2.3	2.3	HLA-B associated transcript 5 (BAT5), transcript variant 1, mRNA.
8081465	BBX	0.4	0.2	1.5	1.2	1.5	0.9	2.1	2.1	bobby sox homolog (Drosophila) (BBX), transcript variant 1, mRNA.
8092691	BCL6	1.3	1.0	1.3	1.3	1.9	1.9	2.4	2.4	B-cell CLL/lymphoma 6 (BCL6), transcript variant 1, mRNA.
8117458	BTN3A1	2.0	1.4	1.6	1.9	0.9	0.7	2.6	2.3	butyrophilin, subfamily 3, member A1 (BTN3A1), transcript variant 4, mRNA.
8117476	BTN3A3	1.8	0.9	1.8	1.7	1.0	0.6	3.2	2.6	butyrophilin, subfamily 3, member A3 (BTN3A3), transcript variant 1, mRNA.
8107934	C5orf56	2.0	1.5	1.5	1.3	2.0	1.4	2.3	2.0	full length insert cDNA clone ZA99C08.
8147112	CA13	1.8	2.1	0.9	1.0	3.0	3.2	2.1	3.3	carbonic anhydrase XIII (CA13), mRNA.
8142585	CADPS2	0.9	1.0	1.2	1.9	1.5	1.1	2.0	2.9	Ca++-dependent secretion activator 2 (CADPS2), transcript variant 1, mRNA.
8077944	CAND2	1.2	1.3	1.1	0.9	1.2	1.0	3.0	5.3	cullin-associated and neddylation-dissociated 2 (putative) (CAND2), transcript variant 1, mRNA.
7999319	CARHSP1	1.6	1.2	0.9	0.8	1.5	1.9	2.3	3.8	calcium regulated heat stable protein 1, 24kDa (CARHSP1), transcript variant 1, mRNA.
8023401	CCDC68	0.6	0.5	1.0	1.2	2.7	3.0	1.9	3.6	coiled-coil domain containing 68 (CCDC68), transcript variant 1, mRNA.
8006433	CCL2	2.0	1.3	1.2	0.5	2.4	2.3	1.8	2.2	chemokine (C-C motif) ligand 2 (CCL2), mRNA.
8097461	CCRN4L	1.9	2.9	1.1	1.9	2.3	2.6	1.7	2.5	CCR4 carbon catabolite repression 4-like (S. cerevisiae) (CCRN4L), mRNA.
8094240	CD38	7.2	0.5	4.5	0.7	3.3	0.4	18.2	6.2	CD38 molecule (CD38), mRNA.
8089299	CD47	1.4	1.7	1.9	2.2	1.9	2.1	2.8	3.6	CD47 molecule (CD47), transcript variant 1, mRNA.
8115147	CD74	1.5	0.5	1.7	0.9	1.4	0.5	5.3	3.6	CD74 molecule, major histocompatibility complex, class II invariant chain (CD74), transcript varia
8026300	CD97	1.3	3.2	1.3	4.1	1.2	3.5	2.2	4.6	CD97 molecule (CD97), transcript variant 1, mRNA.
8060675	CDC25B	1.4	1.2	1.0	0.7	1.0	0.9	3.2	2.7	cell division cycle 25 homolog B (S. pombe) (CDC25B), transcript variant 1, mRNA.
8086517	CDCP1	1.3	10.6	1.5	9.4	1.4	9.2	2.6	9.7	CUB domain containing protein 1 (CDCP1), transcript variant 1, mRNA.
8136187	CPA2	1.3	1.3	1.0	1.4	1.7	2.1	3.6	18.9	carboxypeptidase A2 (pancreatic) (CPA2), mRNA.
8103389	CTSO	0.9	0.9	1.5	1.3	1.4	1.1	3.5	3.1	cathepsin O (CTSO), mRNA.
7919800	CTSS	1.4	0.9	1.6	1.0	1.6	0.9	3.4	2.8	cathepsin S (CTSS), mRNA.
8079993	CYB561D2	2.0	1.9	1.0	1.5	2.3	2.8	1.7	3.4	cytochrome b-561 domain containing 2 (CYB561D2), mRNA.
8051583	CYP1B1	1.4	2.0	0.9	0.6	3.7	2.6	1.7	1.0	cytochrome P450, family 1, subfamily B, polypeptide 1 (CYP1B1), mRNA.
7958425	DAO	2.1	0.7	0.9	0.5	1.6	1.8	5.6	8.0	D-amino-acid oxidase (DAO), mRNA.
7988350	DUOX2	1.0	1.6	1.1	1.2	1.1	1.7	7.6	30.2	dual oxidase 2 (DUOX2), mRNA.
7983405	DUOXA2	1.3	1.9	1.0	1.2	1.6	2.0	6.7	10.7	dual oxidase maturation factor 2 (DUOXA2), mRNA.
7965335	DUSP6	1.2	0.9	1.2	1.6	2.8	2.0	3.4	4.6	dual specificity phosphatase 6 (DUSP6), transcript variant 1, mRNA.
8066716	ELMO2	2.6	1.9	1.3	1.5	1.5	1.2	2.1	2.2	engulfment and cell motility 2 (ELMO2), transcript variant 1, mRNA.
8112274	ELOVL7	1.3	3.3	1.2	7.5	2.6	4.4	2.8	7.8	ELOVL family member 7, elongation of long chain fatty acids (yeast) (ELOVL7), transcript variant
8136954	FAM115C	1.8	2.2	0.9	0.8	3.8	3.7	3.2	4.1	family with sequence similarity 115, member C (FAM115C), transcript variant 3, mRNA.
8047565	FAM117B	1.1	0.9	1.1	1.1	2.2	2.2	5.3	3.0	family with sequence similarity 117, member B (FAM117B), mRNA.
8017867	FAM20A	1.1	0.5	0.8	0.4	1.5	0.6	4.8	2.2	family with sequence similarity 20, member A (FAM20A), transcript variant 1, mRNA.
8152703	FBXO32	2.7	1.3	1.8	1.1	1.4	0.8	3.8	2.7	F-box protein 32 (FBXO32), transcript variant 1, mRNA.
7897728	FBXO6	2.2	1.8	1.6	1.8	1.5	1.3	2.5	2.8	F-box protein 6 (FBXO6), mRNA.
8161964	FRMD3	0.9	1.5	0.9	1.7	0.9	1.3	3.4	4.4	FERM domain containing 3 (FRMD3), mRNA.
8088745	FRMD4B	0.9	1.2	1.6	1.5	2.5	2.6	2.8	3.8	FERM domain containing 4B (FRMD4B), mRNA.
7953943	GABARAPL1	1.6	1.4	1.1	0.8	2.0	2.1	2.2	2.6	GABA(A) receptor-associated protein like 1 (GABARAPL1), mRNA.
7917516	GBP1	1.8	1.8	1.8	1.7	2.7	2.5	3.0	3.1	guanylate binding protein 1, interferon-inducible, 67kDa (GBP1), mRNA.
7917532	GBP2	2.6	1.2	1.3	0.7	5.1	2.6	5.5	5.1	guanylate binding protein 2, interferon-inducible (GBP2), mRNA.
7917548	GBP7	1.3	1.3	0.9	0.7	2.2	1.3	3.7	3.4	guanylate binding protein 7 (GBP7), mRNA.
8151816	GEM	2.7	1.9	1.4	2.4	3.4	2.3	0.8	1.2	GTP binding protein overexpressed in skeletal muscle (GEM), transcript variant 1, mRNA.
7948344	GLYAT	1.2	0.7	0.5	0.3	2.3	1.6	4.0	4.4	glycine-N-acyltransferase (GLYAT), nuclear gene encoding mitochondrial protein, transcript varian
8045336	GPR39	2.0	1.9	1.2	1.8	1.6	1.9	2.0	2.9	G protein-coupled receptor 39 (GPR39), mRNA.
7995362	GPT2	2.2	1.9	1.1	1.6	1.7	1.4	2.9	4.2	glutamic pyruvate transaminase (alanine aminotransferase) 2 (GPT2), transcript variant 1, mRNA.
8081758	GRAMD1C	0.7	0.4	1.2	0.9	1.2	0.7	2.2	2.6	GRAM domain containing 1C (GRAMD1C), transcript variant 1, mRNA.
8014903	GSDMB	1.6	1.2	1.6	1.8	1.5	1.0	2.1	2.0	gasdermin B (GSDMB), transcript variant 3, mRNA.
7991224	HAPLN3	1.8	2.0	1.1	1.0	4.3	5.8	6.0	11.8	hyaluronan and proteoglycan link protein 3 (HAPLN3), mRNA.
8125537	HLA-DMA	1.3	0.6	1.3	0.9	1.0	0.7	8.6	6.9	major histocompatibility complex, class II, DM alpha (HLA-DMA), mRNA.
8125530	HLA-DMB	1.1	0.8	1.2	0.6	0.8	0.6	11.2	6.2	major histocompatibility complex, class II, DM beta (HLA-DMB), mRNA.
8178833	HLA-DOB	1.8	1.4	1.0	1.5	1.7	1.7	4.5	8.5	major histocompatibility complex, class II, DO beta (HLA-DOB), mRNA.
8125556	HLA-DPA1	2.5	0.5	1.9	0.7	1.8	0.6	11.9	7.8	major histocompatibility complex, class II, DP alpha 1 (HLA-DPA1), mRNA.
8179519	HLA-DPB1	1.7	0.8	1.2	0.7	1.3	1.0	7.5	3.8	major histocompatibility complex, class II, DP beta 1 (HLA-DPB1), mRNA.
8125447	HLA-DQB1	2.5	1.0	1.9	1.0	1.9	0.8	14.7	9.9	major histocompatibility complex, class II, DQ beta 1 (HLA-DQB1), mRNA.
8178193	HLA-DRA	2.7	0.3	2.4	0.5	2.7	0.4	17.3	10.0	major histocompatibility complex, class II, DR alpha (HLA-DRA), mRNA.

8125436	HLA-DRB5	1.9	0.4	2.0	0.5	1.5	0.6	7.6	5.4	major histocompatibility complex, class II, DR beta 5 (HLA-DRB5), mRNA.
8179103	HLA-E	2.0	1.8	1.9	2.0	1.6	1.3	2.2	2.4	major histocompatibility complex, class I, E (HLA-E), mRNA.
8025601	ICAM1	1.6	1.6	1.3	1.1	3.8	3.8	3.0	4.2	intercellular adhesion molecule 1 (ICAM1), mRNA.
7942300	IL18BP	2.2	1.6	1.9	1.9	2.2	1.7	5.8	6.3	interleukin 18 binding protein (IL18BP), transcript variant A, mRNA.
7997712	IRF8	1.5	1.0	1.3	0.9	3.9	3.0	3.4	4.1	interferon regulatory factor 8 (IRF8), mRNA.
8154178	JAK2	1.2	1.1	1.6	1.5	5.6	3.0	8.1	6.3	Janus kinase 2 (JAK2), mRNA.
8163002	KLF4	1.7	2.4	1.3	1.9	2.0	2.2	2.3	3.6	Kruppel-like factor 4 (gut) (KLF4), mRNA.
8015387	KRT17	1.3	3.0	1.3	3.2	2.1	5.3	1.9	8.3	keratin 17 (KRT17), mRNA.
7980958	LGMN	1.5	1.3	1.7	1.6	1.1	0.9	2.0	2.2	legumain (LGMN), transcript variant 1, mRNA.
8112803	LHFPL2	0.6	0.8	1.1	0.5	2.3	2.1	1.6	1.3	lipoma HMGIC fusion partner-like 2 (LHFPL2), mRNA.
8072461	LIMK2	2.0	1.8	1.1	1.3	3.4	2.2	2.9	2.7	LIM domain kinase 2 (LIMK2), transcript variant 2b, mRNA.
7969438	LMO7	1.0	1.5	1.7	3.1	3.8	4.4	3.3	4.9	LIM domain 7 (LMO7), transcript variant 1, mRNA.
8040340	LPIN1	1.4	1.1	1.2	1.5	1.6	1.4	2.0	2.0	lipin 1 (LPIN1), mRNA.
8126102	MDGA1	1.5	2.8	1.2	2.6	1.4	3.0	2.4	6.8	MAM domain containing glycosylphosphatidylinositol anchor 1 (MDGA1), mRNA.
8160521	MOBKL2B	0.9	1.5	0.8	2.0	1.8	3.5	2.7	5.4	MOB1, Mps One Binder kinase activator-like 2B (yeast) (MOBKL2B), mRNA.
7912496	MTHFR	1.7	1.3	1.1	1.2	1.8	1.3	2.4	2.1	5,10-methylenetetrahydrofolate reductase (NADPH) (MTHFR), mRNA.
7920642	MUC1	1.7	9.9	1.9	7.3	1.8	5.5	3.5	14.1	mucin 1, cell surface associated (MUC1), transcript variant 2, mRNA.
8178826	NA	1.9	1.6	1.9	1.3	1.9	1.3	14.2	6.8	cDNA FLJ52646 complete cds, highly similar to HLA class II histocompatibility antigen, DQB1*060
8178811	NA	2.0	0.5	1.8	0.5	1.3	0.6	6.4	4.6	cDNA FLJ75018 complete cds.
8180003	NA	2.0	0.5	1.7	0.5	1.3	0.6	6.4	4.5	major histocompatibility complex, class II, DR beta 3 (HLA-DRB3), mRNA.
7917530	NA	2.5	0.9	1.3	0.7	8.8	5.4	8.6	8.2	mRNA; cDNA DKFZp451C2311 (from clone DKFZp451C2311); complete cds.
8117739	NA	1.6	1.4	1.2	0.8	2.5	2.6	4.6	5.4	cdna:pseudogene chromosome:GRCh37:HSCHR6_MHC_APD:29520735:29522057:1 gene:ENSG0
7917528	NA	1.2	1.0	0.9	0.6	7.3	5.5	9.4	10.3	cdna:pseudogene chromosome:GRCh37:1:89569968:89570450:-1 gene:ENSG00000234518
8081818	NA	1.3	0.8	0.9	5.4	3.1	1.7	2.1	3.2	ncrna:misc_RNA chromosome:GRCh37:3:115556715:115557005:1 gene:ENSG00000222510
8053944	NEURL3	2.0	1.7	1.3	1.1	2.3	2.0	2.0	2.1	neuralized homolog 3 (Drosophila) pseudogene (NEURL3), non-coding RNA.
8152340	NUDCD1	1.3	1.8	1.5	2.1	3.2	2.7	2.1	2.6	NudC domain containing 1 (NUDCD1), transcript variant 2, mRNA.
7959251	P2RX7	2.9	1.0	1.5	1.1	3.5	1.3	4.5	4.0	purinergic receptor P2X, ligand-gated ion channel, 7 (P2RX7), mRNA.
8091255	PAQR9	0.9	0.7	0.9	0.9	1.6	1.3	2.9	3.5	progestin and adipoQ receptor family member IX (PAQR9), mRNA.
8105191	PARP8	1.2	1.6	1.5	1.7	1.5	1.3	2.1	2.4	poly (ADP-ribose) polymerase family, member 8 (PARP8), transcript variant 1, mRNA.
7920228	PGLYRP4	1.0	1.7	1.0	1.7	1.0	3.5	2.1	7.2	peptidoglycan recognition protein 4 (PGLYRP4), mRNA.
8081890	PLA1A	2.7	1.4	3.0	1.9	1.2	0.8	5.3	4.6	phospholipase A1 member A (PLA1A), mRNA.
7913216	PLA2G2A	6.3	0.8	2.2	0.5	2.4	0.6	18.0	11.6	phospholipase A2, group IIA (platelets, synovial fluid) (PLA2G2A), transcript variant 1, mRNA.
8091306	PLSCR4	1.0	1.5	1.2	1.3	1.7	1.2	2.9	2.7	phospholipid scramblase 4 (PLSCR4), transcript variant 1, non-coding RNA.
8021470	PMAIP1	1.1	4.2	1.5	5.1	3.3	6.4	2.5	9.1	phorbol-12-myristate-13-acetate-induced protein 1 (PMAIP1), mRNA.
8166705	PRRG1	0.7	1.4	1.3	2.2	2.8	4.8	2.2	5.1	proline rich Gla (G-carboxyglutamic acid) 1 (PRRG1), transcript variant 1, mRNA.
8002133	PSMB10	2.0	1.9	1.8	2.4	2.2	1.6	3.2	4.0	proteasome (prosome, macropain) subunit, beta type, 10 (PSMB10), mRNA.
8180049	PSMB8	2.4	1.4	1.8	1.9	1.6	1.4	2.0	2.8	proteasome (prosome, macropain) subunit, beta type, 8 (large multifunctional peptidase 7) (PSM
7978123	PSME2	2.1	1.5	2.0	1.8	1.5	1.2	2.2	2.4	proteasome (prosome, macropain) activator subunit 2 (PA28 beta) (PSME2), mRNA.
8020110	RAB31	1.1	0.5	0.9	0.5	0.9	0.8	2.3	2.5	RAB31, member RAS oncogene family (RAB31), mRNA.
7905938	RAG1AP1	1.7	1.5	1.1	1.8	1.3	1.6	2.0	2.8	recombination activating gene 1 activating protein 1 (RAG1AP1), transcript variant 1, mRNA.
8091723	RARRES1	1.3	0.8	0.9	0.6	1.3	0.8	7.8	3.4	retinoic acid receptor responder (tazarotene induced) 1 (RARRES1), transcript variant 1, mRNA.
7940775	RARRES3	3.5	1.6	3.1	1.7	3.0	2.8	7.2	8.2	retinoic acid receptor responder (tazarotene induced) 3 (RARRES3), mRNA.
7909214	RASSF5	1.3	1.0	1.3	1.1	5.4	3.9	4.6	7.2	Ras association (RalGDS/AF-6) domain family member 5 (RASSF5), transcript variant 1, mRNA.
8110327	RGS14	1.1	1.2	1.1	1.0	1.8	1.9	2.5	2.9	regulator of G-protein signaling 14 (RGS14), mRNA.
8105596	RGS7BP	1.1	1.2	1.4	1.2	3.1	4.8	3.5	11.6	regulator of G-protein signaling 7 binding protein (RGS7BP), mRNA.
8147206	RIPK2	1.5	2.0	1.5	1.5	2.7	2.7	2.7	3.1	receptor-interacting serine-threonine kinase 2 (RIPK2), mRNA.
7899192	RPS6KA1	1.0	1.6	1.0	1.1	1.3	1.7	2.2	4.0	ribosomal protein S6 kinase, 90kDa, polypeptide 1 (RPS6KA1), transcript variant 1, mRNA.
8174304	SERPINA7	1.1	0.3	1.0	0.3	1.8	0.6	14.0	5.2	serpin peptidase inhibitor, clade A (alpha-1 antiproteinase, antitrypsin), member 7 (SERPINA7), r
7931951	SFMBT2	1.2	1.0	1.0	0.7	1.9	2.2	3.5	5.6	Scm-like with four mbt domains 2 (SFMBT2), mRNA.
7944049	SIDT2	1.4	1.1	1.0	1.0	1.0	1.0	2.2	2.6	SID1 transmembrane family, member 2 (SIDT2), mRNA.
8129666	SLC2A12	1.5	1.5	1.9	1.8	1.7	1.7	4.9	4.9	solute carrier family 2 (facilitated glucose transporter), member 12 (SLC2A12), mRNA.
8143367	SLC37A3	1.9	3.0	1.3	2.4	2.4	4.3	1.6	4.2	solute carrier family 37 (glycerol-3-phosphate transporter), member 3 (SLC37A3), transcript varia
8018864	SOCS3	4.4	1.3	1.1	0.9	5.7	4.2	2.4	7.3	suppressor of cytokine signaling 3 (SOCS3), mRNA.
8048940	SP100	0.7	0.7	2.1	2.1	2.0	1.4	2.5	2.3	SP100 nuclear antigen (SP100), transcript variant 1, mRNA.
8180339	ST6GALNAC6	1.6	1.6	0.8	1.1	1.6	1.7	2.1	2.7	ST6 (alpha-N-acetyl-neuraminyl-2,3-beta-galactosyl-1,3)-N-acetylgalactosaminide alpha-2,6-sialy
8164304	ST6GALNAC6	1.5	1.7	0.8	1.1	1.5	1.7	2.0	2.6	ST6 (alpha-N-acetyl-neuraminyl-2,3-beta-galactosyl-1, 3)-N-acetylgalactosaminide alpha-2,6-sial
8168028	STARD8	1.3	1.6	1.2	1.8	2.2	2.2	1.9	2.5	StAR-related lipid transfer (START) domain containing 8 (STARD8), transcript variant 1, mRNA.
8007212	STAT5A	1.9	1.7	1.4	1.3	1.6	1.3	2.5	3.0	signal transducer and activator of transcription 5A (STAT5A), mRNA.
8165866	STS	0.9	0.7	1.1	0.9	1.6	0.9	3.3	2.8	steroid sulfatase (microsomal), isozyme S (STS), mRNA.
8158059	STXBP1	0.7	1.7	0.9	1.9	0.7	1.8	2.1	4.0	syntaxin binding protein 1 (STXBP1), transcript variant 1, mRNA.
7974920	SYNE2	0.7	0.6	1.0	1.3	2.0	1.0	2.4	4.1	spectrin repeat containing, nuclear envelope 2 (SYNE2), transcript variant 5, mRNA.
7953150	TEAD4	1.7	2.6	1.2	1.4	2.7	3.4	2.3	3.3	TEA domain family member 4 (TEAD4), transcript variant 1, mRNA.
8126086	TMEM217	1.7	2.2	1.0	1.4	2.8	2.8	1.5	3.3	transmembrane protein 217 (TMEM217), transcript variant 1, mRNA.
8179617	TRIM31	1.6	1.0	1.2	0.9	2.8	1.1	18.3	2.0	tripartite motif-containing 31 (TRIM31), mRNA.
8117840	TRIM40	1.4	2.1	1.0	1.3	9.3	20.5	17.6	34.0	tripartite motif-containing 40 (TRIM40), mRNA.
8129637	VNN2	0.9	0.8	0.8	1.1	1.1	1.0	2.8	3.2	vanin 2 (VNN2), transcript variant 1, mRNA.
8040430	VSNL1	1.1	0.4	1.2	0.9	2.5	1.7	7.4	7.5	visinin-like 1 (VSNL1), mRNA.
8091141	XRN1	0.8	0.5	1.9	1.7	3.3	1.9	3.7	3.4	5'-3' exoribonuclease 1 (XRN1), transcript variant 1, mRNA.
8028652	ZFP36	2.2	1.6	1.2	2.0	1.8	2.0	2.2	2.6	zinc finger protein 36, C3H type, homolog (mouse) (ZFP36), mRNA.
8051814	ZFP36L2	0.9	1.0	1.2	1.6	1.5	1.6	2.2	3.2	zinc finger protein 36, C3H type-like 2 (ZFP36L2), mRNA.
7995258	ZNF267	0.3	0.3	1.2	0.9	2.8	1.7	2.3	2.4	zinc finger protein 267 (ZNF267), transcript variant 498723, mRNA.

Supplementary Table IV.

Fold changes of the downregulated genes in IFN-treated PHH. The table shows genes that in PHH from both donors were at least 2-fold downregulated between untreated and IFN-treated PHH samples.

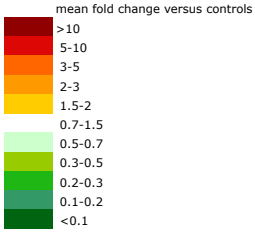

> 2-fold reduced in both donors after IFN-gamma, but not in IFN-alpha

		IFN-alpha				IFN-gamma				
		6h		24h		6h		24h		
probeSetID	Symbol	D1	D2	D1	D2	D1	D2	D1	D2	GeneName
8112920	ACOT12	1.17	0.93	0.72	0.65	1.07	0.82	0.36	0.31	acyl-CoA thioesterase 12 (ACOT12), mRNA.
8006214	ADAP2	0.90	0.39	0.87	0.33	0.41	0.41	0.85	0.39	ArfGAP with dual PH domains 2 (ADAP2), mRNA.
8136336	AKR1B10	1.21	1.41	0.68	0.63	0.79	1.28	0.31	0.46	aldo-keto reductase family 1, member B10 (aldose reductase) (AKR1B10), mRNA.
7925929	AKR1C3	0.81	0.65	0.66	0.41	0.75	0.49	0.47	0.27	aldo-keto reductase family 1, member C3 (3-alpha hydroxysteroid dehydrogenase, type II) (AKR1C3), mRNA.
8161618	APBA1	1.19	1.25	0.88	1.05	0.92	1.08	0.39	0.49	amyloid beta (A4) precursor protein-binding, family A, member 1 (APBA1), mRNA.
7906458	APCS	1.46	1.03	0.85	0.81	1.04	0.87	0.39	0.34	amyloid P component, serum (APCS), mRNA.
7960874	C3AR1	1.28	0.09	1.25	0.06	0.44	0.06	1.33	0.06	complement component 3a receptor 1 (C3AR1), mRNA.
8115397	C5orf4	1.19	1.40	0.92	1.24	0.89	1.05	0.31	0.35	chromosome 5 open reading frame 4 (C5orf4), mRNA.
7996264	CDH5	0.76	0.24	0.85	0.21	0.66	0.20	0.46	0.19	cadherin 5, type 2 (vascular endothelium) (CDH5), mRNA.
7990391	CYP1A1	2.46	4.24	0.93	0.71	5.13	4.32	0.39	0.42	cytochrome P450, family 1, subfamily A, polypeptide 1 (CYP1A1), mRNA.
8141342	CYP3A7	2.05	0.10	0.88	0.13	0.93	0.11	0.43	0.12	cytochrome P450, family 3, subfamily A, polypeptide 7 (CYP3A7), mRNA.
7929664	DHDPSL	1.80	0.64	0.66	0.43	1.26	0.49	0.35	0.36	dihydrodipicolinate synthase-like, mitochondrial (DHDPSL), nuclear gene encoding mitochondrial protein, transcri
8041781	EPAS1	0.96	0.68	0.70	0.38	0.79	0.55	0.47	0.25	endothelial PAS domain protein 1 (EPAS1), mRNA.
7921873	FCGR3A	1.05	0.05	1.49	0.03	0.40	0.05	0.83	0.04	Fc fragment of IgG, low affinity IIIa, receptor (CD16a) (FCGR3A), transcript variant 1, mRNA.
8103326	FGG	1.31	0.65	0.85	0.44	1.09	0.31	0.43	0.16	fibrinogen gamma chain (FGG), transcript variant gamma-B, mRNA.
8030866	FPR3	0.73	0.14	1.85	0.13	0.28	0.10	0.83	0.09	formyl peptide receptor 3 (FPR3), mRNA.
7940135	GLYATL1	1.52	0.20	0.69	0.15	0.82	0.17	0.19	0.10	glycine-N-acyltransferase-like 1 (GLYATL1), mRNA.
7904396	HAO2	0.87	0.24	0.72	0.26	0.57	0.21	0.43	0.09	hydroxyacid oxidase 2 (long chain) (HAO2), transcript variant 2, mRNA.
8115464	HAVCR2	0.85	0.25	0.95	0.22	0.39	0.18	0.90	0.21	hepatitis A virus cellular receptor 2 (HAVCR2), mRNA.
7959234	HNF1A	0.82	0.68	1.15	1.25	0.47	0.49	1.24	0.95	HNF1 homeobox A (HNF1A), mRNA.
7956271	HSD17B6	1.14	0.86	0.56	0.43	0.80	0.56	0.32	0.25	hydroxysteroid (17-beta) dehydrogenase 6 homolog (mouse) (HSD17B6), mRNA.
7951686	IL18	0.96	1.88	0.68	1.12	0.89	1.01	0.35	0.45	interleukin 18 (interferon-gamma-inducing factor) (IL18), mRNA.
8082916	IL20RB	1.85	0.33	1.71	0.73	0.82	0.22	0.46	0.18	interleukin 20 receptor beta (IL20RB), mRNA.
8139207	INHBA	1.02	0.46	1.81	2.35	0.80	0.68	0.29	0.37	inhibin, beta A (INHBA), mRNA.
7956426	INHBE	0.86	0.30	1.05	0.59	0.58	0.33	0.39	0.16	inhibin, beta E (INHBE), mRNA.
7955441	METTL7A	1.27	0.88	0.82	0.66	0.98	0.81	0.47	0.40	methyltransferase like 7A (METTL7A), mRNA.
8136662	MGAM	1.02	0.48	0.86	0.38	0.94	0.39	0.36	0.31	maltase-glucoamylase (alpha-glucosidase) (MGAM), mRNA.
7905329	MLLT11	0.91	1.32	0.92	1.36	0.79	1.30	0.41	0.50	myeloid/lymphoid or mixed-lineage leukemia (trithorax homolog, Drosophila); translocated to, 11 (MLLT11), mRN
7909877	MOSC1	1.08	0.79	0.72	0.61	0.78	0.71	0.43	0.31	MOCO sulphurase C-terminal domain containing 1 (MOSC1), nuclear gene encoding mitochondrial protein, mRNA.
7948364	MPEG1	0.79	0.05	0.83	0.05	0.43	0.06	0.74	0.09	macrophage expressed 1 (MPEG1), mRNA.
7940237	MS4A4A	0.78	0.06	1.11	0.06	0.30	0.06	0.66	0.05	membrane-spanning 4-domains, subfamily A, member 4 (MS4A4A), transcript variant 1, mRNA.
7965884	PAH	0.84	0.54	0.80	0.46	0.79	0.67	0.47	0.28	phenylalanine hydroxylase (PAH), mRNA.
8017599	PECAM1	0.88	0.11	0.93	0.11	0.41	0.09	0.46	0.09	platelet/endothelial cell adhesion molecule (PECAM1), mRNA.
8173120	PFKFB1	2.02	0.64	0.63	0.43	1.41	0.72	0.43	0.17	6-phosphofructo-2-kinase/fructose-2,6-biphosphatase 1 (PFKFB1), mRNA.
8012896	PMP22	0.80	0.84	0.89	0.58	0.29	0.34	0.61	0.43	peripheral myelin protein 22 (PMP22), transcript variant 1, mRNA.
8141052	PON1	1.15	0.39	0.56	0.30	0.81	0.40	0.40	0.19	paraoxonase 1 (PON1), mRNA.
8102468	PRSS12	1.02	0.77	0.71	0.53	0.79	0.71	0.49	0.33	protease, serine, 12 (neurotrypsin, motopsin) (PRSS12), mRNA.
8101304	RASGEF1B	1.04	0.33	1.56	1.19	0.43	0.15	0.59	0.30	RasGEF domain family, member 1B (RASGEF1B), mRNA.
8064790	RASSF2	0.76	0.27	0.84	0.35	0.35	0.24	0.72	0.28	Ras association (RalGDS/AF-6) domain family member 2 (RASSF2), transcript variant 1, mRNA.
7977615	RNASE1	0.74	0.29	1.35	0.46	0.34	0.24	0.51	0.24	ribonuclease, RNase A family, 1 (pancreatic) (RNASE1), transcript variant 3, mRNA.
8146685	RRS1	0.74	0.61	0.92	0.82	0.73	0.68	0.46	0.37	RRS1 ribosome biogenesis regulator homolog (S. cerevisiae) (RRS1), mRNA.
8147461	SDC2	0.88	0.89	0.83	1.04	0.84	0.83	0.50	0.50	syndecan 2 (SDC2), mRNA.
7979878	SLC10A1	1.90	0.39	0.52	0.12	1.23	0.35	0.25	0.08	solute carrier family 10 (sodium/bile acid cotransporter family), member 1 (SLC10A1), mRNA.
8124351	SLC17A3	1.06	0.67	0.51	0.28	0.80	0.46	0.27	0.15	solute carrier family 17 (sodium phosphate), member 3 (SLC17A3), transcript variant 1, mRNA.
7901316	SLC5A9	1.99	0.27	0.66	0.30	1.26	0.30	0.38	0.25	solute carrier family 5 (sodium/glucose cotransporter), member 9 (SLC5A9), transcript variant 1, mRNA.
8060745	SMOX	1.37	0.94	0.91	1.01	0.81	0.74	0.38	0.37	spermine oxidase (SMOX), transcript variant 1, mRNA.
8117165	SOX4	0.71	0.60	0.92	1.25	0.52	0.55	0.35	0.39	SRY (sex determining region Y)-box 4 (SOX4), mRNA.
8051361	SRD5A2	1.20	0.99	0.59	0.59	0.75	1.26	0.32	0.43	steroid-5-alpha-reductase, alpha polypeptide 2 (3-oxo-5 alpha-steroid delta 4-dehydrogenase alpha 2) (SRD5A2)
8002556	TAT	1.15	0.16	1.20	0.30	0.47	0.13	1.48	0.19	tyrosine aminotransferase (TAT), nuclear gene encoding mitochondrial protein, mRNA.
8136557	TBXAS1	0.91	0.29	0.56	0.21	0.49	0.26	0.50	0.25	thromboxane A synthase 1 (platelet) (TBXAS1), transcript variant 3, mRNA.
8005475	TRIM16L	0.92	0.68	0.95	0.56	0.84	0.65	0.41	0.25	tripartite motif-containing 16-like (TRIM16L), mRNA.
8100768	UGT2B11	0.96	0.77	0.75	0.74	0.86	0.81	0.44	0.46	UDP glucuronosyltransferase 2 family, polypeptide B10 (UGT2B10), transcript variant 1, mRNA.
8100784	UGT2B4	0.89	0.82	0.65	0.80	0.69	0.93	0.21	0.29	UDP glucuronosyltransferase 2 family, polypeptide B4 (UGT2B4), mRNA.
8100758	UGT2B7	0.98	0.69	0.72	0.69	1.06	0.84	0.34	0.31	UDP glucuronosyltransferase 2 family, polypeptide B7 (UGT2B7), mRNA.
7952249	USP2	0.74	0.75	0.84	0.50	0.44	0.39	0.63	0.27	ubiquitin specific peptidase 2 (USP2), transcript variant 1, mRNA.
8048319	VIL1	1.31	1.16	0.56	0.42	1.11	1.05	0.46	0.43	villin 1 (VIL1), mRNA.

> 2-fold reduced in both donors after IFN-alpha and IFN-gamma

		IFN-alpha				IFN-gamma				
		6h		24h		6h		24h		
probeSetID	Symbol	D1	D2	D1	D2	D1	D2	D1	D2	GeneName
8114006	–	0.29	0.17	0.92	1.10	0.59	0.83	0.32	0.34	cDNA FLJ44796 fis, clone BRACE3040504.
7906465	–	0.51	0.06	0.85	0.89	0.36	0.13	0.43	0.19	cdna:pseudogene chromosome:GRCh37:1:159568088:159568918:1 gene:ENSG00000158731
7993754	–	0.39	0.26	0.56	0.34	0.39	0.22	2.21	0.39	cDNA FLJ34659 fis, clone KIDNE2018863 gene:ENSG00000226720
8165680	–	0.31	0.41	0.85	0.99	0.23	0.38	0.92	1.14	gi|17981852|ref|NC_001807.4|:12139-12207; gene=TRNH; product=tRNA-His
8165682	–	0.43	0.41	0.83	0.72	0.28	0.36	0.88	0.99	gi|17981852|ref|NC_001807.4|:12208-12266; gene=TRNS2; product=tRNA-Ser
8043375	–	0.68	0.75	0.84	0.66	0.37	0.49	0.73	0.96	gi|17981852|ref|NC_001807.4|:8296-8365; gene=TRNK; product=tRNA-Lys
7961710	ABCC9	0.35	0.24	0.67	0.91	0.72	0.76	0.47	0.51	ATP-binding cassette, sub-family C (CFTR/MRP), member 9 (ABCC9), transcript variant SUR2A, mRNA.
7918533	ADORA3	0.17	0.07	1.02	0.09	0.09	0.05	0.40	0.06	adenosine A3 receptor (ADORA3), transcript variant 1, mRNA.
8149885	ADRA1A	0.35	0.26	0.60	0.28	0.38	0.32	1.54	0.36	adrenergic, alpha-1A-, receptor (ADRA1A), transcript variant 1, mRNA.
7968344	ALOX5AP	0.83	0.18	0.43	0.17	0.33	0.17	0.24	0.13	arachidonate 5-lipoxygenase-activating protein (ALOX5AP), mRNA.
7901883	ANGPTL3	0.36	0.31	0.83	0.73	0.90	0.74	0.38	0.38	angiopoietin-like 3 (ANGPTL3), mRNA.
7993815	ANKS4B	0.52	0.20	0.91	0.60	0.43	0.31	1.32	0.31	ankyrin repeat and sterile alpha motif domain containing 4B (ANKS4B), mRNA.
7954398	C12orf39	0.19	0.28	1.62	1.10	0.53	0.46	0.32	0.24	chromosome 12 open reading frame 39 (C12orf39), mRNA.
7903980	C1orf162	0.41	0.09	0.89	0.09	0.28	0.08	0.74	0.09	chromosome 1 open reading frame 162 (C1orf162), mRNA.
8104758	C5orf23	0.29	0.14	1.22	0.84	0.48	0.32	0.43	0.16	chromosome 5 open reading frame 23, mRNA (cDNA clone MGC:22189 IMAGE:4702775), complete cds.
7953200	CCND2	0.52	0.28	0.74	0.26	0.64	0.24	0.29	0.18	cyclin D2 (CCND2), mRNA.
7960794	CD163	0.41	0.04	0.61	0.04	0.30	0.05	0.49	0.03	CD163 molecule (CD163), transcript variant 1, mRNA.
8127563	COL12A1	0.46	0.68	0.77	0.63	1.09	0.84	0.46	0.34	collagen, type XII, alpha 1 (COL12A1), transcript variant long, mRNA.
8024754	CREB3L3	0.62	0.22	0.98	0.23	0.42	0.16	4.07	1.27	cAMP responsive element binding protein 3-like 3 (CREB3L3), mRNA.
8055465	CXCR4	0.59	0.33	0.84	0.35	0.38	0.26	0.53	0.33	chemokine (C-X-C motif) receptor 4 (CXCR4), transcript variant 1, mRNA.
8141317	CYP3A4	1.62	0.10	0.39	0.10	1.21	0.09	0.36	0.07	cytochrome P450, family 3, subfamily A, polypeptide 4 (CYP3A4), mRNA.
8014063	EVI2B	0.05	0.03	1.00	0.06	0.23	0.03	1.02	0.04	ecotropic viral integration site 2B (EVI2B), mRNA.
8022283	FAM38B	0.36	0.32	0.57	0.60	0.52	0.45	0.42	0.28	family with sequence similarity 38, member B (FAM38B), mRNA.
8089112	FILIP1L	0.35	0.23	1.14	1.40	0.49	0.48	0.45	0.41	filamin A interacting protein 1-like (FILIP1L), transcript variant 1, mRNA.
8105121	GHR	0.44	0.19	0.87	0.46	0.66	0.39	0.35	0.30	growth hormone receptor (GHR), mRNA.
7936322	GPAM	0.38	0.15	0.72	0.87	0.33	0.42	0.21	0.14	glycerol-3-phosphate acyltransferase, mitochondrial (GPAM), nuclear gene encoding mitochondrial protein, mRNA
8131844	GPNMB	0.58	0.05	0.76	0.06	0.42	0.05	0.58	0.05	glycoprotein (transmembrane) nmb (GPNMB), transcript variant 1, mRNA.
8022338	GPR125	0.49	0.34	0.93	0.88	0.92	0.78	0.32	0.42	G protein-coupled receptor 125 (GPR125), mRNA.
8127094	GSTA4	0.62	0.49	0.67	0.42	0.45	0.45	0.53	0.38	glutathione S-transferase alpha 4 (GSTA4), mRNA.
7961673	GYS2	0.37	0.25	0.98	0.40	0.42	0.28	0.21	0.11	glycogen synthase 2 (liver) (GYS2), mRNA.
8115455	HAVCR1	0.44	0.58	0.56	0.49	0.66	0.60	0.32	0.25	hepatitis A virus cellular receptor 1 (HAVCR1), transcript variant 1, mRNA.
8084880	HES1	0.59	0.43	1.06	0.97	0.40	0.35	0.61	0.38	hairy and enhancer of split 1, (Drosophila) (HES1), mRNA.
8103769	HPGD	0.43	0.41	0.75	1.06	0.81	0.64	0.43	0.52	hydroxyprostaglandin dehydrogenase 15-(NAD) (HPGD), transcript variant 1, mRNA.
8040103	ID2	0.61	0.40	0.86	0.71	0.44	0.36	0.80	0.60	inhibitor of DNA binding 2, dominant negative helix-loop-helix protein (ID2), mRNA.

7910950	KMO	0.54	0.26	1.05	0.33	0.62	0.23	0.46	0.16	kynurenine 3-monooxygenase (kynurenine 3-hydroxylase) (KMO), mRNA.
8020551	LAMA3	0.62	0.58	0.79	0.98	0.68	0.60	0.28	0.41	laminin, alpha 3 (LAMA3), transcript variant 1, mRNA.
8044391	MERTK	0.32	0.19	0.93	0.26	0.18	0.19	0.54	0.25	c-mer proto-oncogene tyrosine kinase (MERTK), mRNA.
8083494	MME	0.24	0.15	0.80	0.32	0.59	0.25	0.50	0.25	membrane metallo-endopeptidase (MME), transcript variant 2a, mRNA.
7926410	MRC1	0.10	0.05	0.34	0.05	0.43	0.06	0.14	0.04	mannose receptor, C type 1 (MRC1), mRNA.
7948455	MS4A6A	0.55	0.30	1.75	0.36	0.50	0.26	1.23	0.33	membrane-spanning 4-domains, subfamily A, member 6A (MS4A6A), transcript variant 1, mRNA.
7940259	MS4A7	0.46	0.20	1.30	0.19	0.44	0.19	1.14	0.19	membrane-spanning 4-domains, subfamily A, member 7 (MS4A7), transcript variant 1, mRNA.
8152764	MTSS1	0.47	0.26	1.01	0.69	0.39	0.32	0.93	0.48	metastasis suppressor 1 (MTSS1), mRNA.
7902495	NEXN	0.35	0.23	0.97	1.90	0.69	1.02	0.49	0.64	nexilin (F actin binding protein) (NEXN), transcript variant 1, mRNA.
8104746	NPR3	0.60	0.24	1.24	0.71	0.57	0.38	0.37	0.17	natriuretic peptide receptor C/guanylate cyclase C (atrionatriuretic peptide receptor C) (NPR3), mRNA.
7957835	NR1H4	0.44	0.17	1.13	0.46	0.42	0.19	0.86	0.38	nuclear receptor subfamily 1, group H, member 4 (NR1H4), mRNA.
7903227	PALMD	0.36	0.57	1.08	1.11	0.51	0.69	0.44	0.40	palmdelphin (PALMD), mRNA.
8141094	PDK4	0.44	0.17	1.03	0.45	0.45	0.29	1.83	0.88	pyruvate dehydrogenase kinase, isozyme 4 (PDK4), mRNA.
8126784	PLA2G7	0.35	0.03	1.14	0.05	0.44	0.03	1.03	0.05	phospholipase A2, group VII (platelet-activating factor acetylhydrolase, plasma) (PLA2G7), transcript variant 2, m
8053602	PLGLB2	0.66	0.16	0.54	0.18	0.66	0.17	0.47	0.16	plasminogen-like B2 (PLGLB2), mRNA.
8160297	PLIN2	0.43	0.51	1.05	0.77	0.33	0.47	1.13	0.74	perilipin 2 (PLIN2), mRNA.
7926545	PLXDC2	0.34	0.14	0.58	0.21	0.32	0.17	0.63	0.14	plexin domain containing 2 (PLXDC2), mRNA.
8099633	PPARGC1A	0.37	0.13	1.19	0.74	0.35	0.23	1.00	0.43	peroxisome proliferator-activated receptor gamma, coactivator 1 alpha (PPARGC1A), mRNA.
8106660	RASGRF2	0.47	0.94	0.74	1.03	0.62	1.06	0.47	0.49	Ras protein-specific guanine nucleotide-releasing factor 2 (RASGRF2), mRNA.
8165672	RFC1	0.53	0.43	0.71	0.60	0.14	0.39	0.68	1.18	Human replication factor C large subunit mRNA, complete cds.
8038824	SIGLEC10	0.55	0.20	0.91	0.16	0.35	0.18	0.98	0.19	sialic acid binding Ig-like lectin 10 (SIGLEC10), transcript variant 1, mRNA.
8121515	SLC16A10	0.22	0.15	0.47	0.14	0.30	0.17	0.22	0.17	solute carrier family 16, member 10 (aromatic amino acid transporter) (SLC16A10), mRNA.
7934936	SLC16A12	0.51	0.37	0.71	0.81	0.80	0.72	0.47	0.42	solute carrier family 16, member 12 (monocarboxylic acid transporter 12) (SLC16A12), mRNA.
7924342	SLC30A10	0.39	0.19	0.74	0.39	0.41	0.24	0.39	0.20	solute carrier family 30, member 10 (SLC30A10), mRNA.
8057677	SLC40A1	0.35	0.27	1.01	0.59	0.57	0.33	0.43	0.19	solute carrier family 40 (iron-regulated transporter), member 1 (SLC40A1), mRNA.
8085914	SLC4A7	0.45	0.42	0.67	0.83	0.76	0.72	0.50	0.37	solute carrier family 4, sodium bicarbonate cotransporter, member 7 (SLC4A7), mRNA.
8068361	SLC5A3	0.13	0.10	0.68	0.56	0.41	0.45	0.82	0.64	solute carrier family 5 (sodium/myo-inositol cotransporter), member 3 (SLC5A3), mRNA.
7977933	SLC7A8	0.32	0.28	0.88	0.34	0.23	0.24	0.39	0.38	solute carrier family 7 (amino acid transporter, L-type), member 8 (SLC7A8), transcript variant 1, mRNA.
7942569	SLCO2B1	0.55	0.34	0.90	0.29	0.45	0.35	1.20	1.10	solute carrier organic anion transporter family, member 2B1 (SLCO2B1), transcript variant 2, mRNA.
8104035	SORBS2	0.39	0.38	0.93	1.23	0.47	0.46	0.51	0.58	sorbin and SH3 domain containing 2 (SORBS2), transcript variant 2, mRNA.
8096301	SPP1	0.65	0.12	0.98	0.17	0.63	0.13	0.37	0.06	secreted phosphoprotein 1 (SPP1), transcript variant 1, mRNA.
8146863	SULF1	0.53	0.37	0.82	0.59	0.78	0.49	0.49	0.23	sulfatase 1 (SULF1), transcript variant 1, mRNA.
7970831	UBL3	0.32	0.48	0.95	0.77	0.56	0.68	0.46	0.39	ubiquitin-like 3 (UBL3), mRNA.
8100746	UGT2B15	0.82	0.32	0.41	0.29	1.15	0.33	0.30	0.17	UDP glucuronosyltransferase 2 family, polypeptide B15 (UGT2B15), mRNA.
8056860	WIPF1	0.66	0.30	1.29	0.27	0.41	0.19	0.83	0.26	WAS/WASL interacting protein family, member 1 (WIPF1), transcript variant 1, mRNA.

> 2-fold reduced in both donors after IFN-alpha, but not in IFN-gamma

		IFN-alpha				IFN-gamma				
		6h		24h		6h		24h		
probeSetID	Symbol	D1	D2	D1	D2	D1	D2	D1	D2	GeneName
8045919	MARCH7	0.27	0.26	1.11	1.01	1.06	0.83	0.97	0.85	membrane-associated ring finger (C3HC4) 7 (MARCH7), mRNA.
8132292	SEPT7	0.32	0.32	0.91	0.97	0.90	0.81	0.65	0.74	septin 7 (SEPT7), transcript variant 1, mRNA.
8054467	SEPT10	0.30	0.48	1.11	0.97	0.92	1.06	0.96	1.10	septin 10 (SEPT10), transcript variant 1, mRNA.
8095854	SEPT11	0.35	0.44	0.87	0.93	0.99	1.06	1.11	1.25	septin 11 (SEPT11), mRNA.
7943552	AASDHPPT	0.33	0.37	1.13	0.95	0.72	0.78	0.87	0.67	aminoadipate-semialdehyde dehydrogenase-phosphopantetheinyl transferase (AASDHPPT), mRNA.
8017964	ABCA6	0.36	0.15	1.02	0.69	1.01	0.40	0.91	0.48	ATP-binding cassette, sub-family A (ABC1), member 6 (ABCA6), mRNA.
7903119	ABCD3	0.36	0.26	0.75	0.67	0.91	0.88	0.72	0.68	ATP-binding cassette, sub-family D (ALD), member 3 (ABCD3), transcript variant 1, mRNA.
8097647	ABCE1	0.18	0.23	0.89	0.77	0.80	0.82	0.51	0.47	ATP-binding cassette, sub-family E (OABP), member 1 (ABCE1), transcript variant 1, mRNA.
7902367	ACADM	0.25	0.29	0.90	0.71	0.96	0.76	0.90	0.72	acyl-CoA dehydrogenase, C-4 to C-12 straight chain (ACADM), nuclear gene encoding mitochondrial protein, trans
8092933	ACAP2	0.33	0.26	0.93	1.02	0.96	0.87	1.08	0.99	ArfGAP with coiled-coil, ankyrin repeat and PH domains 2 (ACAP2), mRNA.
7932703	ACBD5	0.38	0.44	1.22	1.08	0.98	0.93	1.43	1.32	acyl-CoA binding domain containing 5 (ACBD5), transcript variant 1, mRNA.
8154733	ACO1	0.97	0.74	0.39	0.29	0.88	0.72	1.01	0.64	aconitase 1, soluble (ACO1), mRNA.
8174474	ACSL4	0.35	0.44	0.91	1.56	0.88	1.74	1.04	1.25	acyl-CoA synthetase long-chain family member 4 (ACSL4), transcript variant 2, mRNA.
7989224	ADAM10	0.32	0.31	1.03	1.06	0.80	0.86	0.95	0.92	ADAM metallopeptidase domain 10 (ADAM10), mRNA.
8146000	ADAM9	0.35	0.38	0.93	1.25	0.94	1.38	0.89	1.28	ADAM metallopeptidase domain 9 (meltrin gamma) (ADAM9), transcript variant 1, mRNA.
8067011	ADNP	0.41	0.49	0.97	0.94	0.72	0.70	0.88	0.74	activity-dependent neuroprotector homeobox (ADNP), transcript variant 1, mRNA.
8106429	AGGF1	0.42	0.45	1.05	1.02	0.95	1.03	0.94	0.86	angiogenic factor with G patch and FHA domains 1 (AGGF1), mRNA.
7903239	AGL	0.17	0.10	0.63	0.42	0.87	0.42	0.81	0.48	amylo-alpha-1, 6-glucosidase, 4-alpha-glucanotransferase (AGL), transcript variant 4, mRNA.
8056220	AHCTF1	0.14	0.10	0.98	1.00	0.89	0.71	0.89	0.72	AT hook containing transcription factor 1 (AHCTF1), mRNA.
8131614	AHR	0.27	0.48	1.08	1.47	0.76	0.97	0.74	0.78	aryl hydrocarbon receptor (AHR), mRNA.
7968835	AKAP11	0.42	0.20	1.06	1.26	1.03	0.68	0.96	0.86	A kinase (PRKA) anchor protein 11 (AKAP11), mRNA.
8134122	AKAP9	0.28	0.12	0.89	0.93	0.72	0.28	0.76	0.72	A kinase (PRKA) anchor protein (yotiao) 9 (AKAP9), transcript variant 2, mRNA.
8081431	ALCAM	0.36	0.24	0.89	0.92	1.04	0.76	0.87	0.83	activated leukocyte cell adhesion molecule (ALCAM), mRNA.
8162884	ALDOB	1.19	0.45	0.48	0.11	0.91	0.38	0.71	0.14	aldolase B, fructose-bisphosphate (ALDOB), mRNA.
8094408	ANAPC4	0.32	0.44	0.97	0.81	0.83	0.77	0.98	0.85	anaphase promoting complex subunit 4 (ANAPC4), mRNA.
8100902	ANKRD17	0.43	0.47	1.08	1.03	0.86	0.93	0.95	0.91	ankyrin repeat domain 17 (ANKRD17), transcript variant 1, mRNA.
8085628	ANKRD28	0.39	0.20	1.10	0.93	0.78	0.52	0.87	0.55	ankyrin repeat domain 28 (ANKRD28), mRNA.
8053801	ANKRD36B	0.35	0.21	0.99	1.11	0.97	0.50	0.97	0.78	ankyrin repeat domain 36 (ANKRD36), mRNA.
8043697	ANKRD36B	0.45	0.28	1.08	1.26	1.11	0.57	1.08	0.86	ankyrin repeat domain 36B (ANKRD36B), mRNA.
8152053	ANKRD46	0.49	0.49	0.96	1.08	0.62	0.80	0.88	0.78	ankyrin repeat domain 46 (ANKRD46), mRNA.
8102720	ANKRD50	0.31	0.31	0.87	1.53	0.82	1.11	0.89	1.07	ankyrin repeat domain 50 (ANKRD50), transcript variant 1, mRNA.
8050619	APOB	0.50	0.20	0.85	0.70	1.02	0.52	0.95	0.73	apolipoprotein B (including Ag(x) antigen) (APOB), mRNA.
8017235	APPBP2	0.36	0.46	1.04	0.89	0.92	0.87	0.95	0.97	amyloid beta precursor protein (cytoplasmic tail) binding protein 2 (APPBP2), mRNA.
8080645	APPL1	0.45	0.46	0.92	0.85	1.13	0.98	0.76	0.61	adaptor protein, phosphotyrosine interaction, PH domain and leucine zipper containing 1 (APPL1), mRNA.
7987325	AQR	0.30	0.31	0.95	0.82	0.92	0.87	0.85	0.84	aquarius homolog (mouse) (AQR), mRNA.
8151149	ARFGEF1	0.26	0.18	0.86	0.85	0.96	0.90	0.79	0.78	ADP-ribosylation factor guanine nucleotide-exchange factor 1(brefeldin A-inhibited) (ARFGEF1), mRNA.
8063242	ARFGEF2	0.50	0.44	0.81	0.80	1.04	0.95	0.82	0.70	ADP-ribosylation factor guanine nucleotide-exchange factor 2 (brefeldin A-inhibited) (ARFGEF2), mRNA.
7932885	ARHGAP12	0.40	0.25	1.07	1.07	1.30	0.87	1.97	1.54	Rho GTPase activating protein 12 (ARHGAP12), mRNA.
8129458	ARHGAP18	0.23	0.23	0.88	0.97	0.92	0.73	0.86	0.84	Rho GTPase activating protein 18 (ARHGAP18), mRNA.
7932554	ARHGAP21	0.33	0.48	1.10	1.42	1.04	1.41	1.18	1.73	Rho GTPase activating protein 21 (ARHGAP21), mRNA.
7917850	ARHGAP29	0.24	0.24	1.19	1.36	1.50	1.08	1.09	1.42	Rho GTPase activating protein 29 (ARHGAP29), mRNA.
7943349	ARHGAP42	0.31	0.30	1.02	0.89	1.15	0.81	1.48	0.95	Rho GTPase activating protein 42 (ARHGAP42), mRNA.
7973840	ARHGAP5	0.26	0.22	0.96	1.02	1.02	0.77	0.93	1.02	Rho GTPase activating protein 5 (ARHGAP5), transcript variant 1, mRNA.
7944560	ARHGEF12	0.42	0.47	0.79	0.74	1.05	0.84	0.93	0.80	Rho guanine nucleotide exchange factor (GEF) 12 (ARHGEF12), mRNA.
7955019	ARID2	0.19	0.22	1.03	0.97	0.89	0.78	1.03	0.70	AT rich interactive domain 2 (ARID, RFX-like) (ARID2), mRNA.
7974621	ARID4A	0.27	0.22	1.08	1.21	0.86	0.63	0.92	0.83	AT rich interactive domain 4A (RBP1-like) (ARID4A), transcript variant 1, mRNA.
8113073	ARRDC3	0.49	0.25	1.21	1.68	1.58	1.16	1.07	1.58	arrestin domain containing 3 (ARRDC3), mRNA.
8149534	ASAH1	0.42	0.46	0.88	0.67	0.62	0.53	0.91	0.57	N-acylsphingosine amidohydrolase (acid ceramidase) 1 (ASAH1), transcript variant 2, mRNA.
8128472	ASCC3	0.25	0.16	0.81	0.67	1.05	0.61	0.89	0.67	activating signal cointegrator 1 complex subunit 3 (ASCC3), transcript variant 1, mRNA.
7920766	ASH1L	0.32	0.23	0.96	0.99	0.99	0.83	1.12	0.87	ash1 (absent, small, or homeotic)-like (Drosophila) (ASH1L), mRNA.
8046997	ASNSD1	0.43	0.48	1.02	0.93	0.99	1.01	0.76	0.69	asparagine synthetase domain containing 1 (ASNSD1), mRNA.
8050875	ASXL2	0.38	0.43	0.94	1.09	0.83	0.98	0.95	0.76	additional sex combs like 2 (Drosophila) (ASXL2), mRNA.
8056909	ATF2	0.47	0.31	1.09	1.09	0.95	0.91	1.18	1.04	activating transcription factor 2 (ATF2), mRNA.
7954104	ATF7IP	0.39	0.37	1.04	1.07	0.66	0.64	1.04	0.88	activating transcription factor 7 interacting protein (ATF7IP), mRNA.
7981217	ATG2B	0.27	0.23	0.85	0.78	0.81	0.86	1.02	1.03	ATG2 autophagy related 2 homolog B (S. cerevisiae) (ATG2B), mRNA.
7901895	ATG4C	0.25	0.26	1.02	0.80	0.60	0.62	0.82	0.62	ATG4 autophagy related 4 homolog C (S. cerevisiae) (ATG4C), transcript variant 7, mRNA.
8128592	ATG5	0.45	0.46	0.98	0.76	0.85	0.78	0.98	0.71	ATG5 autophagy related 5 homolog (S. cerevisiae) (ATG5), mRNA.
7943620	ATM	0.28	0.15	0.97	0.82	1.01	0.45	1.15	0.62	ataxia telangiectasia mutated (ATM), transcript variant 1, mRNA.
8084173	ATP11B	0.29	0.37	0.92	1.03	0.88	0.81	0.89	0.89	ATPase, class VI, type 11B (ATP11B), mRNA.
8175492	ATP11C	0.29	0.16	0.80	0.74	1.04	0.65	1.03	0.85	ATPase, class VI, type 11C (ATP11C), transcript variant 1, mRNA.
8092849	ATP13A3	0.29	0.35	0.85	0.90	1.25	1.29	0.97	0.98	ATPase type 13A3 (ATP13A3), mRNA.
7965359	ATP2B1	0.23	0.11	0.81	1.08	0.70	0.55	0.62	0.51	ATPase, Ca++ transporting, plasma membrane 1 (ATP2B1), transcript variant 1, mRNA.
8168472	ATP7A	0.30	0.32	0.76	1.03	0.65	1.09	0.70	0.69	ATPase, Cu++ transporting, alpha polypeptide (ATP7A), mRNA.
8091190	ATR	0.45	0.17	0.90	0.82	1.70	0.82	1.03	0.93	ataxia telangiectasia and Rad3 related (ATR), mRNA.
8176276	ATRX	0.17	0.15	1.16	1.22	1.12	0.52	1.53	0.89	alpha thalassemia/mental retardation syndrome X-linked (RAD54 homolog, S. cerevisiae) (ATRX), transcript varia
7907310	BAT2L2	0.41	0.47	1.10	1.16	1.18	1.12	1.23	1.28	HLA-B associated transcript 2-like 2 (BAT2L2), mRNA.
7978595	BAZ1A	0.37	0.32	1.26	1.24	1.39	1.24	1.49	1.70	bromodomain adjacent to zinc finger domain, 1A (BAZ1A), transcript variant 1, mRNA.
8056060	BAZ2B	0.44	0.18	1.12	1.05	0.97	0.45	1.24	0.67	bromodomain adjacent to zinc finger domain, 2B (BAZ2B), mRNA.
7965060	BBS10	0.29	0.29	1.25	1.16	0.62	0.75	0.78	0.60	Bardet-Biedl syndrome 10 (BBS10), mRNA.
8081465	BBX	0.37	0.20	1.47	1.24	1.48	0.91	2.13	2.06	bobby sox homolog (Drosophila) (BBX), transcript variant 1, mRNA.
8129773	BCLAF1	0.21	0.22	0.88	0.99	0.90	0.77	1.07	0.87	BCL2-associated transcription factor 1 (BCLAF1), transcript variant 1, mRNA.
8177560	BDP1	0.31	0.14	1.30	1.25	1.07	0.47	0.93	0.75	B double prime 1, subunit of RNA polymerase III transcription initiation factor IIIB (BDP1), mRNA.
7943413	BIRC3	0.47	0.30	1.58	1.59	1.31	0.92	1.61	1.62	baculoviral IAP repeat-containing 3 (BIRC3), transcript variant 1, mRNA.
8041283	BIRC6	0.33	0.16	0.92	0.94	0.99	0.79	0.99	0.81	baculoviral IAP repeat-containing 6 (BIRC6), mRNA.
7926609	BMI1	0.24	0.50	0.98	1.04	0.90	0.85	0.98	0.80	BMI1 polycomb ring finger oncogene (BMI1), mRNA.
8096004	BMP2K	0.30	0.33	1.14	1.36	0.87	1.13	0.92	1.29	BMP2 inducible kinase (BMP2K), transcript variant 1, mRNA.
7989323	BNIP2	0.34	0.40	1.07	1.13	1.21	1.03	1.06	1.10	BCL2/adenovirus E1B 19kDa interacting protein 2 (BNIP2), mRNA.

8009382	BPTF	0.40	0.26	0.93	0.85	0.84	0.66	0.96	0.77	bromodomain PHD finger transcription factor (BPTF), transcript variant 2, mRNA.
8171006	BRCC3	0.20	0.29	0.96	0.96	0.85	0.92	0.89	0.95	BRCA1/BRCA2-containing complex, subunit 3 (BRCC3), transcript variant 1, mRNA.
8070341	BRWD1	0.39	0.24	0.90	0.92	1.02	0.54	0.87	0.60	bromodomain and WD repeat domain containing 1 (BRWD1), transcript variant 2, mRNA.
8173766	BRWD3	0.36	0.28	0.82	1.02	0.97	0.74	0.85	0.74	bromodomain and WD repeat domain containing 3 (BRWD3), mRNA.
7929201	BTAF1	0.45	0.38	1.11	1.10	1.35	1.24	1.02	1.11	BTAF1 RNA polymerase II, B-TFIID transcription factor-associated, 170kDa (Mot1 homolog, S. cerevisiae) (BTAF1)
7936419	C10orf118	0.21	0.13	0.93	1.15	1.02	0.43	0.90	0.76	chromosome 10 open reading frame 118 (C10orf118), mRNA.
7929609	C10orf12	0.32	0.31	0.93	1.21	1.17	1.15	0.77	0.90	chromosome 10 open reading frame 12, mRNA (cDNA clone MGC:17862 IMAGE:3903728), complete cds.
7925978	C10orf18	0.37	0.23	1.08	1.15	1.24	0.96	1.08	0.91	chromosome 10 open reading frame 18 (C10orf18), mRNA.
7961964	C12orf11	0.31	0.29	0.89	0.80	0.99	0.77	0.97	0.80	chromosome 12 open reading frame 11 (C12orf11), mRNA.
7954711	C12orf35	0.26	0.23	1.32	1.36	0.66	0.45	0.98	0.93	chromosome 12 open reading frame 35 (C12orf35), mRNA.
7960411	C12orf4	0.21	0.24	1.02	0.97	1.17	1.16	1.08	1.20	chromosome 12 open reading frame 4 (C12orf4), mRNA.
7953211	C12orf5	0.34	0.48	0.83	0.76	0.77	0.77	0.68	0.67	chromosome 12 open reading frame 5 (C12orf5), mRNA.
7968883	C13orf31	0.30	0.18	0.96	1.02	0.81	0.70	0.77	0.89	chromosome 13 open reading frame 31 (C13orf31), transcript variant 2, mRNA.
7976571	C14orf129	0.36	0.37	0.95	1.01	0.89	0.96	0.93	1.39	chromosome 14 open reading frame 129 (C14orf129), mRNA.
7916506	C1orf168	0.40	0.16	1.07	0.68	1.19	0.56	1.77	2.28	chromosome 1 open reading frame 168 (C1orf168), mRNA.
7908330	C1orf27	0.31	0.43	1.04	0.99	1.17	0.85	0.71	0.76	chromosome 1 open reading frame 27 (C1orf27), transcript variant 1, mRNA.
7909931	C1orf58	0.35	0.45	1.04	0.98	1.12	1.00	1.05	1.13	chromosome 1 open reading frame 58 (C1orf58), mRNA.
7907404	C1orf9	0.24	0.32	1.15	1.71	0.86	0.99	0.92	1.20	chromosome 1 open reading frame 9 (C1orf9), transcript variant 1, mRNA.
8075542	C22orf30	0.39	0.28	1.17	1.15	1.07	0.95	1.14	0.92	chromosome 22 open reading frame 30 (C22orf30), mRNA.
8079170	C3orf23	0.40	0.41	0.93	1.05	1.11	1.18	1.19	1.39	chromosome 3 open reading frame 23 (C3orf23), transcript variant 1, mRNA.
8098512	C4orf41	0.36	0.49	0.92	0.72	0.92	0.83	0.95	0.77	chromosome 4 open reading frame 41 (C4orf41), transcript variant 1, mRNA.
8163839	C5	0.32	0.06	0.84	0.38	0.64	0.22	0.52	0.25	complement component 5 (C5), mRNA.
8108163	C5orf24	0.35	0.38	1.08	1.01	0.82	0.80	0.82	0.71	chromosome 5 open reading frame 24 (C5orf24), transcript variant 2, mRNA.
8111552	C5orf33	0.39	0.47	0.87	0.78	0.84	0.62	0.72	0.45	chromosome 5 open reading frame 33 (C5orf33), transcript variant 1, mRNA.
8110032	C5orf41	0.43	0.29	1.29	0.97	1.09	0.63	1.79	1.23	chromosome 5 open reading frame 41 (C5orf41), transcript variant 1, mRNA.
8105104	C5orf51	0.22	0.35	0.98	1.17	0.93	1.17	1.00	1.08	chromosome 5 open reading frame 51 (C5orf51), mRNA.
8127502	C6orf155	0.45	0.36	0.92	1.26	0.64	0.76	0.79	0.71	chromosome 6 open reading frame 155 (C6orf155), non-coding RNA.
8122818	C6orf211	0.43	0.49	0.90	0.85	0.83	1.06	0.77	0.85	chromosome 6 open reading frame 211, mRNA (cDNA clone MGC:16862 IMAGE:4340090), complete cds.
8156601	C9orf102	0.24	0.12	1.03	0.79	0.98	0.50	1.10	0.76	mRNA; cDNA DKFZp434O1521 (from clone DKFZp434O1521).
8161829	C9orf41	0.30	0.38	1.00	0.88	0.83	0.89	0.68	0.57	chromosome 9 open reading frame 41, mRNA (cDNA clone MGC:24721 IMAGE:4278547), complete cds.
8136347	CALD1	0.49	0.37	0.90	0.89	0.98	0.84	0.80	0.77	caldesmon 1 (CALD1), transcript variant 1, mRNA.
7908614	CAMSAP1L1	0.17	0.18	1.00	1.27	0.91	1.00	0.82	0.98	calmodulin regulated spectrin-associated protein 1-like 1 (CAMSAP1L1), mRNA.
7956910	CAND1	0.43	0.40	1.08	0.98	1.05	0.94	1.09	0.87	cullin-associated and neddylation-dissociated 1 (CAND1), mRNA.
8078110	CAPN7	0.30	0.41	0.88	0.80	0.90	0.74	0.98	0.68	calpain 7 (CAPN7), mRNA.
8134318	CASD1	0.24	0.33	0.92	1.03	0.64	0.81	0.65	0.50	CAS1 domain containing 1 (CASD1), mRNA.
7927889	CCAR1	0.46	0.30	0.95	0.96	0.96	0.75	0.98	0.90	cell division cycle and apoptosis regulator 1 (CCAR1), mRNA.
8090133	CCDC14	0.31	0.25	1.18	1.02	0.83	0.58	1.00	0.68	coiled-coil domain containing 14 (CCDC14), mRNA.
8006112	CCDC55	0.22	0.15	1.08	1.15	0.94	0.73	0.90	1.00	coiled-coil domain containing 55 (CCDC55), transcript variant 1, mRNA.
8052269	CCDC88A	0.17	0.12	0.99	0.77	0.72	0.33	0.82	0.50	coiled-coil domain containing 88A (CCDC88A), transcript variant 1, mRNA.
7954613	CCDC91	0.44	0.27	1.09	0.80	0.94	0.82	0.99	0.87	coiled-coil domain containing 91 (CCDC91), mRNA.
8109830	CCDC99	0.28	0.24	1.13	0.81	0.64	0.69	0.65	0.51	coiled-coil domain containing 99 (CCDC99), mRNA.
8045381	CCNT2	0.43	0.35	1.17	1.16	0.97	1.00	1.19	1.12	cyclin T2 (CCNT2), transcript variant b, mRNA.
8120102	CD2AP	0.37	0.35	1.28	1.57	1.75	1.82	1.91	2.72	CD2-associated protein (CD2AP), mRNA.
7924773	CDC42BPA	0.22	0.19	0.71	0.98	0.94	0.99	0.89	0.83	CDC42 binding protein kinase alpha (DMPK-like) (CDC42BPA), transcript variant B, mRNA.
8140955	CDK6	0.28	0.30	0.95	1.30	0.90	0.87	0.85	0.82	cyclin-dependent kinase 6 (CDK6), transcript variant 1, mRNA.
8113733	CEP120	0.46	0.28	0.89	0.84	0.83	0.72	0.93	0.58	centrosomal protein 120kDa (CEP120), transcript variant 1, mRNA.
7925525	CEP170	0.13	0.10	1.01	0.88	0.77	0.33	0.92	0.69	centrosomal protein 170kDa (CEP170), transcript variant alpha, mRNA.
8180257	CEP170	0.21	0.13	1.13	1.04	0.92	0.56	1.16	0.83	centrosomal protein 170kDa (CEP170), transcript variant gamma, mRNA
8020267	CEP192	0.47	0.42	1.03	0.98	1.13	0.69	1.76	1.15	centrosomal protein 192kDa (CEP192), mRNA.
7907790	CEP350	0.25	0.15	0.95	0.90	1.09	0.45	1.06	0.78	centrosomal protein 350kDa (CEP350), mRNA.
8081362	CEP97	0.26	0.34	1.09	1.45	0.93	1.10	0.76	1.08	centrosomal protein 97kDa (CEP97), mRNA.
8113305	CHD1	0.40	0.20	1.20	1.38	1.33	0.77	1.10	0.97	chromodomain helicase DNA binding protein 1 (CHD1), mRNA.
7995583	CHD9	0.21	0.10	0.89	1.08	0.90	0.42	1.02	0.83	chromodomain helicase DNA binding protein 9 (CHD9), mRNA.
8173892	CHM	0.23	0.19	0.81	0.97	0.81	0.77	0.86	0.88	choroideremia (Rab escort protein 1) (CHM), transcript variant 1, mRNA.
7925500	CHML	0.31	0.19	1.03	1.19	0.88	0.55	0.68	0.55	choroideremia-like (Rab escort protein 2) (CHML), mRNA.
8022666	CHST9	0.31	0.37	0.88	0.87	0.55	0.57	0.58	0.58	carbohydrate (N-acetylgalactosamine 4-0) sulfotransferase 9 (CHST9), mRNA.
7935707	CHUK	0.31	0.48	1.11	1.00	1.18	1.07	0.91	0.85	conserved helix-loop-helix ubiquitous kinase (CHUK), mRNA.
7969243	CKAP2	0.27	0.22	1.22	1.04	0.82	0.74	0.90	1.05	cytoskeleton associated protein 2 (CKAP2), transcript variant 1, mRNA.
7947694	CKAP5	0.31	0.39	1.04	1.26	1.06	1.01	0.87	0.89	cytoskeleton associated protein 5 (CKAP5), transcript variant 1, mRNA.
8098291	CLCN3	0.30	0.41	0.70	0.85	0.85	1.04	0.91	0.89	chloride channel 3 (CLCN3), transcript variant e, mRNA.
7967255	CLIP1	0.36	0.25	1.10	1.08	1.03	0.98	0.98	0.94	CAP-GLY domain containing linker protein 1 (CLIP1), transcript variant 1, mRNA.
8144279	CLN8	0.53	0.61	0.49	0.44	0.79	0.90	0.55	0.32	ceroid-lipofuscinosis, neuronal 8 (epilepsy, progressive with mental retardation) (CLN8), mRNA.
8100428	CLOCK	0.22	0.18	0.94	0.75	0.68	0.72	0.92	0.82	clock homolog (mouse) (CLOCK), mRNA.
8008834	CLTC	0.39	0.46	0.87	0.98	1.05	1.11	0.99	0.96	clathrin, heavy chain (Hc) (CLTC), mRNA.
8056343	COBLL1	0.29	0.34	0.83	1.27	0.94	1.19	1.14	1.63	COBL-like 1 (COBLL1), mRNA.
7968711	COG6	0.26	0.26	0.96	1.29	0.95	1.08	0.95	1.14	component of oligomeric golgi complex 6 (COG6), transcript variant 1, mRNA.
7946703	COPB1	0.28	0.38	0.87	1.01	0.97	1.02	0.91	0.94	coatomer protein complex, subunit beta 1 (COPB1), transcript variant 1, mRNA.
7988605	COPS2	0.19	0.25	0.97	0.86	0.82	0.75	0.80	0.82	COP9 constitutive photomorphogenic homolog subunit 2 (Arabidopsis) (COPS2), transcript variant 1, mRNA.
8006123	CPD	0.29	0.31	0.72	0.91	0.78	0.96	0.99	1.05	carboxypeptidase D (CPD), mRNA.
8110055	CPEB4	0.37	0.27	0.94	1.22	0.57	0.70	0.83	0.67	cytoplasmic polyadenylation element binding protein 4 (CPEB4), mRNA.
7962250	CPNE8	0.39	0.41	1.03	1.03	1.30	1.37	1.31	1.68	copine VIII (CPNE8), mRNA.
7976243	CPSF2	0.36	0.38	1.00	0.77	0.87	0.88	0.98	0.71	cleavage and polyadenylation specific factor 2, 100kDa (CPSF2), mRNA.
8081171	CRYBG3	0.23	0.09	0.95	0.91	1.07	0.61	1.06	0.89	beta-gamma crystallin domain containing 3 (CRYBG3), mRNA.
8063283	CSE1L	0.21	0.32	0.97	0.81	0.87	0.83	0.76	0.68	CSE1 chromosome segregation 1-like (yeast) (CSE1L), mRNA.
8107655	CSNK1G3	0.36	0.34	1.08	1.20	0.96	0.92	0.99	1.08	casein kinase 1, gamma 3 (CSNK1G3), transcript variant 1, mRNA.
7938422	CTR9	0.30	0.32	1.00	0.97	1.00	0.95	0.97	0.88	Ctr9, Paf1/RNA polymerase II complex component, homolog (S. cerevisiae) (CTR9), mRNA.
7933047	CUL2	0.37	0.36	1.12	0.88	1.11	0.99	1.40	1.23	cullin 2 (CUL2), mRNA.
7943580	CUL5	0.31	0.28	0.94	0.85	0.93	0.77	0.80	0.89	cullin 5 (CUL5), mRNA.
8057441	CWC22	0.29	0.26	1.32	1.03	1.09	0.81	1.02	1.02	CWC22 spliceosome-associated protein homolog (S. cerevisiae) (CWC22), mRNA.
8067955	CXADR	0.35	0.45	0.92	1.38	0.74	1.06	0.79	0.89	coxsackie virus and adenovirus receptor (CXADR), mRNA.
8120943	CYB5R4	0.42	0.45	0.91	0.75	0.90	0.85	1.08	0.87	cytochrome b5 reductase 4 (CYB5R4), mRNA.
8166730	CYBB	0.49	0.09	0.62	0.07	1.07	0.10	1.86	0.12	cytochrome b-245, beta polypeptide (CYBB), mRNA.
8028963	CYP2B6	1.94	0.17	0.36	0.05	1.18	0.16	0.55	0.08	cytochrome P450, family 2, subfamily B, polypeptide 6 (CYP2B6), mRNA.
8028955	CYP2B7P1	1.64	0.25	0.34	0.10	1.32	0.23	0.56	0.12	cytochrome P450, family 2, subfamily B, polypeptide 7 pseudogene 1 (CYP2B7P1), non-coding RNA.
7974697	DAAM1	0.38	0.30	1.03	1.19	0.91	1.03	0.92	1.01	dishevelled associated activator of morphogenesis 1 (DAAM1), mRNA.
7918008	DBT	0.41	0.39	1.01	0.99	0.84	0.84	0.76	0.83	dihydrolipoamide branched chain transacylase E2 (DBT), nuclear gene encoding mitochondrial protein, mRNA.
8107356	DCP2	0.50	0.32	0.80	0.69	1.05	0.83	0.80	0.68	DCP2 decapping enzyme homolog (S. cerevisiae) (DCP2), mRNA.
8092321	DCUN1D1	0.30	0.21	1.21	1.01	0.82	0.72	1.11	0.82	DCN1, defective in cullin neddylation 1, domain containing 1 (S. cerevisiae) (DCUN1D1), mRNA.
8095009	DCUN1D4	0.43	0.39	1.08	0.97	1.06	0.90	0.84	0.83	DCN1, defective in cullin neddylation 1, domain containing 4 (S. cerevisiae) (DCUN1D4), transcript variant 1, mR
7979223	DDHD1	0.36	0.43	1.00	1.05	0.90	0.91	1.01	0.80	DDHD domain containing 1 (DDHD1), transcript variant 3, mRNA.
7943690	DDX10	0.38	0.38	1.03	0.90	0.84	0.69	0.71	0.41	DEAD (Asp-Glu-Ala-Asp) box polypeptide 10 (DDX10), mRNA.
8044745	DDX18	0.23	0.33	1.11	0.90	0.83	0.73	0.67	0.61	DEAD (Asp-Glu-Ala-Asp) box polypeptide 18 (DDX18), mRNA.
7927936	DDX21	0.33	0.27	1.26	1.21	1.52	1.82	0.78	1.05	DEAD (Asp-Glu-Ala-Asp) box polypeptide 21 (DDX21), mRNA.
8176624	DDX3Y	0.39	0.20	0.88	0.66	1.02	0.65	0.91	0.78	DEAD (Asp-Glu-Ala-Asp) box polypeptide 3, Y-linked (DDX3Y), transcript variant 1, mRNA.
8108134	DDX46	0.37	0.32	0.91	0.75	1.24	1.15	0.78	0.77	DEAD (Asp-Glu-Ala-Asp) box polypeptide 46 (DDX46), mRNA.
8124144	DEK	0.43	0.29	1.30	0.95	1.33	0.84	0.96	1.02	DEK oncogene (DEK), transcript variant 1, mRNA.
7923131	DENND1B	0.39	0.19	1.14	1.12	1.26	0.78	1.67	1.35	DENN/MADD domain containing 1B (DENND1B), transcript variant 1, mRNA.
7989849	DENND4A	0.39	0.19	0.91	0.75	2.01	1.09	1.57	1.31	DENN/MADD domain containing 4A (DENND4A), transcript variant 1, mRNA.
8154531	DENND4C	0.32	0.20	0.97	0.91	0.85	0.73	1.23	0.89	DENN/MADD domain containing 4C (DENND4C), mRNA.
7962151	DENND5B	0.48	0.49	0.82	0.92	0.84	0.88	1.11	0.71	DENN/MADD domain containing 5B (DENND5B), mRNA.
8112081	DHX29	0.29	0.17	1.03	0.97	0.91	0.88	0.86	0.74	DEAH (Asp-Glu-Ala-His) box polypeptide 29 (DHX29), mRNA.
8091562	DHX36	0.37	0.28	1.01	1.05	1.60	1.02	1.25	1.04	DEAH (Asp-Glu-Ala-His) box polypeptide 36 (DHX36), transcript variant 1, mRNA.
8051637	DHX57	0.43	0.49	1.27	0.97	0.87	0.95	1.00	0.92	DEAH (Asp-Glu-Ala-Asp/His) box polypeptide 57 (DHX57), mRNA.
8168691	DIAPH2	0.36	0.19	0.76	0.82	1.13	0.62	0.75	0.71	diaphanous homolog 2 (Drosophila) (DIAPH2), transcript variant 156, mRNA.
7981111	DICER1	0.21	0.19	0.93	0.89	1.19	1.02	1.06	1.03	dicer 1, ribonuclease type III (DICER1), transcript variant 1, mRNA.
7901565	DIO1	1.93	0.54	0.48	0.20	1.26	0.48	0.71	0.23	deiodinase, iodothyronine, type I (DIO1), transcript variant 1, mRNA.
7971967	DIS3	0.24	0.24	1.15	1.03	0.95	0.93	1.03	1.03	DIS3 mitotic control homolog (S. cerevisiae) (DIS3), transcript variant 1, mRNA.
8093191	DLG1	0.37	0.34	0.78	0.74	0.76	0.78	0.63	0.54	discs, large homolog 1 (Drosophila) (DLG1), transcript variant 1, mRNA.
8133914	DMTF1	0.42	0.36	1.38	1.35	1.61	1.04	1.84	1.46	cyclin D binding myb-like transcription factor 1 (DMTF1), transcript variant 4, non-coding RNA.
8107474	DMXL1	0.26	0.14	0.86	0.80	1.05	0.57	0.84	0.75	Dmx-like 1 (DMXL1), mRNA.
7988789	DMXL2	0.23	0.09	0.99	0.68	0.84	0.43	1.15	0.65	Dmx-like 2 (DMXL2), transcript variant 1, mRNA.
8101934	DNAJB14	0.38	0.40	1.15	1.27	1.34	0.83	1.05	0.90	DnaJ (Hsp40) homolog, subfamily B, member 14 (DNAJB14), transcript variant 1, mRNA.
7902512	DNAJB4	0.29	0.37	1.30	1.31	0.97	1.06	0.79	0.82	DnaJ (Hsp40) homolog, subfamily B, member 4 (DNAJB4), mRNA.
8046759	DNAJC10	0.23	0.35	0.90	1.06	0.92	0.97	0.87	1.13	DnaJ (Hsp40) homolog, subfamily C, member 10 (DNAJC10), mRNA.
8082688	DNAJC13	0.20	0.11	0.75	0.60	0.97	0.66	0.87	0.66	DnaJ (Hsp40) homolog, subfamily C, member 13 (DNAJC13), mRNA.
8141898	DNAJC2	0.46	0.34	1.10	0.99	1.07	0.87	0.92	0.83	DnaJ (Hsp40) homolog, subfamily C, member 2 (DNAJC2), transcript variant 1, mRNA.
7969651	DNAJC3	0.41	0.49	0.70	0.97	1.11	1.07	0.83	1.17	DnaJ (Hsp40) homolog, subfamily C, member 3 (DNAJC3), mRNA.
7954752	DNM1L	0.24	0.23	1.04	0.94	0.92	0.94	0.89	1.03	dynamin 1-like (DNM1L), transcript variant 1, mRNA.

7917771	DNTTIP2	0.30	0.14	1.01	1.16	0.81	0.66	0.68	0.65	deoxynucleotidyltransferase, terminal, interacting protein 2 (DNTTIP2), mRNA.
8142345	DOCK4	0.35	0.33	0.89	0.95	1.12	0.77	2.00	1.33	dedicator of cytokinesis 4 (DOCK4), mRNA.
7916669	DOCK7	0.28	0.27	0.92	0.94	1.13	1.01	1.13	0.99	dedicator of cytokinesis 7 (DOCK7), mRNA.
8147375	DPY19L4	0.47	0.43	1.11	1.09	0.93	0.93	0.84	0.85	dpy-19-like 4 (C. elegans) (DPY19L4), mRNA.
7917912	DPYD	0.49	0.26	0.90	0.73	0.98	0.50	2.13	1.21	dihydropyrimidine dehydrogenase (DPYD), transcript variant 1, mRNA.
8127234	DST	0.29	0.08	0.73	0.88	0.89	0.28	0.68	0.72	dystonin (DST), transcript variant 1eA, mRNA.
8172035	DYNLT3	0.29	0.42	0.78	1.10	1.06	1.18	0.98	1.27	dynein, light chain, Tctex-type 3 (DYNLT3), mRNA.
8129379	ECHDC1	0.37	0.33	0.72	0.58	1.07	0.79	0.92	0.89	enoyl CoA hydratase domain containing 1 (ECHDC1), transcript variant 1, mRNA.
8083941	ECT2	0.34	0.37	1.07	1.35	1.17	1.25	1.13	1.78	epithelial cell transforming sequence 2 oncogene (ECT2), mRNA.
7922823	EDEM3	0.18	0.12	0.97	0.94	0.75	0.68	0.91	0.80	ER degradation enhancer, mannosidase alpha-like 3 (EDEM3), mRNA.
7965436	EEA1	0.15	0.08	0.99	0.98	0.98	0.47	0.83	0.79	early endosome antigen 1 (EEA1), mRNA.
8148333	EFR3A	0.46	0.50	1.06	1.18	1.45	1.27	1.48	1.58	EFR3 homolog A (S. cerevisiae) (EFR3A), mRNA.
8042223	EHBP1	0.38	0.31	1.18	1.13	1.17	1.03	1.40	1.38	EH domain binding protein 1 (EHBP1), transcript variant 1, mRNA.
8092523	EHHADH	0.32	0.31	0.86	0.55	0.74	0.66	0.78	0.60	enoyl-CoA, hydratase/3-hydroxyacyl CoA dehydrogenase (EHHADH), transcript variant 1, mRNA.
7936614	EIF3A	0.38	0.32	0.91	0.95	0.96	1.11	0.84	0.90	eukaryotic translation initiation factor 3, subunit A (EIF3A), mRNA.
8043861	EIF5B	0.26	0.09	1.05	1.16	0.97	0.68	0.82	0.95	eukaryotic translation initiation factor 5B (EIF5B), mRNA.
7917182	ELTD1	0.28	0.18	0.89	0.26	1.70	0.28	2.33	0.35	EGF, latrophilin and seven transmembrane domain containing 1 (ELTD1), mRNA.
8122099	ENPP1	0.42	0.46	0.87	0.53	0.92	0.55	0.78	0.39	ectonucleotide pyrophosphatase/phosphodiesterase 1 (ENPP1), mRNA.
8120061	ENPP4	0.45	0.44	1.17	1.02	1.09	0.99	1.15	1.02	ectonucleotide pyrophosphatase/phosphodiesterase 4 (putative function) (ENPP4), mRNA.
8045619	EPC2	0.35	0.31	1.05	1.07	0.98	0.80	1.06	0.86	enhancer of polycomb homolog 2 (Drosophila) (EPC2), mRNA.
8086141	EPM2AIP1	0.32	0.49	1.05	0.98	0.95	0.91	0.99	0.66	EPM2A (laforin) interacting protein 1 (EPM2AIP1), mRNA.
7924351	EPRS	0.21	0.20	0.81	0.81	0.97	0.89	0.91	0.94	glutamyl-prolyl-tRNA synthetase (EPRS), mRNA.
8105681	ERBB2IP	0.20	0.19	1.04	0.90	0.92	0.76	0.98	0.95	erbb2 interacting protein (ERBB2IP), transcript variant 2, mRNA.
7962013	ERGIC2	0.39	0.36	0.87	0.69	0.81	0.74	0.79	0.74	ERGIC and golgi 2 (ERGIC2), mRNA.
7917707	EVI5	0.32	0.44	0.84	0.87	1.21	0.79	0.77	0.59	ecotropic viral integration site 5 (EVI5), mRNA.
8095163	EXOC1	0.31	0.41	1.15	1.19	1.00	0.98	1.02	1.07	exocyst complex component 1 (EXOC1), transcript variant 3, mRNA.
7979367	EXOC5	0.12	0.15	1.08	0.97	0.95	0.91	0.96	1.05	exocyst complex component 5 (EXOC5), mRNA.
7929288	EXOC6	0.46	0.43	0.87	0.85	0.89	1.01	1.00	1.08	exocyst complex component 6 (EXOC6), transcript variant 1, mRNA.
8170215	F9	0.29	0.09	0.48	0.18	0.88	0.25	0.54	0.20	coagulation factor IX (F9), mRNA.
8180403	FAM115A	0.45	0.36	0.94	0.90	0.87	0.74	0.86	0.82	KIAA0738 gene product (KIAA0738), mRNA
8138553	FAM126A	0.44	0.42	0.78	0.73	1.12	0.94	0.89	1.16	family with sequence similarity 126, member A (FAM126A), mRNA.
8114326	FAM13B	0.40	0.35	1.10	0.99	1.08	0.99	1.14	0.98	family with sequence similarity 13, member B (FAM13B), transcript variant 1, mRNA.
8113083	FAM172A	0.42	0.50	0.68	0.82	0.87	1.04	0.59	0.58	family with sequence similarity 172, member A (FAM172A), transcript variant 1, mRNA.
7931216	FAM175B	0.45	0.49	1.14	0.96	0.98	1.12	0.97	1.10	family with sequence similarity 175, member B (FAM175B), mRNA.
7928800	FAM190B	0.31	0.31	0.88	0.94	1.19	1.09	1.10	1.20	family with sequence similarity 190, member B (FAM190B), mRNA.
7927267	FAM35A	0.29	0.28	0.82	0.72	0.83	0.80	0.82	0.75	family with sequence similarity 35, member B (FAM35B), non-coding RNA.
7927288	FAM35A	0.38	0.31	0.83	0.77	0.91	0.79	0.85	0.73	family with sequence similarity 35, member B2 (FAM35B2), non-coding RNA.
7928909	FAM35A	0.42	0.38	0.88	0.82	0.94	1.07	0.83	0.81	family with sequence similarity 35, member A (FAM35A), mRNA.
7917728	FAM69A	0.32	0.46	1.02	1.23	0.69	0.77	0.67	0.68	family with sequence similarity 69, member A (FAM69A), mRNA.
7902476	FAM73A	0.44	0.43	0.84	1.15	1.29	1.19	0.82	0.85	mRNA; cDNA DKFZp686M07166 (from clone DKFZp686M07166); complete cds.
8148208	FAM91A1	0.39	0.35	1.03	0.96	1.01	1.09	1.11	0.86	family with sequence similarity 91, member A1 (FAM91A1), mRNA.
8047815	FASTKD2	0.44	0.36	1.00	0.72	1.05	0.88	0.78	0.59	FAST kinase domains 2 (FASTKD2), transcript variant 1, mRNA.
8104079	FAT1	0.37	0.38	0.69	0.86	0.70	0.80	0.63	0.52	FAT tumor suppressor homolog 1 (Drosophila) (FAT1), mRNA.
7909992	FBXO28	0.38	0.48	1.00	1.07	1.02	1.13	0.77	0.76	F-box protein 28 (FBXO28), transcript variant 1, mRNA.
8130032	FBXO30	0.40	0.29	1.18	0.85	1.18	0.85	0.80	0.62	F-box protein 30 (FBXO30), mRNA.
8106141	FCHO2	0.25	0.20	1.16	0.99	0.67	0.56	1.26	1.03	FCH domain only 2 (FCHO2), transcript variant 1, mRNA.
7954729	FGD4	0.44	0.40	1.06	1.49	0.71	0.71	0.66	0.68	FYVE, RhoGEF and PH domain containing 4 (FGD4), mRNA.
8097256	FGF2	0.47	0.39	1.05	0.69	0.86	0.70	0.75	0.48	fibroblast growth factor 2 (basic) (FGF2), mRNA.
8056323	FIGN	0.36	0.30	1.09	1.30	0.62	0.63	0.90	0.71	fidgetin (FIGN), mRNA.
8144228	FLJ36840	0.29	0.19	0.89	0.47	1.80	0.41	1.68	0.35	cDNA FLJ36840 fis, clone ASTRO2011461.
8065071	FLRT3	0.39	0.41	1.10	1.04	0.61	0.77	0.59	0.67	fibronectin leucine rich transmembrane protein 3 (FLRT3), transcript variant 2, mRNA.
8045736	FMNL2	0.31	0.29	0.99	0.87	0.73	0.70	1.01	1.05	formin-like 2 (FMNL2), mRNA.
7903092	FNBP1L	0.20	0.20	1.03	1.16	0.76	0.94	0.68	0.82	formin binding protein 1-like (FNBP1L), transcript variant 1, mRNA.
7969060	FNDC3A	0.31	0.25	1.17	1.31	0.93	0.84	1.03	0.91	fibronectin type III domain containing 3A (FNDC3A), transcript variant 1, mRNA.
8113914	FNIP1	0.26	0.23	1.12	1.08	1.09	1.01	1.15	0.90	folliculin interacting protein 1 (FNIP1), transcript variant 1, mRNA.
8129071	FRK	0.25	0.23	0.86	1.03	0.76	0.69	1.01	0.69	fyn-related kinase (FRK), mRNA.
7957043	FRS2	0.38	0.45	1.34	1.32	1.01	1.07	1.13	1.25	fibroblast growth factor receptor substrate 2 (FRS2), transcript variant 1, mRNA.
8100292	FRYL	0.52	0.36	1.01	0.96	1.33	0.89	1.30	1.14	FRY-like (FRYL), mRNA.
8084146	FXR1	0.33	0.40	1.02	0.94	1.03	0.88	0.90	0.82	fragile X mental retardation, autosomal homolog 1 (FXR1), transcript variant 3, mRNA.
8133030	GABPA	0.29	0.20	1.02	1.02	0.73	0.82	0.73	0.98	GA binding protein transcription factor, alpha subunit 60kDa (GABPA), mRNA.
8020903	GALNT1	0.22	0.36	0.80	1.03	0.88	1.15	0.75	0.84	UDP-N-acetyl-alpha-D-galactosamine:polypeptide N-acetylgalactosaminyltransferase 1 (GalNAc-T1) (GALNT1), mR
8044236	GCC2	0.18	0.06	1.30	1.25	0.84	0.32	1.04	0.92	GRIP and coiled-coil domain containing 2 (GCC2), transcript variant 1, mRNA.
8040440	GEN1	0.29	0.22	0.97	0.92	1.29	1.01	1.07	0.87	Gen homolog 1, endonuclease (Drosophila) (GEN1), transcript variant 1, mRNA.
7984517	GLCE	0.33	0.45	0.88	0.91	0.85	0.76	0.97	0.68	glucuronic acid epimerase (GLCE), mRNA.
8180344	GNAQ	0.36	0.48	0.93	1.12	0.98	1.19	0.84	0.99	guanine nucleotide binding protein (G protein), q polypeptide (GNAQ), mRNA
8161906	GNAQ	0.34	0.47	1.00	1.11	1.03	1.10	0.96	0.98	guanine nucleotide binding protein (G protein), q polypeptide (GNAQ), mRNA.
8080419	GNL3	0.42	0.50	1.20	1.18	0.99	1.13	0.63	0.78	guanine nucleotide binding protein-like 3 (nucleolar) (GNL3), transcript variant 2, mRNA.
7965812	GNPTAB	0.33	0.32	0.72	0.75	0.78	0.88	0.81	0.69	N-acetylglucosamine-1-phosphate transferase, alpha and beta subunits (GNPTAB), mRNA.
8078569	GOLGA4	0.21	0.07	0.76	0.74	0.77	0.31	0.78	0.71	golgin A4 (GOLGA4), transcript variant 2, mRNA.
8089930	GOLGB1	0.25	0.15	0.78	0.83	1.03	0.24	1.02	0.80	golgin B1 (GOLGB1), mRNA.
8091954	GOLIM4	0.31	0.23	0.86	0.82	0.83	0.75	0.93	0.72	golgi integral membrane protein 4 (GOLIM4), mRNA.
8129181	GOPC	0.45	0.44	1.02	1.47	0.95	1.03	0.96	1.06	golgi-associated PDZ and coiled-coil motif containing (GOPC), transcript variant 1, mRNA.
8122365	GPR126	0.28	0.27	1.01	1.11	0.83	0.80	0.81	0.72	G protein-coupled receptor 126 (GPR126), transcript variant a1, mRNA.
7980523	GTF2A1	0.37	0.40	0.90	1.01	1.02	1.17	1.07	0.97	general transcription factor IIA, 1, 19/37kDa (GTF2A1), transcript variant 1, mRNA.
8094876	GUF1	0.36	0.38	1.01	0.68	0.97	0.84	0.77	0.63	GUF1 GTPase homolog (S. cerevisiae) (GUF1), mRNA.
7962349	GXYLT1	0.43	0.34	0.85	0.81	0.84	0.66	0.67	0.53	glucoside xylosyltransferase 1 (GXYLT1), transcript variant 1, mRNA.
8132843	HAUS6	0.22	0.20	0.73	0.96	1.06	0.77	0.82	0.55	HAUS augmin-like complex, subunit 6 (HAUS6), mRNA.
7925364	HEATR1	0.25	0.28	0.90	0.72	0.90	0.94	0.60	0.55	HEAT repeat containing 1 (HEATR1), mRNA.
7978492	HEATR5A	0.26	0.28	0.84	0.78	0.86	0.98	0.87	0.79	HEAT repeat containing 5A (HEATR5A), mRNA.
8051464	HEATR5B	0.47	0.43	0.93	0.99	1.03	1.00	1.03	0.87	HEAT repeat containing 5B (HEATR5B), mRNA.
7978449	HECTD1	0.32	0.21	0.83	0.83	0.88	0.89	0.73	0.61	HECT domain containing 1 (HECTD1), mRNA.
8017776	HELZ	0.38	0.34	1.12	1.06	0.88	0.88	1.05	0.97	helicase with zinc finger (HELZ), mRNA.
7974851	HIF1A	0.37	0.35	1.03	0.94	1.00	0.99	1.05	1.27	hypoxia inducible factor 1, alpha subunit (basic helix-loop-helix transcription factor) (HIF1A), transcript variant 1,
7939197	HIPK3	0.34	0.47	1.02	1.15	1.32	1.38	1.14	1.64	homeodomain interacting protein kinase 3 (HIPK3), transcript variant 1, mRNA.
8116910	HIVEP1	0.46	0.44	1.05	1.32	1.26	0.93	1.07	1.07	human immunodeficiency virus type I enhancer binding protein 1 (HIVEP1), mRNA.
8091354	HLTF	0.23	0.12	0.76	0.60	0.93	0.40	0.57	0.43	helicase-like transcription factor (HLTF), transcript variant 1, mRNA.
7919055	HMGCS2	0.73	0.92	0.45	0.26	0.58	0.67	3.02	0.54	3-hydroxy-3-methylglutaryl-CoA synthase 2 (mitochondrial) (HMGCS2), nuclear gene encoding mitochondrial prot
8045499	HNMT	0.45	0.48	0.96	0.97	1.23	0.87	1.72	1.43	histamine N-methyltransferase (HNMT), transcript variant 1, mRNA.
8146243	HOOK3	0.27	0.27	0.74	1.02	0.88	1.01	0.83	0.93	hook homolog 3 (Drosophila) (HOOK3), mRNA.
7902789	HS2ST1	0.40	0.44	0.82	0.99	0.91	0.99	0.73	0.76	heparan sulfate 2-O-sulfotransferase 1 (HS2ST1), transcript variant 1, mRNA.
8157233	HSDL2	0.33	0.41	0.81	0.54	0.71	0.68	0.89	0.78	hydroxysteroid dehydrogenase like 2 (HSDL2), mRNA.
7981335	HSP90AA1	0.43	0.37	1.04	0.82	0.93	0.90	0.98	1.02	heat shock protein 90kDa alpha (cytosolic), class A member 1 (HSP90AA1), transcript variant 1, mRNA.
7947245	HSP90AA2	0.46	0.49	0.88	0.77	0.89	0.97	1.02	1.40	Human heat shock protein 86 mRNA, 5'end.
7958130	HSP90B1	0.50	0.43	0.85	0.94	0.95	0.80	0.84	0.89	heat shock protein 90kDa beta (Grp94), member 1 (HSP90B1), mRNA.
8069532	HSPA13	0.37	0.35	1.00	1.13	1.16	0.94	0.98	1.12	heat shock protein 70kDa family, member 13 (HSPA13), mRNA.
8097335	HSPA4L	0.14	0.08	0.86	0.45	0.75	0.39	0.62	0.35	heat shock 70kDa protein 4-like (HSPA4L), mRNA.
7970864	HSPH1	0.36	0.29	1.13	0.96	1.05	0.87	0.84	0.74	heat shock 105kDa/110kDa protein 1 (HSPH1), mRNA.
8127787	IBTK	0.42	0.19	0.86	1.00	1.38	1.05	0.88	0.96	inhibitor of Bruton agammaglobulinemia tyrosine kinase (IBTK), mRNA.
8127109	ICK	0.47	0.43	1.13	1.07	0.80	0.78	0.87	0.77	intestinal cell (MAK-like) kinase (ICK), transcript variant 2, mRNA.
7935027	IDE	0.29	0.24	0.76	0.77	1.01	1.02	0.79	0.95	insulin-degrading enzyme (IDE), transcript variant 1, mRNA.
8154670	IFT74	0.41	0.41	1.52	1.55	1.17	0.93	0.99	1.33	intraflagellar transport 74 homolog (Chlamydomonas) (IFT74), transcript variant 1, mRNA.
8091737	IFT80	0.22	0.15	1.00	1.17	0.84	0.57	0.92	0.82	intraflagellar transport 80 homolog (Chlamydomonas) (IFT80), mRNA.
7965873	IGF1	0.42	0.49	0.95	0.93	0.85	0.97	0.55	0.95	insulin-like growth factor 1 (somatomedin C) (IGF1), transcript variant 1, mRNA.
7936826	IKZF5	0.43	0.47	1.52	1.43	0.97	1.10	1.13	1.18	IKAROS family zinc finger 5 (Pegasus) (IKZF5), mRNA.
8112139	IL6ST	0.33	0.16	1.02	0.86	1.06	0.63	1.07	1.00	interleukin 6 signal transducer (gp130, oncostatin M receptor) (IL6ST), transcript variant 1, mRNA.
8150906	IMPAD1	0.25	0.39	0.77	0.48	0.58	0.82	0.58	0.66	inositol monophosphatase domain containing 1 (IMPAD1), mRNA.
8058415	INO80D	0.37	0.40	1.12	1.46	1.26	1.04	1.50	1.17	INO80 complex subunit D (INO80D), mRNA.
8017283	INTS2	0.47	0.36	1.15	1.15	1.19	0.95	1.01	0.93	integrator complex subunit 2 (INTS2), transcript variant 2, transcribed RNA.
7933723	IPMK	0.42	0.27	0.97	0.98	0.93	0.96	0.88	0.80	inositol polyphosphate multikinase (IPMK), mRNA.
8105545	IPO11	0.25	0.33	0.84	0.69	0.88	0.87	0.86	0.78	importin 11 (IPO11), transcript variant 2, mRNA.
7938313	IPO7	0.19	0.26	0.89	0.83	0.95	0.83	0.83	0.77	importin 7 (IPO7), mRNA.
7962085	IPO8	0.32	0.46	0.83	0.79	1.17	0.93	0.84	0.84	importin 8 (IPO8), mRNA.
7986010	IQGAP1	0.26	0.40	1.01	1.27	1.09	1.19	1.16	1.27	IQ motif containing GTPase activating protein 1 (IQGAP1), mRNA.
8106354	IQGAP2	0.22	0.09	0.90	0.50	0.84	0.44	1.25	0.57	IQ motif containing GTPase activating protein 2 (IQGAP2), mRNA.
7985166	IREB2	0.33	0.28	1.04	1.01	1.04	0.99	0.92	0.86	iron-responsive element binding protein 2 (IREB2), mRNA.
8046861	ITGAV	0.31	0.27	0.81	0.90	0.97	0.94	0.73	0.88	integrin, alpha V (vitronectin receptor, alpha polypeptide, antigen CD51) (ITGAV), transcript variant 1, mRNA.
8056184	ITGB6	0.29	0.20	0.75	0.56	0.81	0.68	0.78	0.69	integrin, beta 6 (ITGB6), mRNA.
7961900	ITPR2	0.29	0.12	0.56	0.38	1.23	0.48	0.77	0.57	inositol 1,4,5-triphosphate receptor, type 2 (ITPR2), mRNA.

8050719	ITSN2	0.37	0.34	0.94	1.08	1.15	0.93	1.03	0.82	intersectin 2 (ITSN2), transcript variant 1, mRNA.
7933877	JMJD1C	0.39	0.11	1.17	1.06	1.05	0.45	1.08	0.86	jumonji domain containing 1C (JMJD1C), transcript variant 2, mRNA.
8106516	JMY	0.32	0.23	1.00	0.87	0.84	0.63	1.11	0.68	junction mediating and regulatory protein, p53 cofactor (JMY), mRNA.
7970844	KATNAL1	0.39	0.35	0.71	0.83	0.92	0.86	0.69	0.51	katanin p60 subunit A-like 1 (KATNAL1), transcript variant 2, mRNA.
7909745	KCTD3	0.42	0.46	1.00	0.83	0.91	0.84	0.77	0.69	potassium channel tetramerisation domain containing 3 (KCTD3), mRNA.
8159854	KIAA0020	0.39	0.43	0.97	1.10	1.30	0.82	0.58	0.80	KIAA0020 (KIAA0020), mRNA.
8093961	KIAA0232	0.49	0.45	0.93	1.11	0.94	1.09	1.18	1.00	KIAA0232 (KIAA0232), transcript variant 1, mRNA.
7961767	KIAA0528	0.33	0.30	1.07	0.86	0.85	0.61	1.25	0.69	cDNA FLJ60272 complete cds.
7974653	KIAA0586	0.27	0.24	1.07	0.93	0.74	0.66	0.93	0.67	KIAA0586 (KIAA0586), mRNA.
8121161	KIAA0776	0.21	0.13	1.06	0.89	0.83	0.79	0.95	0.84	KIAA0776 (KIAA0776), mRNA.
8104350	KIAA0947	0.36	0.19	1.19	0.98	1.22	1.22	1.21	1.09	KIAA0947 (KIAA0947), mRNA.
8022767	KIAA1012	0.23	0.18	0.79	0.89	0.87	0.88	0.82	0.78	KIAA1012 (KIAA1012), mRNA.
7958216	KIAA1033	0.35	0.22	1.10	0.96	1.34	0.74	1.28	1.03	KIAA1033 (KIAA1033), mRNA.
8097148	KIAA1109	0.24	0.09	0.68	0.61	0.93	0.34	0.89	0.62	KIAA1109 (KIAA1109), mRNA.
7988970	KIAA1370	0.31	0.16	0.98	1.04	0.83	0.81	1.06	0.94	KIAA1370 (KIAA1370), mRNA.
8151842	KIAA1429	0.30	0.34	0.89	0.78	0.93	0.96	0.90	0.89	KIAA1429 (KIAA1429), transcript variant 1, mRNA.
8103979	KIAA1430	0.35	0.27	0.84	0.84	0.85	0.76	0.80	0.72	KIAA1430 (KIAA1430), mRNA.
8021496	KIAA1468	0.45	0.44	1.07	1.02	1.14	1.03	1.30	1.09	KIAA1468 (KIAA1468), mRNA.
8056943	KIAA1715	0.35	0.35	0.68	0.76	0.93	1.00	0.68	0.68	KIAA1715 (KIAA1715), mRNA.
8089647	KIAA2018	0.24	0.18	1.01	1.15	0.82	0.90	1.18	1.05	KIAA2018 (KIAA2018), mRNA.
8160011	KIAA2026	0.15	0.11	0.99	1.13	0.98	0.66	1.16	0.82	KIAA2026 (KIAA2026), mRNA.
8050128	KIDINS220	0.31	0.25	0.89	0.99	0.94	1.02	1.00	0.99	kinase D-interacting substrate, 220kDa (KIDINS220), mRNA.
7962274	KIF21A	0.30	0.14	0.95	1.33	0.95	0.93	0.72	0.77	kinesin family member 21A (KIF21A), transcript variant 1, mRNA.
8105523	KIF2A	0.33	0.36	1.05	1.14	1.40	1.51	1.51	1.72	kinesin heavy chain member 2A (KIF2A), transcript variant 1, mRNA.
7932911	KIF5B	0.22	0.17	0.92	0.98	1.04	0.95	0.94	0.97	kinesin family member 5B (KIF5B), mRNA.
8084219	KLHL24	0.39	0.29	0.92	0.74	0.74	0.57	0.98	0.72	kelch-like 24 (Drosophila) (KLHL24), mRNA.
7978760	KLHL28	0.49	0.44	1.10	1.45	1.23	1.14	1.28	0.86	kelch-like 28 (Drosophila) (KLHL28), mRNA.
7971620	KPNA3	0.31	0.36	0.86	0.90	0.93	0.90	0.89	0.91	karyopherin alpha 3 (importin alpha 4) (KPNA3), mRNA.
8140878	KRIT1	0.39	0.41	1.06	1.10	0.97	0.80	1.08	0.85	KRIT1, ankyrin repeat containing (KRIT1), transcript variant 4, mRNA.
7974483	KTN1	0.32	0.11	1.05	1.01	1.19	0.54	0.95	1.08	kinectin 1 (kinesin receptor) (KTN1), transcript variant 1, mRNA.
7955361	LARP4	0.37	0.27	1.12	1.03	1.28	1.20	1.33	1.37	La ribonucleoprotein domain family, member 4 (LARP4), transcript variant 1, mRNA.
8114861	LARS	0.33	0.49	0.84	0.74	0.83	0.69	0.69	0.48	leucyl-tRNA synthetase (LARS), mRNA.
7929596	LCOR	0.27	0.34	1.09	1.35	1.05	1.04	1.01	1.14	ligand dependent nuclear receptor corepressor (LCOR), transcript variant 1, mRNA.
7988838	LEO1	0.46	0.28	1.39	1.11	0.95	0.96	1.07	1.18	Leo1, Paf1/RNA polymerase II complex component, homolog (S. cerevisiae) (LEO1), mRNA.
7972737	LIG4	0.33	0.19	0.95	1.38	1.25	0.88	1.10	1.21	ligase IV, DNA, ATP-dependent (LIG4), transcript variant 1, mRNA.
7965156	LIN7A	0.48	0.38	0.80	0.86	0.73	0.61	0.70	0.58	lin-7 homolog A (C. elegans) (LIN7A), mRNA.
7947221	LIN7C	0.32	0.28	0.94	0.88	0.98	0.91	0.88	0.75	lin-7 homolog C (C. elegans) (LIN7C), mRNA.
8023561	LMAN1	0.41	0.38	0.84	0.85	0.94	0.89	0.91	1.13	lectin, mannose-binding, 1 (LMAN1), mRNA.
8111533	LMBRD2	0.30	0.23	0.86	0.72	0.81	0.72	0.70	0.71	LMBR1 domain containing 2 (LMBRD2), mRNA.
8085033	LMLN	0.27	0.37	0.90	0.80	0.74	0.76	1.00	0.85	leishmanolysin-like (metallopeptidase M8 family) (LMLN), transcript variant 1, mRNA.
7995697	LPCAT2	0.39	0.27	0.86	0.37	0.69	0.56	1.46	0.51	lysophosphatidylcholine acyltransferase 2 (LPCAT2), mRNA.
7902565	LPHN2	0.23	0.25	0.85	0.71	0.62	0.66	0.63	0.52	latrophilin 2 (LPHN2), mRNA.
8084742	LPP	0.47	0.34	0.74	0.65	1.22	0.83	1.19	0.79	LIM domain containing preferred translocation partner in lipoma (LPP), transcript variant 1, mRNA.
7961339	LRP6	0.44	0.33	0.79	1.14	0.75	0.83	0.76	0.68	low density lipoprotein receptor-related protein 6 (LRP6), mRNA.
8051882	LRPPRC	0.20	0.21	0.87	0.79	0.86	0.93	0.58	0.66	leucine-rich PPR-motif containing (LRPPRC), mRNA.
7916910	LRRC40	0.26	0.23	0.99	0.78	1.03	0.72	0.81	0.61	leucine rich repeat containing 40 (LRRC40), mRNA.
8089830	LRRC58	0.21	0.22	1.02	0.96	0.73	0.84	0.80	0.55	leucine rich repeat containing 58 (LRRC58), mRNA.
8122440	LTV1	0.33	0.40	1.07	0.92	1.01	0.91	0.69	0.58	LTV1 homolog (S. cerevisiae) (LTV1), mRNA.
8113064	LYSMD3	0.18	0.21	0.92	1.16	1.02	1.13	0.90	0.96	LysM, putative peptidoglycan-binding, domain containing 3 (LYSMD3), mRNA.
7925257	LYST	0.24	0.20	1.14	1.12	0.78	0.51	0.86	0.70	lysosomal trafficking regulator (LYST), mRNA.
7904340	MAN1A2	0.38	0.33	0.85	1.16	1.11	1.25	0.79	0.80	mannosidase, alpha, class 1A, member 2 (MAN1A2), mRNA.
8107234	MAN2A1	0.31	0.35	0.83	1.01	1.10	1.06	1.01	0.99	mannosidase, alpha, class 2A, member 1 (MAN2A1), mRNA.
8121144	MANEA	0.23	0.17	0.96	0.95	0.85	0.66	1.10	0.86	mannosidase, endo-alpha (MANEA), mRNA.
8106098	MAP1B	0.29	0.45	0.83	1.84	0.78	1.63	0.75	1.12	microtubule-associated protein 1B (MAP1B), mRNA.
8105436	MAP3K1	0.30	0.48	1.32	1.73	0.79	1.21	1.00	1.09	mitogen-activated protein kinase kinase kinase 1 (MAP3K1), mRNA.
8054997	MAP3K2	0.17	0.20	1.04	1.02	0.82	0.82	1.02	0.81	mitogen-activated protein kinase kinase kinase 2 (MAP3K2), mRNA.
8051707	MAP4K3	0.40	0.35	1.16	1.49	0.66	0.82	1.02	0.97	mitogen-activated protein kinase kinase kinase kinase 3 (MAP4K3), mRNA.
7978997	MAP4K5	0.33	0.47	1.06	1.42	1.11	1.38	1.00	1.15	mitogen-activated protein kinase kinase kinase kinase 5 (MAP4K5), transcript variant 2, mRNA.
8175369	MAP7D3	0.28	0.30	0.97	0.82	0.79	0.90	0.67	0.60	MAP7 domain containing 3 (MAP7D3), transcript variant 1, mRNA.
7983763	MAPK6	0.21	0.26	0.89	0.71	0.90	0.80	1.04	0.80	mitogen-activated protein kinase 6 (MAPK6), mRNA.
8108403	MATR3	0.40	0.31	1.09	0.95	1.06	0.79	0.89	0.88	matrin 3 (MATR3), transcript variant 1, mRNA.
8083429	MBNL1	0.34	0.27	0.94	1.01	0.99	0.73	0.86	0.61	muscleblind-like (Drosophila) (MBNL1), transcript variant 1, mRNA.
7969677	MBNL2	0.34	0.18	1.06	0.94	0.75	0.59	0.82	0.71	muscleblind-like 2 (Drosophila) (MBNL2), transcript variant 1, mRNA.
8175177	MBNL3	0.50	0.23	0.63	0.40	0.81	0.49	0.83	0.88	muscleblind-like 3 (Drosophila) (MBNL3), transcript variant 1, mRNA.
8060813	MCM8	0.26	0.35	0.91	0.69	0.79	0.71	0.74	0.52	minichromosome maintenance complex component 8 (MCM8), transcript variant 1, mRNA.
7956989	MDM2	0.39	0.37	1.05	0.76	0.86	0.64	1.06	0.72	Mdm2 p53 binding protein homolog (mouse) (MDM2), transcript variant MDM2, mRNA.
8017312	MED13	0.40	0.40	1.22	1.41	1.31	1.12	1.24	1.18	mediator complex subunit 13 (MED13), mRNA.
8129522	MED23	0.36	0.46	1.08	1.05	0.99	0.96	1.08	1.02	mediator complex subunit 23 (MED23), transcript variant 1, mRNA.
8097066	METTL14	0.39	0.32	1.54	1.23	1.02	0.94	1.19	0.88	methyltransferase like 14 (METTL14), mRNA.
8109403	MFAP3	0.28	0.37	0.92	0.87	0.79	0.94	0.83	0.82	microfibrillar-associated protein 3 (MFAP3), transcript variant 3, non-coding RNA.
8103695	MFAP3L	0.49	0.45	0.95	0.94	0.93	0.92	0.66	0.71	microfibrillar-associated protein 3-like (MFAP3L), transcript variant 1, mRNA.
7982957	MGA	0.35	0.26	1.24	1.08	1.08	0.77	1.17	0.85	MAX gene associated (MGA), transcript variant 1, mRNA.
8054135	MGAT4A	0.23	0.27	0.94	0.77	0.74	0.75	1.17	1.32	mannosyl (alpha-1,3-)-glycoprotein beta-1,4-N-acetylglucosaminyltransferase, isozyme A (MGAT4A), transcript va
7909898	MIA3	0.43	0.41	1.14	1.41	0.95	0.89	1.20	1.45	melanoma inhibitory activity family, member 3 (MIA3), mRNA.
8020423	MIB1	0.39	0.35	0.73	0.77	1.06	0.84	0.60	0.58	mindbomb homolog 1 (Drosophila) (MIB1), mRNA.
7902166	MIER1	0.46	0.48	1.38	1.58	1.69	1.13	1.65	1.65	mesoderm induction early response 1 homolog (Xenopus laevis) (MIER1), transcript variant 1, mRNA.
8112182	MIER3	0.40	0.31	1.39	1.49	1.19	1.13	1.39	1.31	mesoderm induction early response 1, family member 3 (MIER3), mRNA.
8131479	MIOS	0.21	0.29	0.91	0.60	0.67	0.53	0.61	0.34	missing oocyte, meiosis regulator, homolog (Drosophila) (MIOS), mRNA.
7993310	MKL2	0.37	0.42	1.02	1.11	0.86	1.08	1.05	1.17	MKL/myocardin-like 2 (MKL2), mRNA.
7980246	MLH3	0.42	0.30	1.10	0.98	1.04	0.59	1.20	0.85	mutL homolog 3 (E. coli) (MLH3), transcript variant 1, mRNA.
8143988	MLL3	0.34	0.32	0.94	1.11	0.97	0.88	1.02	0.95	myeloid/lymphoid or mixed-lineage leukemia 3 (MLL3), mRNA.
8135277	MLL5	0.25	0.22	1.24	1.22	0.97	0.91	1.12	1.04	myeloid/lymphoid or mixed-lineage leukemia 5 (trithorax homolog, Drosophila) (MLL5), transcript variant 1, mRN
8095566	MOBKL1A	0.47	0.26	0.87	0.90	1.25	0.77	1.08	0.71	MOB1, Mps One Binder kinase activator-like 1A (yeast) (MOBKL1A), mRNA.
8047228	MOBKL3	0.24	0.42	1.07	1.07	0.90	1.07	0.91	1.09	MOB1, Mps One Binder kinase activator-like 3 (yeast) (MOBKL3), transcript variant 2, mRNA.
7956697	MON2	0.37	0.39	0.91	0.98	1.15	0.95	1.08	0.87	MON2 homolog (S. cerevisiae) (MON2), mRNA.
8166140	MOSPD2	0.24	0.19	1.05	1.09	1.14	0.93	1.19	1.19	motile sperm domain containing 2 (MOSPD2), transcript variant 1, mRNA.
8160088	MPDZ	0.26	0.15	0.85	0.62	0.81	0.46	0.84	0.49	multiple PDZ domain protein (MPDZ), mRNA.
8042588	MPHOSPH10	0.37	0.45	1.08	0.97	0.82	0.84	0.63	0.77	M-phase phosphoprotein 10 (U3 small nucleolar ribonucleoprotein) (MPHOSPH10), mRNA.
7967386	MPHOSPH9	0.29	0.18	1.13	0.95	0.84	0.67	1.10	0.78	M-phase phosphoprotein 9 (MPHOSPH9), mRNA.
7975203	MPP5	0.42	0.43	0.91	0.94	1.21	1.27	0.93	0.93	membrane protein, palmitoylated 5 (MAGUK p55 subfamily member 5) (MPP5), mRNA.
8106633	MSH3	0.48	0.38	0.95	0.99	1.08	0.98	0.97	0.86	mutS homolog 3 (E. coli) (MSH3), mRNA.
8149448	MSR1	0.47	0.06	1.04	0.06	0.63	0.07	1.20	0.06	macrophage scavenger receptor 1 (MSR1), transcript variant SR-AII, mRNA.
8169949	MST4	0.38	0.49	0.86	0.91	0.85	0.94	0.66	0.66	serine/threonine protein kinase MST4 (MST4), transcript variant 1, mRNA.
8052250	MTIF2	0.42	0.36	0.92	0.75	1.09	0.84	0.83	0.66	mitochondrial translational initiation factor 2 (MTIF2), nuclear gene encoding mitochondrial protein, transcript var
8170428	MTM1	0.35	0.41	0.90	1.10	0.83	0.98	1.14	0.88	myotubularin 1 (MTM1), mRNA.
7970655	MTMR6	0.33	0.32	0.91	0.99	0.96	0.86	0.81	0.74	myotubularin related protein 6 (MTMR6), mRNA.
7974566	MUDENG	0.43	0.45	1.02	0.96	0.82	0.84	1.09	0.96	MU-2/AP1M2 domain containing, death-inducing (MUDENG), transcript variant 1, mRNA.
8126860	MUT	0.45	0.46	0.83	0.79	1.18	1.01	0.94	0.91	methylmalonyl Coenzyme A mutase (MUT), nuclear gene encoding mitochondrial protein, mRNA.
7972069	MYCBP2	0.36	0.21	0.90	0.73	1.35	0.75	1.19	0.94	MYC binding protein 2 (MYCBP2), mRNA.
7988921	MYO5A	0.37	0.28	0.74	0.50	1.04	0.84	0.82	0.56	myosin VA (heavy chain 12, myoxin) (MYO5A), transcript variant 1, mRNA.
8120783	MYO6	0.39	0.40	0.90	1.05	1.28	1.14	1.34	1.13	myosin VI (MYO6), mRNA.
7916592	MYSM1	0.22	0.12	1.14	0.81	0.85	0.51	0.96	0.52	Myb-like, SWIRM and MPN domains 1 (MYSM1), mRNA.
8150491	MYST3	0.36	0.39	1.24	1.17	1.04	0.95	1.10	0.92	MYST histone acetyltransferase (monocytic leukemia) 3 (MYST3), transcript variant 1, mRNA.
7928491	MYST4	0.41	0.31	0.99	0.99	0.77	0.68	1.17	0.89	MYST histone acetyltransferase (monocytic leukemia) 4 (MYST4), mRNA.
7970907	N4BP2L2	0.44	0.31	0.97	0.87	1.06	0.55	1.11	0.55	NEDD4 binding protein 2-like 2 (N4BP2L2), transcript variant 2, mRNA.
8161556	–	0.30	0.15	0.50	0.14	0.53	0.18	1.09	0.14	cdna:pseudogene chromosome:GRCh37:2:95403082:95403994:1 gene:ENSG00000213355
8176253	–	0.25	0.14	0.61	0.61	0.59	0.31	0.75	0.60	cDNA FLJ40916 fis, clone UTERU2005533.
8083445	–	0.14	0.13	1.14	0.92	0.68	0.26	1.18	0.37	ncrna:misc_RNA chromosome:GRCh37:3:152167061:152167173:1 gene:ENSG00000201217
7957549	–	0.33	0.23	0.47	0.56	0.71	0.79	0.52	0.51	cDNA FLJ37555 fis, clone BRCAN2028460.
8171024	–	0.22	0.13	0.63	0.63	0.73	0.30	0.97	0.75	cDNA FLJ45551 fis, clone BRTHA2037247.
8092081	–	0.19	0.10	0.79	0.69	0.78	0.48	0.76	0.69	ncrna:snRNA chromosome:GRCh37:3:170712659:170712822:-1 gene:ENSG00000199488
8063444	–	0.45	0.27	1.03	0.59	0.79	0.48	1.14	0.67	Teashirt homolog 2 gene:ENSG00000182463
8054557	–	0.24	0.18	0.90	0.91	0.84	0.66	0.82	0.78	RANBP2-like and GRIP domain containing 5 (RGPD5), transcript variant 2, mRNA.
8054532	–	0.23	0.17	0.88	0.98	0.87	0.64	0.82	0.82	RANBP2-like and GRIP domain containing 5 (RGPD5), transcript variant 1, mRNA.
7927799	–	0.45	0.43	0.94	0.99	0.97	1.05	1.04	0.99	receptor accessory protein 3 (REEP3), mRNA.
8041170	–	0.43	0.22	0.81	0.68	0.98	0.46	0.79	0.38	ncrna:snoRNA chromosome:GRCh37:2:29150849:29150926:1 gene:ENSG00000212326
7933593	–	0.31	0.40	0.81	0.99	1.07	0.64	1.32	0.59	ncrna:snoRNA chromosome:GRCh37:10:51383526:51383726:1 gene:ENSG00000223182
7947989	–	0.35	0.34	0.89	0.89	1.07	0.76	1.47	0.71	ncrna:misc_RNA chromosome:GRCh37:11:47748446:47748544:-1 gene:ENSG00000200090

8149248	–	0.43	0.24	0.54	0.35	1.34	0.23	1.18	0.22	liver-related low express protein 1 (LRLE1) mRNA, complete cds.
8145766	–	0.25	0.14	1.06	0.33	2.22	0.61	1.44	1.07	MSTP131 gene:ENSG00000227478
7939374	–	0.41	0.29	0.88	0.90	2.60	0.55	2.32	0.43	PNAS-17 mRNA, complete cds.
8126093	–	0.35	0.45	0.75	1.14	2.68	1.48	2.30	1.96	ncrna:snoRNA chromosome:GRCh37:6:37218980:37219082:-1 gene:ENSG00000238375
8097480	NAA15	0.21	0.20	0.80	0.91	1.12	1.14	0.79	0.89	N(alpha)-acetyltransferase 15, NatA auxiliary subunit (NAA15), mRNA.
7966462	NAA25	0.37	0.35	1.19	1.14	1.39	1.34	1.07	0.98	N(alpha)-acetyltransferase 25, NatB auxiliary subunit (NAA25), mRNA.
8112478	NAIP	0.37	0.27	1.21	0.69	1.08	0.45	1.25	0.46	NLR family, apoptosis inhibitory protein (NAIP), transcript variant 1, mRNA.
8141872	NAPEPLD	0.46	0.41	1.18	1.23	1.11	0.98	2.83	1.71	N-acyl phosphatidylethanolamine phospholipase D (NAPEPLD), transcript variant 1, mRNA.
7989347	NARG2	0.23	0.20	1.03	1.02	1.01	0.95	0.97	0.82	NMDA receptor regulated 2 (NARG2), transcript variant 1, mRNA.
8047606	NBEAL1	0.23	0.07	0.67	0.83	0.99	0.41	0.86	0.76	neurobeachin-like 1 (NBEAL1), mRNA.
8151711	NBN	0.27	0.29	1.25	1.27	1.32	0.97	1.27	1.26	nibrin (NBN), mRNA.
8082911	NCK1	0.42	0.44	1.34	1.23	0.81	0.80	1.02	1.03	NCK adaptor protein 1 (NCK1), mRNA.
8057517	NCKAP1	0.30	0.37	0.84	0.86	1.01	0.95	0.89	1.01	NCK-associated protein 1 (NCKAP1), transcript variant 1, mRNA.
8040552	NCOA1	0.47	0.46	1.00	0.82	0.91	0.88	1.02	0.85	nuclear receptor coactivator 1 (NCOA1), transcript variant 2, mRNA.
8151254	NCOA2	0.49	0.36	1.24	1.18	0.99	0.86	1.29	1.01	nuclear receptor coactivator 2 (NCOA2), mRNA.
8012961	NCOR1	0.44	0.50	1.11	1.12	0.99	0.94	1.25	1.06	nuclear receptor co-repressor 1 (NCOR1), mRNA.
7957715	NEDD1	0.39	0.48	1.10	1.43	1.61	1.13	1.25	1.11	neural precursor cell expressed, developmentally down-regulated 1 (NEDD1), transcript variant 1, mRNA.
7989094	NEDD4	0.22	0.24	0.87	1.00	0.75	0.87	0.76	0.79	neural precursor cell expressed, developmentally down-regulated 4 (NEDD4), transcript variant 1, mRNA.
7908543	NEK7	0.39	0.50	1.03	1.49	1.22	1.31	1.01	1.23	NIMA (never in mitosis gene a)-related kinase 7 (NEK7), mRNA.
8006239	NF1	0.29	0.27	0.92	0.87	0.97	0.87	0.97	0.76	neurofibromin 1 (NF1), transcript variant 1, mRNA.
7996954	NFAT5	0.35	0.33	1.10	1.17	1.35	0.96	1.24	1.04	nuclear factor of activated T-cells 5, tonicity-responsive (NFAT5), transcript variant 1, mRNA.
8056977	NFE2L2	0.35	0.42	1.20	1.42	1.16	1.35	1.07	1.45	nuclear factor (erythroid-derived 2)-like 2 (NFE2L2), transcript variant 1, mRNA.
7901788	NFIA	0.41	0.25	0.85	0.77	0.55	0.53	0.82	0.57	nuclear factor I/A (NFIA), transcript variant 1, mRNA.
8160138	NFIB	0.42	0.44	0.93	1.06	0.73	0.78	0.84	0.67	nuclear factor I/B (NFIB), mRNA.
8100179	NFXL1	0.36	0.44	1.04	1.18	1.05	0.83	0.89	0.66	nuclear transcription factor, X-box binding-like 1 (NFXL1), mRNA.
7930614	NHLRC2	0.29	0.29	1.01	1.04	0.93	0.93	0.84	0.72	NHL repeat containing 2 (NHLRC2), mRNA.
8104944	NIPBL	0.26	0.18	1.08	1.18	1.01	0.55	1.06	0.89	Nipped-B homolog (Drosophila) (NIPBL), transcript variant B, mRNA.
8079079	NKTR	0.42	0.18	1.06	0.91	1.22	0.69	1.15	0.77	natural killer-tumor recognition sequence (NKTR), mRNA.
8083757	NMD3	0.23	0.21	1.04	1.03	0.72	0.81	0.60	0.67	NMD3 homolog (S. cerevisiae) (NMD3), mRNA.
7935146	NOC3L	0.29	0.24	1.35	1.14	1.04	0.93	0.71	0.82	nucleolar complex associated 3 homolog (S. cerevisiae) (NOC3L), mRNA.
8162352	NOL8	0.22	0.17	1.21	1.15	0.82	0.64	0.94	0.84	nucleolar protein 8 (NOL8), transcript variant 2, non-coding RNA.
8047518	NOP58	0.27	0.33	1.04	1.05	0.91	0.97	0.81	0.71	NOP58 ribonucleoprotein homolog (yeast) (NOP58), mRNA.
7951497	NPAT	0.28	0.19	1.21	1.08	0.83	0.43	1.20	0.68	nuclear protein, ataxia-telangiectasia locus (NPAT), mRNA.
8078272	NR1D2	0.43	0.46	1.23	1.19	1.16	1.08	1.22	1.08	nuclear receptor subfamily 1, group D, member 2 (NR1D2), transcript variant 1, mRNA.
8069553	NRIP1	0.28	0.15	1.32	0.85	1.29	0.78	1.32	0.77	nuclear receptor interacting protein 1 (NRIP1), mRNA.
7938687	NUCB2	0.44	0.37	1.05	1.44	1.10	1.10	1.22	1.87	nucleobindin 2 (NUCB2), mRNA.
8113413	NUDT12	0.40	0.37	0.97	0.88	0.72	0.78	0.77	0.93	nudix (nucleoside diphosphate linked moiety X)-type motif 12 (NUDT12), mRNA.
8013908	NUFIP2	0.29	0.33	1.02	1.17	1.08	0.99	0.89	0.90	nuclear fragile X mental retardation protein interacting protein 2 (NUFIP2), mRNA.
8046804	NUP35	0.48	0.45	1.15	0.80	1.08	0.76	0.76	0.53	nucleoporin 35kDa (NUP35), mRNA.
7916570	OMA1	0.38	0.37	0.83	0.46	0.72	0.44	0.72	0.42	OMA1 homolog, zinc metallopeptidase (S. cerevisiae) (OMA1), mRNA.
8084844	OPA1	0.30	0.21	0.80	0.81	1.01	0.84	0.66	0.69	optic atrophy 1 (autosomal dominant) (OPA1), nuclear gene encoding mitochondrial protein, transcript variant 8,
8121043	ORC3L	0.35	0.35	1.15	1.12	1.02	0.94	1.01	0.94	origin recognition complex, subunit 3-like (yeast) (ORC3L), transcript variant 1, mRNA.
8055645	ORC4L	0.42	0.47	1.12	1.04	1.08	0.85	0.91	1.00	origin recognition complex, subunit 4-like (yeast) (ORC4L), transcript variant 2, mRNA.
8090277	OSBPL11	0.29	0.42	0.98	0.79	0.80	0.82	1.22	0.94	oxysterol binding protein-like 11 (OSBPL11), mRNA.
7965064	OSBPL8	0.14	0.14	0.79	0.89	0.88	0.68	0.78	0.78	oxysterol binding protein-like 8 (OSBPL8), transcript variant 1, mRNA.
7901385	OSBPL9	0.35	0.38	1.06	1.00	0.83	0.86	0.89	0.83	oxysterol binding protein-like 9 (OSBPL9), transcript variant 6, mRNA.
8147262	OTUD6B	0.25	0.21	1.12	1.44	0.75	0.61	0.90	0.73	OTU domain containing 6B (OTUD6B), mRNA.
8116848	PAK1IP1	0.39	0.43	1.16	1.05	0.86	0.91	0.62	0.56	PAK1 interacting protein 1 (PAK1IP1), mRNA.
8000329	PALB2	0.44	0.41	1.19	1.08	0.90	0.88	1.21	0.90	partner and localizer of BRCA2 (PALB2), mRNA.
7976598	PAPOLA	0.25	0.29	0.86	0.77	0.84	0.92	0.95	0.95	poly(A) polymerase alpha (PAPOLA), mRNA.
8087951	PBRM1	0.37	0.32	0.91	1.02	1.25	1.14	1.12	1.05	polybromo 1 (PBRM1), transcript variant 1, mRNA.
7942839	PCF11	0.44	0.35	0.97	0.95	1.12	0.83	0.98	0.91	PCF11, cleavage and polyadenylation factor subunit, homolog (S. cerevisiae) (PCF11), mRNA.
8144812	PCM1	0.22	0.10	0.90	0.71	0.95	0.47	1.03	1.03	pericentriolar material 1 (PCM1), mRNA.
8150714	PCMTD1	0.25	0.39	1.03	1.08	0.74	0.82	1.03	1.01	protein-L-isoaspartate (D-aspartate) O-methyltransferase domain containing 1 (PCMTD1), mRNA.
8099926	PDS5A	0.28	0.23	1.01	0.89	0.97	0.82	0.92	0.80	PDS5, regulator of cohesion maintenance, homolog A (S. cerevisiae) (PDS5A), transcript variant 1, mRNA.
7936559	PDZD8	0.39	0.41	0.91	0.94	0.85	0.99	0.77	0.74	PDZ domain containing 8 (PDZD8), mRNA.
8140915	PEX1	0.33	0.40	0.82	0.78	0.77	0.77	0.90	0.79	peroxisomal biogenesis factor 1 (PEX1), mRNA.
8148358	PHF20L1	0.32	0.32	0.90	1.08	0.96	0.99	0.91	0.83	PHD finger protein 20-like 1 (PHF20L1), transcript variant 1, mRNA.
8120441	PHF3	0.20	0.07	0.99	0.86	0.80	0.43	1.03	0.68	PHD finger protein 3 (PHF3), mRNA.
8169969	PHF6	0.36	0.25	0.98	1.05	0.79	0.74	0.86	0.82	PHD finger protein 6 (PHF6), transcript variant 2, mRNA.
8127698	PHIP	0.27	0.15	0.91	0.82	1.11	0.47	0.93	0.52	pleckstrin homology domain interacting protein (PHIP), mRNA.
7995382	PHKB	0.31	0.47	0.76	0.63	0.83	0.73	0.96	0.71	phosphorylase kinase, beta (PHKB), transcript variant 2, mRNA.
8081590	PHLDB2	0.50	0.31	1.05	1.24	1.36	0.97	1.03	0.99	pleckstrin homology-like domain, family B, member 2 (PHLDB2), transcript variant 2, mRNA.
8023133	PIAS2	0.44	0.48	0.90	0.84	0.90	0.83	1.07	0.86	protein inhibitor of activated STAT, 2 (PIAS2), transcript variant beta, mRNA.
7946815	PIK3C2A	0.13	0.07	0.92	0.97	0.85	0.49	1.01	0.90	phosphoinositide-3-kinase, class 2, alpha polypeptide (PIK3C2A), mRNA.
7954208	PIK3C2G	0.40	0.18	0.90	0.90	0.88	0.38	1.26	0.84	phosphoinositide-3-kinase, class 2, gamma polypeptide (PIK3C2G), mRNA.
8084016	PIK3CA	0.20	0.17	1.03	1.11	1.13	0.91	1.04	1.04	phosphoinositide-3-kinase, catalytic, alpha polypeptide (PIK3CA), mRNA.
8105778	PIK3R1	0.20	0.16	1.12	1.04	0.66	0.78	1.10	1.01	phosphoinositide-3-kinase, regulatory subunit 1 (alpha) (PIK3R1), transcript variant 1, mRNA.
8113469	PJA2	0.25	0.21	0.98	1.21	0.99	1.01	0.95	1.04	praja ring finger 2 (PJA2), mRNA.
7902822	PKN2	0.25	0.22	1.08	1.09	0.99	0.80	1.16	0.92	protein kinase N2 (PKN2), mRNA.
8092134	PLD1	0.44	0.49	1.03	1.31	0.72	0.73	0.60	0.50	phospholipase D1, phosphatidylcholine-specific (PLD1), transcript variant 1, mRNA.
7983502	PLDN	0.29	0.44	0.83	0.78	1.18	0.99	0.68	0.73	pallidin homolog (mouse) (PLDN), mRNA.
7954245	PLEKHA5	0.36	0.40	0.83	1.32	0.96	0.89	0.92	0.92	pleckstrin homology domain containing, family A member 5 (PLEKHA5), transcript variant 1, mRNA.
8083146	PLS1	0.24	0.24	0.91	0.91	1.16	0.93	0.79	0.86	plastin 1 (PLS1), transcript variant 3, mRNA.
8169473	PLS3	0.44	0.47	0.95	0.85	1.16	0.95	1.06	1.26	plastin 3 (PLS3), transcript variant 1, mRNA.
7957570	PLXNC1	0.36	0.44	0.88	1.52	0.47	0.69	1.13	1.14	plexin C1 (PLXNC1), mRNA.
8047038	PMS1	0.48	0.38	1.04	0.88	0.78	0.61	0.78	0.62	PMS1 postmeiotic segregation increased 1 (S. cerevisiae) (PMS1), transcript variant 1, mRNA.
7974066	PNN	0.41	0.32	1.07	0.93	0.88	0.74	0.80	0.68	pinin, desmosome associated protein (PNN), mRNA.
8142307	PNPLA8	0.28	0.30	0.96	1.15	1.22	1.08	0.90	1.05	patatin-like phospholipase domain containing 8 (PNPLA8), mRNA.
8021275	POLI	0.37	0.27	0.86	0.78	0.97	0.71	0.94	0.72	polymerase (DNA directed) iota (POLI), mRNA.
8106303	POLK	0.16	0.10	1.20	1.09	1.04	0.48	0.97	1.01	polymerase (DNA directed) kappa (POLK), mRNA.
8100495	PPAT	0.40	0.27	1.27	0.99	1.01	0.80	0.76	0.67	phosphoribosyl pyrophosphate amidotransferase (PPAT), mRNA.
8130087	PPIL4	0.45	0.43	1.15	0.89	1.18	1.00	0.92	0.96	peptidylprolyl isomerase (cyclophilin)-like 4 (PPIL4), mRNA.
8107164	PPIP5K2	0.17	0.14	0.94	0.71	0.84	0.68	1.07	0.78	diphosphoinositol pentakisphosphate kinase 2 (PPIP5K2), mRNA.
7965123	PPP1R12A	0.25	0.24	0.99	1.05	1.10	0.99	1.35	1.26	protein phosphatase 1, regulatory (inhibitor) subunit 12A (PPP1R12A), transcript variant 2, mRNA.
8082869	PPP2R3A	0.41	0.48	0.83	1.42	1.31	1.77	0.71	0.87	protein phosphatase 2 (formerly 2A), regulatory subunit B'', alpha (PPP2R3A), transcript variant 1, mRNA.
8101971	PPP3CA	0.34	0.50	0.78	0.73	0.92	0.80	0.68	0.65	protein phosphatase 3, catalytic subunit, alpha isozyme (PPP3CA), transcript variant 1, mRNA.
8080973	PPP4R2	0.47	0.28	0.95	1.06	1.25	1.07	0.91	1.01	protein phosphatase 4, regulatory subunit 2 (PPP4R2), mRNA.
8105633	PPWD1	0.32	0.31	0.90	0.95	1.07	0.66	1.11	0.64	peptidylprolyl isomerase domain and WD repeat containing 1 (PPWD1), mRNA.
8051928	PREPL	0.25	0.29	0.71	0.62	0.71	0.78	0.76	0.68	prolyl endopeptidase-like (PREPL), transcript variant 1, mRNA.
8111796	PRKAA1	0.43	0.38	1.07	0.98	0.84	0.94	0.86	0.87	protein kinase, AMP-activated, alpha 1 catalytic subunit (PRKAA1), transcript variant 2, mRNA.
7902594	PRKACB	0.38	0.36	0.89	0.79	1.42	0.86	1.18	0.87	protein kinase, cAMP-dependent, catalytic, beta (PRKACB), transcript variant 1, mRNA.
8150599	PRKDC	0.29	0.38	0.56	0.59	1.00	0.86	0.64	0.55	protein kinase, DNA-activated, catalytic polypeptide (PRKDC), transcript variant 1, mRNA.
7924817	PRO2012	0.29	0.26	0.87	1.15	0.96	0.33	2.07	0.77	hypothetical protein PRO2012, mRNA (cDNA clone IMAGE:4995736).
7909681	PROX1	0.39	0.29	1.16	1.08	0.73	0.69	1.21	1.16	prospero homeobox 1 (PROX1), mRNA.
7903519	PRPF38B	0.46	0.42	0.91	1.00	0.92	1.08	0.81	0.69	PRP38 pre-mRNA processing factor 38 (yeast) domain containing B (PRPF38B), mRNA.
8055913	PRPF40A	0.24	0.24	1.14	1.14	1.08	0.96	0.96	0.94	PRP40 pre-mRNA processing factor 40 homolog A (S. cerevisiae) (PRPF40A), mRNA.
8116664	PRPF4B	0.41	0.24	1.34	1.24	1.11	0.95	1.12	1.10	PRP4 pre-mRNA processing factor 4 homolog B (yeast) (PRPF4B), mRNA.
8149551	PSD3	0.19	0.12	0.57	0.76	0.70	0.75	0.57	0.55	pleckstrin and Sec7 domain containing 3 (PSD3), transcript variant 1, mRNA.
8161632	PTAR1	0.27	0.34	1.10	1.23	0.99	0.99	1.10	0.92	protein prenyltransferase alpha subunit repeat containing 1 (PTAR1), mRNA.
7903188	PTBP2	0.48	0.36	0.91	0.73	1.43	0.55	1.11	0.44	polypyrimidine tract binding protein 2 (PTBP2), mRNA.
7926356	PTER	0.35	0.34	0.84	0.74	1.18	0.86	1.13	1.29	phosphotriesterase related (PTER), transcript variant 1, mRNA.
7958846	PTPN11	0.37	0.40	0.62	0.54	0.90	0.88	0.58	0.54	protein tyrosine phosphatase, non-receptor type 11 (PTPN11), mRNA.
8133788	PTPN12	0.40	0.43	1.04	1.04	0.81	0.87	0.91	1.01	protein tyrosine phosphatase, non-receptor type 12 (PTPN12), transcript variant 1, mRNA.
8160040	PTPRD	0.46	0.26	0.75	0.46	0.70	0.42	0.94	0.44	protein tyrosine phosphatase, receptor type, D (PTPRD), transcript variant 1, mRNA.
8050565	PUM2	0.36	0.41	1.16	1.00	0.96	0.97	1.03	0.88	pumilio homolog 2 (Drosophila) (PUM2), mRNA.
8052418	PUS10	0.29	0.33	1.21	1.44	0.52	0.75	1.20	0.86	pseudouridylate synthase 10 (PUS10), mRNA.
8081548	PVRL3	0.41	0.39	0.86	0.88	0.82	0.74	0.79	0.72	poliovirus receptor-related 3 (PVRL3), mRNA.
7954382	PYROXD1	0.30	0.31	0.84	1.17	0.94	1.04	0.69	0.95	pyridine nucleotide-disulphide oxidoreductase domain 1 (PYROXD1), mRNA.
7939158	QSER1	0.20	0.22	0.80	0.81	1.06	0.79	0.97	0.74	glutamine and serine rich 1 (QSER1), mRNA.
7936567	RAB11FIP2	0.25	0.21	1.18	1.28	1.01	0.88	0.92	0.55	RAB11 family interacting protein 2 (class I) (RAB11FIP2), mRNA.
7950743	RAB30	0.38	0.47	0.99	1.42	0.51	0.67	0.86	0.86	RAB30, member RAS oncogene family (RAB30), mRNA.
7924405	RAB3GAP2	0.38	0.34	1.05	1.04	1.01	1.05	0.96	1.11	RAB3 GTPase activating protein subunit 2 (non-catalytic) (RAB3GAP2), mRNA.
8004111	RABEP1	0.29	0.28	0.94	0.81	1.01	0.81	0.88	0.68	rabaptin, RAB GTPase binding effector protein 1 (RABEP1), transcript variant 1, mRNA.
8177478	RAD17	0.29	0.39	1.22	1.19	0.71	0.87	0.84	0.96	RAD17 homolog (S. pombe) (RAD17), transcript variant 1, mRNA.
8085145	RAD18	0.41	0.45	0.86	0.92	1.02	0.94	0.94	0.73	RAD18 homolog (S. cerevisiae) (RAD18), mRNA.
8152477	RAD21	0.40	0.37	1.15	1.07	1.14	1.04	1.06	1.10	RAD21 homolog (S. pombe) (RAD21), mRNA.
8107942	RAD50	0.20	0.09	1.11	0.95	1.03	0.53	0.97	0.72	RAD50 homolog (S. cerevisiae) (RAD50), mRNA.

8104788	RAI14	0.40	0.46	1.11	1.40	1.09	1.09	0.76	0.77	retinoic acid induced 14 (RAI14), transcript variant 6, mRNA.
8180364	RALGAPA1	0.27	0.18	1.03	0.91	0.91	0.64	1.04	0.67	GTPase activating Rap/RanGAP domain-like 1 (GARNL1), transcript variant 1, mRNA
8180365	RALGAPA1	0.27	0.18	1.03	0.91	0.91	0.64	1.04	0.67	GTPase activating Rap/RanGAP domain-like 1 (GARNL1), transcript variant 2, mRNA
7978653	RALGAPA1	0.46	0.33	1.26	0.86	1.03	0.78	1.70	0.92	Ral GTPase activating protein, alpha subunit 1 (catalytic) (RALGAPA1), transcript variant 1, mRNA.
7907657	RALGPS2	0.39	0.43	0.90	0.97	0.93	1.19	1.24	1.29	Ral GEF with PH domain and SH3 binding motif 2 (RALGPS2), mRNA.
8044263	RANBP2	0.27	0.13	0.96	0.84	0.80	0.43	0.87	0.69	RAN binding protein 2 (RANBP2), mRNA.
8160016	RANBP6	0.23	0.23	1.10	1.10	1.36	1.19	0.73	0.82	RAN binding protein 6 (RANBP6), transcript variant 1, mRNA.
7969693	RAP2A	0.29	0.46	0.68	0.82	1.10	0.99	0.84	0.94	RAP2A, member of RAS oncogene family (RAP2A), mRNA.
8106784	RASA1	0.30	0.34	0.94	1.10	0.92	0.87	0.80	0.77	RAS p21 protein activator (GTPase activating protein) 1 (RASA1), transcript variant 1, mRNA.
7969017	RB1	0.22	0.21	0.98	0.92	0.99	0.90	1.16	1.21	retinoblastoma 1 (RB1), mRNA.
8150757	RB1CC1	0.30	0.12	0.78	0.62	0.86	0.38	0.86	0.63	RB1-inducible coiled-coil 1 (RB1CC1), transcript variant 1, mRNA.
8020468	RBBP8	0.35	0.26	1.11	0.94	1.01	0.78	1.32	0.98	retinoblastoma binding protein 8 (RBBP8), transcript variant 1, mRNA.
7972190	RBM26	0.46	0.37	1.31	1.12	1.04	0.92	0.97	0.94	RNA binding motif protein 26 (RBM26), mRNA.
8108927	RBM27	0.29	0.38	1.18	1.24	0.98	1.00	1.13	1.08	RNA binding motif protein 27 (RBM27), mRNA.
8094460	RBPJ	0.19	0.27	1.10	0.97	0.90	0.95	0.95	0.93	recombination signal binding protein for immunoglobulin kappa J region (RBPJ), transcript variant 1, mRNA.
7922432	RC3H1	0.32	0.43	1.13	1.40	1.10	1.34	1.14	1.11	ring finger and CCCH-type zinc finger domains 1 (RC3H1), mRNA.
7909529	RCOR3	0.39	0.40	1.10	1.00	0.72	0.68	1.10	0.87	REST corepressor 3 (RCOR3), transcript variant 1, mRNA.
7951554	RDX	0.28	0.25	0.88	0.76	1.07	1.00	0.97	1.18	radixin (RDX), mRNA.
7961654	RECQL	0.48	0.34	1.28	1.40	1.34	0.88	1.18	1.21	RecQ protein-like (DNA helicase Q1-like) (RECQL), transcript variant 1, mRNA.
8095262	REST	0.40	0.29	1.03	1.33	1.05	1.15	1.03	0.98	RE1-silencing transcription factor (REST), mRNA.
8128894	REV3L	0.26	0.20	1.03	0.97	1.02	0.52	1.15	0.77	REV3-like, catalytic subunit of DNA polymerase zeta (yeast) (REV3L), mRNA.
8099860	RFC1	0.23	0.22	1.15	1.13	1.02	0.88	1.32	1.23	replication factor C (activator 1) 1, 145kDa (RFC1), mRNA.
7989132	RFX7	0.32	0.29	1.08	0.96	0.78	0.70	1.24	0.93	regulatory factor X, 7 (RFX7), mRNA.
8081343	RG9MTD1	0.36	0.41	1.13	1.18	0.99	1.17	0.82	0.88	RNA (guanine-9-) methyltransferase domain containing 1 (RG9MTD1), nuclear gene encoding mitochondrial prote
8053622	RGPD1	0.26	0.19	0.87	0.90	0.82	0.67	0.78	0.75	RANBP2-like and GRIP domain containing 1 (RGPD1), mRNA.
8054414	RGPD3	0.21	0.16	0.86	0.89	0.83	0.61	0.79	0.76	RANBP2-like and GRIP domain containing 3 (RGPD3), mRNA.
8044161	RGPD4	0.21	0.16	0.87	0.91	0.85	0.62	0.80	0.77	RANBP2-like and GRIP domain containing 4 (RGPD4), mRNA.
8044304	RGPD6	0.23	0.17	0.89	0.98	0.88	0.67	0.83	0.82	RANBP2-like and GRIP domain containing 6 (RGPD6), transcript variant 1, mRNA.
8106986	RHOBTB3	0.34	0.44	0.90	0.76	0.64	0.80	0.88	0.67	Rho-related BTB domain containing 3 (RHOBTB3), mRNA.
8006345	RHOT1	0.39	0.49	0.83	0.80	0.78	0.75	0.86	0.79	ras homolog gene family, member T1 (RHOT1), transcript variant 1, mRNA.
8045697	RIF1	0.25	0.19	1.33	1.32	1.22	0.50	1.00	0.83	RAP1 interacting factor homolog (yeast) (RIF1), transcript variant 1, mRNA.
8113286	RIOK2	0.24	0.28	1.21	1.11	0.96	0.90	0.96	0.76	RIO kinase 2 (yeast) (RIOK2), transcript variant 1, mRNA.
7900395	RLF	0.38	0.20	1.36	1.32	1.25	0.93	1.07	1.13	rearranged L-myc fusion (RLF), mRNA.
8069711	RNF160	0.18	0.14	0.98	0.92	1.05	0.65	0.90	0.72	ring finger protein 160 (RNF160), mRNA.
8022441	ROCK1	0.20	0.13	0.97	0.97	0.98	0.63	0.85	0.88	Rho-associated, coiled-coil containing protein kinase 1 (ROCK1), mRNA.
8050302	ROCK2	0.33	0.16	1.25	1.31	1.56	0.90	1.27	1.25	Rho-associated, coiled-coil containing protein kinase 2 (ROCK2), mRNA.
7902992	RPAP2	0.32	0.28	0.92	0.86	0.73	0.67	0.89	0.74	RNA polymerase II associated protein 2 (RPAP2), mRNA.
8022914	RPRD1A	0.38	0.49	0.97	1.01	1.04	1.15	0.89	0.77	regulation of nuclear pre-mRNA domain containing 1A (RPRD1A), mRNA.
8171762	RPS6KA3	0.35	0.45	0.90	0.88	1.10	1.02	1.10	1.23	ribosomal protein S6 kinase, 90kDa, polypeptide 3 (RPS6KA3), mRNA.
8152133	RRM2B	0.14	0.13	1.12	0.70	0.86	0.69	1.50	1.15	ribonucleotide reductase M2 B (TP53 inducible) (RRM2B), transcript variant 1, mRNA.
7994565	RRN3	0.64	0.50	1.20	0.69	0.85	0.60	0.84	0.57	RRN3 RNA polymerase I transcription factor homolog (S. cerevisiae) (RRN3), mRNA.
7950606	RSF1	0.43	0.26	1.41	1.45	1.48	0.66	1.42	1.12	remodeling and spacing factor 1 (RSF1), mRNA.
8083605	RSRC1	0.36	0.40	0.84	0.75	1.00	0.79	0.86	0.66	arginine/serine-rich coiled-coil 1 (RSRC1), mRNA.
7933999	RUFY2	0.29	0.32	1.19	1.19	1.03	1.04	0.94	0.98	RUN and FYVE domain containing 2 (RUFY2), transcript variant 1, mRNA.
8079346	SACM1L	0.22	0.33	0.96	0.98	0.90	0.91	0.78	0.85	SAC1 suppressor of actin mutations 1-like (yeast) (SACM1L), mRNA.
7970569	SACS	0.29	0.25	0.84	1.10	1.27	0.55	0.67	0.57	spastic ataxia of Charlevoix-Saguenay (sacsin) (SACS), mRNA.
7967420	SBNO1	0.29	0.15	0.69	0.72	0.92	0.82	0.70	0.61	strawberry notch homolog 1 (Drosophila) (SBNO1), transcript variant 1, mRNA.
8106479	SCAMP1	0.34	0.38	1.22	1.07	0.86	0.87	0.79	0.89	secretory carrier membrane protein 1 (SCAMP1), mRNA.
7920875	SCARNA4	1.50	0.43	0.49	0.26	1.26	0.09	1.15	0.13	small Cajal body-specific RNA 4 (SCARNA4), guide RNA.
7973770	SCFD1	0.32	0.28	0.88	0.95	0.92	0.83	0.88	0.90	sec1 family domain containing 1 (SCFD1), transcript variant 1, mRNA.
8056491	SCN9A	0.36	0.42	0.69	1.00	1.49	1.53	1.17	1.72	sodium channel, voltage-gated, type IX, alpha subunit (SCN9A), mRNA.
8097521	SCOC	0.42	0.44	0.82	0.76	0.88	0.96	0.62	0.70	short coiled-coil protein (SCOC), transcript variant 4, mRNA.
8046502	SCRN3	0.30	0.34	0.78	0.66	0.59	0.70	0.71	0.68	secernin 3 (SCRN3), mRNA.
7957806	SCYL2	0.18	0.25	0.98	0.94	0.99	1.05	1.04	1.19	SCY1-like 2 (S. cerevisiae) (SCYL2), mRNA.
8101099	SDAD1	0.35	0.32	1.10	1.19	1.56	1.17	1.27	1.29	SDA1 domain containing 1 (SDAD1), mRNA.
7978866	SDCCAG1	0.25	0.15	0.96	0.97	0.80	0.48	0.82	0.79	serologically defined colon cancer antigen 1 (SDCCAG1), mRNA.
8083826	SEC62	0.23	0.18	0.97	0.97	0.87	0.81	0.65	0.73	SEC62 homolog (S. cerevisiae) (SEC62), mRNA.
8128650	SEC63	0.34	0.34	0.87	0.95	1.05	0.93	0.85	1.03	SEC63 homolog (S. cerevisiae) (SEC63), mRNA.
7988581	SECISBP2L	0.35	0.29	1.12	1.34	1.10	1.18	1.20	1.23	SECIS binding protein 2-like (SECISBP2L), mRNA.
7980547	SEL1L	0.40	0.25	0.78	0.79	0.89	0.80	0.79	0.86	sel-1 suppressor of lin-12-like (C. elegans) (SEL1L), mRNA.
8120758	SENP6	0.36	0.20	1.10	0.92	1.14	0.87	0.90	0.83	SUMO1/sentrin specific peptidase 6 (SENP6), transcript variant 1, mRNA.
8099696	SEPSECS	0.40	0.31	1.09	1.14	0.80	0.65	1.24	0.81	Sep (O-phosphoserine) tRNA:Sec (selenocysteine) tRNA synthase (SEPSECS), mRNA.
8128698	SESN1	0.30	0.33	0.95	0.52	0.65	0.37	0.87	0.51	sestrin 1 (SESN1), mRNA.
8086706	SETD2	0.34	0.23	1.16	1.03	0.96	0.84	1.18	0.85	SET domain containing 2 (SETD2), mRNA.
8164701	SETX	0.41	0.26	1.19	1.27	1.55	0.91	1.44	1.58	senataxin (SETX), mRNA.
8058024	SF3B1	0.30	0.33	0.96	0.92	0.92	0.80	1.03	0.85	splicing factor 3b, subunit 1, 155kDa (SF3B1), transcript variant 1, mRNA.
8112337	SFRS12IP1	0.19	0.25	0.92	1.33	0.89	1.04	0.84	0.70	SFRS12-interacting protein 1 (SFRS12IP1), mRNA.
8128394	SFRS18	0.45	0.26	1.00	1.00	0.80	0.67	1.00	0.78	splicing factor, arginine/serine-rich 18 (SFRS18), transcript variant 1, mRNA.
8146717	SGK3	0.39	0.36	0.91	0.69	1.15	0.76	1.35	0.71	serum/glucocorticoid regulated kinase family, member 3 (SGK3), transcript variant 1, mRNA.
8168557	SH3BGRL	0.45	0.32	1.22	0.95	0.77	0.60	1.08	0.92	SH3 domain binding glutamic acid-rich protein like (SH3BGRL), mRNA.
7930470	SHOC2	0.20	0.24	0.94	1.09	0.89	0.74	1.02	1.00	soc-2 suppressor of clear homolog (C. elegans) (SHOC2), mRNA.
7918847	SIKE1	0.49	0.47	1.08	1.08	0.92	0.93	0.86	0.82	suppressor of IKBKE 1 (SIKE1), transcript variant 1, mRNA.
8105353	SKIV2L2	0.24	0.13	0.83	0.65	0.95	0.63	0.73	0.47	superkiller viralicidic activity 2-like 2 (S. cerevisiae) (SKIV2L2), mRNA.
7956658	SLC16A7	0.37	0.23	0.64	0.73	1.13	0.77	0.72	0.61	solute carrier family 16, member 7 (monocarboxylic acid transporter 2) (SLC16A7), mRNA.
8104930	SLC1A3	0.38	0.12	1.00	0.15	0.60	0.13	1.29	0.17	solute carrier family 1 (glial high affinity glutamate transporter), member 3 (SLC1A3), transcript variant 1, mRNA
8140814	SLC25A40	0.38	0.45	0.85	0.69	0.62	0.69	0.78	0.73	solute carrier family 25, member 40 (SLC25A40), nuclear gene encoding mitochondrial protein, mRNA.
8092083	SLC2A2	0.38	0.35	0.87	0.75	0.73	0.63	0.79	0.84	solute carrier family 2 (facilitated glucose transporter), member 2 (SLC2A2), mRNA.
8094848	SLC30A9	0.34	0.46	0.95	0.74	1.17	1.07	0.88	0.84	solute carrier family 30 (zinc transporter), member 9 (SLC30A9), mRNA.
7903281	SLC35A3	0.24	0.26	0.87	0.79	0.83	0.99	0.59	0.61	solute carrier family 35 (UDP-N-acetylglucosamine (UDP-GlcNAc) transporter), member A3 (SLC35A3), mRNA.
7962559	SLC38A4	0.40	0.18	1.35	1.23	0.67	0.38	2.75	1.69	solute carrier family 38, member 4 (SLC38A4), transcript variant 1, mRNA.
8047174	SLC39A10	0.30	0.48	0.82	1.49	1.32	1.35	1.01	1.09	solute carrier family 39 (zinc transporter), member 10 (SLC39A10), transcript variant 1, mRNA.
8095585	SLC4A4	0.34	0.36	0.74	0.75	1.03	1.12	0.73	0.66	solute carrier family 4, sodium bicarbonate cotransporter, member 4 (SLC4A4), transcript variant 1, mRNA.
7954356	SLCO1B1	0.38	0.12	0.71	0.21	1.14	0.36	0.70	0.20	solute carrier organic anion transporter family, member 1B1 (SLCO1B1), mRNA.
7930276	SLK	0.31	0.12	0.97	1.18	1.28	0.96	1.10	1.24	STE20-like kinase (yeast) (SLK), mRNA.
8080685	SLMAP	0.35	0.46	1.12	1.26	1.15	1.25	1.11	1.32	sarcolemma associated protein (SLMAP), mRNA.
7989253	SLTM	0.31	0.22	0.99	0.82	0.89	0.76	0.76	0.74	SAFB-like, transcription modulator (SLTM), transcript variant 1, mRNA.
8115606	SLU7	0.41	0.47	1.29	1.19	1.05	1.17	1.19	1.20	SLU7 splicing factor homolog (S. cerevisiae) (SLU7), mRNA.
8023191	SMAD2	0.21	0.31	0.52	0.74	1.23	1.01	0.85	0.61	SMAD family member 2 (SMAD2), transcript variant 1, mRNA.
8096463	SMARCAD1	0.23	0.14	1.17	1.08	0.96	0.76	0.99	0.85	SWI/SNF-related, matrix-associated actin-dependent regulator of chromatin, subfamily a, containing DEAD/H box
7930422	SMC3	0.15	0.09	1.10	0.93	0.89	0.43	1.01	0.83	structural maintenance of chromosomes 3 (SMC3), mRNA.
8083709	SMC4	0.19	0.12	1.18	1.34	0.76	0.55	0.85	0.91	structural maintenance of chromosomes 4 (SMC4), transcript variant 1, mRNA.
8155770	SMC5	0.49	0.16	1.08	0.84	1.32	0.71	0.92	0.66	structural maintenance of chromosomes 5 (SMC5), mRNA.
8050443	SMC6	0.26	0.16	0.95	0.86	1.18	0.62	0.93	0.85	structural maintenance of chromosomes 6 (SMC6), transcript variant 1, mRNA.
8019885	SMCHD1	0.39	0.18	1.82	1.45	1.33	0.78	1.60	1.36	structural maintenance of chromosomes flexible hinge domain containing 1 (SMCHD1), mRNA.
8052307	SMEK2	0.30	0.28	0.81	0.79	0.92	0.84	0.93	0.77	SMEK homolog 2, suppressor of mek1 (Dictyostelium) (SMEK2), transcript variant 1, mRNA.
8131957	SNX10	0.40	0.24	1.07	0.60	1.19	0.69	1.62	0.92	sorting nexin 10 (SNX10), mRNA.
8138401	SNX13	0.37	0.29	0.88	0.89	0.97	0.78	0.90	0.90	sorting nexin 13 (SNX13), mRNA.
8107613	SNX2	0.41	0.47	1.11	0.63	0.79	0.67	1.03	0.82	sorting nexin 2 (SNX2), mRNA.
7907702	SOAT1	0.42	0.49	0.98	0.58	0.75	0.56	1.05	0.60	sterol O-acyltransferase 1 (SOAT1), transcript variant 688113, mRNA.
7974447	SOCS4	0.34	0.30	0.96	1.10	0.91	0.86	0.82	0.81	suppressor of cytokine signaling 4 (SOCS4), transcript variant 1, mRNA.
8051670	SOS1	0.30	0.44	1.05	1.06	1.00	1.18	1.44	1.31	son of sevenless homolog 1 (Drosophila) (SOS1), mRNA.
7978932	SOS2	0.19	0.18	1.12	1.17	0.77	0.85	1.13	0.87	son of sevenless homolog 2 (Drosophila) (SOS2), mRNA.
8041236	SPAST	0.41	0.29	0.96	0.91	0.88	0.82	0.78	0.69	spastin (SPAST), transcript variant 1, mRNA.
7988286	SPG11	0.42	0.33	0.96	0.72	1.01	0.73	1.14	0.76	spastic paraplegia 11 (autosomal recessive) (SPG11), transcript variant 1, mRNA.
7970999	SPG20	0.28	0.16	0.93	0.32	0.78	0.25	0.85	0.27	spastic paraplegia 20 (Troyer syndrome) (SPG20), transcript variant 1, mRNA.
8045514	SPOPL	0.30	0.38	1.07	1.00	0.83	0.86	1.06	0.97	speckle-type POZ protein-like (SPOPL), mRNA.
8083183	SR140	0.31	0.18	1.20	1.14	1.11	0.93	1.12	1.01	U2-associated SR140 protein (SR140), mRNA.
8107578	SRFBP1	0.40	0.27	1.26	1.02	1.74	1.21	1.09	1.29	serum response factor binding protein 1 (SRFBP1), mRNA.
8095230	SRP72	0.42	0.49	0.94	0.83	0.99	1.00	0.85	0.97	signal recognition particle 72kDa (SRP72), mRNA.
7962499	SRSF2IP	0.26	0.18	1.07	1.09	0.94	0.70	1.03	0.96	splicing factor, arginine/serine-rich 2, interacting protein (SFRS2IP), mRNA.
8046201	SSB	0.50	0.43	1.07	0.93	1.19	0.92	0.88	0.84	Sjogren syndrome antigen B (autoantigen La) (SSB), mRNA.
7917255	SSX2IP	0.31	0.29	0.84	0.67	0.87	0.80	1.04	1.48	synovial sarcoma, X breakpoint 2 interacting protein (SSX2IP), transcript variant 5, mRNA.
8169750	STAG2	0.23	0.10	1.06	0.96	0.83	0.59	1.15	1.16	stromal antigen 2 (STAG2), transcript variant 2, mRNA.
8051443	STRN	0.37	0.43	0.88	1.03	1.18	1.07	1.13	1.12	striatin, calmodulin binding protein (STRN), mRNA.
7903541	STXBP3	0.29	0.26	1.16	1.09	1.12	0.86	1.02	0.93	syntaxin binding protein 3 (STXBP3), mRNA.
7974387	STYX	0.30	0.37	0.97	0.94	0.99	1.01	0.95	0.91	serine/threonine/tyrosine interacting protein (STYX), transcript variant 1, mRNA.
7971541	SUCLA2	0.24	0.37	0.74	0.87	0.76	0.79	0.81	0.89	succinate-CoA ligase, ADP-forming, beta subunit (SUCLA2), nuclear gene encoding mitochondrial protein, mRNA.
8100798	SULT1B1	0.28	0.17	0.90	0.76	0.55	0.45	1.20	0.89	sulfotransferase family, cytosolic, 1B, member 1 (SULT1B1), mRNA.

8006325	SUZ12	0.27	0.22	1.11	0.97	0.88	0.75	1.16	0.79	suppressor of zeste 12 homolog (Drosophila) (SUZ12), mRNA.
8152553	TAF2	0.26	0.28	1.04	0.88	0.93	0.93	0.90	0.76	TAF2 RNA polymerase II, TATA box binding protein (TBP)-associated factor, 150kDa (TAF2), mRNA.
8173732	TAF9B	0.33	0.42	0.84	0.87	1.03	1.08	0.82	0.84	TAF9B RNA polymerase II, TATA box binding protein (TBP)-associated factor, 31kDa (TAF9B), mRNA.
8006030	TAOK1	0.33	0.26	0.86	1.03	0.98	0.81	0.90	0.84	TAO kinase 1 (TAOK1), mRNA.
8131975	TAX1BP1	0.33	0.42	0.96	1.06	1.11	0.95	1.04	0.98	Tax1 (human T-cell leukemia virus type I) binding protein 1 (TAX1BP1), transcript variant 1, mRNA.
8081256	TBC1D23	0.22	0.23	1.08	1.00	0.98	0.87	0.82	0.74	TBC1 domain family, member 23 (TBC1D23), mRNA.
8102171	TBCK	0.30	0.38	1.05	0.93	0.95	0.96	1.41	1.46	TBC1 domain containing kinase (TBCK), transcript variant 1, mRNA.
7956795	TBK1	0.30	0.34	1.27	1.10	1.23	0.90	1.10	0.82	TANK-binding kinase 1 (TBK1), mRNA.
8092201	TBL1XR1	0.24	0.17	0.88	0.74	0.77	0.60	0.97	0.74	transducin (beta)-like 1 X-linked receptor 1 (TBL1XR1), mRNA.
7983843	TCF12	0.34	0.30	1.11	1.00	0.88	0.80	0.93	0.87	transcription factor 12 (TCF12), transcript variant 1, mRNA.
8023415	TCF4	0.45	0.17	1.03	0.21	0.54	0.19	0.80	0.22	transcription factor 4 (TCF4), transcript variant 1, mRNA.
7938544	TEAD1	0.35	0.41	0.98	1.16	0.84	1.02	0.92	0.96	TEA domain family member 1 (SV40 transcriptional enhancer factor) (TEAD1), mRNA.
8096675	TET2	0.27	0.27	1.36	1.29	0.81	0.54	1.57	0.95	tet oncogene family member 2 (TET2), transcript variant 1, mRNA.
8057599	TFPI	0.34	0.45	0.94	1.18	0.99	1.06	0.91	1.05	tissue factor pathway inhibitor (lipoprotein-associated coagulation inhibitor) (TFPI), transcript variant 1, mRNA.
8093053	TFRC	0.49	0.37	0.79	0.69	1.00	0.92	0.56	0.47	transferrin receptor (p90, CD71) (TFRC), mRNA.
8180324	THAP5	0.33	0.36	1.18	1.34	0.75	1.25	0.98	1.45	THAP domain containing 5 (THAP5), mRNA
8021924	THOC1	0.28	0.35	1.07	0.71	0.91	0.68	0.96	0.58	THO complex 1 (THOC1), mRNA.
8174893	THOC2	0.26	0.09	1.26	1.14	1.06	0.52	1.15	0.88	THO complex 2 (THOC2), mRNA.
8000003	THUMPD1	0.37	0.34	1.09	0.94	0.97	0.93	1.17	1.02	THUMP domain containing 1 (THUMPD1), mRNA.
8157524	TLR4	0.23	0.19	1.09	0.56	0.62	0.49	1.04	0.48	toll-like receptor 4 (TLR4), transcript variant 3, non-coding RNA.
8131539	TMEM106B	0.33	0.33	0.97	0.90	0.64	0.70	0.87	0.78	transmembrane protein 106B (TMEM106B), transcript variant 1, mRNA.
7943369	TMEM133	0.41	0.15	1.00	0.98	0.97	0.93	1.23	1.04	transmembrane protein 133 (TMEM133), mRNA.
7942964	TMEM135	0.48	0.37	0.90	1.20	1.23	0.98	1.44	1.10	transmembrane protein 135 (TMEM135), transcript variant 1, mRNA.
8113023	TMEM161B	0.43	0.49	1.14	1.18	0.91	0.82	0.90	0.92	transmembrane protein 161B (TMEM161B), mRNA.
8112967	TMEM167A	0.37	0.45	0.90	0.94	0.78	0.90	0.65	0.86	transmembrane protein 167A (TMEM167A), mRNA.
8123062	TMEM181	0.41	0.43	0.78	0.83	0.82	0.89	0.86	0.86	transmembrane protein 181 (TMEM181), mRNA.
8127637	TMEM30A	0.41	0.50	1.02	0.92	1.00	0.99	1.01	0.93	transmembrane protein 30A (TMEM30A), transcript variant 1, mRNA.
8172022	TMEM47	0.46	0.43	0.99	1.14	0.83	0.94	0.83	0.79	transmembrane protein 47 (TMEM47), mRNA.
7903162	TMEM56	0.41	0.47	0.76	0.81	1.01	0.95	0.71	0.59	transmembrane protein 56 (TMEM56), mRNA.
8088700	TMF1	0.25	0.18	1.00	1.26	1.00	0.75	0.90	0.85	TATA element modulatory factor 1 (TMF1), mRNA.
7983744	TMOD3	0.41	0.42	0.97	1.15	1.00	1.35	0.94	1.06	tropomodulin 3 (ubiquitous) (TMOD3), mRNA.
7957478	TMTC3	0.20	0.16	0.91	0.96	0.82	0.65	0.79	0.72	transmembrane and tetratricopeptide repeat containing 3 (TMTC3), mRNA.
8106122	TNPO1	0.26	0.37	1.01	1.02	0.98	1.04	0.88	0.97	transportin 1 (TNPO1), transcript variant 1, mRNA.
8008547	TOM1L1	0.46	0.47	0.86	0.82	0.88	0.88	0.72	0.78	target of myb1 (chicken)-like 1 (TOM1L1), mRNA.
8085815	TOP2B	0.24	0.14	0.80	0.56	1.07	0.65	0.74	0.51	topoisomerase (DNA) II beta 180kDa (TOP2B), mRNA.
8090772	TOPBP1	0.27	0.17	0.90	0.79	0.95	0.76	0.73	0.64	topoisomerase (DNA) II binding protein 1 (TOPBP1), mRNA.
8160581	TOPORS	0.43	0.33	1.17	1.30	1.01	0.99	0.94	0.89	topoisomerase I binding, arginine/serine-rich (TOPORS), mRNA.
7969881	TPP2	0.26	0.33	0.95	1.03	0.92	0.90	0.96	0.81	tripeptidyl peptidase II (TPP2), mRNA.
7922912	TPR	0.25	0.11	1.05	0.99	0.91	0.38	1.05	0.92	translocated promoter region (to activated MET oncogene) (TPR), mRNA.
8097841	TRIM2	0.31	0.43	0.81	1.13	0.93	1.02	0.80	0.85	tripartite motif-containing 2 (TRIM2), transcript variant 1, mRNA.
8136473	TRIM24	0.44	0.45	1.05	1.10	0.71	0.80	1.35	1.17	tripartite motif-containing 24 (TRIM24), transcript variant 1, mRNA.
7918725	TRIM33	0.35	0.42	1.12	1.03	0.95	0.95	1.08	1.00	tripartite motif-containing 33 (TRIM33), transcript variant a, mRNA.
7980923	TRIP11	0.16	0.11	0.83	0.83	0.84	0.40	0.88	0.84	thyroid hormone receptor interactor 11 (TRIP11), mRNA.
7908421	TROVE2	0.21	0.18	1.02	0.94	0.95	0.72	0.88	0.74	TROVE domain family, member 2 (TROVE2), transcript variant 2, mRNA.
7988713	TRPM7	0.25	0.11	0.94	0.71	0.92	0.58	0.82	0.65	transient receptor potential cation channel, subfamily M, member 7 (TRPM7), mRNA.
8152453	TRPS1	0.20	0.14	0.80	0.14	0.79	0.15	1.12	0.13	trichorhinophalangeal syndrome I (TRPS1), mRNA.
8068522	TTC3	0.14	0.10	0.54	0.55	0.80	0.62	0.61	0.46	tetratricopeptide repeat domain 3 (TTC3), transcript variant 1, mRNA.
8113157	TTC37	0.19	0.08	1.00	0.98	0.95	0.59	0.90	0.87	tetratricopeptide repeat domain 37 (TTC37), mRNA.
7917199	TTLL7	0.40	0.15	0.78	0.36	1.58	0.51	1.15	0.74	tubulin tyrosine ligase-like family, member 7 (TTLL7), mRNA.
8072407	TUG1	0.33	0.47	0.99	0.94	0.87	0.98	0.83	0.86	taurine upregulated 1 (non-protein coding) (TUG1), non-coding RNA.
8013906	TWF1	0.23	0.33	0.91	0.88	1.11	0.95	1.08	0.98	twinfilin, actin-binding protein, homolog 1 (Drosophila) (TWF1), mRNA.
8166230	TXLNG	0.30	0.31	1.05	0.91	0.93	0.80	0.74	0.72	taxilin gamma (TXLNG), transcript variant 1, mRNA.
7990054	UACA	0.42	0.30	1.16	2.24	1.45	1.10	2.56	1.82	uveal autoantigen with coiled-coil domains and ankyrin repeats (UACA), transcript variant 1, mRNA.
8100615	UBA6	0.49	0.33	1.47	1.50	1.49	1.01	1.73	1.96	ubiquitin-like modifier activating enzyme 6 (UBA6), mRNA.
7986769	UBE3A	0.37	0.41	1.00	0.92	1.05	1.07	0.95	0.84	ubiquitin protein ligase E3A (UBE3A), transcript variant 3, mRNA.
8109597	UBLCP1	0.15	0.21	1.03	0.97	0.80	0.77	1.01	0.86	ubiquitin-like domain containing CTD phosphatase 1 (UBLCP1), mRNA.
7987981	UBR1	0.32	0.35	0.91	0.92	1.20	1.43	1.24	1.40	ubiquitin protein ligase E3 component n-recognin 1 (UBR1), mRNA.
8046213	UBR3	0.32	0.22	0.77	0.82	1.14	0.94	0.94	0.68	ubiquitin protein ligase E3 component n-recognin 3 (putative) (UBR3), mRNA.
8152148	UBR5	0.40	0.34	0.83	0.84	1.07	0.86	0.98	0.77	ubiquitin protein ligase E3 component n-recognin 5 (UBR5), mRNA.
8146544	UBXN2B	0.46	0.24	0.88	0.62	0.85	0.59	0.63	0.72	UBX domain protein 2B (UBXN2B), mRNA.
8045455	UBXN4	0.35	0.33	1.03	1.09	1.19	1.17	1.24	1.17	UBX domain protein 4 (UBXN4), mRNA.
7947027	UEVLD	0.34	0.35	0.87	0.95	1.03	0.97	1.11	0.98	UEV and lactate/malate dehyrogenase domains (UEVLD), transcript variant 1, mRNA.
8095402	UGT2A3	0.38	0.15	0.76	0.73	0.54	0.32	0.87	0.53	UDP glucuronosyltransferase 2 family, polypeptide A3 (UGT2A3), mRNA.
7965723	UHRF1BP1L	0.29	0.23	0.94	0.79	0.84	0.80	0.91	0.78	UHRF1 binding protein 1-like (UHRF1BP1L), transcript variant 1, mRNA.
7932041	UPF2	0.46	0.21	1.42	1.19	1.18	0.90	1.21	1.23	UPF2 regulator of nonsense transcripts homolog (yeast) (UPF2), transcript variant 1, mRNA.
8095773	USO1	0.23	0.24	0.77	0.97	1.12	0.82	1.06	0.96	USO1 vesicle docking protein homolog (yeast) (USO1), mRNA.
8180323	USP12	0.49	0.43	1.00	0.86	1.29	1.13	1.28	1.09	ubiquitin specific peptidase 12 (USP12), mRNA
7956670	USP15	0.38	0.31	1.48	1.32	1.54	0.90	1.70	1.65	ubiquitin specific peptidase 15 (USP15), mRNA.
8068062	USP16	0.28	0.22	1.00	1.01	1.04	0.93	0.90	0.89	ubiquitin specific peptidase 16 (USP16), transcript variant 1, mRNA.
7916443	USP24	0.31	0.27	0.75	0.62	1.04	0.83	0.83	0.64	ubiquitin specific peptidase 24 (USP24), mRNA.
8052443	USP34	0.27	0.14	0.75	0.79	0.99	0.62	0.82	0.58	ubiquitin specific peptidase 34 (USP34), mRNA.
8097570	USP38	0.41	0.41	1.02	1.00	0.98	0.85	0.97	0.75	ubiquitin specific peptidase 38 (USP38), mRNA.
7938448	USP47	0.30	0.18	1.11	1.17	1.19	0.91	0.89	0.84	ubiquitin specific peptidase 47 (USP47), mRNA.
8097098	USP53	0.46	0.15	1.18	1.50	1.32	0.73	0.72	0.68	ubiquitin specific peptidase 53 (USP53), mRNA.
7983663	USP8	0.18	0.19	0.79	0.87	0.88	0.70	0.90	0.77	ubiquitin specific peptidase 8 (USP8), transcript variant 1, mRNA.
8166826	USP9X	0.33	0.23	0.76	0.79	0.95	0.97	0.95	0.93	ubiquitin specific peptidase 9, X-linked (USP9X), transcript variant 3, mRNA.
7968333	USPL1	0.42	0.36	1.15	1.10	1.03	0.86	1.00	0.80	ubiquitin specific peptidase like 1 (USPL1), mRNA.
7957890	UTP20	0.26	0.18	0.90	0.78	1.05	0.98	0.60	0.54	UTP20, small subunit (SSU) processome component, homolog (yeast) (UTP20), mRNA.
8122464	UTRN	0.32	0.18	0.72	0.95	1.33	0.88	1.86	2.08	utrophin (UTRN), mRNA.
8151118	VCPIP1	0.46	0.45	1.10	1.16	1.32	1.18	1.24	1.25	valosin containing protein (p97)/p47 complex interacting protein 1 (VCPIP1), mRNA.
8165658	VIPR2	0.46	0.76	1.05	1.44	0.30	0.53	1.00	2.07	gi|17981852|ref|NC_001807.4|:5513-5580; gene=TRNW; product=tRNA-Trp
8155946	VPS13A	0.31	0.16	0.75	0.62	0.93	0.28	0.83	0.53	vacuolar protein sorting 13 homolog A (S. cerevisiae) (VPS13A), transcript variant A, mRNA.
8147580	VPS13B	0.41	0.25	0.86	0.87	1.16	0.70	1.25	0.83	vacuolar protein sorting 13 homolog B (yeast) (VPS13B), transcript variant 5, mRNA.
7989387	VPS13C	0.25	0.10	0.81	0.67	1.45	0.43	1.52	1.05	vacuolar protein sorting 13 homolog C (S. cerevisiae) (VPS13C), transcript variant 2A, mRNA.
7927972	VPS26A	0.37	0.47	1.00	1.00	0.94	0.93	0.91	0.97	vacuolar protein sorting 26 homolog A (S. pombe) (VPS26A), transcript variant 1, mRNA.
8139165	VPS41	0.42	0.48	0.70	0.69	1.21	0.69	0.93	0.68	vacuolar protein sorting 41 homolog (S. cerevisiae) (VPS41), transcript variant 1, mRNA.
7934812	WAPAL	0.41	0.45	1.02	1.15	1.05	1.09	0.88	0.86	wings apart-like homolog (Drosophila) (WAPAL), mRNA.
8101511	WDFY3	0.32	0.39	0.81	0.84	0.91	0.73	0.79	0.59	WD repeat and FYVE domain containing 3 (WDFY3), transcript variant 1, mRNA.
8107282	WDR36	0.34	0.35	1.16	0.87	1.12	0.96	0.82	0.89	WD repeat domain 36 (WDR36), mRNA.
7979565	WDR89	0.45	0.37	1.31	1.17	1.09	0.98	0.79	0.69	WD repeat domain 89 (WDR89), transcript variant 2, mRNA.
7952986	WNK1	0.44	0.49	0.87	0.82	0.90	0.68	1.34	0.72	hereditary sensory neuropathy, type II (HSN2), mRNA.
8147156	WWP1	0.32	0.32	0.93	0.89	0.78	0.81	0.91	0.73	WW domain containing E3 ubiquitin protein ligase 1 (WWP1), mRNA.
8052526	XPO1	0.25	0.21	1.15	1.10	0.76	0.66	0.93	0.91	exportin 1 (CRM1 homolog, yeast) (XPO1), mRNA.
7970473	XPO4	0.32	0.38	0.90	0.83	0.89	0.94	0.69	0.56	exportin 4 (XPO4), mRNA.
8021984	YES1	0.38	0.27	0.95	0.82	1.09	0.91	1.00	0.91	v-yes-1 Yamaguchi sarcoma viral oncogene homolog 1 (YES1), mRNA.
8107375	YTHDC2	0.29	0.20	0.96	0.89	1.12	1.01	1.04	1.14	YTH domain containing 2 (YTHDC2), mRNA.
8146637	YTHDF3	0.29	0.38	0.88	0.92	0.86	0.91	0.87	0.86	YTH domain family, member 3 (YTHDF3), mRNA.
7975068	ZBTB1	0.37	0.38	1.25	1.10	1.16	0.87	1.00	0.99	zinc finger and BTB domain containing 1 (ZBTB1), transcript variant 1, mRNA.
8089234	ZBTB11	0.39	0.30	1.11	1.17	1.08	1.12	1.00	0.98	zinc finger and BTB domain containing 11 (ZBTB11), mRNA.
8169683	ZBTB33	0.30	0.28	1.19	0.97	0.80	0.75	1.02	0.78	zinc finger and BTB domain containing 33 (ZBTB33), mRNA.
8083092	ZBTB38	0.20	0.12	0.98	0.90	0.69	0.64	1.14	0.74	zinc finger and BTB domain containing 38 (ZBTB38), mRNA.
7923119	ZBTB41	0.13	0.15	1.14	1.24	1.13	0.91	1.28	1.13	zinc finger and BTB domain containing 41 (ZBTB41), mRNA.
8180263	ZC3H11A	0.42	0.38	1.11	1.01	1.01	0.93	1.00	1.02	zinc finger CCCH-type containing 11A (ZC3H11A), mRNA
7908978	ZC3H11A	0.38	0.31	0.97	0.69	1.27	0.80	0.79	0.88	zinc finger CCCH-type containing 11A (ZC3H11A), mRNA.
7971422	ZC3H13	0.49	0.31	1.10	1.05	1.02	0.69	1.03	0.95	zinc finger CCCH-type containing 13 (ZC3H13), mRNA.
8046848	ZC3H15	0.30	0.38	1.05	0.91	0.98	0.79	0.76	0.84	zinc finger CCCH-type containing 15 (ZC3H15), mRNA.
7916185	ZCCHC11	0.36	0.24	1.12	0.91	0.79	0.64	0.95	0.59	zinc finger, CCHC domain containing 11 (ZCCHC11), transcript variant 1, mRNA.
8162147	ZCCHC6	0.37	0.14	1.01	0.93	0.79	0.71	0.90	0.67	zinc finger, CCHC domain containing 6 (ZCCHC6), mRNA.
7957277	ZDHHC17	0.44	0.44	0.96	1.39	1.18	0.97	0.98	0.71	zinc finger, DHHC-type containing 17 (ZDHHC17), mRNA.
8160151	ZDHHC21	0.35	0.32	1.02	1.01	1.01	0.96	0.91	0.87	zinc finger, DHHC-type containing 21 (ZDHHC21), mRNA.
7926916	ZEB1	0.30	0.18	1.24	1.04	1.63	0.63	1.77	1.45	zinc finger E-box binding homeobox 1 (ZEB1), transcript variant 2, mRNA.
7964937	ZFC3H1	0.41	0.23	1.07	1.12	1.22	0.85	0.84	0.97	zinc finger, C3H1-type containing (ZFC3H1), mRNA.
8166500	ZFX	0.43	0.42	1.06	1.09	1.26	0.87	1.37	0.89	zinc finger protein, X-linked (ZFX), mRNA.
8106602	ZFYVE16	0.28	0.16	0.97	0.93	1.19	0.57	1.13	0.84	zinc finger, FYVE domain containing 16 (ZFYVE16), transcript variant 1, mRNA.
8152656	ZHX1	0.19	0.21	0.99	0.96	0.72	0.62	1.08	0.87	zinc fingers and homeoboxes 1 (ZHX1), transcript variant 1, mRNA.
8092230	ZMAT3	0.41	0.31	0.81	0.63	1.01	0.93	0.83	0.78	zinc finger, matrin type 3 (ZMAT3), transcript variant 1, mRNA.
7967900	ZMYM2	0.39	0.21	1.11	1.14	0.87	0.81	0.97	0.98	zinc finger, MYM-type 2 (ZMYM2), mRNA.
7899957	ZMYM4	0.36	0.32	1.01	0.95	0.96	1.01	1.08	1.04	zinc finger, MYM-type 4 (ZMYM4), mRNA.

8033789	ZNF121	0.29	0.32	1.09	1.40	0.86	1.05	0.84	0.93	zinc finger protein 121 (ZNF121), mRNA.
8105136	ZNF131	0.42	0.38	1.07	1.11	0.83	1.00	0.81	0.88	zinc finger protein 131 (ZNF131), mRNA.
8028186	ZNF146	0.18	0.13	1.28	1.05	0.92	0.75	0.62	0.60	zinc finger protein 146 (ZNF146), transcript variant 1, mRNA.
8090237	ZNF148	0.28	0.16	1.08	0.94	0.91	0.70	1.07	0.91	zinc finger protein 148 (ZNF148), mRNA.
8156935	ZNF189	0.29	0.37	1.01	0.94	0.77	0.75	1.13	0.81	zinc finger protein 189 (ZNF189), transcript variant 1, mRNA.
8117646	ZNF192	0.34	0.28	1.10	0.93	0.98	0.68	0.94	0.61	zinc finger protein 192 (ZNF192), mRNA.
7945864	ZNF195	0.35	0.30	1.07	1.12	0.80	0.70	0.84	0.58	zinc finger protein 195 (ZNF195), transcript variant 1, mRNA.
8022882	ZNF24	0.38	0.39	1.15	1.07	1.12	1.41	1.15	1.44	zinc finger protein 24 (ZNF24), mRNA.
8036324	ZNF260	0.16	0.16	1.37	1.61	0.66	0.83	0.77	0.91	zinc finger protein 260 (ZNF260), transcript variant 1, mRNA.
7995258	ZNF267	0.33	0.29	1.17	0.92	2.83	1.66	2.26	2.40	zinc finger protein 267 (ZNF267), transcript variant 498723, mRNA.
8020898	ZNF271	0.40	0.46	0.70	0.77	0.80	0.83	0.69	0.82	zinc finger protein 271 (ZNF271), transcript variant 1, non-coding RNA.
8135497	ZNF277	0.49	0.46	1.12	1.11	1.06	1.06	1.23	1.33	zinc finger protein 277 (ZNF277), mRNA.
8175076	ZNF280C	0.29	0.29	1.47	1.07	1.37	1.18	1.39	1.06	zinc finger protein 280C (ZNF280C), mRNA.
7989159	ZNF280D	0.45	0.39	0.99	0.95	0.81	0.67	0.94	0.70	zinc finger protein 280D (ZNF280D), transcript variant 1, mRNA.
8120992	ZNF292	0.37	0.15	1.35	1.47	0.94	0.50	1.36	1.05	zinc finger protein 292 (ZNF292), mRNA.
8028194	ZNF382	0.24	0.33	1.16	0.97	0.70	0.82	0.89	0.86	zinc finger protein 382 (ZNF382), mRNA.
8030908	ZNF480	0.38	0.46	1.19	1.01	0.66	0.73	0.82	0.79	zinc finger protein 480 (ZNF480), mRNA.
8027439	ZNF507	0.32	0.23	1.11	0.94	0.83	0.72	0.99	0.75	zinc finger protein 507 (ZNF507), transcript variant 1, mRNA.
7929562	ZNF518A	0.25	0.20	1.17	1.18	1.11	0.60	1.53	0.93	zinc finger protein 518A (ZNF518A), mRNA.
8030980	ZNF525	0.26	0.46	1.13	0.96	0.76	0.81	0.71	0.93	zinc finger protein 525 (ZNF525), non-coding RNA.
8042601	ZNF638	0.32	0.21	0.91	0.87	0.91	0.46	1.12	0.77	zinc finger protein 638 (ZNF638), transcript variant 1, mRNA.
7917604	ZNF644	0.26	0.12	1.06	1.00	1.11	0.58	0.99	0.73	zinc finger protein 644 (ZNF644), transcript variant 1, mRNA.
8081069	ZNF654	0.16	0.20	1.19	1.42	1.20	0.97	1.13	1.33	zinc finger protein 654 (ZNF654), mRNA.
8098758	ZNF721	0.23	0.12	1.16	0.99	1.00	0.48	1.22	0.67	zinc finger protein 721 (ZNF721), mRNA.
8035793	ZNF737	0.27	0.40	1.04	2.16	0.55	0.71	0.69	0.81	zinc finger protein 737 (ZNF737), mRNA.
7987361	ZNF770	0.26	0.17	0.84	0.83	0.93	0.67	0.69	0.43	zinc finger protein 770 (ZNF770), mRNA.
8142730	ZNF800	0.49	0.43	1.03	1.03	0.93	0.96	1.09	0.99	zinc finger protein 800 (ZNF800), mRNA.
7960143	ZNF84	0.45	0.40	1.19	1.27	0.94	0.86	1.05	1.00	zinc finger protein 84 (ZNF84), transcript variant 1, mRNA.
8035842	ZNF91	0.16	0.08	0.92	0.77	0.69	0.41	0.93	0.55	zinc finger protein 91 (ZNF91), mRNA.
7917359	ZNHIT6	0.35	0.38	1.14	1.11	1.36	1.41	0.78	0.69	zinc finger, HIT type 6 (ZNHIT6), transcript variant 1, mRNA.
7916969	ZRANB2	0.29	0.24	1.19	1.10	0.88	0.64	0.82	0.80	zinc finger, RAN-binding domain containing 2 (ZRANB2), transcript variant 2, mRNA.
7901479	ZYG11B	0.32	0.35	0.90	0.83	0.91	1.00	1.01	0.81	zyg-11 homolog B (C. elegans) (ZYG11B), mRNA.
7917103	ZZZ3	0.34	0.20	1.11	1.03	1.02	0.84	1.01	0.88	zinc finger, ZZ-type containing 3 (ZZZ3), mRNA.

Supplementary Table V.

PHH-derived gene sets used for GSEA. The table shows genes that are preferentially induced by IFN alpha or IFN gamma in PHH (at least at one time point the fold difference of expression induced by the two cytokines is higher than 2, with the corresponding p-value below 0.05).

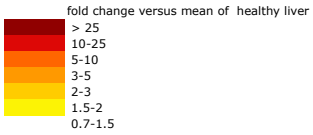

Genes preferentially induced by IFN gamma (IFN gamma signature)

ID	Symbol	alpha		gamma		Genename
		6h	24h	6h	24h	
8075695	APOL3	6.6	3.6	5.9	11.1	apolipoprotein L, 3
7954527	ARNTL2	0.9	0.8	1.9	2.1	aryl hydrocarbon receptor nuclear translocator-like 2
7953993	BCL2L14	7.1	1.9	4.6	7.1	BCL2-like 14 (apoptosis facilitator)
8023401	CCDC68	0.5	0.9	2.5	2.4	coiled-coil domain containing 68
8060675	CDC25B	1.5	1.0	1.1	3.4	cell division cycle 25 homolog B (S. pombe)
8103389	CTSO	1.2	1.8	1.6	4.3	cathepsin O
8101131	CXCL11	42.0	55.0	65.3	112.5	chemokine (C-X-C motif) ligand 11
7958425	DAO	1.6	0.9	2.2	8.5	D-amino-acid oxidase
7983405	DUOXA2	1.5	1.1	1.8	8.3	dual oxidase maturation factor 2
7965335	DUSP6	1.0	1.4	2.3	3.9	dual specificity phosphatase 6
8125993	ETV7	4.8	2.7	3.8	7.4	ets variant 7
8136940	FAM115C	1.9	0.8	3.6	3.4	family with sequence similarity 115, member C
8047565	FAM117B	1.0	1.1	2.2	4.0	family with sequence similarity 117, member B
7917561	GBP4	34.1	11.8	50.2	78.4	guanylate binding protein 4
7917576	GBP5	7.5	3.0	23.3	195.0	guanylate binding protein 5
7917548	GBP7	1.8	1.1	2.4	4.9	guanylate binding protein 7
7984001	GCNT3	1.0	0.9	1.9	2.1	glucosaminyl (N-acetyl) transferase 3, mucin type
8180086	HLA-DMA	1.1	1.2	1.0	9.5	major histocompatibility complex, class II, DM alpha
8125530	HLA-DMB	1.4	1.2	1.0	12.2	major histocompatibility complex, class II, DM beta
8125447	HLA-DQB1	1.9	1.7	1.5	15.0	major histocompatibility complex, class II, DQ beta 1
8025601	ICAM1	1.7	1.3	4.1	3.8	intercellular adhesion molecule 1
7942300	IL18BP	2.1	2.1	2.1	6.6	interleukin 18 binding protein
8114010	IRF1	6.7	2.5	13.2	13.5	interferon regulatory factor 1
8154178	JAK2	1.1	1.5	4.0	7.1	Janus kinase 2
8028744	LGALS17A	3.0	1.3	6.4	52.7	lectin, galactoside-binding, soluble, 14 pseudogene
8112803	LHFPL2	0.9	1.0	2.9	1.8	lipoma HMGIC fusion partner-like 2
8072461	LIMK2	1.7	1.1	2.5	2.6	LIM domain kinase 2
8141872	NAPEPLD	0.4	1.2	1.0	2.2	N-acyl phosphatidylethanolamine phospholipase D
8091255	PAQR9	1.0	1.1	1.8	3.8	progestin and adipoQ receptor family member IX
8091306	PLSCR4	1.2	1.2	1.4	2.7	phospholipid scramblase 4
8115997	RAB24	1.4	1.1	1.7	2.3	RAB24, member RAS oncogene family
7909214	RASSF5	1.0	1.1	4.1	5.2	Ras association (RalGDS/AF-6) domain family member 5
8110327	RGS14	1.3	1.1	2.1	3.0	regulator of G-protein signaling 14
8064766	RNF24	2.2	1.0	1.9	2.1	ring finger protein 24
8017039	SEPT4	1.2	1.0	1.2	3.5	septin 4
7998637	SEPX1	1.5	0.8	1.7	2.0	selenoprotein X, 1
7931951	SFMBT2	1.2	1.0	2.2	4.9	Scm-like with four mbt domains 2
8129666	SLC2A12	1.5	1.8	1.7	4.9	solute carrier family 2 (facilitated glucose transporter), member 12
7999423	SOCS1	5.1	1.7	4.5	9.0	suppressor of cytokine signaling 1
8060997	SPTLC3	0.7	0.9	1.6	2.4	serine palmitoyltransferase, long chain base subunit 3
8180339	ST6GALNAC6	1.4	0.9	1.4	2.1	ST6 (alpha-N-acetyl-neuraminyl-2,3-beta-galactosyl-1,3)-N-acetylgalactosaminide alpha-2,6-sialyltransferase 6
8007212	STAT5A	1.8	1.3	1.4	2.7	signal transducer and activator of transcription 5A
8165866	STS	0.9	1.2	1.5	3.7	steroid sulfatase (microsomal), isozyme S
7938812	TMEM86A	1.2	1.0	1.1	2.4	transmembrane protein 86A
7977046	TNFAIP2	1.6	1.0	2.2	2.3	tumor necrosis factor, alpha-induced protein 2
8117840	TRIM40	1.6	1.0	12.6	22.2	tripartite motif-containing 40
8178295	UBD	2.4	1.4	4.2	7.8	ubiquitin D
8129637	VNN2	0.9	1.0	1.2	3.4	vanin 2
8040430	VSNL1	1.1	1.6	3.2	11.8	visinin-like 1

Genes preferentially induced by IFN alpha (IFN alpha signature)

ID	Symbol	alpha		gamma		Genename
		6h	24h	6h	24h	
8073062	APOBEC3B	4.6	1.8	1.3	1.1	apolipoprotein B mRNA editing enzyme, catalytic polypeptide-like 3B
8073081	APOBEC3F	4.9	2.4	1.4	3.0	apolipoprotein B mRNA editing enzyme, catalytic polypeptide-like 3F
8073088	APOBEC3G	9.5	5.2	1.3	5.9	apolipoprotein B mRNA editing enzyme, catalytic polypeptide-like 3G
8035304	BST2	2.5	3.9	1.2	2.5	bone marrow stromal cell antigen 2
7996403	C16orf70	2.4	1.6	1.1	1.6	chromosome 16 open reading frame 70
8126371	CCND3	2.2	1.8	1.1	1.6	cyclin D3
8007188	CNP	3.8	2.3	1.3	2.1	2',3'-cyclic nucleotide 3' phosphodiesterase
8169995	FAM122C	3.9	2.3	1.2	2.2	family with sequence similarity 122C
8152812	FAM84B	2.3	1.3	1.0	1.0	family with sequence similarity 84, member B
8117034	GMPR	5.6	3.5	1.2	2.7	guanosine monophosphate reductase
7976443	IFI27	3.3	16.7	1.4	6.5	interferon, alpha-inducible protein 27
7902553	IFI44	11.9	28.4	4.1	11.4	interferon-induced protein 44
7929065	IFIT1	85.6	83.3	3.3	17.5	interferon-induced protein with tetratricopeptide repeats 1
8078729	MYD88	2.9	1.9	1.3	1.6	myeloid differentiation primary response gene (88)
8108080	PHF15	3.5	2.5	1.2	2.5	PHD finger protein 15
8038225	PLEKHA4	4.9	2.3	1.5	1.7	pleckstrin homology domain containing, family A (phosphoinositide binding specific) member 4
8037794	PRKD2	4.5	2.3	1.3	1.2	protein kinase D2
8132031	PRR15	3.0	1.1	1.1	1.6	proline rich 15
7941865	RAD9A	2.6	1.3	1.0	1.4	RAD9 homolog A (S. pombe)
7927120	RET	4.8	3.4	1.1	1.5	ret proto-oncogene
8084732	RTP4	11.4	9.4	4.9	6.2	receptor (chemosensory) transporter protein 4
8140967	SAMD9	1.4	12.4	1.4	4.7	sterile alpha motif domain containing 9
8081710	SIDT1	5.5	2.4	1.0	1.7	SID1 transmembrane family, member 1
7916403	SSBP3	2.2	1.4	0.9	1.4	single stranded DNA binding protein 3
7990839	STARD5	5.7	2.9	2.1	4.6	StAR-related lipid transfer (START) domain containing 5
7964119	STAT2	6.1	4.5	3.0	6.6	signal transducer and activator of transcription 2, 113kDa
8156060	TLE4	6.8	2.6	1.3	2.5	transducin-like enhancer of split 4 (E(sp1) homolog, Drosophila)
8088054	TMEM110	3.1	1.8	1.1	1.9	transmembrane protein 110
8087485	UBA7	3.6	4.2	1.0	1.4	ubiquitin-like modifier activating enzyme 7
8071155	USP18	14.3	10.0	2.4	4.8	ubiquitin specific peptidase 18
7979757	ZFYVE26	2.4	1.3	1.1	1.3	zinc finger, FYVE domain containing 26

Supplementary Table VI.

Amount of positive cells per high power field in AHC liver biopsies.

Patient 1	pSTAT1	CD3	CD8	CD20	CD56	CD123
1	4	9	10	0	0	0
2	8	25	10	1	1	0
3	32	53	25	2	4	3
4	3	11	14	0	0	0
5	1	11	11	0	0	0
Mean	9.6	21.8	14	0.6	1	0.6

Patient 2	pSTAT1	CD3	CD8	CD20	CD56	CD123
1	32	47	*65*	1	-	-
2	38	53	*55*	2	-	-
3	44	43	*45*	3	-	-
4	30	59	*39*	1	-	-
5	38	40	*60*	2	-	-
Mean	36.4	48.4	52.8	1.8	-	-

Patient 3	pSTAT1	CD3	CD8	CD20	CD56	CD123
1	62	33	148	1	0	0
2	11	30	32	0	0	1
3	5	23	35	0	0	1
4	16	34	37	1	0	1
5	0	22	18	1	1	0
Mean	18.8	28.4	30.5	0.6	0.2	0.6

Patient 4	pSTAT1	CD3	CD8	CD20	CD56	CD123
1	46	47	33	11	0	2
2	15	20	27	0	0	1
3	10	10	19	1	0	0
4	15	18	19	2	0	0
5	10	16	8	1	0	1
Mean	19.2	22.2	21.2	3	0	0.8

Patient 5	pSTAT1	CD3	CD8	CD20	CD56	CD123
1	36	39	31	1	0	-
2	47	49	60	1	0	-
3	24	26	39	0	0	-
4	31	24	29	1	0	-
5	23	28	35	0	0	-
Mean	32.2	33.2	38.8	0.6	0	-

Patient 6	pSTAT1	CD3	CD8	CD20	CD56	CD123
1	12	49	41	1	0	0
2	11	41	34	0	0	1
3	16	31	29	2	0	0
4	3	29	34	0	0	0
5	12	34	42	1	0	0
Mean	10.8	36.8	36	0.8	0	0.2

Supplementary Table VII.

Primer sequences used for real-time RT-PCR analysis

Gene	Forward primer sequence	Reverse primer sequence
GAPDH	5' GCTCCTCCTGTTCGACAGTCA 3'	5' ACCTTCCCCATGGTGTCTGA 3'
IFNγ	5' GAAATATTTTAATGCAGGTCATTCAG 3'	5' TCTTTTGGATGCTCTGGTCA 3'
USP18	5' CTCAGTCCCGACGTGGAACT 3'	5' ATCTCTCAAGCGCCATGCA 3'
IFI27	5' GGCAGCCTTGTGGCTACTCT 3'	5' CCCAGGATGAACTTGGTCAATC 3'
IFIT1	5' CCCTGCAGAACGGCTGCCTA 3'	5' TCAGGGCTTCCTCATTCTGGCCT 3'
GBP5	5' CGCAAAGGTTGGCGGCGATT 3'	5' AGCTGTGCAGCCTGTTCCTGC 3'
HLA-DMB	5' ACCAACAGGACACGGCCACCA 3'	5' TGCGCACTGCTGTGAGGCAT 3'
IFNα	5' GACCTGGAAGCCTGTGTGA 3'	5' GACAACCTCCCAGGCACAA 3'
IFNβ	5' TGCTCTGGCACAACAGGTAG 3'	5' GCTGCAGCTGCTTAATCTCC 3'

Supplementary Table VIII.

Primary antibodies used for immunohistochemistry or Western Blot

Antibody	Dilution IHC	Dilution WB	Catalogue No.	Company
PY701-STAT1	1:300	1:1000	#9171	Cell Signalling
USP18	1:50	1:1000	#4813	Cell Signalling
CD3	1:600	-	#A0452	DAKO
CD8	1:1000	-	#M7103	DAKO
CD20	1:500	-	#M0755	DAKO
CD56	1:200	-	NCL-CD56-1B6	Novocastra
CD123	1:50	-	#554527	BD Biosciences
STAT1	-	1:1000	#610186	BD Biosciences
MAVS	-	1:500	ALX-804-847	Enzo Life Sciences
β-Actin	-	1:2000	A5441	Sigma

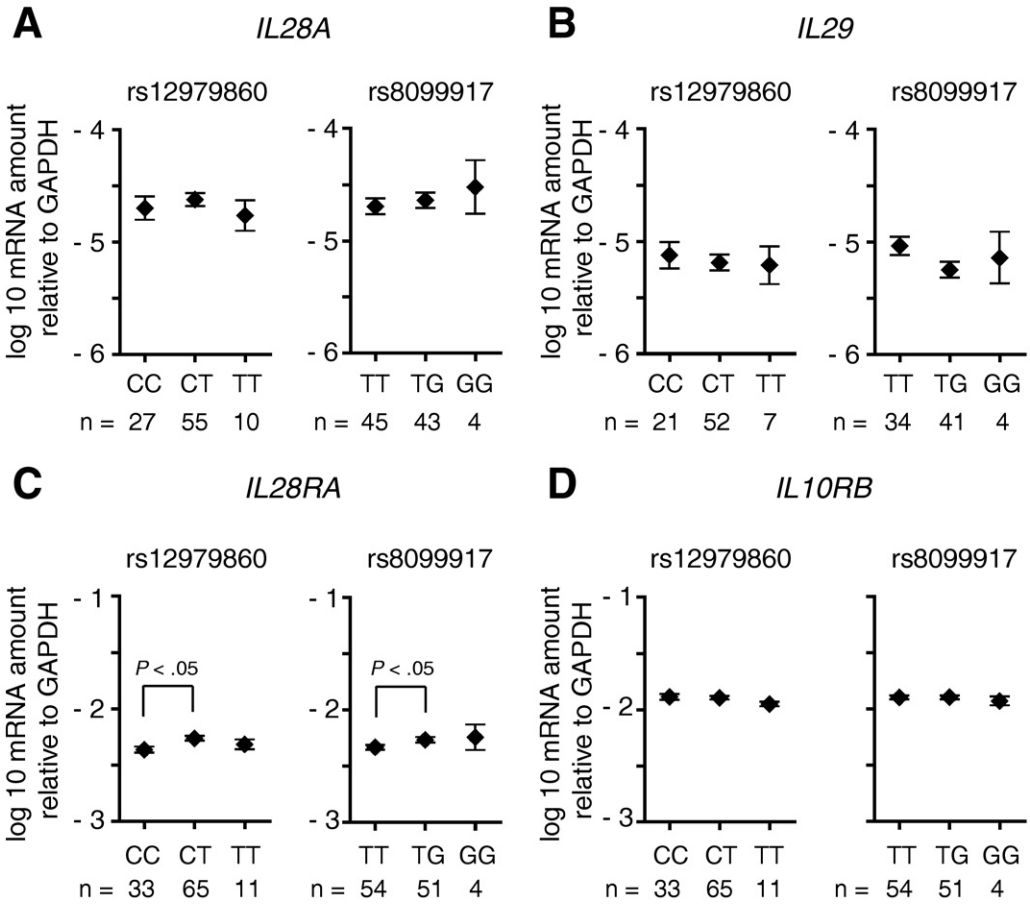

Supplementary Figure 1. Association of *IL28B* SNPs with hepatic mRNA expression of (*A*) *IL28A*, (*B*) *IL29* (IFNλ1), (*C*) *IL28RA*, and (*D*) *IL10Rβ*. Expression levels were determined by quantitative reverse-transcription polymerase chain reaction and normalized relative to GAPDH mRNA. Shown are the mean values (±SEM) after $\log_{10}$ transformation. The only statistical significant differences (Student *t* test) were found for *IL28RA* between the rs12979860 CC and CT groups and the rs8099917 TT and TG groups.

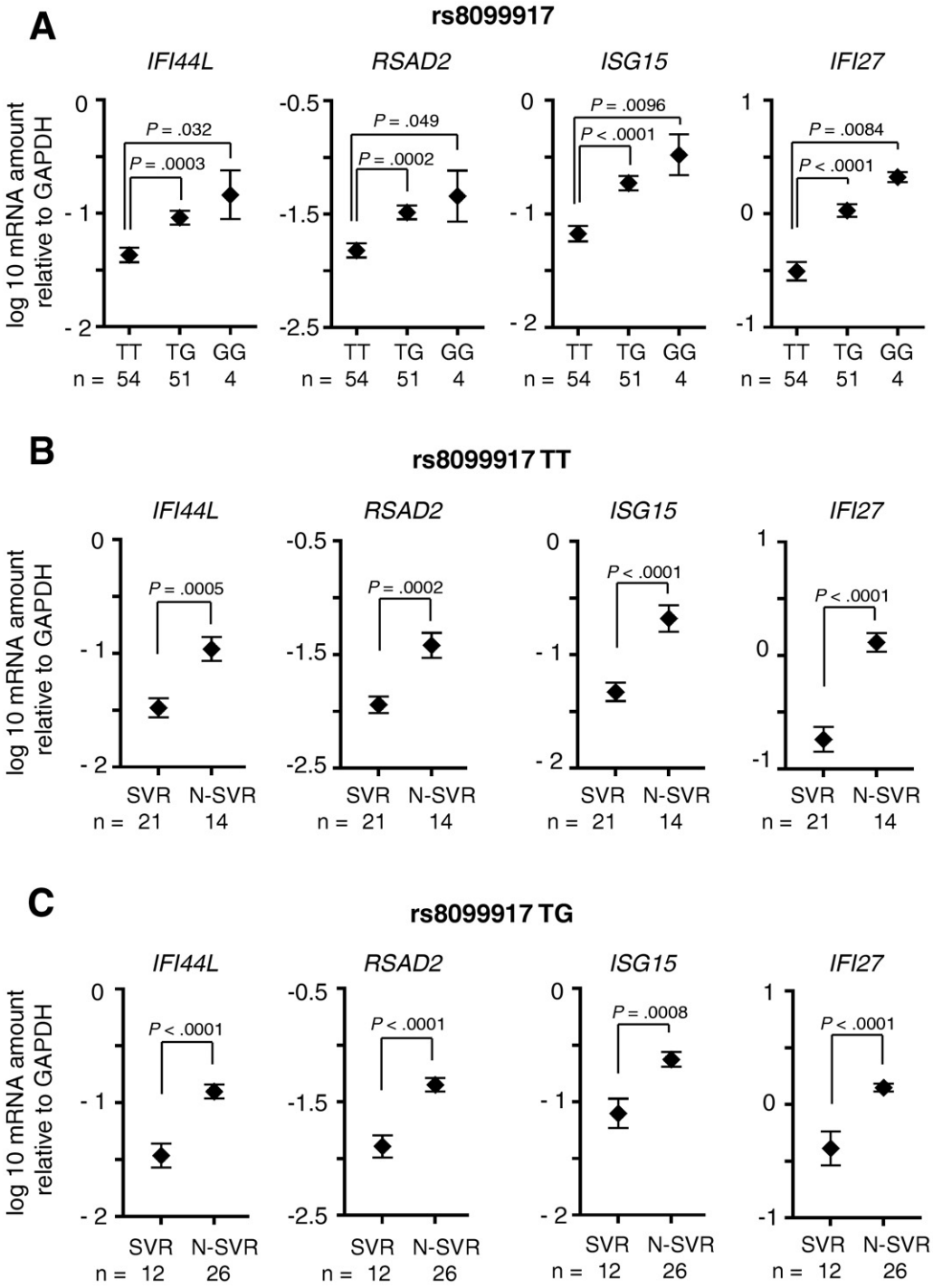

Supplementary Figure 2. Hepatic ISG expression according to *IL28B* genotypes (SNP = rs8099917). (*A*) Expression of 4 ISGs (*IFI44L*, *RSAD2*, *ISG15*, *IFI27*) in the liver according to the *IL28B* genotype (rs8099917) in 109 patients with CHC. (*B*) Hepatic expression of 4 ISGs (*IFI44L*, *RSAD2*, *ISG15*, *IFI27*) in 35 patients with rs8099917 TT genotype, stratified according to treatment response (SVR vs non-SVR). (*C*) Hepatic expression of 4 ISGs (*IFI44L*, *RSAD2*, *ISG15*, *IFI27*) in 38 patients with rs8099917 TG genotype, stratified according to treatment response (SVR vs non-SVR). Shown are mean values (±SEM) after log transformation. *P* values were obtained with Student *t* test. The number of patients in each group is shown below the plots.

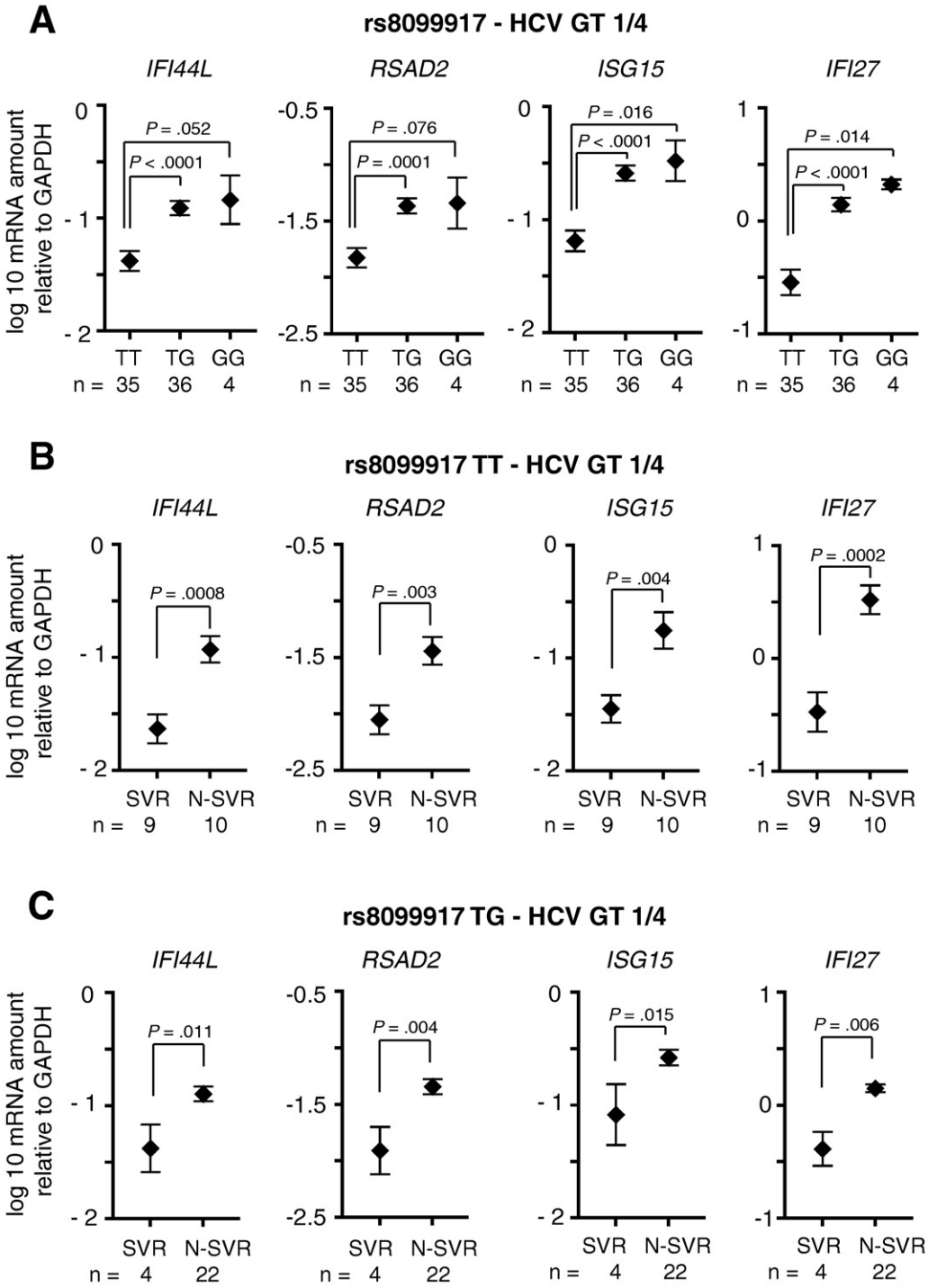

Supplementary Figure 3. Hepatic ISG expression according to *IL28B* genotypes (SNP = rs8099917) in patients infected with HCV genotype 1 or 4. (*A*) Expression of 4 ISGs (*IFI44L*, *RSAD2*, *ISG15*, *IFI27*) in the liver according to the *IL28B* genotype (rs8099917) in 75 patients with CHC infected with HCV genotype 1 or 4. (*B*) Hepatic expression of 4 ISGs (*IFI44L*, *RSAD2*, *ISG15*, *IFI27*) in 19 patients with rs8099917 TT genotype, stratified according to treatment response (SVR vs non-SVR). (*C*) Hepatic expression of 4 ISGs (*IFI44L*, *RSAD2*, *ISG15*, *IFI27*) in 26 patients with rs8099917 TG genotype, stratified according to treatment response (SVR vs non-SVR). Shown are mean values (±SEM) after log transformation. *P* values were obtained with Student *t* test. The number of patients in each group is shown below the plots.

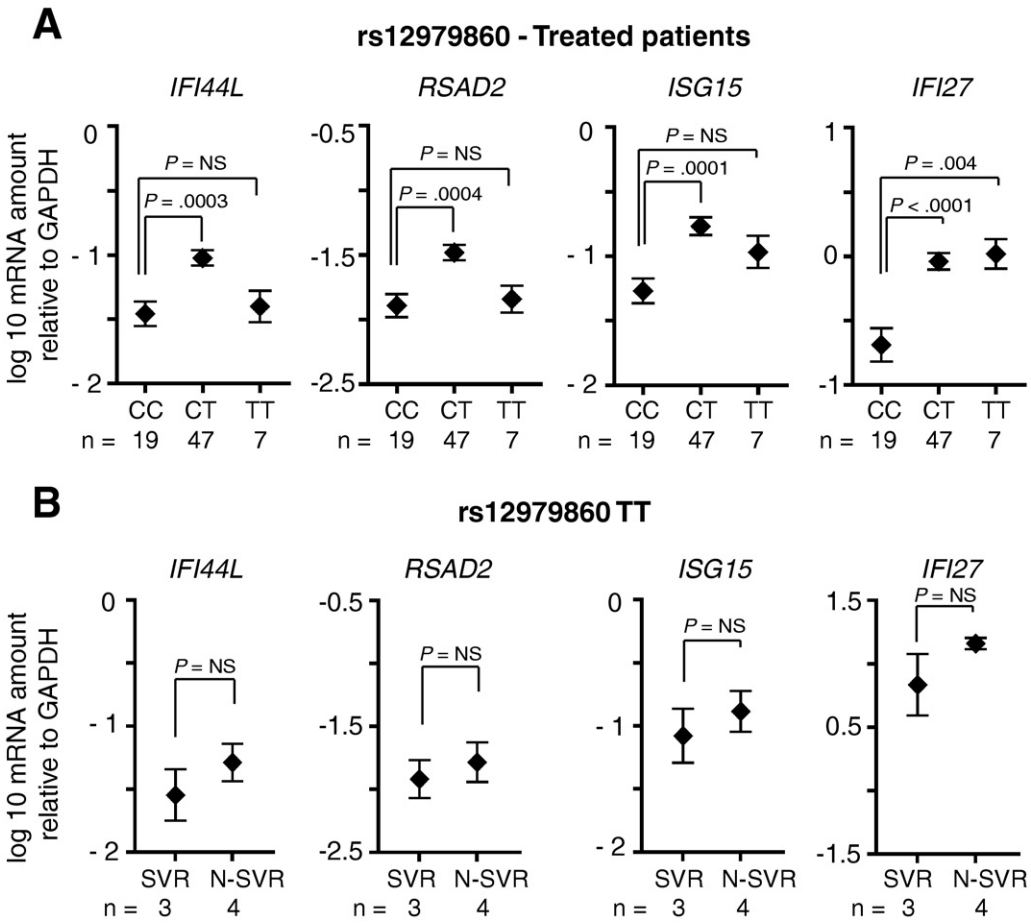

Supplementary Figure 4. (*A*) Expression of 4 ISGs (*IFI44L*, *RSAD2*, *ISG15*, *IFI27*) in the liver according to the *IL28B* genotype (rs12979860) in the subset of 73 patients with CHC who have undergone treatment with pegIFN-α and ribavirin. (*B*) Hepatic expression of 4 ISGs (*IFI44L*, *RSAD2*, *ISG15*, *IFI27*) in 7 patients with the rs12979860 TT genotype, stratified according to treatment response (SVR vs non-SVR). Due to the small number of patients, the difference is not significant. Shown are mean values (±SEM) after log transformation. *P* values were obtained with Student *t* test. The number of patients in each group is shown below the plots.

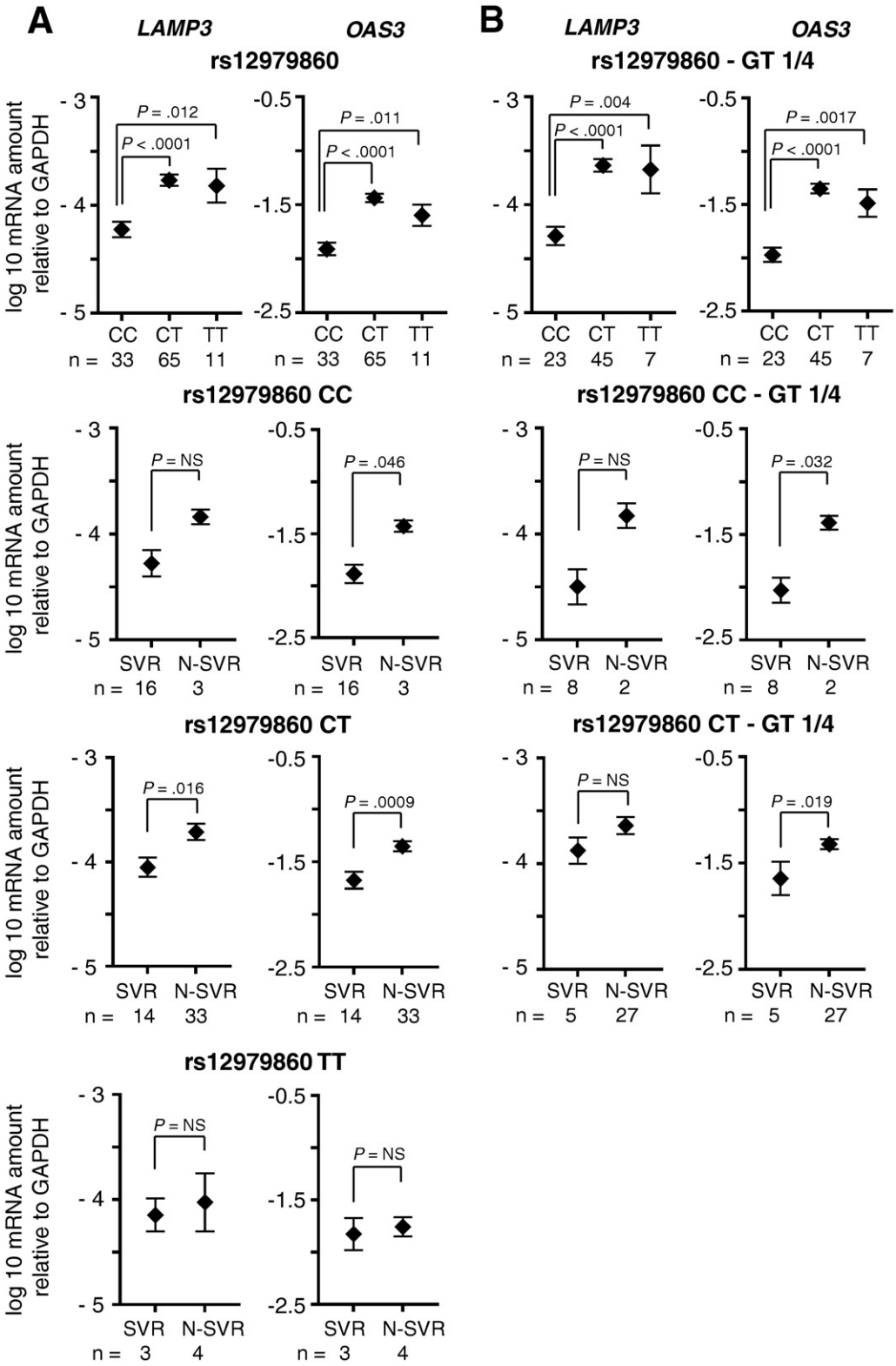

Supplementary Figure 5. (*A*) Expression of 2 ISGs (*LAMP3*, *OAS3*) in the liver according to the *IL28B* genotype (rs12979860) in all 109 patients with CHC and in patients with either CC, CT, or TT *IL28B* genotype stratified according to treatment response (SVR vs non-SVR). (*B*) Expression of 2 ISGs (*LAMP3*, *OAS3*) in the liver according to the *IL28B* genotype (rs12979860) in all 75 patients infected with HCV genotype 1 or 4 and in patients with either CC or CT *IL28B* genotype stratified according to treatment response (SVR vs non-SVR). Shown are mean values (±SEM) after log transformation. *P* values were obtained with Student *t* test. The number of patients in each group is shown below the plots.

Supplementary Table 1. Patient Characteristics and SNP Genotypes

No.	Sex	Age (*y*)	HCV genotype	Viral load (*IU/mL*)	METAVIR score	Treatment	rs12979860	rs8099917
1	M	37	3a	247,290	A2/F2	SVR	TT	TG
2	M	37	3a	78,684	A1/F2	SVR	CT	TT
3	M	38	1a	9,638,894	A2/F1	SVR	CC	TT
4	F	63	2a/c	3,306,636	A2/F3	SVR	CT	TT
5	F	53	2a/c	1,196,303	A2/F3	SVR	CT	TG
6	M	61	4f	14,552,681	A3/F4	SVR	CT	TG
7	M	47	2b	4,663,883	A3/F4	SVR	CT	TG
8	M	33	3a	1,683,442	A2/F1	SVR	CC	TT
9	M	49	3a	12,381,160	A2/F2	SVR	CC	TT
10	F	38	1b	8,002,763	A2/F3	SVR	CC	TT
11	M	40	3a	2,531,993	A3/F3	SVR	CT	TT
12	M	41	3a	15,538,256	A1/F1	SVR	CC	TT
13	M	44	1b	67,587	A2/F4	SVR	CT	TG
14	F	24	1b	440	A2/F2	SVR	CC	TT
15	F	50	1b	16,639,113	A1/F2	SVR	CC	TT
16	F	24	3a	805,551	A2/F3	SVR	CC	TT
17	M	38	4	12,000	A2/F2	SVR	CC	TT
18	F	54	3a	75,644	A2/F4	SVR	CC	TT
19	M	49	4	165,330	A3/F4	SVR	CT	TT
20	M	34	4	173,000	A2/F2	SVR	CT	TG
21	M	45	4	1,331,047	A2/F2	SVR	CC	TT
22	F	47	3a	7850	A3/F4	SVR	CT	TT
23	F	48	3a	13,790	A1/F1	SVR	CT	TT
24	M	44	3	419,083	A2/F2	SVR	TT	TG
25	F	20	2a	87,375	A1/F2	SVR	TT	TG
26	M	29	1b	384,525	A2/F2	SVR	CT	TG
27	F	48	3a	28,368	A2/F3	SVR	CC	TT
28	F	42	3a	234,210	A3/F4	SVR	CC	TG
29	M	34	3a	3,145,764	A3/F2	SVR	CC	TT
30	F	44	3a	319,000	A2/F3	SVR	CT	TG
31	M	35	4	4,491,065	A2/F3	SVR	CC	TT
32	F	31	3a	249,240	A1/F1	SVR	CT	TG
33	M	27	1b	3102	A3/F4	SVR	CC	TT
34	M	36	3a	1,480,000	A1/F1	PNR	CT	TG
35	M	67	1b	2,137,002	A1/F2	No EoTR	CT	TG
36	F	47	1a	1,444,062	A2/F2	PNR	CT	TG
37	M	48	1b	713,046	A3/F4	PNR	CT	TG
38	F	52	1a	4,458,717	A2/F2	PNR	CT	TG
39	F	38	2	5,780,000	A2/F3	No EoTR	TT	TT
40	M	41	1	12,328,724	A2/F3	PNR	CT	TT
41	M	59	1b	191,299	A3/F3	PNR	CT	TG
42	M	63	1	1,752,158	A3/F4	No EoTR	CT	TG
43	M	56	1b	7,790,643	A2/F3	PNR	CT	TG
44	M	48	1b	2,949,376	A2/F4	PNR	CT	TT
45	M	48	1a	36,108,528	A1/F2	PNR	CT	TT
46	F	58	2	5,262,008	A2/F4	No EoTR	CT	TG
47	F	37	1a	953,556	A3/F3	PNR	CT	TG
48	M	61	1a	5,545,733	A2/F4	PNR	TT	TG
49	M	62	1a	5,624,281	A3/F4	PNR	TT	TG
50	M	54	1	222,053	A3/F4	No EoTR	CC	TT
51	M	45	4	321,000	A2/F2	PNR	CT	TG
52	F	41	1a	321,000	A2/F2	PNR	CT	TG
53	F	36	1a	717,000	A2/F2	PNR	CT	TG
54	M	51	1b	851,138	A3/F4	PNR	CT	TG
55	M	49	4c	371,535	A1/F2	No EoTR	CT	TG
56	F	50	3	1,123,718	A3/F4	PNR	CT	TG
57	F	48	1a	2,834,081	A3/F2	PNR	CT	TT
58	M	50	1	6,216,555	A3/F2	PNR	CT	TT
59	F	38	1	362,282	A1/F2	PNR	CT	TG
60	M	48	1b	245,062	A2/F4	PNR	CT	TG
61	M	48	4b	3,201,553	A2/F4	No-EoTR	TT	TT
62	M	42	1a	4,291,956	A2/F3	No EoTR	CT	TG
63	M	60	1b	4,326,723	A3/F3	PNR	CT	TG

Supplementary Table 1. Continued

No.	Sex	Age (*y*)	HCV genotype	Viral load (*IU/mL*)	METAVIR score	Treatment	rs12979860	rs8099917
64	M	55	1a	1,710,592	A3/F4	PNR	CT	TT
65	M	45	1b	2,910,319	A1/F4	EoTR, relapse	CT	TG
66	F	52	2a/c	72,157	A2/F4	EoTR, relapse	CC	TT
67	F	48	3a	13,538,256	A2/F3	EoTR, relapse	CT	TT
68	M	42	3	2,085,698	A1/F2	EoTR, relapse	CT	TG
69	M	40	1a	15,900,000	A3/F4	EoTR, relapse	CC	TT
70	M	44	1a	3,884,688	A2/F3	EoTR, relapse	CT	TG
71	M	53	1b	770,000	A2/F4	EoTR, relapse	CT	TT
72	M	55	3	578,305	A2/F2	EoTR, relapse	CT	TT
73	F	34	1b	36,000	A1/F2	EoTR, relapse	CT	TG
74	M	35	1b	1,578,381	A1/F2	EoTR	CT	TT
75	F	56	3a	712,846	A2/F2	EoTR	CT	TT
76	M	37	3a	828,467	A2/F3	EoTR	CC	TT
77	M	36	3a	1,140,000	A2/F3	EoTR	CT	TG
78	M	51	1b	241,223	A1/F2	EoTR	CT	TG
79	M	43	1b	1,089,515	A2/F2	EoTR	CT	TG
80	M	49	1a	1,484,271	A2/F2	EoTR	CC	TT
81	M	35	1b	17,594	A1/F2	EoTR	CC	TT
82	M	58	1b	57,791	A2/F2	Ongoing	TT	GG
83	M	37	3a	6,420,826	A2/F2	Ongoing	CT	TT
84	F	47	1	7,500,000	A3/F3	Ongoing	CC	TT
85	M	48	4	45,523	A1/F4	Ongoing	TT	GG
86	M	45	1	5,632,925	A2/F3	Ongoing	CC	TT
87	F	48	1a	3,107,291	A3/F4	Ongoing	CC	TT
88	M	46	1b	69,000,000	A1/F2	Interrupted	CC	TT
89	M	55	1a	788,024	A1/F1	Interrupted	CC	TT
90	M	46	1a	1,218,968	A1/F1	Interrupted	TT	GG
91	M	39	1a	3,427,262	A1/F2	Interrupted	CC	TT
92	M	42	1a	3,556,921	A1/F1	No treatment	CT	TG
93	M	43	1a	792,776	A1/F1	No treatment	CT	TG
94	F	41	1a	4,519,497	A2/F1	No treatment	CC	TT
95	F	48	4	88,216	A1/F1	No treatment	TT	GG
96	M	51	4e	864,372	A3/F4	No treatment	CT	TG
97	M	57	1	10,327,448	A1/F1	No treatment	CT	TG
98	F	53	1	–	A3/F4	No treatment	CT	TG
99	F	69	1b	1,686,605	A1/F2	No treatment	CT	TG
100	F	67	3a	265,382	A3/F4	No treatment	CT	TG
101	M	35	1a	3,378,710	A1/F1	No treatment	CT	TT
102	M	50	1b	2,230,542	A1/F1	No treatment	CC	TT
103	M	54	1a	4,625,025	A2/F2	No treatment	CC	TT
104	F	53	3a	228,439	A2/F4	No treatment	CT	TG
105	F	44	1	90,124	A1/F1	No treatment	CT	TG
106	M	45	1	135,556	A3/F2	No treatment	CC	TT
107	F	47	1b	10,527,018	A3/F3	No treatment	CT	TT
108	F	45	1a	551,185	A1/F1	No treatment	CT	TG
109	M	46	1a	3,380,665	A2/F2	No treatment	CC	TT

M, male; F, female; PNR, primary non-response: < 2 log 10 reduction of viral load after 12 weeks of treatment; EoTR, end of treatment response: negative viral load at the end of treatment; SVR, sustained virological response: negative viral load 6 months after end of treatment.

Supplementary Table 2. Primer Sequences Used for Real-Time Reverse-Transcription Polymerase Chain Reaction Analysis

Gene	Forward primer sequence	Reverse primer sequence
GAPDH	5′ GCTCCTCCTGTTCGACAGTCA 3′	5′ ACCTTCCCCATGGTGTCTGA 3′
IFI44L	5′ GCTGCGGGCTGCAGAT 3′	5′ CTCTCTCAATTGCACCAGTTTCC 3′
RSAD2	5′ CTTTGTGCTGCCCCTTGAG 3′	5′ TCCATACCAGCTTCCTTAAGCAA 3′
ISG15	5′ TCCTGCTGGTGGTGGACAA 3′	5′ TTGTTATTCCTCACCAGGATGCT 3′
IFI27	5′ GGCAGCCTTGTGGCTACTCT 3′	5′ CCCAGGATGAACTTGGTCAATC 3′
LAMP3	5′ GCGGCCGCGCTCTT 3′	5′ TTTGACTGCCATCGTGCAA 3′
OAS3	5′ TCTCCCATCAAAGTGATCAAGGT 3′	5′ CCACGAGGTCGGCATCTG 3′
LGALS3BP	5′ GGCTGGCTGAAGAGCAACTG 3′	5′ GTGGGTGCTCCTGGTTTCAT 3′
HTATIP2	5′ GGGCGGAGGGATTTGTTC 3′	5′ TGCCAGCTCTGCAGACTTCA 3′
IL28A	5′ GACCCAGCCCTGGTGGAC 3′	5′ CTGGATACAGGCCCGGAA 3′
IL28B	5′ GGCCTTTAAGAGGGCCAAAG 3′	5′ GGCGGGAGCGGCACT 3′
IL29	5′ CACAGGAGCTAGCGAGCTTCA 3′	5′ TTTTCAGCTTGAGTGACTCTTCCA 3′
IL28RA	5′ TGACCTATTTTGTGGCCTATCAGA 3′	5′ GTTCCCGCACACTCTTCCA 3′
IL10RB	5′ GCAAACAACCCATGACGAAA 3′	5′ CCGAGGCCATGAGGATGAC 3′

Supplementary Table 3. Gene Expression Relative to GAPDH (log_{10} transformed)

No.	*IFI44L*	*RSAD2*	*ISG15*	*IFI27*	*LAMP3*	*OAS3*	*LGALS3BP*	*HTATIP2*	*IL28A*	*IL28B*	*IL29*	*IL28RA*	*IL10RB*
1	−1.2312	−1.6843	−0.6969	0.3176	−3.8908	−1.5518	−0.3281	−1.3983	−5.1276	−4.8029	Undetected	−2.2788	−1.8950
2	−1.5217	−1.8890	−1.3817	−0.9663	−4.4823	−1.9733	−0.8640	−1.2192	−3.9896	−6.1944	Undetected	−2.2457	−1.7746
3	−1.8905	−2.2472	−1.4374	−1.1364	−4.5335	−2.1102	−0.8323	−1.4675	−5.1412	−4.2750	−5.5028	−2.3510	−1.8589
4	−1.4675	−2.0485	−1.5006	−0.8098	−4.5847	−1.7746	−0.7511	−1.4254	−4.9727	−4.5275	−5.1476	−2.4700	−1.9973
5	−1.7475	−2.2502	−1.4389	−1.0340	−4.1045	−1.8513	−0.8474	−1.4826	−4.3454	−4.5586	−5.8881	−2.4865	−2.0666
6	−1.8844	−2.3902	−1.3426	−1.2884	−4.3469	−2.1208	−0.6653	−1.3245	−4.5877	−4.5060	Undetected	−2.3149	−1.8002
7	−1.6948	−2.0621	−1.4630	−0.7360	−4.1723	−1.7625	−0.5720	−1.4720	−5.2883	−5.6367	−5.8114	−2.4504	−2.0982
8	−2.0455	−2.3721	−1.9130	−0.9964	−4.7262	−2.3390	−0.9693	−1.4796	−5.3076	Undetected	Undetected	−2.5572	−2.1614
9	−1.2177	−1.7204	−1.1259	−0.1039	−3.9796	−1.5563	−0.4004	−1.4811	−4.3604	−5.9748	−4.5817	−2.4429	−2.0816
10	−1.7415	−2.2457	−1.5292	−1.2523	−4.8240	−2.3525	−1.0672	−1.1800	Undetected	Undetected	−5.4336	−2.2306	−1.7941
11	−1.4449	−1.9311	−1.2222	−0.4094	−4.3574	−1.6858	−0.4305	−1.1409	−4.6802	Undetected	Undetected	−2.2698	−1.8860
12	−1.4495	−1.9371	−1.6000	−1.0521	−4.6494	−1.9898	−0.8128	−1.4043	Undetected	−4.4011	Undetected	−2.6355	−1.9356
13	−1.5127	−2.1283	−1.7068	−0.7435	−3.8667	−1.9206	−0.5990	−1.4464	Undetected	Undetected	−4.5320	−2.2713	−1.8107
14	−1.5473	−2.0846	−1.7053	−0.8128	−3.8306	−1.8483	−0.6261	−1.4284	Undetected	−4.6961	−5.9092	−2.3405	−1.8664
15	−2.0470	−2.4052	−1.4991	−1.7821	−4.5862	−2.1659	−1.0822	−1.2523	Undetected	−4.2460	Undetected	−2.2306	−1.8905
16	−1.8257	−2.1930	−1.2523	−0.9934	−3.9134	−1.8528	−0.7089	−1.2688	−4.2174	−4.6855	Undetected	−2.2517	−1.5834
17	−2.2231	−2.6024	−2.1238	−1.4570	−5.1401	−2.5467	−1.1499	−1.5669	−5.3265	Undetected	Undetected	−2.6235	−2.0997
18	−0.7947	−1.3622	−0.5689	0.0602	−3.4016	−1.1981	−0.1656	−1.2688	−4.2927	−4.7066	−4.4778	−2.0380	−1.6120
19	−1.1695	−1.5112	−0.8489	−0.0060	−3.7839	−1.3637	−0.2920	−1.4359	−4.5591	−4.4869	−4.8105	−2.4203	−2.0922
20	−0.9121	−1.5924	−0.7767	0.2724	−3.7569	−1.4781	−0.7014	−1.3712	−4.3032	−5.0633	−4.6991	−2.5211	−1.9748
21	−1.0672	−1.4645	−1.1123	−0.5494	−4.8391	−1.5036	−0.6021	−1.3381	−4.3695	Undetected	−5.0137	−2.0816	−1.8047
22	−1.4163	−1.9763	−1.4495	−0.5765	−3.9962	−1.7294	−0.5449	−1.3983	−4.7533	−4.8406	Undetected	−2.3510	−1.7520
23	−1.0145	−1.5533	−0.8895	−0.0166	−3.9013	−1.5036	−0.7450	−1.1800	−5.3050	Undetected	Undetected	−2.1584	−1.8092
24	−1.9281	−2.2005	−1.4374	−0.4034	−4.4342	−2.0831	−0.7119	−1.3622	−5.4476	−5.4216	−5.8144	−2.4022	−2.0244
25	−1.4826	−1.8694	−1.1018	−0.4109	−4.1151	−1.8408	−0.6954	−1.4269	−4.7849	−5.5751	−5.2936	−2.4323	−1.9386
26	−1.1981	−1.5262	−0.5118	0.2785	−3.6214	−1.3456	−0.5388	−1.4645	Undetected	−5.0874	−5.6037	−2.1253	−1.7234
27	−1.0717	−1.5879	−0.9151	−0.1279	−3.8938	−1.5217	−0.5464	−1.4645	−4.4720	−4.7317	−5.0754	−2.3014	−2.0741
28	−1.4314	−1.8333	−1.1168	−0.4666	−3.9600	−1.6918	−0.2619	−1.4359	−3.6590	−5.4104	−6.1651	−2.4820	−1.9657
29	−1.1138	−1.7384	−1.0446	−0.7782	−3.9209	−1.7746	−0.7345	−1.1590	Undetected	Undetected	−4.7442	−1.9597	−1.5684
30	−0.8143	−1.2357	−0.2378	−0.1430	−3.4016	−1.0130	−0.4832	−1.5051	Undetected	−4.6976	−5.3418	−1.9973	−1.6060
31	−1.5157	−2.0365	−1.5473	−0.9844	−4.4041	−1.9025	−0.6999	−1.3260	−5.2205	Undetected	−5.8746	−2.4594	−1.8814
32	−1.7309	−1.9281	−1.4028	−0.2845	−4.3409	−1.9236	−0.6412	−1.2839	−4.9809	−5.0918	Undetected	−2.2382	−1.6888
33	−1.4841	−1.8694	−1.2297	−0.7872	−3.8306	−1.7971	−0.6939	−1.2974	−4.3970	−4.3657	−4.8225	−2.4895	−1.8679
34	−1.1861	−1.6903	−1.2448	0.0271	−4.1783	−1.7144	−0.8113	−1.5337	−4.0323	−4.2129	Undetected	−2.5226	−1.9657
35	−1.0792	−1.2538	−0.7977	0.0075	−3.4950	−1.3531	−0.4741	−1.3531	−4.5372	−5.5555	−5.2138	−2.4293	−2.0094
36	−0.2438	−0.7466	0.0978	0.3883	−3.0223	−0.8384	−0.0015	−1.2177	−4.3348	−5.6232	−4.8270	−1.7911	−1.7099
37	−1.1830	−1.3802	−0.5705	0.0211	−3.3324	−1.4103	−0.2920	−1.3938	Undetected	Undetected	−5.1566	−2.4022	−1.9928
38	−0.8941	−1.3260	−0.5388	−0.3658	−3.4664	−1.2282	−0.2213	−1.1575	−4.7081	−5.2523	−5.4562	−2.1539	−1.9040
39	−1.3832	−1.7866	−0.5464	0.2890	−3.8502	−1.6933	−0.4395	−1.2673	Undetected	−5.0395	Undetected	−2.4158	−1.9371
40	−0.2529	−0.7315	0.1008	0.5358	−3.0088	−0.8730	0.1054	−0.9528	−3.9164	−5.2261	−4.5275	−1.8122	−1.6406
41	−0.6472	−1.2568	−0.4591	0.1626	−3.4257	−1.3592	−0.2393	−1.2553	−5.3493	−4.9027	−4.6374	−2.2637	−2.0515
42	−0.6999	−1.2086	−0.6382	0.1731	−3.3219	−1.1966	−0.1325	−1.3020	Undetected	−5.1633	−4.8827	−2.2382	−1.9115
43	−0.8038	−1.3847	−0.5178	0.3131	−3.4889	−1.3682	−0.1144	−1.3471	−4.2838	−5.4493	−4.9881	−1.9447	−1.7309
44	−0.7541	−1.3381	−0.7661	−0.0045	−3.9811	−1.5337	−0.4079	−1.2839	Undetected	−4.9233	−5.1807	−2.4218	−1.9447
45	−0.7526	−1.2658	−0.2860	0.3658	−3.5973	−1.3050	−0.5750	−1.2538	−4.5425	−5.1024	−5.3884	−2.1945	−1.9266
46	−0.4726	−0.9768	−1.0295	−0.0421	−4.6870	−1.4058	−0.3221	−1.3306	Undetected	−4.4929	−4.2325	−2.3902	−1.9130
47	−0.5509	−0.8835	−0.1505	0.4470	−3.6741	−1.0295	−0.2815	−1.3004	−4.0940	−4.9158	−5.2003	−2.0997	−1.9191
48	−1.6210	−2.1162	−1.2764	0.1264	−4.8225	−2.0274	−1.0973	−1.4118	−4.5440	−5.1551	Undetected	−2.3315	−2.0711
49	−0.9136	−1.3637	−0.7134	0.1340	−3.5461	−1.6195	−0.4184	−1.3531	−4.6122	−5.8415	−4.8074	−2.2833	−1.9657
50	−0.8956	−1.3080	−0.7195	0.0692	−3.9435	−1.4540	−0.5539	−1.4480	−4.5804	Undetected	−4.5576	−2.2412	−1.8935
51	−0.7797	−1.1981	−0.1595	0.5178	−3.4814	−1.2794	−0.1550	−1.2026	−4.5757	−5.8294	−4.5320	−2.1238	−1.9040
52	−1.1228	−1.4043	−0.5087	0.1656	−3.9706	−1.4766	−0.4425	−1.1620	−4.6044	Undetected	−5.2259	−2.3691	−2.0034
53	−0.4862	−0.9212	−0.3356	0.2724	−3.3414	−1.0145	−0.0512	−1.2026	−4.7217	−5.7753	−5.1536	−2.2231	−1.6993
54	−0.6141	−1.0416	−0.3943	0.1460	−3.2075	−1.0235	−0.0467	−1.2598	−4.5675	−4.6690	−4.9444	−2.2246	−1.9025
55	−0.8579	−1.3787	−0.6021	0.2860	−3.5296	−1.2929	−0.1942	−1.3998	−4.6178	−5.4818	−5.5495	−2.3465	−2.0651
56	−0.6969	−1.2899	−0.4832	0.1912	−3.7418	−1.2794	−0.3898	−1.1319	−4.4989	−5.3922	−5.5073	−2.3119	−1.9221
57	−0.8263	−1.1996	−0.2453	0.2167	−3.3956	−1.1364	−0.2649	−1.4269	−4.1647	−4.4430	−4.8481	−2.1840	−2.0034
58	−0.9016	−1.4856	−0.8188	0.0873	−4.0037	−1.5232	−0.5268	−1.3441	−4.4702	Undetected	−4.8707	−2.3104	−1.9477
59	−1.3607	−1.8047	−1.0942	0.0978	−4.3619	−1.8950	−0.4862	−1.3170	−5.4772	−4.3803	Undetected	−2.4293	−2.0485
60	−0.8910	−1.3426	−0.7962	0.0722	−3.7298	−1.3516	−0.2980	−1.4224	−4.6569	−5.1920	−5.6759	−2.2472	−2.0380
61	−1.2387	−1.8709	−1.0039	0.0888	−3.8848	−1.6858	−0.5930	−1.4314	−5.0327	−5.0113	Undetected	−2.3525	−1.9040
62	−1.1575	−1.6963	−0.7812	0.2589	−3.9676	−1.5247	−0.5975	−1.2884	−4.5140	−5.1126	−5.0558	−2.3661	−1.8528
63	−0.8929	−1.3592	−0.8615	0.1045	−4.4876	−1.6600	−0.3537	−1.3501	−5.1759	−5.0059	−5.5329	−2.6129	−2.0034
64	−1.0021	−1.6174	−0.9839	0.1801	−4.6302	−1.7397	−0.4440	−1.1459	−4.9280	−4.7759	−5.1792	−2.3556	−1.9221
65	−0.8173	−1.3983	−0.3582	0.1671	−3.1443	−1.1635	−0.2318	−1.0717	Undetected	−5.4486	Undetected	−2.0259	−1.8829
66	−1.0747	−1.4028	−0.9046	0.0813	−3.8637	−1.5036	−0.3382	−1.1634	−4.5297	−5.1227	−4.4688	−2.3029	−1.8965
67	−1.8920	−2.3375	−1.7294	−0.8098	−4.3815	−2.1162	−0.6871	−1.4392	−5.4532	−5.8249	Undetected	−2.4188	−2.0711
68	−1.3456	−1.5804	−0.7887	0.1701	−3.9631	−1.3381	−0.3628	−1.3604	Undetected	Undetected	−6.0296	−2.2216	−1.8739
69	−1.2267	−1.5307	−0.7526	0.0060	−3.7102	−1.3230	−0.4199	−1.2252	−4.3051	−4.4011	−4.1693	−2.2713	−1.8062
70	−1.0100	−1.2974	−0.3447	0.0467	−3.7298	−1.2839	−0.5569	−1.1575	−4.5707	−4.7623	Undetected	−2.2728	−1.7008
71	−0.6337	−1.0506	−0.4666	0.3507	−3.5928	−1.2643	−0.4275	−1.2824	−4.0792	Undetected	−4.0218	−2.2954	−2.0304
72	−0.6322	−0.9332	−0.4079	0.1565	−3.2842	−1.0867	−0.3928	−1.3501	−4.5313	−4.0731	−5.2936	−2.4323	−1.8303
73	−1.1093	−1.7971	−0.9513	−0.0181	−3.8728	−1.5834	−0.7706	−1.5819	−5.0318	−4.9252	−5.6142	−2.2984	−1.8754
74	−0.7661	−1.0912	−0.5012	0.0105	−3.7794	−1.2177	−0.6246	−1.5337	Undetected	Undetected	−4.8150	−2.1915	−2.0018
75	−1.2402	−1.6226	−0.8098	0.0346	−3.9585	−1.6873	−0.2507	−1.1191	−5.1209	−4.5659	Undetected	−2.2020	−1.8694
76	−1.8167	−2.3194	−1.7309	−1.0717	−4.4086	−2.2367	−0.8425	−1.3869	−4.9046	−4.3665	Undetected	−2.5618	−2.1223
77	−1.2342	−1.7776	−1.1003	−0.1460	−4.1151	−1.6948	−0.7119	−1.2779	−4.8150	−5.1100	−5.5495	−2.3435	−1.9913
78	−0.6578	−1.1394	−0.2785	0.5659	−3.1969	−1.0882	−0.2950	−1.2312	−4.6121	Undetected	−4.7232	−2.0952	−1.7670
79	−1.3712	−1.8604	−1.1153	−0.0542	−4.1918	−1.8137	−0.8053	−1.2478	−4.4837	−4.9773	Undetected	−2.2923	−1.7866

Supplementary Table 3. Continued

No.	*IFI44L*	*RSAD2*	*ISG15*	*IFI27*	*LAMP3*	*OAS3*	*LGALS3BP*	*HTATIP2*	*IL28A*	*IL28B*	*IL29*	*IL28RA*	*IL10RB*
80	−1.9537	−2.3586	−1.6557	−0.9994	−4.4251	−2.0094	−0.6833	−1.3622	−4.8661	−4.2784	Undetected	−2.4308	−1.7264
81	−2.2653	−2.6596	−1.9070	−1.3050	−4.6539	−2.5076	−0.9937	−1.3968	−5.3689	−4.9498	Undetected	−2.3074	−1.9567
82	−0.8775	−1.4540	−0.6292	0.2423	−3.2030	−1.2854	−0.2576	−1.3595	−4.9324	−5.4757	−5.2635	−2.4218	−2.0395
83	−1.1710	−1.6797	−0.7721	−0.1942	−3.9871	−1.5021	−0.6705	−1.2210	−4.7601	−5.0100	−5.8912	−2.4910	−1.9717
84	−1.6993	−2.1599	−1.4284	−1.0912	−4.2867	−1.8513	−0.5665	−1.2672	−4.6105	−4.1547	−5.2725	−2.4955	−1.9326
85	−1.3456	−1.8875	−0.7827	0.2544	−3.8487	−1.5789	Not measured	Not measured	−4.9338	−4.9866	−4.6148	−2.4504	−1.8739
86	−0.9814	−1.4510	−1.1243	−0.5223	−4.2972	−1.8047	−0.6517	−1.3576	Undetected	−4.9881	−5.1025	−2.3992	−1.8378
87	−1.6903	−2.1584	−1.6978	−0.8158	−4.8767	−1.9672	−0.5780	−1.3351	−5.5253	−4.8691	−5.5390	−2.4097	−1.8558
88	−2.0726	−2.5542	−1.9130	−1.5398	−4.2536	−2.2938	Not measured	Not measured	−5.2673	−5.1642	Undetected	−2.4835	−2.0214
89	−1.0235	−1.4194	−0.8775	0.2318	−4.0308	−1.5940	Not measured	Not measured	−4.1895	−5.5224	−4.5922	−2.3255	−1.9025
90	−0.8293	−1.2177	−0.5464	0.4109	−3.1608	−1.1710	Not measured	Not measured	−4.1193	−5.8129	−4.9805	−2.1057	−1.9266
91	−1.9115	−2.2637	−1.6632	−1.2764	−4.1632	−2.1253	Not measured	Not measured	−5.4894	−4.4823	−5.4938	−2.3586	−1.7701
92	−1.3245	−1.8604	−0.9482	0.3507	−3.7629	−1.6436	Not measured	Not measured	−4.7404	−4.9625	−5.1040	−2.2472	−1.6331
93	−0.4410	−0.7405	0.0241	0.4531	−3.1473	−0.8339	Not measured	Not measured	−3.8622	−4.9956	−5.0001	−2.1403	−1.9281
94	−1.6030	−2.0952	−1.5789	−1.2508	−3.7569	−1.9266	Not measured	Not measured	−4.6341	−4.6001	Undetected	−2.4233	−1.8453
95	−0.2965	−0.8068	0.0391	0.3838	−3.2556	−1.0386	Not measured	Not measured	−4.0955	−4.2446	−5.7015	−1.9973	−1.8694
96	−0.2935	−0.7932	−0.0376	0.4726	−2.9832	−0.9091	Not measured	Not measured	−3.9013	−4.7578	−4.9414	−2.1268	−1.8769
97	−0.8534	−1.3110	−0.5434	0.2769	−3.7885	−1.3682	Not measured	Not measured	−4.4944	−4.3667	−5.6850	−2.4037	−1.9717
98	−1.0566	−1.4901	−0.5945	0.2739	−3.6093	−1.4329	Not measured	Not measured	−4.1392	−5.6636	−5.3568	−2.3014	−1.8980
99	−0.6021	−1.0897	−0.2423	0.3296	−3.5326	−1.1981	Not measured	Not measured	−4.1346	Undetected	−5.5314	−2.1283	−1.9326
100	−1.7580	−2.0771	−1.0807	−0.5629	−3.9209	−1.7670	Not measured	Not measured	−5.3553	−4.7141	−5.9589	−2.4308	−2.0681
101	−0.8083	−1.2207	−0.5975	0.1791	−3.3956	−1.2132	Not measured	Not measured	−4.6514	−4.6584	−5.1085	−2.1494	−1.9808
102	−1.7640	−2.0891	−1.4525	−0.3808	−3.8908	−1.8062	Not measured	Not measured	−3.7975	−5.3780	Undetected	−2.4700	−1.8468
103	−1.9793	−2.3556	−1.7369	−0.7134	−4.4342	−2.2984	Not measured	Not measured	−5.4285	−4.2433	−5.3493	−2.3525	−1.9687
104	−1.4480	−2.0365	−1.3140	−0.2363	−3.7915	−1.8152	Not measured	Not measured	−5.6959	−5.3703	Undetected	−2.1373	−1.6587
105	−0.4937	−0.9166	−0.0798	0.4892	−3.4664	−1.1003	Not measured	Not measured	−4.4314	−5.2498	−4.7352	−1.8799	−1.7430
106	−1.5684	−2.2126	−1.6692	−1.1349	−3.7343	−2.0500	Not measured	Not measured	−4.3306	−4.4488	−5.4246	−2.4067	−1.9431
107	−1.2643	−1.7746	−1.1484	−0.4410	−3.7448	−1.7806	Not measured	Not measured	−4.0708	−5.0373	−4.6750	−2.3134	−1.8167
108	−0.4395	−0.8053	−0.2845	−0.0256	−3.3685	−1.2402	Not measured	Not measured	−4.7310	−4.8335	−5.1627	−2.1463	−1.9070
109	−1.7068	−2.1870	−1.6948	−1.1695	−4.2114	−2.1509	−0.8921	−1.5543	−4.2516	−4.3741	Undetected	−2.2833	−1.8724